Limbic connections with the ventral tegmental area in the nonhuman primate

Dissertation

zur Erlangung des Grades eines
Doktors der Naturwissenschaften

der Mathematisch-Naturwissenschaftlichen Fakultät
und
der Medizinischen Fakultät
der Eberhard-Karls-Universität Tübingen

vorgelegt
von

Diana Hernandez
aus *Barcelona*,*Spain*

2016

Tag der mündlichen Prüfung: 4th Februar

Dekan der Math.-Nat. Fakultät: Prof. Dr. W. Rosenstiel
Dekan der Medizinischen Fakultät: Prof. Dr. I. B. Autenrieth

1. Berichterstatter: Prof. Dr. Uwe ilg

2. Berichterstatter: Prof. Dr. Ricardo Insausti

Prüfungskommission: Prof. Dr. Uwe Ilg

Prof. Dr. Dr Ricardo Insauti

Dr. Henry Evrard

Dra. Monica Muñoz

Erklärung:

Ich erkläre, dass ich die zur Promotion eingereichte Arbeit mit dem Titel: “Limbic connections with the ventral tegmental area in the nonhuman primate“ selbständig verfasst, nur die angegebenen Quellen und Hilfsmittel benutzt und wörtlich oder inhaltlich übernommene Stellen als solche gekennzeichnet habe. Ich versichere an Eides statt, dass diese Angaben wahr sind und dass ich nichts verschwiegen habe. Mir ist bekannt, dass die falsche Abgabe einer Versicherung an Eides statt mit Freiheitsstrafe bis zu drei Jahren oder mit Geldstrafe bestraft wird.

Tübingen, den 4 Februar 2016

The present dissertation has been accomplished under a framework of joint supervision between the University of Tübingen/Max Planck Institute (Tübingen, Germany) and the University of Castilla-La Mancha (Albacete, Spain)

EBERHARD KARLS
UNIVERSITÄT
TÜBINGEN

UCLM
UNIVERSIDAD DE CASTILLA-LA MANCHA

Tübingen, ..., 2015

Rector of the University of Castilla-La Mancha
.....
Prof. Dr. Miguel Ángel Collado Yurrita

Rector of the University of Tübingen
.....
Prof. Dr. Bernd Engler

Chairman of the doctorate
University of Castilla-La Mancha
.....
Prof. Dr. José María Ruiz Moreno

Chairman of the doctorate
University of Tübingen
.....
Prof. Dr. Matthias Bethge

Thesis supervisor
University of Castilla-La Mancha
.....
Prof. Dr. Ricardo Insausti Serrano

Thesis supervisor
University of Tübingen
.....
Prof. Dr. Uwe Ilg

Thesis supervisor
Max Planck Institute /
Centre for Integrative Neuroscience
Werner Reichardt
.....
Dr. Henry Evrard

Doctoral Student
.....
Ms. Diana Hernández Mombiela

Acknowledgments

Quiero dar las gracias en primer lugar al Dr. Ricardo por darme la oportunidad de cumplir hoy mi sueño, estudiar el cerebro y ser doctora. Gracias al Dr. Henry, por haber estado a mi lado 726 días ayudándome y guiándome. Gracias al Dr. Nikos quien sin él, nunca hubiese sido posible engrandecer mi sueño ni de desarrollarme como la científica que he llegado a ser. Gracias a mi hermano quien me apoyo desde el primer día en que me concedieron la beca para estudiar mi doctorado. Hoy por fin, podré usar el boli que me regalo con el grabado de Dra. que siempre me animaba a seguir caminado cuando ya no podía más. Gracias a mis padres, quienes comprendieron mi “vida loca”, compartieron conmigo todos los veranos y siempre estuvieron orgullosos de mí. Gracias a mi compi de aventuras, Emmanuel Rojas, que hasta en los peores momentos nunca me dejo sola. Gracias a mi compañera, casi una hermana Mar Ubero, sin la cual sé que hoy no estaría aquí. Gracias al ministerio de educación y ciencia por promover y apoyar el talento Español, por confiar en mí y por qué lo siga haciendo con más estudiantes para que el mañana pueda ser un futuro mejor. Gracias a todos mis compañeros del laboratorio de neuroanatomía, nunca pensé el primer día que llegue Albacete, que se convertirían en mi familia. Gracias a la sociedad del Max Planck y a todos los alemanes que con su contribución hicieron posible que pudiese realizar este proyecto, del que espero haya podido poner un granito de arena para un mejor tratamiento en pacientes con enfermedades neurodegenerativas. Gracias a todos mis compañeros por haberme hecho sentir en casa, me llevo de cada uno de vosotros un trocito de vuestra cultura, de vuestro país de nuestras vivencias y sobretodo y aunque me quejara muchas veces del frio y de los horarios, de mi Alemania, mi segundo hogar.

Contents

1. Brief summary and goals

Addictive behaviors consist in the lack of freedom against a range of stimuli to which the individual has lost the ability to control their own impulses. Large amount of experimental work has been done to elucidate the neurobiological mechanisms underlying addiction especially in rodents. Addictive behaviors in experimental models show deficits in cognitive functions that depend on the frontal lobe, particularly the medial prefrontal cortex (MPFC) and orbitofrontal (OPFC). In the most acute stage of addiction (craving), there exist also alterations in conditioned reinforcement that depend on the amygdala and that contextualized the information processing within the hippocampus (Koob and Volkow, 2010).

Functional testing in patients with drug addiction showed a decrease in attention, cognitive flexibility and deferred reward (functions dependent on the frontal lobe), and deficits in spatial memory, verbal and visual recognition (functions dependent on the hippocampus) (Aharonovich et al., 2006). Therefore, reward systems (altered by addictions in their pathological side) are an essential component of human behavior. Their imbalance causes severe behavioral disturbances that end in the destruction of the individual.

Reward systems involve a series of brain structures and neurochemicals that regulate nerve transmission. The brain structures include deep brain structures such as the ventral tegmental area (VTA) and the locus coruleus (LC). VTA and LC have as common denominators that they are neuromodulators of the cathecolaminergic system producing dopamine (DA) and noradrenaline (NE), and that they are heavily interconnected with limbic centers such as the Amygdala (Amy) and the Prefrontal Cortex (PFC). The organization of these neuronal interconnections is crucial and needs to be completely elucidated, not only in rodents, but also in nonhuman primate models closer to humans.

A first step in the study of this system is to translate what we already know about those connections from rodents to the nonhuman primate's function. The present project aims to study the cross-connectivity of the brain structures of the limbic network in the macaque monkey, with a specific focus on the connections between the prefrontal cortex (PFC), Amy, and HF with VTA and to a lesser extent LC. So far, the only connections that have been extensively described are indirect polysynaptic connections from PFC, Amy, and HF to VTA (and LC) via interposed nuclei such as the nucleus accumbens (NA) of the ventral striatum (VS) (Haber et al., 1999), the medial thalamus that projects in fact mainly to the substantia nigra (SN) (Ikemoto et al., 2007). Even though PFC, Amy and HF are known to be very well connected with one another with direct monosynaptic projections, and although all of these regions are known to directly project to other monoaminergic nuclei (e.g., the cholinergic basal nucleus; Gaykema et al., 1991; Jankowski and Sesack, 2004), there is to date little evidence that they also directly project to VTA and LC.

We hypothesize that declarative memory in humans plays an important role in decision-making and reward/reinforcement behaviour, and that this is made possible through a loop that begins and

ends in the VTA and LC. In this study, we demonstrated the precise topography of the direct projections from the cortex (MPFC and OPFC), HF and Amy to the main sources of DA and NE in the brain. Moreover, since both neuromodulator pathways seem to have a similar origin in the PFC, HF and Amy, we postulated the inclusion of those projections in a neural network of reward and reinforcement of learning in the nonhuman primate Macaca fascicularis.

1. Breve sumario con los principales objetivos

Las conductas adictivas consisten en la perdida de libertad frente a una variedad de estímulos en los que el individuo ha perdido la capacidad de controlar sus propios impulsos. Gran cantidad de trabajos experimentales se ha hecho para descubrir los mecanismos neurobiológicos subyacentes en la adicción, especialmente en los roedores. Conductas adictivas observadas en modelos experimentales muestran déficits en las funciones cognitivas que dependen del lóbulo frontal, en particular en la actividad de la Corteza Prefrontal medial (mPFC) y en la Corteza Orbitofrontal (OFC). En la etapa más aguda de la adicción (craving), existen también alteraciones en el refuerzo condicionado dependientes de la amígdala y que contextualiza el procesamiento de la información para el hipocampo (Koob y Volkow, 2010).

Pruebas funcionales en pacientes con adicción a las drogas mostró una disminución en la atención, en la flexibilidad cognitiva y en la recompensa diferida (funciones dependientes del lóbulo frontal), también en el déficit en la memoria espacial, en la verbal y en el reconocimiento visual (funciones dependientes del hipocampo) (Aharonovich et al., 2006). Por lo tanto, los sistemas de recompensa (alterados por las adicciones en su lado patológico) son un componente esencial de la conducta humana. Su desequilibrio provoca trastornos graves de conducta que terminan en la destrucción del individuo.

Los sistemas de recompensa implican una serie de estructuras cerebrales y neuroquímicas que regulan la transmisión nerviosa, estas estructuras cerebrales incluyen a las estructuras profundas del cerebro, tales como el área ventral tegmental (VTA) y el Locus Coruleus (LC). VTA y LC tienen como denominador común que ambos son neuromoduladores del sistema catecolinérgico, el cual produce la Dopamina (DA) y la Noradrenalina (NE), y que también están fuertemente interconectados con los centros límbicos, tales como la Amígdala (Amy) y la Corteza Prefrontal (PFC). La organización de estas interconexiones neuronales es crucial y necesita ser completamente esclarecida, pero no sólo en roedores sino también en modelos de primates no humanos cercanos a los seres humanos.

Un primer paso en el estudio de este sistema es tomar lo que ya sabemos acerca de esas conexiones en los roedores y traducirlo a la función de los primates no humanos. El presente proyecto tiene como objetivo estudiar la conectividad cruzada de las estructuras de la red límbica en el cerebro del macaco, con un enfoque específico en las conexiones entre la Corteza Prefrontal (PFC), Amy y HF con la VTA y en menor medida con el LC. Hasta el momento, las únicas

conexiones que se han descrito ampliamente son las conexiones polisinápticas indirectas de PFC, Amy, y HF con la VTA (y con el LC) a través de núcleos intermediarios, como son el Núcleo Accumbens (NA) del Estriado Ventral (VS) (Haber et al., 1999) y el Tálamo Medial, el cual se proyecta, principalmente a la sustancia negra (SN) (Ikemoto et al., 2007). A pesar de que la PFC, Amy y HF se sepan que están muy bien conectados entre sí con las proyecciones directas monosinápticas, y aunque todas estas regiones se sabe que proyectan directamente a otros núcleos monoaminérgicos (por ejemplo, el núcleo basal colinérgico; Gaykema et al, 1991; Jankowski y Sesack, 2004), pero hasta la fecha hay poca evidencia de que también proyectan directamente a VTA y LC.

Nuestra hipótesis es que la memoria declarativa en el ser humano juega un papel importante en la toma de decisiones y en el comportamiento de la recompensa y el refuerzo; esto es posible gracias a un bucle que comienza y termina en el VTA y LC. En este estudio hemos demostrado la topografía exacta de las proyecciones directas de la corteza (mPFC y OFC), HF y Amy a las principales fuentes de DA y NE en el cerebro. Además, dado que ambas vías neuromoduladores parecen tener un origen similar en con la PFC, HF y Amy, hemos postulado incluir esas proyecciones a una red neuronal de la recompensa y del refuerzo del aprendizaje en el primate no humano Macaca Fasicularis.

1. Kurze Zusammenfassung und Ziele

Suchtverhalten entsteht durch eine Einschränkung vieler Reize, welche dazu führen, dass das Individuum die Fähigkeit zur Kontrolle der eigenen Impulse verliert. Es wurden bereits zahlreiche Experimente durchgeführt, insbesondere bei Nagern, um die der Sucht zugrunde liegenden neurobiologischen Mechanismen aufzuklären. Experimentelle Modelle zeigen, dass Suchtverhalten sich durch Defizite in kognitiven Funktionen äußern, welche abhängig vom Frontallappen, dem medialen präfrontalen Cortex (MPFC) und dem orbitofrontalen Cortex (OPFC) sind.Im akutesten Stadium der Sucht (craving) entsteht eine Veränderung der konditionierten Verstärkung, welche von der Amygdala (Amy) abhängig ist und die Informationsverarbeitung innerhalb des Hippocampus beeinflusst (Koob and Volkow, 2010).

Funktionelle Tests bei Patienten mit einer Drogenabhängigkeit zeigten eine Abnahme in der Aufmerksamkeit, der kognitiven Flexibilität und dem verzögerten Belohnungslernen (allesamt Funktionen die vom Frontallappen abhängig sind). Zudem wiesen diese Patienten defizite im räumlichen Gedächtnis, sowie bei der verbalen und visuellen Erkennung auf (allesamt Funktionen die vom Hippocampus abhängig sind).Darum sind Belohnungssysteme (durch Sucht pathologisch veränderbar) essentielle Bestandteile des menschlichen Verhaltens. Ein Missverhältnis führt zu schwerwiegenden Verhaltensstörungen die letztendlich das Individuum zerstören.

Belohnungssysteme schließen eine Reihe von Hirnstrukturen und Neurochemikalien (Regulation von Nervenübertragungen) ein. Dabei handelt es sich um tiefe Hirnstrukturen, wie dem ventral

tegmentalen Bereich (VTA) und dem locus coeruleus (LC). VTA und LC haben eine Gemeinsamkeit: Sie sind beide Neuromodulatoren der kathekolamineregen Systeme, welche Dopamin und Noradrenalin produzieren. Des Weiteren sind sie sehr stark mit den limbischen Zentren (Amygdala, präfrontaler Kortex) vernetzt. Die Organisation dieser neuronalen Verbindungen ist von großer Bedeutung und sollte nicht nur für Nager sondern auch für nicht-menschlichen Primaten (die den Menschen ähnlicher sind) ausgiebig erforscht werden.

Ein erster Schritt zur Erforschung dieses Systems ist es, die bereits bei Nagern gewonnen Erkenntnisse auf nicht-menschliche Primaten zu übertragen.Dieses Projekt beschäftigt sich mit der Erforschung der Vernetzungen in den Hirnstrukturen des limbischen Netzwerks von Makaken. Dabei liegt der Fokus auf der Verbindung zwischen dem präfrontalen Kortex, der Amy, der hippocampalen Formation (HF) und dem VTA (und zu einem geringeren Maße dem LC).Die bisher einzigen Verbindungen die ausführlich beschrieben wurden, sind die indirekten polysynaptischen Verbindungen vom präfrontalen Kortex, der Amy und dem HF zur VTA (und LC) über Zwischenkerne wie dem Nucleus accumbens (NA) des ventral striatum (VS) und dem medialen Thalamus, welcher vorwiegend in die Substantia nigra (SN) projiziert. Obwohl man weiß, dass PFC, Amy und HF über monosynaptische Projektionen miteinander verbunden sind, und auch, dass all diese Regionen zu anderen monoaminergen Nuclei projizieren, gibt es bis heute nur wenige Beweise für ihre direkte Projektion in das VTA und LC.

Wir behaupten, dass das deklarative Gedächtnis bei Menschen eine wichtige Rolle für Entscheidungen und Belohnungs-/Bestärkungsverhalten spielt, und dass dies durch eine Schleife ermöglicht wird, die ihren Anfang und ihr Ende im VTA und LC hat.Mit dieser Studie zeigen wir die präzise Topographie der direkten Projektionen vom Kortex (MPFC und OPFC), HF und Amy zu den Hauptquellen des DA und NE im Gehirn. Darüber hinaus postulieren wir aufgrund des scheinbar gleichen Ursprungs beider neuromodulatorischer Wege in PFC, HF und Amy, dass ihre Projektionen dem neuronalen Netzwerk für Belohnung und Bestärkung beim Lernen in nichtmenschlichen Primaten (in diesem Fall Macaca fascicularis), zugehörig sind.

2. Introduction

Our main interest is to elucidate the anatomical projections from the prefrontal cortex, hippocampus and amygdala that mediate signals of reward and memory through neurotransmitters release from the Locus Coruleus (LC) and Ventral Tegmental Area (VTA).

2.1 Interconnections of the reward and memory network

The neuronal network that substantiates memory and reward includes several parallel and segregated pathways that heavily rely on the release of, and the regulation of the release of monoamine transmitters such as dopamine (DA) and noradrenaline (norepinephrine; NE). Two pathways that have a key role in regulating the release of monoamine transmitters originate in the prefrontal cortex (PFC) and in the medial temporal lobes amygdala (Amy) and hippocampal formation (HF). They end in monoaminergic neuromodulatory midbrain centers such as the ventral tegmental area (VTA) and the locus coeruleus (LC) either through direct neuronal projections or through indirect projections involving intermediate structures such as the ventral striatum (VS) and ventral pallidum (VP), the mediodorsal nucleus of the thalamus (MD), and the lateral septum (LS). These direct and indirect projections enable enhancing adaptive behaviors, developing appropriate plans and inhibiting inappropriate choices on the basis of earlier experience (Haber et al., 2010).

2.1.1. Interconnections via the Ventral Striatum

Each general function of the striatum (limbic, associative, and sensorimotor) is represented in a specific region within each distinct structure of the basal ganglia (Alexander et al., 1990; Parent et al., 1995). The behavior derived from each region is regulated by glutamate projections originating in cortical and subcortical structures, and converging in the nucleus accumbens (NA) of the VS. The NA has repercussion in the effect of this glutamatergic influence to the rest of the brain, including the VTA.

There is to this date no evidence of direct projections between VS and LC. In fact, only scattered NE terminals occur in the striatum, particularly in the most caudal part of the shell of NA (Berrigde et al., 1997; Schoroeter et al., 2000). This could presumably have a strong effect on the striatum due to the high turn over of the neurotransmitter (Fornai et al., 1996; Fornai et al., 1996; Fulceri et al., 2006). In contrast, there are strong anatomical connections between VTA and VS. The rostral part of VTA sends strong projections to the ventral part of the striatum, and the most lateral part of VTA projects mainly to the dorsal-middle part of VS (Haber et al., 1999, 2000). Furthermore, Haber et al (1990) demonstrated this organization by showing that different anterograde injections in the medio-lateral parts of VS produced differences in density and rostro-caudal distribution of the labeling within VTA. For example, injections in the most lateral parts of VS and central striatum produced labeling only in the lateral VTA. All together, this indicated that VS is a possible interposed structure for the indirect polysynaptic projections of various cortical and subcortical regions to VTA.

Studies carried out by Haber et al. (1995, 2010) confirmed this idea by showing that dense cortical projections to VS arise from medial PFC (MPFC), with relatively much less projections from orbital PFC (OPFC). Further studies from the same authors completed this pathway by showing projections back from VS to PFC. These projections included broad targets in both MPFC and OPFC, in contrast to other parts of the striatum (central and lateral parts) that presented only light and restricted projections to PFC (Haber et al., 2000). Interestingly, in the present thesis (see Results and Discussion), we observed that the areas of PFC that project most heavily to VTA such as area 25, also project strongly to VS (NA shell) whereas other areas such as area 11 that project weakly to VTA, target the middle striatum. Therefore, the flow of information from PFC to the deep brain structures is very likely organized across parallel pathways including both fast direct projections and more elaborated indirect projections.

Additional afferent projections to the shell of VS have also been described from the basal nucleus of Amy (B) and from HF (Groenewegen et al., 1999). Interestingly, the HF projections are restricted only to VS (Strange et al., 2014). The input that originates primarily in CA1 and in the Subiculum ends in the medial and ventral parts of VS, as well as in the shell of NA. These projections are topographically organized in a decreasing dorso-ventral gradient (septal to temporal) similar to the dorso-caudal axis in NA (from the core to the shell) (Groenewegen et al.1987; Brog et al.1993; Kelley and Domesick et al., 1982; McGeorge and Faull. 1989; Voorn et al. 2004; Sesack and Grace. 2010). Some authors suggested that the caudomedial ventral Subiculum tends to receive the strongest hippocampal input, while the rostrolateral ventral Subiculum receive a relatively weaker input. In addition, in the dorsal Subiculum, the proximal Subiculum has denser projections to VS than does the distal Subiculum (Groenewegen et al. 1987; Witter et al. 1990). All together suggest that the direct projections described from the Subiculum to VTA, come from the region of the Subiculum that is most interconnected with VS.

Topographically organized projections from EC to VS have been reported. The lateral EC preferentially targets lateral aspects of VS throughout the entire rostrocaudal axis (Deshmukh et al. 2014), while the medial EC targets preferentially the medial VS (Derdikman and Moser 2014; Phillipson and Griffiths 1985; Totterdell and Meredith 1997). However, in contrast to PFC, these projections are not reciprocal.

On the basis of the existence of these connections and of our general hypothesis (see “1. Brief summary and goals”), we propose that the HF regions that project to VTA via the VS in an indirect pathway also project directly to VTA. The prior observations suggest that the only possible origin of these direct projections would be CA1, S and some parts of EC. The topographical distribution of the convergent inputs in the VS from PFC and HF places the VS as a key entry for processing of emotional and motivational information that in turn drives basal ganglia action output (Haber et al., 2010).

In the case of Amy, previous experiments in monkeys described by Russchen et al. (1985) pointed out that the density and distribution of the projections to VS varied depending on the Amy nucleus. Particularly, projections from the ventral and central striatum to Amy showed more labeling within the most medial and ventral parts of B, while injections in the most lateral and dorsal striatum showed labeling in the most lateral parts of Amy. Projections back from Amy to VS (Nucleus Accumbens) seemed to be also distributed heterogeneously. Interestingly, it has been observed that the heterogeneity of the projections from the different parts of the basal and lateral nucleus of Amy in rodents differentially regulates conditional neural responses within the core and shell of NA (Jones et al., 2010). Other Amy nuclei such as the medial part of the central nucleus (CeM), the peryamigdaloid cortex (PAC) and the medial nucleus of Amy are largely interconnected with the shell of NA (Haber et al., 2010). In contrast, the amygdaloid hippocampal area (AHA) and lateral nucleus (L) showed minor inputs to VS (Fudge et al., 2002) compared to the B nucleus and magnocellular divisions of the basal area (BA) (Russchen et al., 1985; Fudge et al., 2002). However, the main projections from Amy to the striatum, in general, target more to the caudate, putamen and the dorsal and middle parts of the striatum than VS (Nucleus Accumbens) (Mc Donald et al., 1991).

These data suggest that the connections between Amy and the midbrain may not be conveyed via VS but via another structure. Among the other possible structures, it has been shown that Amy sends strong projections to the thalamus (Russchen et al., 1987) and ventral pallidum (Haber et al., 1990; Hedreen et al., 1991; Parent et al., 1997). Another possible candidate gateway from Amy could be the amygdalofugal pathway (CE), the stria terminalis and the lateral septum (LS) (Price et al., 1981). Interestingly, in the results of this thesis, only the nuclei described with strong projections with NA have been found to also project to VTA.

2.1.2. Interconnections via the thalamus

In the study of the interconnections from PFC, HF and Amy to VTA, one of the possible intermediate relay is the thalamus, since is the gateway for the modulation of the flow of information to the cortex. So far there have not been described direct projections from the thalamus to LC. However, it has been found projections from the mediodorsal nucleus of the thalamus (MD) and central nucleos to the VTA in rodents (Watabe-Uchida et al., 2012). In the opposite direction, the VTA targets maily the mediodorsal nucleus of the thalamus (MD) followed by the lateral dorsal (LD) nucleus (Mitchell. 2015). Connections were also found with the ventral lateral and ventral posterior somatosensory thalamus (VPM and VPL); however the density was not homogenous; it was clearly abundant in VPL but sparse in VPM (Whitsel et al., 1978).

PFC has complex reciprocal thalamocortical connections, particularly with the MD nuclei. MPFC and OPFC are generally related to the medial part of MD while the lateral PFC (LPFC) is related to the more lateral parts of MD (Ray and Price 1993; Ikemoto et al., 2007; for a complete review of the MD connections see Hsu et al., 2007). Moreover, in the description of the projections back to the

PFC through the MD it has been also shown connections with the Amy (Timbie et al., 2014; Miyashita et al., 2007). Particularly, the projections between the MD and the Amy are reciprocal and particularly well organized (Russchen et al., 1987). For example, midline nuclei (such as reuniens) and intralaminar nuclei send projections to the magnocellular divisions of the basal nucleus, the medial nucleus, and the central nucleus of Amy (Aggleton et al., 1980; Aggleton & Mishkin, 1984; Mehler, 1980). Portions of the medial geniculate send projections to the lateral nucleus, the accessory basal nucleus, the medial nucleus, and the central nucleus of the amygdala (Amaral et al., 1992; Mehler, 1980). Finally, modest projections from the medial nucleus of the pulvinar to the lateral nucleus have also been reported (Aggleton et al., 1980; Jones & Burton, 1976). Projections back to the thalamus have also been described with origins in different parts of Amy. The parvicellular division of the basal nucleus of the amygdala terminates in the magnocellular portion of the nucleus MD (Aggleton & Mishkin, 1984; Amaral, & Price, 1987). The lateral nucleus, the magnocellular division of the basal nucleus, the accessory basal nucleus, the periamygdaloid cortex, and the amygdalohippocampal area also contribute to these projections (Aggleton & Mishkin, 1984). These projections terminate in distinct patches with a high degree of specificity. In particular, the parvicellular division of the basal nucleus and the periamygdaloid cortex project to different patches within the ventromedial region of the magnocellular portion of the MD, while the magnocellular division of the basal nucleus, the accessory basal nucleus, and the lateral nucleus, all project to specific patches within the ventrolateral region of the magnocellular portion of the MD nucleus (Russchen et al., 1987). Although this thalamic nucleus is the main recipient of amygdalothalamic projections, it does not reciprocate these connections. A second amygdalothalamic connection extends from the medial nucleus, the central nucleus, and the amygdalohippocampal area to the nucleus of the midline (reuniens) and the intralaminar nuclei (Aggleton & Mishkin, 1984; Price & Amaral, 1981). Finally, the central nucleus of the amygdala sends additional projections to the pulvinar (Price & Amaral, 1981).

According with the current knowledge, this prior tracing data suggests that despite the fact that that MPFC and Amy's B nucleus are strongly connected with the thalamus, the thalamus itself is not or is very unlikely to be an intermediate relay for PFC and Amy to LC and VTA.

2.1.3. Interconnections via the ventral pallidum

The Ventral Pallidum (VP) has been shown as the central point of convergence of inputs of limbic structures such as PFC (Funahashi, 1983), Amy, EC (Manns et al., 2001) to mediate reward and motivation functions (Marice et al., 1997; Kalivas et al., 1999; Smith et al., 2009).

There is no evidence of direct projections from the VP to the LC. However, projections in the opposite direction have been suggested (Berridge et al., 1997). In contrast, reciprocal projections with the VTA have been reported (Groenewegen et al., 1993; Luo et al., 2011; Beckestead et al., 1979, Taylor et al., 2014)

In turn, at least in rodents, reciprocal connections have been described with the mPFC (Root et al., 2015). However, to the best of our knowledge, there is no anatomical evidence of connections between VP and HF (Yang et al.,1985). However VP is anatomically linked to the lateral habernula (Nagy et al., 1978; Nauta et al., 1958), which directly connects with the septal nucleus, which in turn projects to the hippocampus (Nauta et al., 1966), and whose back projections reach VP via the nucleus accumbens. This pathway is important since it regulates indirectly the neuromodulation of the DA system via disinhibition from VP to VTA (Sabatino et al., 1986). According to this pathway, the afferent connections of the limbic system via the accumbens to VTA support the hypothesis that limbic structures such as the hippocampus can influence DA-dependent activities by way of NA and its efferent projection to ventral pallidal regions (Yang et al., 1985).

Anatomical studies show that Amy directly projects to cholinergic neurons in the VP (Zaborszky et al., 1984, 1986b; Carlsen et al., 1985; Poulin et al., 2006). These projections are predominantly glutamatergic (Fuller et al., 1987). The stimulation of the Amy produced two different effects, inhibition and excitation in separate populations of VP neurons. Specifically, excitation has been observed more in the medial side than the lateral VP (Yim and Mogenson, 1983; Maslowski-Cobuzzi and Napier, 1994; Mitrovic and Napier, 1998). Furthermore, reciprocal projections from the VP, mainly cholinergic (Carlsen et al., 1985; Zaborszky et al., 1986a, 1986b) target the Basolateral Amygdala (BLA) (Conrad and Pfaff, 1976b; Troiano and Siegel, 1978b; Haber et al., 1985; Carlsen et al., 1985; Mascagni and McDonald, 2009).

Although those results confirm a possible indirect pathway from Amy to VTA through the VP, further detailed studies need to be carried out in order to know if the same parts of the VP interact with both Amy and VTA, or whether the connections of Amy and VTA with VP are unrelated.

2.1.4. Interconnections between the HF and the PFC

Complementarily, we also considered the interconnections of the cingulum. It includes projections between PFC passing through the Subiculum, hippocampal cortex and Amy (Mufson et al., 1984).

Most of the projections between HF and PFC are reciprocal. The Subiculum and MPFC are reciprocally connected (Barbas et al., 1995; Carmichael et al., 1995) and some areas such as the prelimbic cortex or area 32 in primates, received additional excitatory inputs from CA1 (Jay et al., 1991, 1992; Insausti and Muñoz, 2001).

There are also reciprocal connections between EC and PFC (Barbas et al., 1995; Carmichael et al., 1995; Muñoz and Insausti, 2005; Legidos, 2014) although; the target in PFC depends on the rostro-caudal origin of the EC projections (Legidos, 2014). These projections are responsible for the role of HF and MPFC in spatial memory, goal directed behaviors, anxiety and cognition (Adhikari et al., 2010).

Projections from E_O show reciprocal connections with OPFC (areas 12 and 13) and MPFC (24 and 32 areas). Likewise, E_C showed reciprocal projections from the areas mentioned above (Insausti

et al., 1987; Muñoz and Insausti, 2005). Projections from E_R present connections with areas 12, 13 but also 11 and 14 of OPFC, and with MPFC (area 25) (Muñoz and Insausti, 2005). Projections from E_{LR} target the same areas as E_R but with area 24 of MPFC (Muñoz and Insausti, 2005). Projections from E_I to the PFC added the frontopolar projections (area 10), in addition to the areas specified above. In contrast, projections from E_{CL} are far less dense to the OPFC and MPFC (Muñoz and Insausti, 2005; Legidos, 2014).

Despite of the lack of the knowledge of all the interconnections, those observations suggest that not all the areas are reciprocally connected and that the density of the projections varies according to the specific portion of the HF considered. Alternative pathways include the relay via the mammillary bodies and the thalamus (Hok et al., 2005), such as the lateral OPFC that presents weak connections (Carmichael & Price 1995a). The study of those connections is significant since it has been suggested that the modulatory role of VTA on PFC is evoked by the HF influence, as the DA projections from VTA converge in the same areas of PFC that receive projections from HF (Jay et al. 1995).

2.1.5. Interconnections between the Amy and the PFC

Studies carried out by Krettek et al. (1977) showed that the connections between PFC and Amy are reciprocal. In primates, they are organized in such a way that the medial PFC is primarily connected with the ventrolateral part of the B nucleus while areas of the orbital prefrontal cortex are rather interconnected with the ventromedial parts of the B nucleus. A more extensive description of the terminal distribution within the nucleus was carried by Bonda (2000) who showed that the lateral part of Bi and Bmpc are more interconnected with MPFC, while the medial part of B is more interconnected with OPFC.

Further details reported by Carmichael and Price (1995) showed that different groups of cells within the same Amy nuclei project to different parts of PFC. For example, area 13b receives projections from the most medial parts of B (Bi, very low from Bpc) and not from L, while area 14 receives projections from only the most central part of the same nuclei. Particularly, area 14r receives projections from B and ABpc, while area 14c receives projections from Bi, Bpc and Co. Area 12o receives projections from the lateral part of B. Other examples of sub specializations of the projections between PFC areas and Amy show also differences within area 11. Finally, not all the connections are reciprocal, for example area 13a does not receive projections from Amy although it projects to Bpc, Bi, low to AB, and also to CE.

Other areas of the lateral PFC receive projections from Amy. Area 9d receives projections from the dorsal part of B and areas 12r, 45 and 46 and project to Bmc and Ld. The insular cortex areas Iai, Iamp, and Ial present projections with Amy that are more or less reciprocal but the targets are not the same. Area Iai receives projections from several nuclei but projects only to Bpc. Iamp receives projections from ABmc, Bi and Bpc but only projects to CE and AB. Area Iam receives

projections from Bmc and Bi; it projects back to BI. These observations are pertinent because in the present thesis we found similar patterns of “patchy projection” with VTA, and also because regions from Amy with strong projections the VTA also present substantial projections to MPFC.

2.1.6. Interconnections between HF and Amy

There are also interactions between Amy, EC and hippocampus (Amaral et al., 1986, 1992). Particularly, the rostral parts of EC (E_O, E_R and E_{LR}) seems to be more interconnected with all the Lateral (L) nuclei of Amy (Ld, Li, Ldi, Lvi, Lv) and some parts of the Basal nucleus (specifically with the Bi/Bpc and Bpc/PL areas) and have also some connections with the Accessory Basal nucleus. The rest of the EC subfields, E_{LC}, E_I and E_C/E_{CL}, present almost no connections with Amy except for E_I, which receives only projections from the most ventral parts of L (Lvi and Lv). This is very interesting because Pitaken et al. (2002) showed that those projections are organized in different routes. Projections that arise directly from the L nuclei project to E_{LR}, E_R and E_O and not to the hippocampus, however projections arising from the L that make an intermediate synapsis with the B nucleus, target EC (areas mentioned above) and the Subiculum. Moreover, sensory information that target not only L but also AB with an intermediate synapsis in the B nucleus targets not only EC but also the Dentate Gyrus. Finally, sensory projections to the PAC, along with the previous steps in B and BA, target EC and Subiculum.

In turn, Amy could also be modulated by EC (particularly from the rostral half), to CA1 subfield and the Subiculum. The amygdala nuclei receiving the heaviest inputs are the L, B, AB, CE and the amygdalohippocampal area. Moreover, all the areas of the HF that project to the amygdala innervate the lateral nucleus except for the CA1 subfield, which innervates the B nucleus, and the amygdalohippocampal area.

Memory related information might become associated with information processed in various amygdala nuclei and this might help “fine tune” in parallel the different components of the behavioral response that the amygdala generates (Pitkanen et al., 2000).

2.2 Functional Aspects of Reward and Memory

2.2.1 Reward and addiction

Since the mid 1970 a number of theories on the role of DA in reward have been put forth. They include hedonic effects on reward (Wise et al., 1978), reinforcement (Beninger, 1983; white and Milner 1992), incentive-motivation (Wise and Bozarth 1987), motivation for action (Salamone 1991), reward prediction error (Schultz 1997), reward learning (Horvitz et al., 2007) and incentive salience attribution (Berridge et al., 1998).

A role for DA in the incentive-motivational (approach) effects of primary reward has also been demonstrated (Wise et al., 2004); the neurons can also habituate to the stimuli and not respond

anymore (Ljunberg et al., 1998). Several studies explored the contribution of release of phasic DA by rewards and found that primary rewards (such as food or drug abuse) enhance DA transmission in terminal regions of the mesocorticolimbic DA system, particularly in NA (Haber et al., 2010). On the other hand, with opposite stimuli such as foot shock, an increase of DA has been observed in the shell of the NA but not in the core (Kalivas et al., 1995) suggesting that the core and the shell of the NA are implicated in different functions. Moreover, responses in the DA neurons of the different parts of VTA have been reported in the dorsal PBP and PN but with opposite modulation effects, reducing and increasing the firing, respectively (Ungless et al., 2004; Brischoux et al., 2009). Several lines of evidence strongly argue in favour of the involvement of reward circuitry for the processing of aversive stimuli such as foot shock so as to encode behaviour to avoid these aversive stimuli. Specifically, DA is involved in behaviours predicting reward (approach) or punishment (avoidance). However, recording studies pointed out that the cells excited during aversive stimuli were the non-DA cells (Ungless et al., 2004).

Studies carried out by Bouret et al. (2014) suggested that the activity of LC and PFC is related to reward anticipation. LC neurons exhibit experience-dependent plasticity related to reward-contingency regulating learning and memory. Neuromodulator properties of NA suggest that the coruleus-cortical projection should play an important role in attention and memory processes. LC cells respond to novelty or change in incoming information but do not have a sustained response to stimuli, even when they have a high level of biological significance. The gating and tuning action of NA released in target sensory systems would promote selective attention to relevant stimuli at the critical moment of change. The adaptive behavioral outcome would result from the integration of retrieved memory with the sensory information selected from the environment (Sara et al., 1994).

Furthermore, clinical observations have converged on the hypothesis that addiction represents the pathological usurpation of neural processes that normally serve reward-related learning. The major substrates of persistent compulsive drug use are hypothesized to be molecular and cellular mechanisms that underlie long-term associative memories in several forebrain circuits (involving the ventral and dorsal striatum and prefrontal cortex) that receive input from midbrain DA neurons (Hyman et al., 2006).

2.2.2. Memory

Memory allows to acquire, encode, store and retrieve information that gives the human being a biography and a set of facts that are used as a guide through the world and to interact in their environment. Learning and memory are closely related processes; however, learning is the process of acquiring new information while the memory refers to the persistence of learning; memory is usually the result of learning (Hilgard and Marquis 1940).

Memory is classified conventionally and according to its temporal scope into two types: short-term memory and long-term memory. The short-term memory retains an isolated sensory stimulus

or temporary thinking waiting to be stored. This is mainly regulated by the dorsolateral prefrontal cortex (responsible of attention) and left pre-silvian zone (which manipulates verbal information). The long-term memory is the result of a permanent strengthening and reinforcement of synaptic changes that result in a warehouse of ideas, events, etc. In general, where these vivid memories are stored, is also our knowledge about the world, images, concepts, strategies for action, etc.

In turn, long term-memory is subdivided into two types according to their content: implicit or procedural (skills that are stored unconsciously) and explicit or declarative memory (reportable through language). The later is responsible for the use of the knowledge learnt during the experiences to provide new ways to solve future situations (Eichenbaum, Braver, 2001). It subdivides into episodic (that stores events of daily life) and semantics (which specializes in acquiring knowledge of the environment and the meaning of words) and its function depend mainly on the integrity of the hippocampal formation. Adjacent structures such as temporopolar, perirhinal and parahippocampal are also able to achieve the evocation and consolidation of those memories (Preston et al, 2004). Procedural memory in contrast, includes the store of skeletal and cognitive abilities, dependent on the basal ganglia structures, the amygdala, cerebral cortex, etc. In addition, for emotional associative memory (procedural) it has been found that the main responsible is the amygdala, which performs tasks such as the relation between object-punishment and the reward action. For that reason both structures HF and Amy are involved in the recognition of objects and situations, but in their own different nature (Parkinson et al, 1988).

2.3. Cytoarchitecture of the principal components of reward and memory network

2.3.1 Prefrontal Cortex

Traditionally PFC was defined as a region with prominent connections with the thalamus (Uylingis et al., 2003), particularly with the medial thalamus whose interconnections have been used actually to delineate the borders of the different areas of PFC (Groenewegen et al., 1990). PFC is also connected with the brainstem (Williams et al., 1998 and Frankle et al., 2006), locus coruleus (Ongur et al., 2000; Heidbreder et al., 2003), Amy (especially to the BLA) (Freese et al., 2009), the HF and Entorhinal Cortex (Quirk et al., 2003).

Twenty-two distinct cortical areas have been identified in the Orbital and Medial Prefrontal Cortex (OMPFC) in the macaque monkey (Carmichael et al., 1994) (see figure 1). These areas are characterized by their unique histological staining characteristics and by different interconnections (Ongur et al., 2000). The medial network comprises strong interconnected areas along of the medial wall (10m, 32, 25,24b and 24a), the medial edge of the orbital cortex (10o, 11m, 14r and 14c) and the lateral orbital surface called the intermediate agranular insula. Moreover, within the mPFC we found the agranular Insula (Rose, 1928; Amaral and Price, 1984) composed by five subdivisions (Iam, Iai, Ial, Iapm, and Iapl). Further subdivisions of the mPFC divide it into five areas based on

cytoarchitecture and connections (Vogt et al., 1987): areas 25 and 32 and three subdivisions of the granular area 24: 24a, 24b, and 24c.

Those areas can be distinguished based on the anatomical features of layer V. particularly; area 32 has horizontal striations of pyramidal cells in layer V while area 24b arranges them in the vertical axis. In contrast, area 24c which has a less vertical organization in layer V contains aggregates or clumps of medium-sized pyramidal neurons in layers V but also laminar VI. However, area 24a has been shown to have a rudimentary lamination that consists of only four layers. On the other hand, area 25 lacks a clear radial organization, and consists of densely packed layer V and a less dense layer II/III, plus a very thin layer VI. The structure of 25 becomes more elaborate from caudal to rostral. Furthermore, the caudal part of area 32 resembles 25, which makes it difficult to recognize a precise boundary between these two areas.

The orbital network however, includes strong interconnected areas 11l, 12r, 12m, 12l, 13m and 13l as well as several parts of the agranular insular cortex. A few areas (13a, 13b and 12o) appear to be connected to both networks and termed medial/orbital network (Hsu et al., 2007). Further details of the cytoarchitecture shows that area 13a is an agranular area characterized by a sublaminated layer V in which the two cellular rows are composed of aggregates of densely staining pyramidal cells. Moreover, we found the lateral orbital surface of the cortex, which can be designated by its topographic position within Walker's original area 12: rostral 12 (12r), lateral 12 (12l), medial 12 (12m), and orbital 12 (12o). They principally distinguish by the degree of granularity of layer IV and the pattern of pyramidal cell staining in layers III and V. The most rostral area, 12r, is a dysgranular field with prominent vertical striations in the arrangement of pyramidal cells in layers III and V. Layer V is not sublaminated. Area 12m, within the lateral orbital sulcus, has a clearly sublaminated layer V and a more granular layer IV than the surrounding areas 12r, 13l, and 12o. Area 12m can be distinguished from caudally adjacent 13l by its more compact and darkly staining layer V. Area 12o has a very thin and weakly staining layer IV and no obvious sublamination in layer V. In contrast, area 12l is a sharply laminated, granular field; with prominent sublamination of layers III and V. Area 12l is bordered dorsally by area 45 (Walker, 1940), which can be distinguished by a population of very large pyramidal cells in deep layer III. Caudal to area 12l, the precentral opercular cortex is much less granular and has a pattern of vertical and radial striations of pyramidal neurons not seen in area 12l.

Finally, the rostral orbital cortex contains two areas, medial 11 (11m) and lateral 11 (11l), and the frontal pole, which contains orbital and medial areas (10o and 10m, respectively). Areas 10 and 11 constitute the granular cortex rostral to 13m. In 11m and 11l, layer V is thinner and has more trilaminate appearance than in 13m. Area 11m differs from 11l in that the outer and inner sublaminae are broken up into aggregates of neurons rather than forming the continuous bands seen in 11l. Area 11m also lacks the horizontal and vertical striations of cells that typify the adjacent area 13b. Rostrally, areas 11m and 11l border the thinner, less distinctly laminated area 10o. Area 10o

appears more granular than 11m and 11l, but layer IV is not well demarcated. Layer V is markedly thinner in 10o than in either 11m or 11l and is not as prominently sublaminated. Area 10o also contains vertical and horizontal cross striations of cells in layers III and V. In both the orbital and the medial subdivisions of area 10, layer VI is thin and not well separated from layer V. The distinguishing feature of 10m in the Nissl stain is the presence of horizontal striations of granule cells in layer IV. This feature clearly demarcates layer IV from layers III and V and, as a result, distinguishes area 10m from the surrounding cortical areas, which are either agranular (areas 14c and 32) or dysgranular (area 14r). Area 14 can be subdivided into rostral and caudal divisions (14r and 14c) in addition to the areas that occupy the medial bank of the medial orbital sulcus (13a and 13b). Areas 14c and 14r can be differentiated by the appearance of layer IV. Area 14c is agranular, whereas 14r is dysgranular. Additionally, there is no distinguishable layer II in 14c, while in 14r layer II is recognizable as a distinct population of small cells. Finally, on the medial wall, area 10m can be distinguished from 14c and 14r by its granular layers II and IV and its characteristic criss-cross pattern of horizontal and vertical striations of cells in layers III, IV, and V.

Moreover, in the classic cytoarchitectonic maps of the primate and human cerebral cortex (Brodmann 1908, 1909; Sarkissov et al. 1955) there are a few more areas that do not have equivalence in rodents on the mid-lateral prefrontal cortex. In monkeys, area 9 is defined by a poorly developed layer IV and the presence of large pyramidal cells in the deeper part of layer III. In contrast, area 46 has a well-developed layer IV with deeply stained pyramidal neurons in the lower part of layer III. Moreover, in the ventral part of the lateral PFC lies area 44, a dysgranular area in which layer IV is present but not well-developed, characterized by large pyramidal neurons in the lower part of layer III and in layer V (Petrides & Pandya 1994 and 1999; Amunts et al. 1999). Area 44 is succeeded rostrally by area 45 which differs from area 44 by the presence of a well-developed layer IV and strikingly large pyramidal neurons in the deeper part of layer III. Rostroventral to area 44 we found area 45 that extends to the most orbital surface.

Supported by functional studies it has been suggested that those subspecialisations of the areas in the PFC have related different functions, described for the anterior, posterior and lateral OPFC by O'Doherty et al in 2001. Interestingly, the columnar organization of those areas based in six layers it is not homogeneous and depend on the structures related to it. For example, PFC limbic areas lack of layer 4, which is poorly mielinizated (Mesulam et al., 1982; Barbas et al., 1989 and 2015). Those areas occupied a ring around the corpus callosum. Laminar pattering beyond the limbic core appears progressively differentiate in successive eulaminates areas. This is important to account since in our results we have shown that the area's most projecting from the PFC are the ones closest to the medial line in the PFC or limbic cortex. However, in the study of the projections back from the DA nucleus, the study of the regional distribution of the DA fibbers within the PFC showed that the area's most projecting are not the ones receiving the most DA input. The results showed that the greater density of DA fibres was in area 9 (dorsomedial) and area 24 (anterior cingulate).

Medium levels were found in area 25 (medial surface), 12 (lateral), 11 and 13 (orbital) followed by low levels in areas 46 (dorsolateral) and 10 (frontal pole) (Bjorklund et al., 1978; Brown et al., 1979). This pattern was similar for NE fibbers distributions but less dense and with one exception, the area higher received NE input was the 24 instead of area 9 (Briand et al., 2009).

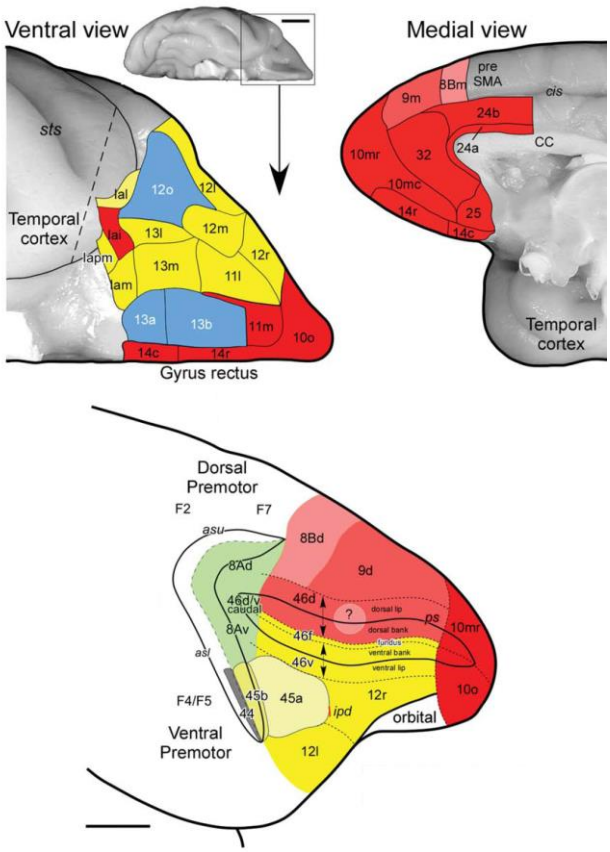

Figure 1: Line drawings of the subdivisions of the Prefrontal Cortex in monkey. In yellow the OPFC network, in red the MPFC network and in blue the orbital/medial (intermediate areas). Scale bar 5mm. Modified from Saleem et al., 2014.

2.3.2 Amygdala

The term Amygdala (Amy) refers to a group of subregions that together form a key component of the emotion network. Amy is implicated in the recognition of negative and unpleasant emotions such as fear but also in reward-related events. The Amy interacts with cortical and subcortical structures such as NA, midbrain and PFC (particularly OPFC). In addition to “emotion” sensu stricto, Amy can also be affected by other functions such as learning processes related to HF. It has been postulated that learning and memory can be influenced by motivation and emotion, and the responsible Amy region for that influence is the Basolateral Amy (Almaguer et al., 2003). In fact, several distinct subnuclei of the Amy contribute differently to the acquisition of an avoidance strategy and to the consolidation of avoidance memories (Ilango et al., 2014).

The Amy is not a single functional or structural unit; it is composed by several subnuclei that have been suggested to constitute at least three different networks (Swanson et al., 1998). The olfactory network that involves the Medial nucleus of the Amy (ME); the cortical network that involves the Basal and Lateral Amy; and the autonomic network, which involves the Central nucleus of the Amy (CE).

The nonhuman primate amygdaloid complex can be further divided into 13 nuclei and cortical areas (Amaral & Bassett, 1989; Amaral et al., 1992; Gloor, 1997; Price et al., 1987) (see figure 2 from Stefanacci and Amaral., 2000).

For convenience, these often are classified as “deep nuclei” (the lateral nucleus (L), basal nucleus (B), Accessory Basal nucleus (AB), and paralaminar nucleus (PL)); “superficial nuclei” (the medial nucleus (ME), the anterior cortical nucleus (COa), the posterior cortical nucleus (Cop) and the periamygdaloid cortex (PAC)); and “remaining nuclei” (the anterior amygdaloid area (AAA), the central nucleus (CE), the amygdalohippocampal area (AHA), and the intercalated cells(I)(Bienvenue et al.,2015).

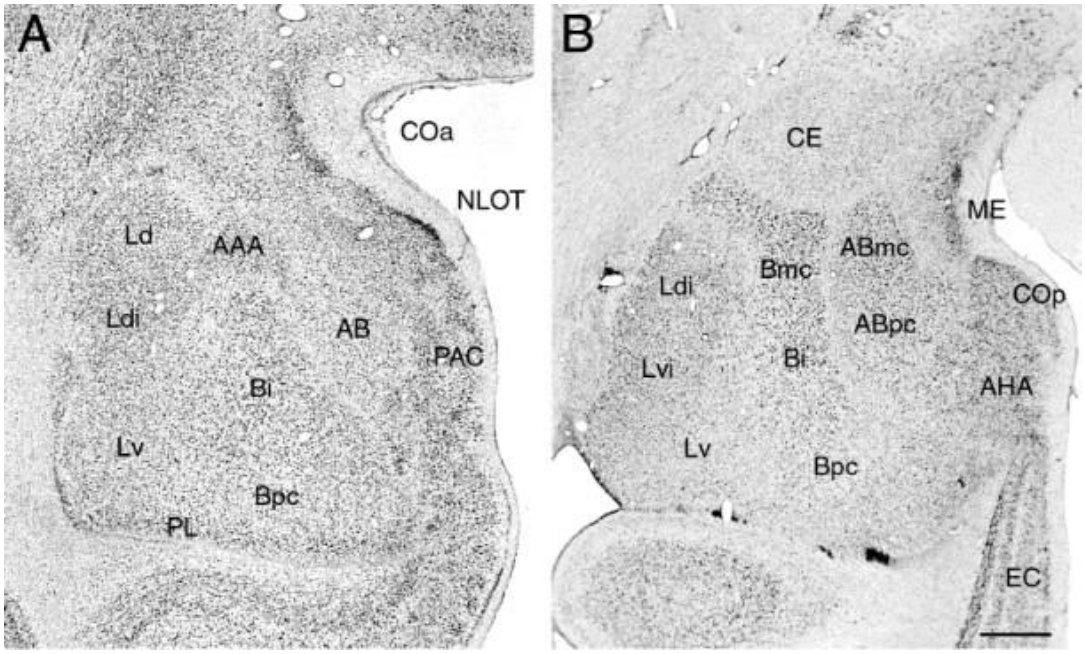

Figure 2: Photomicrographs (A-B) of coronal sections stained with Nissl of rostral levels of the amygdala, showing the different nuclei subdivisions. Source: Stefanacci and Amaral, 2000. Scale 1mm.

In detail, the lateral nucleus is subdivided into dorsal (Ld), dorsal intermediate (Ldi), ventral intermediate (Lvi) and ventral (Lv) divisions (Pitkänen & Amaral, 1998; Price et al., 1987). Connections within the lateral nucleus originate mainly in the dorsal divisions and terminate in the ventral divisions (Pitkänen & Amaral, 1998). Also based on cytoarchitectonics, the basal nucleus is parcelled into magnocellular (Bmc), intermediate (Bi), and parvicellular (Bpc) divisions (Amaral &

Bassett, 1989; Price et al., 1987). The most medial of the deep nuclei is the accessory basal nucleus (AB); it is subdivided into magnocellular (ABmc), parvicellular (ABpc), and ventromedial (ABvm) divisions (Price et al., 1987). The magnocellular and parvicellular divisions of the accessory basal nucleus are interconnected (Amaral et al., 1992; Price et al., 1987). The paralaminar nucleus is a narrow band of densely packed, darkly Nissl stained cells situated along the ventral and rostral limits of the amygdala (Pitkänen & Amaral, 1998). The medial nucleus is composed of a large portion of gammaaminobutyric acid-ergic cells (GABAergic). Rostrally continuous with the medial nucleus, there is the anterior cortical nucleus that includes a wide, cell-free layer I, thick diffuse lightly stained cells in layer II and an even less dense layer III. The anterior cortical nucleus is differentiated from the medial nucleus because its layers II and III form nearly a continuous mass, whereas the medial nucleus has a distinct layer II. The posterior cortical nucleus is caudally positioned and contains only two cell layers. Layer I is quite thin, while layer II is slightly thicker and consists of medium-sized lightly stained neurons. The Nucleus of the Lateral Olfactory tract (NLOT) is located in the rostral half of the amygdaloid complex and is identifiable by the moderately dense layer II and an overall intense staining for AChE. Although it is a prominent nucleus in the rat and cat, it is often difficult to discern its borders in primates (Price et al., 1987). The periamygdaloid cortex (PAC) is located on the medial surface that extends along the rostrocaudal amygdala. It is a heterogeneous region that has been given many different names and subdivided in a number of ways (Jimenez-Castellanos, 1949; Johnston, 1923; Price et al., 1987). The periamygdaloid cortex has been divided into PAC2, PAC3, and PACs subdivisions (Amaral & Bassett, 1989). In PAC2, layer II is thin and dense and contains darkly stained cells in Nissl material, whereas layer III contains scattered lightly stained cells. A cell-free zone often separates the two layers. PAC3 is located caudal to PAC2. Furthermore, like the nucleus of the lateral olfactory tract, the anterior amygdaloid area is less prominent in monkeys than in rats and cats. It is located in the rostral half of the amygdala and contains small and medium-sized cells. The central nucleus (CE) located in the caudal half of the primate amygdala. It is typically subdivided into medial and lateral divisions, based on its cytoarchitecture (Price et al., 1987). The medial division contains a heterogeneous mixture of lightly stained small and medium-sized cells. Neurons in the lateral division are more homogeneous in appear. A distinguishing feature of CE is that it is strongly immunoreactivity for GABA and glutamic acid decarboxylase (GAD), a precursor to GABA. This suggests that many projections of the central nucleus are GABAergic. The amygdalohippocampal area (AHA) is located at the caudal pole of the amygdala. Rostrally, the neurons of AHA are lightly packed in contrast with the dense packed cells of the most caudal parts. Finally, there is the intercalated nucleus (I) with separated cell masses located in different areas of the amygdala. There has been enormous interest in the intercalated nucleus in the rodent brain (Paré, Quirk, & LeDoux, 2004; Royer, Martina, & Paré, 1999; Royer & Paré, 2002). However, much less is known about its organization in the nonhuman primate brain. In general, they tend to be relatively less prominent in the primate brain than in the rodent

brain. They receive mainly projections from the lateral and accessory basal nuclei (Aggleton, 1985; Pitkänen & Amaral, 1998) and have a spread location within the amygdala. Some are located between the basal and accessory basal nuclei; others are located between the basal and lateral nuclei; and still others are found among passing fibres just ventral to the central nucleus.

2.3.3. Hippocampal Formation

The Hippocampal Formation (HF) is composed of: Ammon's field, Subicular Complex, Dentate Gyrus (DG) and Entorhinal Cortex (EC) (see figure 3; Courtesy of Dr. Mohedano-Moriano). These regions have been observed to form intrinsic connections organized into rostro-caudal (in primates) or ventral-dorsal (in rodents) orientation (Strange et al., 2014). The most rostral parts of EC (E_O) are interconnected with the rostral HF while the most caudal parts (E_{LR} and E_C) are interconnected with the caudal HF (Chorbak et al., 2007) suggesting that the EC projections may be organized into separate networks.

It is remarkable that in rodents this organization has been shown to imply a dorso-ventral segregation of the functions within the HF and EC. Particularly in rodents, the dorsal hippocampus has been shown to impact spatial memory providing contextual information via CA1 to the retrosplenial cortex (Cenquizca et al., 2007) and provides reward-context information via dorsal CA3 projections to the Lateral Septum (LS) that disinhibits the VTA (Luo et al., 2011). In the ventral axis however, the ventral CA1 and ventral Subiculum, the major output from the HF, provides novelty-evoked signals (Legault and Wise 2001; Valenti et al., 2011) and it induces the activity of VTA during stress trough projections to NA (Christie et al., 1987).

The Subiculum presents also a dorso-ventral gradient acting as pivotal structure between the HF and EC. The dorsal part is strongly interconnected with the cortical areas related to mnemonic, spatial memory and environmental movement while the ventral part is more interconnected with subcortical structures related to stress and vestibular movement (O'Mara et al., 2005). Also, the ventral Subiculum, along with Pedunculo Pontino Tract (PPT), has been shown to regulate the phasic and tonic release of DA cells. Particularly, the Subiculum induces a significant increase of the burst of the DA neurons and phasic release to encode reward (Lodge et al., 2006) in the NA (Blaha et al., 1997) that in turn inhibits the VP (GABAergic) afferents to VTA (Floresco et al., 2001).

Another circuit that deserves particularly attention involves projections from the ventral Subiculum to the PFC (Swanson et al., 1981 and Jay et al., 1991), which in turn provides glutamatergic inputs to the VTA (Sesack and Pickel 1990).

Although at first glance the appearance of HF is different between the species (rat, monkey and human) humans and primates have a similar cytoarchitectonic organization in the Ammon's fields, divided into three CA1, CA2 and CA3 fields (Amaral and Insausti, 1990; Bakst and Amaral, 1984) whose layer fields are described below: Alveus, formed by transversally oriented axons of the pyramidal cells that form the exit way out of the hippocampus.

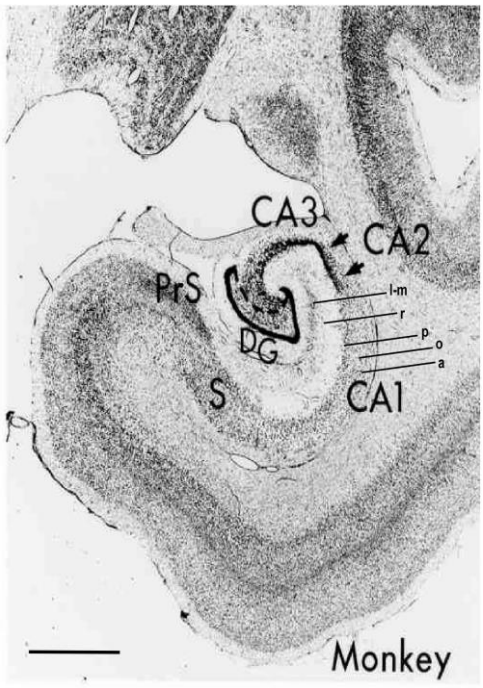

Figure 3: Microphotography of coronal section of the hippocampal formation of the primate. The anatomical boundaries separate the following regions: Ammon's fields: CA1, CA2, CA3; Dentate Gyrus (DG) with their respective layers (a: alveus or stratum oriens; p: piramidale stratum; r: stratum radiatum; l-m: stratum lacunosummoleculare); Subiculum and Presubiculum. Photomicrograph modified from Insausti and 2004. Scale 1mm.

The stratum Oriens, situated below the stratum piramidale with a limited fibber number of cells (basal dendrites of pyramidal cells). The stratum piramidale, which contains the most interneurons a part from the cell bodies of the pyramidal cells and their basal dendrites. The stratum lucidum is only present in CA3 and is situated just above the pyramidal layer occupied by mossy fibber axons coming from the Dentate Gyrus. The stratum radiatum is above the stratum lucidum in CA3 and immediately superficial to the CA1 and CA2 pyramidal layer that contains apical cells. Finally is the stratum lacunosum-molecular which is the most external layer of the hippocampus. It contains the apical dendrites from the pyramidal cells and the axon fascicles that form the fibbers of the perforant pathway from the entorhinal cortex, which run parallel in the hippocampal fissure.

Enveloping the end of the pyramidal cells of CA3, it is situated the dentate gyrus (DG), also divided into three layers: molecular, granule and polymorph (also referred to it as the hilus). The molecular layer is located superficial to the granule cell layer that contains sparse cells of varying sizes and the fibbers of the perforant pathway. The granular layer, which contains an extensive number of small, densely packed and uniformly sized cells. The polymorph layer, enclosed by the granular and molecular layer, which contains sparsely, distributed large polymorphic cells whose major prominent cell is the mossy cell (Amaral et al., 2007). Finally, at the interface of the granular and polymorph layer, it lays the subgranular zone, one of the few regions in the brain in which adult neurogenesis occur.

Continued to the Ammon's field we found the Subiculum (among others) which is the origin of major subcortical projections to the septal complex, nucleus accumbens, anterior thalamus, and mammillary nuclei, as well as projections to the entorhinal cortex, and to some cortical regions in the non-human primate (Rosene and Van Hoesen, 1978; Insausti and Munoz, 2001). However, these projections are poorly understood as long as the cellular and laminar organization of this region. As noted earlier, the Subiculum and field CA1 of the hippocampus overlap at their border. The laminar organization of both regions is complex in this zone. Medially (closer to the Presubiculum), the Subiculum can easily be divided into three layers. Superficially, there is a wide molecular layer into which the apical dendrites of the subicular pyramidal cells extend (Braak, 1972). Particularly specify the superficial limit of the external pyramidal cell layer contains islands of small, darkly stained cells that enable to distinguish the Subiculum from CA1. Moreover, the deepest portion of the subicular pyramidal cell layer contains a variety of smaller neurons called the polymorphic layer in the monkey (Bakst and Amaral, 1984). In addition, the most rostral uncal flexure of the hippocampus formed by the Subiculum is designated the hippocampoamygdaloid transitional area (HATA) by Rosene and Van Hoesen (1987).

On the other hand, the laminar organization of the Presubiculum and parasubiculum is complex and only poorly understood. It is perhaps most useful to consider that the Presubiculum consists of a single, superficially located cellular layer made up of an external principal (layer II) and an internal principal cellular layer (Braak, 1980), which is formed by densely packed, small, modified pyramidal cells. Layer II of the Presubiculum tends to be narrow and continuous at posterior levels of the hippocampal formation but breaks up into larger-diameter islands at more rostral levels. As in the monkey (Bakst and Amaral, 1984), layer II can be further divided into a narrow, superficial rim that contains more densely packed and darkly stained neurons and a broader band of more widely separated cells. The parasubiculum in turn, contains also a single cellular layer that is difficult to clearly differentiate from the Presubiculum. The layer II cells of the parasubiculum tend to be somewhat larger than those in the Presubiculum and more widely spaced.

So far we have described the non-cortical components of the Hippocampal formation but there is also a cortical structure named the entorhinal cortex that in rodents it is generally subdivided into two domains, the lateral and medial entorhinal (Witter et al., 1989). In primates however we can distinguish 7 rostro-caudal subdivisions (E_O, E_R, E_{LR}, E_{LC}, E_I, E_C, E_{CL}) (Insausti et al., 1987b) with a structure of six layers. Layer I contains fibbers and a few neurons. Layer II is prominent and contains a special type of modified pyramidal cell who's most characteristic features is the clustering in cell islands in many species. Layer III, made up of medium pyramids that are arranged in clusters medially and are more columnar laterally. Layer IV, that corresponds to a cell-poor or cell-free stratum in the middle of the cortex (lamina dissecans) (Rose, 1927). However this lamina it is only present in certain portions of the entorhinal cortex. In contrast, Layer V contains big, deeply stained pyramid cells. Authors who follow the nomenclature of the layers set by Lorente de No (1933) refer

to this layer as layer IV and reserve the name of layer V for the most superficial part of layer VI. Finally, Layer VI is multi-layered and therefore can be broken down into different substrata.

2.3.4. VTA

The classical description of the ventral tegmental area of Tsai in 1925 situated it lying in the midbrain and was classified by Dahlstrom and Fuxe (1964) inside the A10 dopamine group. In 1987, Oades defined the borders of that region, bilaterally distributed along the midline over the interpeduncularis nucleus (IP), under the oculomotor fibres of the third cranial nerve (NIII) and medial to the substantia nigra (SN). This description fits with the C10 (Hubbart et al., 1974) and M10 (Garver et al., 1975) groups defined in monkey. The A10 area consists in three groups (A10c, A10dc, and A10dr). VTA is in A10c along with the Edinger-Westphal nucleus (EW), central and rostral linear nuclei (CLi and CrLi respectively) and interfascicularis (IF).

So far there exists no consensus on the cytoarchitecture or on the exact borders of the VTA (See figure 4). In monkeys previous studies pointed out the existence of two main nuclei in the VTA (Smeets WJ et al., 2000): paranigral and parabrachial pigmented nuclei. Other authors referred to VTA as a whole, A10, (such as Cho in 2010; Schofield in 1981 and Felten in 1983; Martin *et al*., 1996) or did not include the parabrachial nuclei in the VTA (Mc Ritchie in 1998).

Figure 4: (From left to right) Coronal drawings of the primate brain that illustrate the boundaries of the VTA defined by different authors. Left: VTA named as A10 occupied the middle line of the brainstem (Gaver et al., 1975); in the center, the VTA is subdivided into PPB and PN (Schofield et al., 1981); on the right hand side, the VTA lies intermingled with fibers of the third cranial nerve but not underneath the red nucleus, as in the previous diagrams (Felten et al., 1983).

Neither of this parcellation is comparable with the parcellation of VTA in rodents. Previous anatomical studies in rats suggested the existence of up to 8 DA nuclei (Gasbarri *et al*., 1994b). Concretely one rostral named rostral VTA (VTAR), 3 situated in the middle line (Cli, Rli, IF), 3 more lateral (PBP, PIF, PN) and one more caudal named the Rostromedial Tegmentum (RMT) or tail of the VTA (tVTA). Despite the fact that RMT in many studies is not differentiated from VTA itself

(Olson et al., 2007) some authors consider it as a nucleus apart. The tail of the VTA (tVTA) was first described in rats as bilateral clusters of GABA neurons within VTA. It extends 6 to 7 mm from the bregma (Bourdy et al., 2012) and has been described also in monkeys (Simon et al., 2011).

It receives dense projections from the Lateral Habenula (LHAB) and projects strongly to the main VTA. Particularly, these projections are GABAergic and exert an inhibitory effect on the main VTA (Matsuri et al., 2011). Further detailed studies of the projections with the LHAB showed that the most medial parts of LHAB projected to the VTA while the most lateral parts of the area projected to the tVTA (Geiser et al., 2005) suggesting that tVTA could in fact belong to the VTA. Further evidences although suggested the contrary, during particular functions such as response to aversive stimuli and/or reward omission and drug administration it has been observed an increase of the expression of c-Fos only in the RMT (tVTA) (Lavezzi et al., 2011; Perroti et al., 2005) during error prediction, and motor control responses (Jhou et al., 2009). Physiological evidences also supported the exclusion of this group. During recordings in vivo, it has been observed that firing rate of the tVTA neurons covers a large range (1-60Hz) (Jalabert et al., 2011; Lecca et al., 2011) similar to monkeys (17.8 Hz) (Hong et al., 2011) but totally different to the VTA (1-8Hz) (Grace and Bunney, 1984b).Functional studies have found that the VTA contains DA neurons with different electrophysiological profiles (Lammel et al., 2008) suggesting that VTA DA neurons could be involved in different neurocircuits (Bromberg et al., 2010); and so, many anatomical studies began to classify the VTA neurons based on their projection targets (Beckley et al., 2013; Ikemoto et al., 2007; Margolis et al., 2006 and 2008). Moreover, those projections seem to not overlap in the targets and so the ascending projections could be conceptualized as independent parallel lines (Fallon et al., 1981; Albanese et al., 1983). For example, DA neurons in the PN and medial PBP project selectively to the medial shell of the NA, mPFC and BLA while the cells from the lateral PBP project to the lateral shell (Lammel et al., 2014). Further studies demonstrated the existence of distinctive mesocortical (projections to PFC and HF), mesolimbic (projections to Amy) and mesoestriatal (Accumbens) at a single level (Bjorklund et al., 2007 Aransay et al., 2015) that are not spatially segregated within the VTA. Further genetically studies supported this idea by showing that the different DA neuron types of the VTA maybe not be anatomically segregated but rather intermingled (Poulin et al., 2014). The combination of information about the neurotransmitter content, the target structures and the axonal branching that might funnel information simultaneously to multiple structures, provide a more complex and functional relevant, the study of the connections of the VTA. Insofar as VTA have long sparsely branching dendrites (Phillipson et al., 1979) contacted by many afferent fibbers which, in general arborize relatively sparsely within the VTA even scarce projections arising to this area should elicit simultaneous activation of diverse neurons.

2.3.5. Locus Coruleus

The locus coeruleus (LC) is a densely packed cluster of NE producing cells located in the upper part of the pons near the floor of the fourth ventricle. In spite of its limited size, the LC is the largest accumulation of NE containing neurons in the mammalian brain. LC supplies NE to the entire central nervous system via extensive efferent projections grouped into two major ascending fiber systems, the dorsal noradrenergic bundle and the rostral limb of the dorsal periventricular pathway. Through these projections, LC innervates limbic regions such as the hippocampus, as well as the whole neocortex (Klimek et al., 1999). Before 1977, studies revealed that the nucleus of the nonhuman primate is similarly located to that of the rat LC and is also composed of NE-containing neurons (Battista et al 1972, Demirjian 1976, German et al 1975). While the NE system was initially proposed to be involved in learning and memory (Crow et al., 1968, 1973; Kety et al., 1970), several theories concerning the functional role of this system have been formulated more recently, proposing links to vigilance, attention, and memory processes, as well as development of higher-order functions concerning prediction errors, decision making, and unexpected uncertainty (Aston-Jones et al., 1991; Servan-Schreiber et al., 1990; Sara and Segal, 1991; Sara et al., 1994; Clayton et al., 2004). Studies in monkeys and rats have demonstrated that LC neurons are activated within behavioral contexts that require a cognitive shift, that is, an interruption of ongoing behavior and adaptation. This kind of LC activation occurs whenever there is a change in environmental imperative, such as the appearance of a novel, unexpected event, or a change in stimulus-reinforcement contingency within a formal learning situation. Within trials, LC neurons are driven by stimuli that require a rapid behavioral adjustment such as a preparatory signal or an unexpected reward (Bouret and Sara, 2005). Central NE, derived from the LC in particular, is hypothesized to play an important role in attention, arousal, and behavioral activation (Aston-Jones et al., 1991; Aston-Jones et al., 2000; Charney et al., 1990; Foote et al., 1983; Puumala et al., 1997; Siegel and Rogawski, 1988). Furthermore, up regulation of the activity of tyrosine hydroxylase (TH), the rate-limiting enzyme in the synthesis of catecholamine's, has been suggested to lead to changes in NE transmission that contribute to behavioral, cognitive, emotional, and physiological manifestations of depression and anxiety (Persson et al., 1997; Sands et al., 2000).

LC is composed mostly of medium-size neurons. Melanin granules inside the neurons of LC contribute to its blue color. The neuromelanin is formed by the polymerization of NE and is analogous to the black dopamine-based neuromelanin in the substantia nigra (Grzanna et al, 1980). In rodents four contiguous but cytological distinct sets of neurons composing the LC have been observed: the LC proper (Swanson et al, 1976), the dorsal division of LC or the A4 cell group (Dahlstrom and Fuxe 1964), the ventral division (Swanson et al, 1976) and a group of cells that are DBH reactive and extend anteriorly from the LC.

2.4 Neurotransmitters

Dopamine (DA) of the ventral tegmental area (VTA) plays critical roles into the integration of various forms of information relative to the internal state: stress, fear, aggression, thermoregulation, appetite, arousal, error detection, liking and wanting with the integration of external information; novelty, aversive or reward stimuli to learn and decide to enlist the appropriate behaviour enhancing motor or sexual responses to survive (Haber et al., 2010; Ikemoto S, 2007; Wise, 2004; Schultz et al., 1997; 2000; 2007; Krebs et al., 2011; Kalivas and Duffy, 1993; Lammel et al., 2014; Pezze and Feldon, 2004; Salamone and Correa, 2002). Lesions in the A10 DA nucleus with 6-OHDA injections resulted in permanently disturbed behaviour, manifested by hyperactivity, hipoemotivity, hipoexploration, confusion and disorganisation of orderly sequencing in rats (Galey et al., 1977; Pioli et al., 2008).

VTA signalling is thought to increase an organism probability of survival and to be pathologically altered in neurodegenerative diseases such as Alzheimer, Parkinson and Huntington, as well as in neuropsychiatric illnesses such as schizophrenia, certain affective and stress-related disorders and drug addiction (Bogerts et al., 1983; Howes et al., 2009; Jahanshahi et al 2013; Lodje et al., 2011; Nestler et al., 2001; Sara et al., 2009; Rodriguez et al., 2012).

Studies in both rats and monkeys showed that VTA not only contains DA (principals cells), which represents the 60-65% of the cells, but also a large population of non-DA cells (secondary cells) including cells producing GABA (30%) and glutamate (5%) (Gasbarri et al., 1994b; Margolis et al., 2006; Lammelle et al., 2011; Haber et al., 1995; Carr et al., 2000; Dobi et al., 2010; Chuhma *et al.,* 2004; Yamaguchi et al., 2007; Kosaka et al., 1997; Williams et al., 1998; 2007; Cho et al., 2010; Felten et al., 1983; McRitchie et al.,1998; Battista et al.,1972). The exact ratio of DA and non-DA cells varies throughout the rostro-caudal extent of the VTA. GABAergic neurons are situated dorsally to DAergic cells (Gonzalez M. et al., 2011) and significantly separated from the glutamatergic population that is mainly located in the rostro-medial portions of the VTA (Yamaguchi et al., 2007; Nair et al., 2008).

DA and is an amine that belongs to the catecholamine family. A specific marker for DAergic cells -when there are non-noradrenergic neurons- in the ventral midbrain is the tyrosine hydroxylase (TH). TH removes the carboxyl group from a molecule of L-DOPA and has no specific pattern distribution within VTA (Javoy-Agid et al., 1981). Despite that the general assumption is that the DA has an excitatory role, the effect of DA depends on the type of DA receptor to which it binds. There are at least five subtypes of dopamine receptors, D1, D2, D3, D4, and D5 grouped in two types of families The D1-like family (D1 and D5) and the D2 family (including the D2, D3 and D4 receptors). At a global level, D1-2 receptors have widespread expression throughout the brain and are associated with mesolimbic pathways (Jaber et al., 1996). Particularly, D1 and D2 receptors are found at 10-100 higher levels than the D3-5 subtypes. The distribution of D1 and D2 is complemen-

tary in several brain regions suggesting that dopamine may exert different effects by virtue of the different signal transduction mechanisms of the subtypes and their anatomic compartimentation. The majority cortical areas and hippocampus had relatively low levels of D1 and D2 immunoreactivity, although neurons expressing either subtype were detected in limbic regions (e.g., piriform, entorhinal, Subiculum, and retrosplenial cortex). In the amygdala, D1 was in the intercalated and basolateral nuclei, and D2 was in the central nucleus. Diencephalon and most hindbrain regions displayed little or no immunoreactivity (Levey *et al*., 1993). Basal ganglia areas present both receptors in the striatum, where the D2 receptor is located both pre and postsynaptic, while the D1 receptors are postsynaptic. In the midbrain, studies realized in monkeys by Haber in 1995, found high levels of hybridization for of D2 receptor in the ventral tier, calbindin-negative neurons and relatively low levels in the dorsal, calbindin-positive tier.

In addition to DA, the VTA contains other neurotransmitters such as GABA (*gamma*-Aminobutyric acid) that have been shown to have similar targets than of DA neurons (Nair-Roberts *et al*., 2008). It projects for example to the NA, PFC, VP, MD, Amy and LC (Taylor et al., 2014). Also, VTA has been shown to have glutamatergic projections to Amy, VP, NA and PFC. VTA also contain other minor neurotransmitters: Serotonin, Noradrenaline, Acetylcholine, Orexin and neuropeptides, opioids and aminoacids.

Given the heterogeneity of the VTA it is not surprising that DA neurons play different roles ranging from signalling reward to encoding aversion and novelty. Additional complexity became evident after the discovery of DA co-transmission with glutamate in the shell of the NA (Stuber et al., 2010) and with GABA in the dorsal striatum (Trisch et al., 2012) and lateral habenula (Stamakis et al., 2013).

On the other hand, the Noradrenergic system of the LC plays an important role in the regulation of executive circuits (Chandelier et al., 2014) since it has been found to be the exclusive provider of NE to the cortex (Jones et al., 1977; Waterhouse et al., 1983) (Further information see Berridge et al., 2003). Immunohistochemical studies of the distribution of terminals expressing TH or dopamine beta-hydroxylase (DBH; limiting enzyme for the synthesis of DA into NE) concluded that LC and VTA in monkeys project massively to the entire brain without any specific topographical organization (Campbell et al., 1987; Ginsberg et al., 1993; Lewis et al., 1986; Lewis et al., 1988; Lewis and Morrison, 1989; Morrison and Foote, 1986). However, these studies recognized a difference in the TH and DBH fibre density in different cortical areas (Lewis et al., 1979; Morrison et al., 1979; 1982). Prior seminal tracing and immunohistochemical studies showed that most LC projecting neurons are both DBH- and TH-positive (Lewis et al., 1987; Sharma et al., 2010) suggesting that LC-projecting neurons could release both NA and DA in cortical and subcortical structures. Recent physiological and neurochemical evidence in the rat shows that dopamine transmission in rodents can be mediated by noradrenergic projections when TH and VTA dopamine transport are blocked by delivery of siRNA directly into VTA (Smith and Greene, 2012). Similarly, stimulation of LC induced

releases of DA in medial prefrontal in the rat brain despite of the blockage of VTA (Devoto et al., 2003; 2005; 2008). There exist evidences of co-localization of TH and DBH in LC rodent that co-release DA and NA in the terminals, however, there is a discrepancy due too the absence of immunohistochemical co-localization of TH and DBH in the terminals of the cortex (Lewis et al., 1987). Those results beg to wonder by which mechanism LC projections could possibly release DA and why LC terminals in cortex do not express detectable levels of TH.

Finally, while the global pattern of VTA and LC projections is well known, there is only one study to account for the differences of the projections from VTA and LC (Aransay et al., 2015) suggesting a parallel and topographical organization of the projection within this two structures.

2.5 Limitations of the present study

As explained in section 2.2, the present thesis relied essentially on neuronal tract-tracing in macaque monkeys. Tract-tracing presents several considerable inherent difficulties. The overall procedure is made of many different steps that can each be subject to a fatal mistake or accident. For example, reaching deep brain targets such as VTA is not evident, even with MRI guidance and any misplaced injection must be repeated in a different animal. (In fact, so far there is only one published macaque tract-tracing study that targeted VTA (Haber et al., 2000). Tracers can easily spread to adjacent brain regions, in particular in ill-defined regions like VTA that is crossed by many fibres.

Tract-tracing in nonhuman primates is time-consuming and long periods of time are needed between the processing of two separate monkeys. Steps requiring anaesthesia are separated by two weeks interval and the survival period after tracer injection is minimum two weeks as well. Tracer injections require full anaesthesia, a procedure that is delicate in monkeys and that sometimes fail to be optimal, leading to cancellation of the experiment and postponing by minimum two weeks. Each tract-tracing experiment requires a full staff (surgeon, assistant, veterinarian…), fully equipped surgical suite, functional MRI equipment, and many home-made devices. Any sudden technical or staff problems (in the MRI setup, the surgery room, etc.) can also lead to postponing an experiment. The number of monkeys is highly-controlled and limited. Once the brain has been extracted, the entire histological procedure and the analysis of the material at the microscope can take up to a month of work, unlike with the smaller rat brain. Any technical problems with the perfusion or histology can dramatically alter the quality of the data.

Finally, other factors that can and did dramatically alter the pace of the work are the general hygiene issues and external political events that relate to animal research. The first half of this thesis was strongly affected by massive epidemics of tuberculosis and later with staphylococcus that basically all together “shut down” monkey research for more than a year. The second half of this

thesis was historically massively impaired by attacks from animal activists; most monkey works either temporarily stopped or was slowed down in order to care for the consequences of the attacks.

In order to cope with the two later factors, a large part of this thesis relied in the end on the examination of tract-tracing material readily available at two other neuroanatomy labs in United States of America (USA), the first in Davis (California) and next in St-Louis (Missouri). This very valuable material was collected in the frame of other studies. While it provided great data, it was also limited by the fact that some of the labelling had faded or the injection sites were not clearly visible. Finally, in addition to some injections made in VTA at the Max Planck Institute (Tuebingen, Germany), successful injections could be made in another lab at the University of Castilla La Mancha (Albacete, Spain). These injections in VTA provided the necessary retrograde confirmation of the anterograde data collected in the USA.

2.6. Bibliography

Adhikari, A., Topiwala, M. A., & Gordon, J. A. (2010). Synchronized activity between the ventral hippocampus and the medial prefrontal cortex during anxiety. Neuron, 65, 257-269.

Aggleton, JP, & Mishkin, M. (1984). Projections of the amygdala to the thalamus in the cynomolgus monkey. Journal of Comparative Neurology, 222, 56–68.

Aggleton, JP, Burton, M. J., & Passingham, R. E. (1980). Cortical and subcortical afferents to the amygdala of the rhesus monkey (Macaca mulatta). Brain Research, 190(2), 347–368.

Aggleton, JP. (1985). A description of intra-amygdaloid connections in Old World monkeys. Experimental Brain Research, 57, 390–399.

Aharonovich, E., Hasin, D. S., Brooks, A. C., Liu, X., Bisaga, A., & Nunes, E. V. (2006). Cognitive deficits predict low treatment retention in cocaine dependent patients. Drug and alcohol dependence, 81, 313-322.

Albanese, A., Minciacchi, D., (1983). Organization of the ascending projections from the ventral tegmental area: a multiple fluorescent retrograde tracer study in the rat. J. Comp. Neurol. 216, 406e420.

Amaral D. G., Scharfman H. E., Lavenex P. (2007). The dentate gyrus: fundamental neuroanatomical organization (dentate gyrus for dummies). Prog. Brain Res.

Amaral D.G. and R. Insausti (1990). The Human Nervous System, chapter Hippo-campal formation, pages 771–755.

Amaral D.G, Insausti R. (1992) Retrograde transport of D-[3H]-aspartate injected into the monkey amygdaloid complex. Exp Brain Res.;88:375–388.

Amaral D.G. (1986). Amygdalohippocampal and amygdalocortical projections in the primate brain. In *Excitatory amino acids and epilepsy* . Springer US.

Amaral D.G., & Bassett, J. L. (1989). Cholinergic innervation of the monkey amygdala: An immunohistochemical analysis with antisera to choline acetyltransferase. Journal of Comparative Neurology, 281(3), 337–361.

Amaral D.G., Price, J. L., Pitkänen, A., & Carmichael, T. (1992). Anatomical organization of the primate amygdaloid complex. In J. Aggleton (Ed.), The amygdala: Neurobiological aspects of emotion, memory, and mental dysfunction. New York: Wiley-Liss.

Amaral, D.G., and J.L. Price (1984) Amygdalo-cortical projections in the monkey (Macaca fascicularis). J. Comp. Neurol. 230.465496.

Amunts K, Schleicher A, Burgel U, Mohlberg H, Uylings H.B.M, Zilles K (1999). Broca's region revisited: cytoarchitecture and intersubject variability. J. Comp. Neurol; 412:319–341.

Aransay, A., Rodríguez-López, C., García-Amado, M., Clascá, F., & Prensa, L. (2015). Long-range projection neurons of the mouse ventral tegmental area: a single-cell axon tracing analysis. *Frontiers in Neuroanatomy*, *9*, 59.

Aston-Jones G, Chiang C, Alexinsky T (1991). Discharge of noradrenergic locus coeruleus neurons in behaving rats and monkeys suggests a role in vigilance. Prog Brain Res; 88:501–520.

Aston-Jones G, Rajkowski J, Cohen J (2000). Locus coeruleus and regulation of behavioral flexibility and attention. Prog Brain Res; 126:165–182.

Bakst I. and D.G. Amaral (1984). The distribution of acetylcholinestirase in the hippocampal formation of the monkey. The Journal Comparative of Neurology, 225:344–371.

Barbas H, Blatt G.J. (1995) Topographically specific hippocampal projections target functionally distinct prefrontal areas in the rhesus monkey Hippocampus, 5, pp. 511–533

Barbas H, Pandya DN (1989). Architecture and intrinsic connections of the prefrontal cortex in the rhesus monkey. J Comp Neurol; 286:353–375

Barbas, H. (2015). General cortical and special prefrontal connections: principles from structure to function. Annual review of neuroscience, Dopamine Efflux in the Rat Nucleus Accumbens. *European Journal of Neuroscience*, *9*, 902-911.

Battista A, Fuxe K, Goldstein M, Ogawa M (1972). Mapping of central monoamine neurons in the monkey. Experientia. Jun 15;28688-90.

Beckstead RM (1979): An autoradiographic examination of corticocortical and subcortical projections of the mediodorsal-projection (prefrontal) cortex in the rat. *J Comp Neurol* 184:43–62

Beckley, J.T., Evins, C.E., Fedarovich, H., Gilstrap, M.J., Woodward, J.J., (2013). Medial prefrontal cortex inversely regulates toluene-induced changes in markers of synaptic plasticity of mesolimbic dopamine neurons. J. Neurosci. 33, 804e813.

Beninger, R.J. (1983). The role of dopamine in locomotor activity and learning. Brain Res. Rev. 6, 173–196.

Berridge, C. W., & Waterhouse, B. D. (2003). The locus coeruleus–noradrenergic system: modulation of behavioral state and state-dependent cognitive processes. *Brain Research Reviews*, *42*(1), 33-84.

Berridge, C.W.; Stratford, T.L.; Foote, S.L.; Kelley, A.E (1997) Distribution of dopamine beta hydroxylase-like immunoreactive fibers within the shell subregion of the nucleus accumbens. Synapse, 27, 230-241.

Berridge, K. C., & Robinson, T. E. (1998). What is the role of dopamine in reward: hedonic impact, reward learning, or incentive salience?. *Brain Research Reviews*, *28*, 309-369.

Bienvenu, T. C., Busti, D., Micklem, B. R., Mansouri, M., Magill, P. J., Ferraguti, F., & Capogna, M. (2015). Large intercalated neurons of amygdala relay noxious sensory information. *The Journal of Neuroscience*, *35*(5), 2044-2057.

Blaha, C. D., Yang, C. R., Floresco, S. B., Barr, A. M., & Phillips, A. G. (1997). Stimulation of the Ventral Subiculum of the Hippocampus Evokes Glutamate Receptor-mediated Changes in

Bogerts B, Häntsch J, Herzer M (1983). A morphometric study of the dopamine-containing cell groups in the mesencephalon of normals, Parkinson patients, and schizophrenics. Biol Psychiatry. Sep;18:951-69.

Bonda E (2000). Organization of connections of the basal and accessory basal nuclei in the monkey amygdala. Eur J Neurosci. Jun;12:1971-92.

Bourdy R, Barrot M. (2012). A new control center for dopaminergic systems: pulling the VTA by the tail. Trends Neurosci. Nov;35:681-90.

Bouret S, Sara S (2005). Network reset: Simplified overarching theory od locus coeruleus noradreline function. Trends Neurosci; 28:574–582.
Bouret, S, & Sara, S. J. (2004). Reward expectation, orientation of attention and locus coeruleus medial frontal cortex interplay during learning. European Journal of Neuroscience, 20, 791-802.
Braak H (1972): Zur Pigmentarchitektonic der Grosshirnrinde des Menschen. I. Regio entorhinalis, Z Zellforsch Mikrosk Anat 127:407–438.
Braak H (1980): Architectonics of the Human Telencephalic Cortex, New York, Springer-Verlag.
Briand LA, Blendy JA (2009).Molecular and genetic substrates linking stress and addiction. Published online 2009 NovBrain Res. 2010 Feb 16;1314:219-34
Brischoux, F., Chakraborty, S., Brierley, D. I., & Ungless, M. A. (2009). Phasic excitation of dopamine neurons in ventral VTA by noxious stimuli. Proceedings of the National Academy of Sciences, 106, 4894-4899.
Brodmann K (1908). Beitraege zur histologischen Lokalisation der Grosshirnrinde. VI. Mitteilung: Die Cortexgliederung des Menschen. J. Psychol. Neurol. (Lzp);10:231–246T.
Brodmann K. Barth; Leipzig: (1909). Vergleichende localisationslehre der grosshirnrinde in ihren prinzipien dargestellt auf grund des zellenbaues.
Brog J, Salyapongse A, Deutch A, Zahm D (1993) the patterns of afferent innervation of the core and shell in the "accumbens" part of the rat ventral striatum: immunohistochemical detection of retrogradely transported fluoro-gold. J Comp Neurol 338:255–278
Bromberg-Martin, E.S., Matsumoto, M., Hikosaka, O., (2010). Dopamine in motivational control: rewarding, aversive, and alerting. Neuron 68, 815e834.
Brown, R. M., Crane, A. M., & Goldman, P. S. (1979). Regional distribution of monoamines in the cerebral cortex and subcortical structures of the rhesus monkey: concentrations and in vivo synthesis rates. *Brain research*, *168*, 133-150.
Campbell MJ, Lewis DA, Foote SL, Morrison JH (1987): The distribution of choline acetyltransferase-,serotonin-, dopamine-/~-hydroxylase-, and tyrosine hydroxylase-immunoreactive fibers in monkey primary auditory cortex. J. Comp. Neurol., 261, 209-220.
Carlsen, J., Za´borszky, L., Heimer, L., (1985). Cholinergic projections from the basal forebrain to the basolateral amygdaloid complex: a combined retrograde fluorescent and immunohistochemical study. J. Comp. Neurol. 234, 155–167.
Carmichael ST, Price JL (1994). Architectonic subdivision of the orbital and medial prefrontal cortex in the macaque monkey. J Comp Neurol.346:366–402.
Carmichael ST, Price JL (1995) Limbic connections of the orbital and medial prefrontal cortex in macaque monkeys. J Comp Neurol.;363:615–641.
Carr DB, Sesack SR (2000). GABA-containing neurons in the rat ventral tegmental area project to the prefrontal cortex. Synapse. Nov; 38:114-23.
Cenquizca, L. A., & Swanson, L. W. (2007). Spatial organization of direct hippocampal field CA1 axonal projections to the rest of the cerebral cortex. Brain research reviews, 56, 1-26.
Charney DS, Woods SW, Nagy LM, Southwick SM, Krystal JH, Heninger GR (1990). Noradrenergic function in panic disorder. J Clin Psychiatry. 1990;51(Suppl A):5–11.
Cho YT, Fudge JL (2010). Heterogeneous dopamine populations project to specific subregions of the primate amygdala. Neuroscience.Feb 17;165:1501-18.
Christie, M. J., Summers, R. J., Stephenson, J. A., Cook, C. J., & Beart, P. M. (1987). Excitatory amino acid projections to the nucleus accumbens septi in the rat: A retrograde transport study utilizingd [3 H] aspartate and [3 H] GABA. Neuroscience, 22, 425-439.
Chuhma N, Zhang H, Masson J, Zhuang X, Sulzer D, Hen R, Rayport S (2004). Dopamine neurons mediate a fast excitatory signal via their glutamatergic synapses. J Neurosci.Jan 28;24:972-81.
Clayton EC, Rajkowski J, Cohen JD, Aston-Jones G (2004). Phasic activation of monkey locus coeruleus neurons by simple decisions in a forced-choice task. J Neurosci. 2004;24:9914–9920.
Conrad, L.C., Pfaff, D.W., (1976). Efferents from medial basal forebrain and hypothalamus in the rat. I. An autoradiographic study of the medial preoptic area. J. Comp. Neurol. 169 (2), 185–219.
Crow TJ. (1968)Cortical synapses and reinforcement: a hypothesis. Nature. 1968;219:736–737.
Crow TJ (1973)The coeruleo–cortical norepinehrine system and learning. In: Usdin E, Snyder S, editors. Frontiers in Catecholamine Research. Pergamon Press; Oxford UK: 1973. pp. 723–726.
Dahlstrom A, Fuxe K (1964). Evidence for the existence of monoamine-containing neurons in the central nervous system. I. Demonstration of monoamine in the cell bodies of brain stem neurons. Acta Physiol Scand; 62(suppl 232):1–55.
Demirjian, C., R. Grossman, R. Meyer, and R. Katzman (1976) the catecholamine pontine cellular groups locus coeruleus, A4, and subcoeruleus in the primate Cebus apella. Brain Res. 115:395-411.
Derdikman D, Moser EI (2014) Spatial maps in the entorhinal cortex and adjacent structures. In: Derdikman D, Knierim JJ (eds) Space, time and memory in the hippocampal formation. Springer, Heidelberg
Deshmukh SS (2014) Spatial and nonspatial representations in the lateral entorhinal cortex. In: Derdikman D, Knierim JJ (eds) Space, time and memory in the hippocampal formation. Springer, Heidelberg.
Devoto P et al. (2008) 6-Hydroxydopamine lesion in the ventral tegmental area fails to reduce extracellular dopamine in the cerebral cortex. Journal of Neuroscience Research Volume 86, Issue 7, pages 1647–1658.
Devoto P, Flore G, Saba P, Fa M, Gessa GL (2005). Stimulation of the locus coeruleus elicits noradrenaline and dopamine release in the medial prefrontal and parietal cortex. J Neurochem 92: 368.
Devoto P, Flore G, Vacca G, Pira L, Arca A, Casu MA et al (2003). Co-release of noradrenaline and dopamine from noradrenergic neurons in the cerebral cortex induced by clozapine, the prototype atypical antipsychotic. Psychopharmacology 167: 79–84.

Dobi A, Margolis EB, Wang HL, Harvey BK, Morales M (2010). Glutamatergic and nonglutamatergic neurons of the ventral tegmental area establish local synaptic contacts with dopaminergic and nondopaminergic neurons. J Neurosci Jan 6;30:218-29.
Fallon, J.H., (1981). Collateralization of monoamine neurons: mesotelencephalic dopamine projections to caudate, septum, and frontal cortex. J. Neurosci. 1, 1361e1368.
Felten DL, Sladek JR Jr (1983). Monoamine distribution in primate brainV. Monoaminergic nuclei: anatomy, pathways and local organization. Brain Res Bull.Feb;10:171-284.
Foote SL, Bloom FE, Aston-Jones G (1983). Nucleus locus coeruleus: new evidence of anatomical and physiological specificity. Physiol Rev. 1983;63:844–914.
Fornai, F.; Bassi, L.; Torracca, M.T.; Alessandrì, M.G.; Scalori, V.; Corsini, G.U. (1996) Region- and neurotransmitter-dependent species and strain differences in DSP-4-induced monoamine depletion in rodents. Neurodegeneration, 5, 241-249.
Fornai, F.; Torracca, M.T.; Bassi, L.; D'Errigo, D.A.; Scalori, V.; Corsini, G.U. (1996) Norepinephrine loss selectively enhances chronic nigrostriatal dopamine depletion in mice and rats. Brain Res., 735, 349-353.
Frankle, W. G., Laruelle, M., & Haber, S. N. (2006). Prefrontal cortical projections to the midbrain in primates: evidence for a sparse connection. *Neuropsychopharmacology*, *31*, 1627-1636.
Freese, J.L. and Amaral, D.G. (2009) Neuroanatomy of the primate amygdala. In The Human Amygdala (Whalen, P.J. and Phelps, E.A., eds), pp. 3–42, Guildford Press
Fudge JL, Kunishio K, Walsh P, Richard C, Haber SN (2002). Amygdaloid projections to ventromedial striatal subterritories in the primate. Neuroscience;110:257-75.
Fulceri, F.; Biagioni, F.; Lenzi, P.; Falleni, A.; Gesi, M.; Ruggieri, S.; Fornai, F (2206). Nigrostriatal damage with 6-OHDA: validation of routinely applied procedures. Ann. N.Y. Acad. Sci., , 1074, 344-348
Fuller, T.A., Russchen, F.T., Price, J.L., (1987). Sources of presumptive glutamergic/ aspartergic afferents to the rat ventral striatopallidal region. J. Comp. Neurol. 258 (3), 317–338.
Funahashi S (1983). Responses of monkey prefrontal neurons during a visual tracking task reinforced by substantia innominata self-stimulation. Brain Res. 276, 267–276.
Galey D, Simon H, Le Moal M (1977). Behavioral effects of lesions in the A10 dopaminergic area of the rat. Brain Res. Mar 18;124:83-97.
Garver DL, Sladek JR Jr (1975). Monoamine distribution in primate brain. I Catecholamine-containing perikarya in the brain stem of Macaca speciosa. J Comp Neurol. 1975 Feb 1;159:289-304.
Gasbarri A, Verney C, Innocenzi R, Campana E, Pacitti C (1994). Mesolimbic dopaminergic neurons innervating the hippocampal formation in the rat: a combined retrograde tracing and immunohistochemical study. Brain Res 668:71-9.
Gaykema RP, Van Weeghel R, Hersh LB, Luiten PG. (1991). Prefrontal cortical projections to the cholinergic neurons in the basal forebrain. J Comp Neurol. 303:563-583.
Geisler S, Zahm DS (2005). Afferents of the ventral tegmental area in the rat-anatomical substratum for integrative functions. J Comp Neurol. Sep 26;490:270-94.
German, D.C., and D.M. Bowden (1975) Locus ceruleus in rhesus monkey (Macaca mulatta): A combined histochemical fluroescence, Nissl and silver study. J. Comp. Neurol. 161:19-30.
Ginsberg SD, Hof PR, Young WG, Morrison JH (1993): Noradrenergic innervation of the hypothalamus of rhesus monkeys: Distribution of dopamine-fl-hydroxylase-immunoreactive fibers and quantitative analysis of varicosities in the paraventricular nucleus. J. Comp. Neurol., 327, 597-611.
Gloor, P. (1997). The amygdaloid system. In P. Gloor (Ed.), The temporal lobe and limbic system (pp. 591–721). New York: Oxford University Press.
Gonzalez C, Bolam JP, Mena-Segovia J (2011) Topographical organization of the pedunculopontine nucleus. Frontiers in Neuroanatomy 5.
Grace, A. A., & Bunney, B. S. (1984). The control of firing pattern in nigral dopamine neurons: burst firing. *The Journal of neuroscience*, *4*, 2877-2890.
Groenewegen HJ, Der Zee EV-V, Te Kortschot A, Witter MP (1987) Organization of the projections from the subiculum to the ventral striatum in the rat. A study using anterograde transport of Phaseolus vulgaris leucoagglutinin. Neuroscience 23:103–120
Groenewegen H. J., Berendse H. W., Wolters J. G., Lohman A. H. (1990). The anatomical relationship of the prefrontal cortex with the striatopallidal system, the thalamus and the amygdala: evidence for a parallel organization. Prog. Brain Res. 85, 95–116 discussion: 116–118.
Groenewegen, H. J., Berendse, H. W., & Haber, S. N. (1993). Organization of the output of the ventral striatopallidal system in the rat: ventral pallidal efferents. *Neuroscience*, *57*(1), 113-142.
Groenewegen, H. J., Wright, C. I., Beijer, A. V., & Voorn, P. (1999). Convergence and segregation of ventral striatal inputs and outputs. *Annals of the New York academy of sciences*, *877*, 49-63.
Grzanna R, Molliver ME (1980). The locus coeruleus in the rat: an immunohistochemical delineation. Neuroscience. 1980;5:21–40.
Haber SN, Fudge JL, McFarland NR (2000). Striatonigrostriatal pathways in primates form an ascending spiral from the shell to the dorsolateral striatum. J Neurosci. Mar 15;20:2369-82.
Haber SN, Kunishio K, Mizobuchi M, Lynd-Balta E (1995). The orbital and medial prefrontal circuit through the primate basal ganglia. J Neurosci.Jul;15:4851-67.
Haber SN, Lynd E, Klein C, Groenewegen HJ (1999). Topographic organization of the ventral striatal efferent projections in the rhesus monkey: an anterograde tracing study. J Comp Neurol. Mar8; 293:282-98.
Haber, S. N., & Knutson, B. (2010). The reward circuit: linking primate anatomy and human imaging. *Neuropsychopharmacology*, *35*(1), 4-26.

Haber, S. N., Lynd, E., Klein, C., & Groenewegen, H. J. (1990). Topographic organization of the ventral striatal efferent projections in the rhesus monkey: an anterograde tracing study. Journal of Comparative Neurology, 293, 282-298.
Haber, S.N., Groenewegen, H.J., Grove, E.A., Nauta, W.J., (1985). Efferent connections of the ventral pallidum: evidence of a dual striato pallidofugal pathway. J. Comp. Neurol. 235 (3), 322–335.
Hedreen, J. C., & Delong, M. R. (1991). Organization of striatopallidal, striatonigral, and nigrostriatal projections in the macaque. Journal of Comparative Neurology, 304, 569-595.
Heidbreder, C. A., & Groenewegen, H. J. (2003). The medial prefrontal cortex in the rat: evidence for a dorso-ventral distinction based upon functional and anatomical characteristics. *Neuroscience & Biobehavioral Reviews*, *27*, 555-579.
Hok, V., Save, E., Lenck-Santini, P. P., & Poucet, B. (2005). Coding for spatial goals in the prelimbic/infralimbic area of the rat frontal cortex. Proceedings of the National Academy of Sciences of the United States of America, 102, 4602-4607.
Hong S, Jhou TC, Smith M, Saleem KS, Hikosaka O (2011) Negative reward signals from the lateral habenula to dopamine neurons are mediated by rostromedial tegmental nucleus in primates. J Neurosci 31:11457–11471.
Horvitz, J.C. (2000). Mesolimbocortical and nigrostriatal dopamine responses to salient non-reward events. Neuroscience 96, 651–655.
Horvitz, J.C., Choi, W.Y., Morvan, C., Eyny, Y. and Balsam, P.D. (2007). A "good parent" function of dopamine: transient modulation of learning and performance during early stages of training. Ann. NY Acad. Sci. 1104, 270–288.
Howes OD, Egerton A, Allan V, McGuire P, Stokes P, Kapur S (2009). Mechanisms underlying psychosis and antipsychotic treatment response in schizophrenia: insights from PET and SPECT imaging. Curr Pharm Des 15:2550-9.
Hsu, D. T., & Price, J. L. (2007). Midline and intralaminar thalamic connections with the orbital and medial prefrontal networks in macaque monkeys. Journal of Comparative Neurology, 504, 89-111.
Hubbard JE, Di Carlo V (1974). Fluorescence histochemistry of monoamine-containing cell bodies in the brain stem of the squirrel monkey (Saimiri sciureus). II.Catecholamine-containing groups. J Comp Neurol. Feb 15;153:369-84.
Hyman, S. E., Malenka, R. C., & Nestler, E. J. (2006). Neural mechanisms of addiction: the role of reward-related learning and memory. *Annu. Rev. Neurosci.*, *29*, 565-598.
Ikemoto S (2007). Dopamine reward circuitry: two projection systems from the ventral midbrain to the nucleus accumbens-olfactory tubercle complex. Brain Res Rev. Nov; 56:27-78. Review.
Ilango, A., Shumake, J., Wetzel, W., & Ohl, F. W. (2014). Contribution of emotional and motivational neurocircuitry to cue-signaled active avoidance learning. Frontiers in behavioral neuroscience, 8.
Insausti R, Amaral D.G, and Cowan W.M (1987b). The entorhinal cortex of the monkey. II. Cortical afferents. The Journal of Comparative Neurology, 264:356–395.
Insausti R, Munoz M (2001): Cortical projections of the non-entorhinal hippocampal formation in the cynomolgus monkey (Macaca fascicularis), Eur J Neurosci 14:435–451.
Jaber M., Robinson S.W., Missale C., Caron M.G (1996). Dopamine receptors & brain function. Neuropharmacology.;35:1503–1519.
Jahanshahi M. (2013). Contributions of the basal ganglia to temporal processing: evidence from Parkinson's disease. Timing Time Percept. 1 1–41.
Jalabert M, Bourdy R, Courtin J, Veinante P, Manzoni OJ, Barrot M, Georges F (2011). Neuronal circuits underlying acute morphine action on dopamine neurons. Proc Natl Acad Sci U S A. Sep 27;108:16446-50.
Jankowski MP, Sesack SR. (2004). Prefrontal cortical projections to the rat dorsal raphe nucleus: Ultrastructural features and associations with serotonin and gamma-aminobutyric acid neurons. J Comp Neurol. 468:518-529.
Javoy-Agid F, Ploska A, Agid Y (1981). Microtopography of tyrosine hydroxylase, glutamic acid decarboxylase, and choline acetyltransferase in the substantia nigra and ventral tegmental area of control and Parkinsonian brains. J Neurochem. Nov; 37:1218-27.
Jay, T. M., Glowinski, J., & Thierry, A. M. (1995). Inhibition of hippocampo-prefrontal cortex excitatory responses by the mesocortical DA system. Neuroreport, 6, 1845-1848.
Jay, T. M., Thierry, A. M., Wiklund, L., & Glowinski, J. (1992). Excitatory Amino Acid Pathway from the Hippocampus to the Prefrontal Cortex. Contribution of AMPA Receptors in Hippocampo-prefrontal Cortex Transmission. European journal of neuroscience, 4, 1285-1295.
Jay, T.M & Witter, M.P (1991) Distribution of hippocampal CA1 and subicular efferents in the prefrontal cortex of the rat studied by means of anterograde transport of phaseolus vulgaris-leucoagglutinin. J. Comp. Neurol., 313, 547-586.
Jhou TC, Fields HL, Baxter MG, Saper CB, Holland PC (2009). The rostromedial tegmental nucleus (RMTg), a GABAergic afferent to midbrain dopamine neurons, encodes aversive stimuli and inhibits motor responses. Neuron. Mar 12;61:786-800.
Jimenez-Castellanos, J. (1949). The amygdaloid complex in monkey studies by reconstructional methods. Journal of Comparative Neurology, 91(3), 507–526.
Johnston, J. B. (1923). Further contributions to the study of the evolution of the forebrain. Journal of Comparative Neurology, 35, 337–481.
Jones, B. E., & Moore, R. Y. (1977). Ascending projections of the locus coeruleus in the rat. II. Autoradiographic study. *Brain research*, *127*, 23-53.
Jones, E. G., & Burton, H. (1976). A projection from the medial pulvinar to the amygdala in primates. Brain Research, 104, 142–147.
Jones, J. L., Day, J. J., Wheeler, R. A., & Carelli, R. M. (2010). The basolateral amygdala differentially regulates conditioned neural responses within the nucleus accumbens core and shell. *Neuroscience*, *169*, 1186-1198.
Kalivas P. W & Duffy, P. (1993) Neurotransmitter regulation of dopamine neurons in the ventral tegmental area. Brain Res Brain Res Rev. Jan-Apr;18:75-113.
Kalivas PW, Nakamura M (1999). Neural systems for behavioral activation and reward. Curr Opin Neurobiol;9:223–7.
Kalivas, P. W. & Duffy, P. (1995). Selective activation of dopamine transmission in the shell of the nucleus accumbens by stress. Brain research, 675, 325-328.

Kelley A, Domesick V (1982) The distribution of the projection from the hippocampal formation to the nucleus accumbens in the rat: an anterograde and retrograde-horseradish peroxidase study. Neuroscience 7:2321–2335
Klimek V, Rajkowska G, Luker SN, Dilley G, Meltzer HY, Overholser JC, Stockmeier CA, Ordway GA. (1999) Brain noradrenergic receptors in major depression and schizophrenia. Neuropsychopharmacology.;21:69–81.
Koob, G. F., & Volkow, N. D. (2010). Neurocircuitry of addiction. *Neuropsychopharmacology*, *35*, 217-238.
Kosaka T, Kosaka K, Hataguchi Y, Nagatsu I, Wu JY, Ottersen OP, Storm-Mathisen J, Hama K. (1987). Catecholaminergic neurons containing GABA-like and/or glutamic acid decarboxylase-like immunoreactivities in various brain regions of the rat. Exp Brain Res 66:191–210.
Krebs RM, Heipertz D, Schuetze H, Duzel E (2011). Novelty increases the mesolimbic functional connectivity of the substantia nigra/ventral tegmental area (SN/VTA) during reward anticipation: Evidence from high-resolution fMRI. Neuroimage. Sep 15;58:647-55.
Lammel S, Ion DI, Roeper J, Malenka RC (2011). Projection-specific modulation of dopamine neuron synapses by aversive and rewarding stimuli. Neuron. Jun 9;70:855-62. doi: 10.1016/j.neuron.2011.03.025.
Lammel S, Lim BK, Malenka RC (2014) Reward and aversion in a heterogeneous midbrain dopamine system. Neuropharmacology 76 Pt B:351–359.
Lammel, S., Hetzel, A., Hackel, O., Jones, I., Liss, B., Roeper, J., (2008). Unique properties of mesoprefrontal neurons within a dual mesocorticolimbic dopamine system. Neuron 57, 760e773.
Lavezzi HN, Zahm DS (2011). The mesopontine rostromedial tegmental nucleus: an integrative modulator of the reward system. Basal Ganglia. Nov;1(4):191-200.
Lecca S, Melis M, Luchicchi A, Ennas MG, Castelli MP, Muntoni AL, Pistis M (2011) Effects of drugs of abuse on putative rostromedial tegmental neurons, inhibitory afferents to midbrain dopamine cells. Neuropsychopharmacology 36:589 –602.
Legault, M., & Wise, R. A. (2001). Novelty-evoked elevations of nucleus accumbens dopamine: dependence on impulse flow from the ventral subiculum and glutamatergic neurotransmission in the ventral tegmental area. European Journal of Neuroscience, 13, 819-828.
Levey AI, Hersch SM, Rye DB, Sunahara RK, Niznik HB, Kitt CA, Price DL, Maggio R, Brann MR, Ciliax BJ (1993). Localization of D1 and D2 dopamine receptors in brain with subtype-specific antibodies. Proc Natl Acad Sci U S A. Oct 1;90:8861-5.
Lewis DA, Campbell MJ, Foote SL, Morrison JH (1986): The monoaminergic innervation of primate neocortex. Hum. Neurobiol., 5, 181-188.
Lewis DA, Foote SL, Goldstein M, Morrison JH (1988). The dopaminergic innervation of monkey prefrontal cortex: a tyrosine hydroxylase immunohistochemical study. Brain Res. May 24;449 225-43.
Lewis DA, Morrison JH (1989) Noradrenergic innervation of monkey prefrontal cortex: a dopamine-beta-hydroxylase immunohistochemical study. J Comp Neurol. 15;282(3):317-30
Lewis MS, Molliver ME, Morrison JH, Lidow HGW (1979) Complementarity of dopaminergic and noradrenergic innervation in anterior cingulate cortex of the rat. Brain Res 164:328–333.
Lewis, E.J., Harrington, C.A., and Chikaraishi, D.M. (1987). Transcrip-tional regulation of the tyrosine hydroxylase gene by glucocorticoid and cyclic AMP. Proc. Natl. Acad. Sci. USA84, 3550–3554
Lisman, J. E., & Grace, A. A. (2005). The hippocampal-VTA loop: controlling the entry of information into long-term memory. Neuron, 46, 703-713.
Lodge, D. J., & Grace, A. A. (2006). The hippocampus modulates dopamine neuron responsivity by regulating the intensity of phasic neuron activation. *Neuropsychopharmacology*, *31*, 1356-1361.
Lorente de No. (1933) Studies on the structure of the cerebral cortex. I. The area entorhinalis. J Psychol Neurol 45:381-438.
Manns, I.D., Mainville, L., Jones, B.E (2001). Evidence for glutamate, in addition to acetylcholine and GABA, neurotransmitter synthesis in basal forebrain neurons projecting to the entorhinal cortex. Neuroscience 107 (2), 249–263.
Margolis, E.B., Lock, H., Hjelmstad, G.O., Fields, H.L., (2006). The ventral tegmental area revisited: is there an electrophysiological marker for dopaminergic neurons? J. Physiol. 577, 907e924.
Margolis, E.B., Mitchell, J.M., Ishikawa, J., Hjelmstad, G.O., Fields, H.L., (2008). Midbrain dopamine neurons: projection target determines action potential duration and dopamine D(2) receptor inhibition. J. Neurosci. 28, 8908e8913.
Martin RF, Bowden DM (1996). A stereotaxic template atlas of the macaque brain for digital imaging and quantitative neuroanatomy. Neuroimage. Oct;4:119-50
Mascagni, F., McDonald, A.J., (2009). Parvalbumin-immunoreactive neurons and GABAergic neurons of the basal forebrain project to the rat basolateral amygdala. Neuroscience 160 (4), 805–812.
Maslowski-Cobuzzi, R.J., Napier, T.C., (1994). Activation of dopaminergic neurons modulates ventral pallidal response evoked by amygdala stimulation. Neuroscience 62, 103–1120.
McGeorge AJ, Faull RL (1989) The organization of the projection from the cerebral cortex to the striatum in the rat. Neuroscience 29:503–537.
McRitchie DA, Cartwright H, Pond SM, van der Schyf CJ, Castagnoli N Jr, van der Nest DG, Halliday GM (1998). The midbrain dopaminergic cell groups in the baboon Papio ursinus. Brain Res Bull. Dec;47:611-23.
Mehler, W. R. (1980). Subcortical afferent connections of the amygdala in the monkey. Journal of Comparative Neurology, 190, 733–762.
Mitchell. A (2015) the mediodorsal thalamus as a higher order thalamic relay nucleus important for learning and decision-making Neuroscience & Biobehavioral Reviews Volume 54, July 2015, Pages 76–88
Mitrovic, I., Napier, T.C., (1998). Substance P attenuates and DAMGO potentiates amygdala glutamatergic neurotransmission within the ventral pallidum. Brain Res. 792 (2), 193–206.
Miyashita, T. et al. (2007) Differential modes of termination of amygdalothalamic and amygdalocortical projections in the monkey. J. Comp. Neurol. 502, 309–324.

Morrison JH, Foote SL (1986): Noradrenergic and serotonergic innervation of cortical and thalamic visual structures in old and new world monkeys. J. Comp. Neurol., 243, 117-138.
Morrison JH, Foote SL, O'Connor D, Bloom FE (1982): Laminar, tangential, and regional organization of the noradrenergic innervation of monkey cortex: Dopamine-/~-hydroxylase immunohistochemistry. Brain Res. Bull., 9, 309-319.
Morrison, J. U., Molliver, M. E. & Grzanna, R. (1979) Noradrenergic innervation of cerebral cortex: Widespread effects of local cortical lesions. Science 205, 313-6.
Mufson, E. J., & Pandya, D. N. (1984). Some observations on the course and composition of the cingulum bundle in the rhesus monkey. *Journal of Comparative Neurology*, *225*, 31-43.
Muñoz M, Insausti R. (2005). Cortical efferents of the entorhinal cortex and the adjacent parahippocampal region in the monkey (Macaca fascicularis) . Eur J Neurosci 22 : 1368 – 88 .
Nagy, J.I., Carter, D.A., McLehmann, J. and Fibiger, H.C. (1978): Evidence for a GABA-containing projectionfrom the entopeduncular nucleus to the lateral habenula in the rat, Brain Res., 145 360-364.
Nair-Roberts RG, Chatelain-Badie SD, Benson E, White-Cooper H, Bolam JP, Ungless MA (2008). Stereological estimates of dopaminergic, GABAergic and glutamatergic neurons in the ventral tegmental area, substantia nigra and retrorubral field in the rat. Neuroscience. Apr 9;152:1024-31.
Nauta, W.J.H. (1958): Hippocampal projection and related neural pathways to the midbrain of the cat, Brain, 81. 319-340.
Nauta, W.J.H. and Mehler, W.R. (1966): Projections of the lentiform nucleus in the monkey, Brain Res., 1 3-42.
Nestler EJ (2001). Molecular basis of long-term plasticity underlying addiction. Nat Rev Neurosci. Feb;2:119-28.
Oades RD, Halliday GM (1987). Ventral tegmental (A10) system: neurobiology. 1. Anatomy and connectivity. Brain Res. May; 434:117-65. Review.
O'Doherty, J., Kringelbach, M. L., Rolls, E. T., Hornak, J., & Andrews, C. (2001). Abstract reward and punishment representations in the human orbitofrontal cortex. *Nature neuroscience*, *4*, 95-102
Olson VG, Nestler EJ (2007). Topographical organization of GABAergic neurons within the ventral tegmental area of the rat. Synapse. Feb;61:87-95.
O'Mara, S. (2005). The subiculum: what it does, what it might do, and what neuroanatomy has yet to tell us. *Journal of anatomy*, *207*, 271-282.
Öngür, D., & Price, J. L. (2000). The organization of networks within the orbital and medial prefrontal cortex of rats, monkeys and humans. *Cerebral cortex*, *10*, 206-219.
Paré, D., Quirk, G. J., & LeDoux, J. E. (2004). New vistas on amygdala networks in conditioned fear. Journal of Neurophysiology, 92(1), 1–9.
Persson ML, Wasserman D, Geijer T, Jonsson EG, Terenius L (1997). Tyrosine hydroxylase allelic distribution in suicide attempters. Psychiatry Res. 1997;72:73–80.
Petrides M, Pandya D.N (1994). Comparative architectonic analysis of the human and the macaque frontal cortex. In: Boller F, Grafman J, editors. Handbook of neuropsychology. vol. 9. Elsevier; Amsterdam. pp. 17–58.
Petrides M, Pandya D.N (1999). Dorsolateral prefrontal cortex: Comparative cytoarchitectonic analysis in the human and the macaque brain and corticocortical connection patterns. Eur. J. Neurosci;11:1011–1036.
Pezze MA, Feldon J (2004) Mesolimbic dopaminergic pathways in fear conditioning. Prog Neurobiol 74:301–320.
Phillipson O. T. (1979). A Golgi study of the ventral tegmental area of Tsai and interfascicular
Phillipson OT, Griffiths AC (1985) the topographic order of inputs to nucleus accumbens in the rat. Neuroscience 16:275–296
Pioli EY, Meissner W, Sohr R, Gross CE, Bezard E, Bioulac BH (2008). Differential behavioral effects of partial bilateral lesions of ventral tegmental area or substantia nigra pars compacta in rats. Neuroscience. Jun 2;153:1213-24.
Pitkänen, A., & Amaral, D. G. (1998). Organization of the intrinsic connections of the monkey amygdaloid complex: Projections originating in the lateral nucleus. Journal of Comparative Neurology, 398(3), 431–458.
Poulin, A., Gurci, A., Mestikawy, S.E., Semba, K., 2006. Vesicular glutamate transporter 3 immunoreactivity is present in cholinergic basal forebrain neurons projecting to the basolateral amygdala in rat. J. Comp. Neurol. 498, 690–711.
Poulin, J. F., Zou, J., Drouin-Ouellet, J., Kim, K. Y. A., Cicchetti, F., & Awatramani, R. B. (2014). Defining midbrain dopaminergic neuron diversity by single-cell gene expression profiling. *Cell reports*, *9*, 930-943.
Price, J. L., & Amaral, D. G. (1981). An autoradiographic study of the projections of the central nucleus of the monkey amygdala. *The journal of Neuroscience*, *1*, 1242-1259.
Price, J. L., Russchen, F. T., & Amaral, D. G. (1987). The limbic region: II. The amygdaloid complex. In A. Bjorklund, T. Hokfelt, & L. W. Swanson (Eds.), Handbook of chemical neuroanatomy: Vol. 5. Integrated systems of the CNS (Part I, pp. 279–388). Amsterdam: Elsevier Science.
Puumala T, Riekkinen P, Sr., Sirvio J (1997). Modulation of vigilance and behavioral activation by alpha-1 adrenoceptors in the rat. Pharmacol Biochem Behav. 1997;56:705–712.
Quirk, G.J. et al. (2003) Stimulation of medial prefrontal cortex decreases the responsiveness of central amygdala output neurons. J. Neurosci. 23, 8800–8807
Ray , J.P., and J.L. Price (1993) The organization of the projections from the mediodorsal nucleus of the thalamus to orbital and medial prefrontal cortex in the monkey. J. Comp. Neurol. 337:l-31.
Rodriguez Parkitna J, Engblom D (2012). Addictive drugs and plasticity of glutamatergic synapses on dopaminergic neurons: what have we learned from genetic mouse models? Front Mol Neurosci.;5:89.
Root, D. H., Melendez, R. I., Zaborszky, L., & Napier, T. C. (2015). The ventral pallidum: subregion-specific functional anatomy and roles in motivated behaviors. *Progress in neurobiology*, *130*, 29-70.
Rose, M. (1928) Die Inselrinde des Menschen und der Tiere. J. Psychol. Neurol. 37:467-624.
Rosene D. L. Van Hoesen, G. W (1978). Non-entorhinal projections to the subiculum from temporal neocortex in the rhesus monkey. Anat. Rec., 190: 570.

Rosene DL, Van Hoesen GW (1987): The hippocampal formation of the primate brain. A review of some comparative aspects of cytoarchitecture connections. In Jones EG, Peters A, editors: Cerebral Cortex, vol 6, New York, Plenum Press, pp 345–456.
Royer, S., & Paré, D. (2002). Bidirectional synaptic plasticity in intercalated amygdala neurons and the extinction of conditioned fear responses. Neuroscience, 115(2), 455–462.
Royer, S., Martina, M., & Paré, D. (1999). An inhibitory interface gates impulse traffic between the input and output stations of the amygdala. Journal of Neuroscience, 19(23), 10575–10583.
Russchen FT, Amaral DG, Price JL (1987) The afferent input to the magnocellular division of the mediodorsal thalamic nucleus in the monkey, Macaca fascicularis. Journal of Comparative Neurology, 256(2), 175–210.
Russchen FT, Bakst I, Amaral DG, Price JL (1985). The amygdalostriatal projections in the monkey. An anterograde tracing study. Brain Res. Mar 11;329:241-57.
Sabatino, M., Savatteri, V., Liberti, G., Vella, N., & La Grutta, V. (1986). Effects of substantia nigra and pallidum stimulation on hippocampal interictal activity in the cat. *Neuroscience letters*, *64*(3), 293-298.
Salamone JD, Correa M (2002) Motivational views of reinforcement: implications for understanding the behavioral functions of nucleus accumbens dopamine. Behav Brain Res 137:3–25.
Salamone, J.D. (1991). Behavioral Pharmacology of Dopamine Systems: A New Synthesis. In: The Mesolimbic Dopamine System: From Motivation to Action, P. Willner and J. Scheel-Kruger, eds.(Hoboken, NJ: John Wiley & Sons), pp. 599–613
Sands SA, Strong R, Corbitt J, Morilak DA (2000). Effects of acute restraint stress on tyrosine hydroxylase mRNA expression in locus coeruleus of Wistar and Wistar-Kyoto rats. Mol Brain Res. 2000;75:1–7.
Sara SJ (2009). The locus coeruleus and noradrenergic modulation of cognition. Nat Rev Neurosci 10:211-23.
Sara SJ, Segal M (1991). Plasticity of sensory responses of locus coeruleus neurons in the behaving rat: implications for cognition. Prog Brain Res. 1991;88:571–585.
Sara, S. J., Vankov, A., & Hervé, A. (1994). Locus coeruleus-evoked responses in behaving rats: a clue to the role of noradrenaline in memory. *Brain research bulletin*, *35*(5), 457-465.
Sarkissov S.A, Filimonoff I.N, Kononowa E.P, Preobraschenskaja I.S, Kukuew L.A. Medgiz; Moscow: (1955). Atlas of the cytoarchitectonics of the human cerebral cortex.\
Schofield SP, Everitt BJ (1981). The organisation of catecholamine-containing neurons in the brain of the rhesus monkey (Macaca mulatta). J Anat. May;132:391-418.
Schultz W (2000) Multiple reward signals in the brain. Nat Rev Neurosci 1:199–207.
Schultz W, Dayan P, Montague PR (1997). A neural substrate of prediction and reward. Science. Mar 14;275:1593-9.
Schultz, P. W., Nolan, J. M., Cialdini, R. B., Goldstein, N. J., & Griskevicius, V. (2007). The constructive, destructive, and reconstructive power of social norms. Psychological Science, 18, 429-434
Servan-Schreiber D, Printz H, Cohen JD (1990). A network model of catecholamine effects: gain, signal-to-noise ratio, and behavior. Science. 1990;249:892–895.
Sesack SR, Grace AA (2010) Cortico-Basal Ganglia reward network: microcircuitry. Neuropsychopharmacology 35:27–47.
Sesack, S. R. & Prickel. V. M (1990) Prefrontal cortical efferents in the rat synapse on unlabeled neuronal targets of catecholamine terminals in the nucleus accumbens septi and on dopamine neurons of the ventral tegmental area. Brain. Res., 506, 166-168.
Sharma N (2010), Deppmann CD, Harrington AW, St Hillaire C, Chen ZY, Lee FS, Ginty DD. Long-distance control of synapse assembly by target-derived NGF. Neuron. 2010;67:422–434.
Siegel JM, Rogawski MA (1988). A function for REM sleep: regulation of noradrenergic receptor sensitivity. Brain Res. 1988;472:213–233.
Simon N.W, K.S. Montgomery, B.S. Beas, M.R. Mitchell, C.L. LaSarge, I.A. Mendez, C. Banuelos, C.M. Vokes, A.B. Taylor, R.P. Haberman, J.L. Bizon, B. Setlow (2011) Dopaminergic modulation of risky decision-making J. Neurosci., 31 pp. 17460–17470.
Smeets WJ, González A (2000). Catecholamine systems in the brain of vertebrates: new perspectives through a comparative approach. Brain Res Brain Res Rev. Sep; 33:308-79. Review.
Smith C. C., Greene R. W. (2012). CNS dopamine transmission mediated by noradrenergic innervation. J. Neurosci. 32 6072–6080 10.1523/JNEUROSCI.6486-11.2012.
Smith, K. S., Tindell, A. J., Aldridge, J. W., & Berridge, K. C. (2009). Ventral pallidum roles in reward and motivation. Behavioural brain research, 196, 155-167.
Stefanacci, L., & Amaral, D. G. (2000). Topographic organization of cortical inputs to the lateral nucleus of the macaque monkey amygdala: a retrograde tracing study. *Journal of Comparative Neurology*, *421*(1), 52-79.
Strange, B. A., Witter, M. P., Lein, E. S., & Moser, E. I. (2014). Functional organization of the hippocampal longitudinal axis. *Nature Reviews Neuroscience*, *15*, 655-669.
Stuber, G. D., Hnasko, T. S., Britt, J. P., Edwards, R. H., & Bonci, A. (2010). Dopaminergic terminals in the nucleus accumbens but not the dorsal striatum corelease glutamate. The Journal of neuroscience, 30, 8229-8233.
Swanson L.W. (1981), A direct projection from Ammon's horn to prefrontal cortex in the rat. Brain Res. 217, 150-154.
Swanson LW (1982). The projections of the ventral tegmental area and adjacent regions: a combined fluorescent retrograde tracer and immunofluorescence study in the rat. Brain Res Bull. Jul-Dec;9:321-53**.**
Swanson, L. W., & Petrovich, G. D. (1998). What is the amygdala? Trends in neurosci ences, 21, 323-331.
Swanson, L.W. (1976) The locus coeruleus: A cytoarchitectonic Golgi and immunohistochemical study in the albino rat as studied by the Golgi method. Brain Res., 110:39-56.
Taylor, S. R., Badurek, S., Dileone, R. J., Nashmi, R., Minichiello, L., & Picciotto, M. R. (2014). GABAergic and glutamatergic efferents of the mouse ventral tegmental area. *Journal of Comparative Neurology*, *522*, 3308-3334.
Timbie, C. and Barbas, H. (2014) Specialized pathways from the primate amygdala to posterior orbitofrontal cortex. J. Neurosci. 34, 8106–8118

Totterdell S, Meredith GE (1997) Topographical organization of projections from the entorhinal cortex to the striatum of the rat. Neuroscience 78:715–729
Troiano, R., Siegel, A., (1978). Efferent connections of the basal forebrain in the cat: the substantia innominata. Exp. Neurol. 61 (1), 198–213.
Ungless, M. A., Magill, P. J., & Bolam, J. P. (2004). Uniform inhibition of dopamine neurons in the ventral tegmental area by aversive stimuli. Science, 303, 2040-2042.
Valenti, O., Lodge, D. J., & Grace, A. A. (2011). Aversive stimuli alter ventral tegmental area dopamine neuron activity via a common action in the ventral hippocampus. The Journal of Neuroscience, 31, 4280-4289.
Vogt, B.A., D.N. Pandya, and D.I. Rosene (1987) Cingulate cortex of the Rhesus monkey: I. Cytoarchitecture and thalamic afferents. J. Comp. Neurol. 262: 25 6-2 70.
Voorn P, Vanderschuren LJ, Groenewegen HJ, Robbins TW, Pennartz CM (2004) Putting a spin on the dorsal-ventral divide of the striatum. Trends Neurosci 27:468–474.
Walker, A.E. (1940) A cytoarchitectural study of the prefrontal area of the macaque monkey. J. Comp. Neurol. 73:59-86.
Waterhouse, B. D., Lin, C. S., Burne, R. A., & Woodward, D. J. (1983). The distribution of neocortical projection neurons in the locus coeruleus. *Journal of Comparative Neurology*, *217*, 418-431.
Watabe-Uchida M, Zhu L, Ogawa SK, Vamanrao A, Uchida N (2012). Whole-brain mapping of direct inputs to midbrain dopamine neurons. Neuron. Jun 7;74:858-73**.**
White, N.M. and Milner, P.M. (1992). The psychobiology of reinforcers. Annu. Rev. Psychol. 43, 443–471.
Whitsel BL, Rustioni A, Dreyer DA, Loe PR, Allen EE, Metz CB. (1978). Thalamic projections to S-I in macaque monkey. The Journal of comparative neurology 178:385-409.
Williams JT. Beckstead MJ (2007). Long-term depression of a dopamine IPSC. J Neurosci 27:2074–2080.
Williams SM, Goldman-Rakic PS (1998). Widespread origin of the primate mesofrontal dopamine system. Cereb Cortex. Jun;8:321-45.
Wise, R.A. (2004). Dopamine, learning and motivation. Nat. Rev. Neurosci. *5*, 483–494.
Wise, R.A. and Bozarth, M.A. (1987). A psychomotor stimulant theory of addiction. Psychol. Rev. *94*, 469–492
Wise, R.A., Spindler, J., deWit, H., and Gerber, G.J. (1978). Neuroleptic-induced “anhedonia” in rats: pimozide blocks reward quality of food. Science 201, 262–264.
Witter MP, Groenewegen HJ (1990) The subiculum: cytoarchitectonically a simple structure, but hodologically complex. Prog Brain Res 83:47–58
Witter MP, Ostendorf RH, Groenewegen HJ (1990) Heterogeneity in the dorsal subiculum of the rat. Distinct neuronal zones project to different cortical and subcortical targets. Eur J Neurosci 2:718–725.
Witter W.P, Van Hoesen G.W, and Amaral D.G (1989). Topographical organization of the entorhinal projection to the dentate gyrus of the monkey. The Journal of Neuroscience, 95:216–228, 1989.
Yamaguchi T, Sheen W, Morales M (2007). Glutamatergic neurons are present in the rat ventral tegmental area. Eur J Neurosci. Jan;25:106-18.
Yang, C. R., & Mogenson, G. J. (1985). An electrophysiological study of the neural projections from the hippocampus to the ventral pallidum and the subpallidal areas by way of the nucleus accumbens. *Neuroscience*, *15*(4), 1015-1024.
Yim, C.Y., Mogenson, G.J., (1983). Response of ventral pallidal neurons to amygdala stimulation and its modulation by dopamine projections to nucleus accumbens. J. Neurophysiol. 50 (1), 148–161.
Zaborszky, L. Heimer, L., (1984). Ultrastructural evidence of amygdalofugal axons terminating on cholinergic cells of the rostral forebrain. Neurosci. Lett. 52 (3), 219–225.
Zaborszky, L., Heimer, L., Eckenstein, F., Leranth, C., (1986b). GABAergic input to cholinergic forebrain neurons: an ultrastructural study using retrograde tracing of HRP and double immunolabeling. J. Comp. Neurol. 250, 282–295.
Zarborszky, L., Carlsen, J., Brashear, H.R., Heimer, L., (1986a). Cholinergic and GABAergic afferents to the olfactory bulb in the rat with special emphasis on the projection neurons in the nucleus of the horizontal limb of the diagonal band. J. Comp. Neurol. 243 (4), 488–509.

3. Set of contributions

All the projects were realized under the joint supervision of Dr. Henry Evrard by the Max Planck Institute (University of Tubingen, Germany) and Prof. Dr Ricardo Insausti by the University of Castilla-La Mancha (Spain)

Additional collaboration was stablish with Prof Joseph Price at the Washington University (St. Louis, USA) and Prof. David Amaral at the MIND institute (UC Davis, California, USA)

1. Heterogeneous prefrontal projections to the midbrain ventral tegmental area in the macaque monkey.

The following persons collaborated in this project and are listed in alphabetic order.

Hernandez Diana*: First author. Conception. Adquisition of the data. Analysis of the data. Interpretation of the results and writting the manuscript
Evrard Henry: Conception. Adquisition of the data. Interpretation of the results and writting the manuscript
Insausti Ricardo: Conception.Adquisition of the data. Interpretation of the results and writting the manuscript
Logothetis Nikos: Adquisition of the data
Price Joel: Adquisition of the data
Ubero Mar: Conception. Adquisition of the data.

2. Hippocampal formation and Amygdala projections to the ventral tegmental area in the macaque monkey

The following persons collaborated in this project listed in alphabetic order.

Hernandez Diana*: First author. Conception. Acquisition of the data. Analysis of the data Interpretation of the results and writting the manuscript
Amaral David: Acquisition of the data
Evrard Henry: Conception. Acquisition of the data. Interpretation of the results and writting the manuscript
Insausti Ricardo: Conception. Acquisition of the data. Interpretation of the results and writting the manuscript
Logothetis Nikos: Acquisition of the data
Ubero Mar: Conception. Acquisition of the data.

3. Hippocampal formation and amygdaloid projections to the Locus Coruleus in the nonhuman primate

Ubero Mar: First author. Conception. Acquisition of the data. Analysis of the data Interpretation of the results and writting the manuscript
Evrard Henry: Conception. Acquisition of the data. Interpretation of the results and writting the manuscript
Hernandez Diana: Conception. Acquisition of the data.
Insausti Ricardo: Conception. Acquisition of the data. Interpretation of the results and writting the manuscript
Logothetis Nikos: Acquisition of the data
Price Joel: Acquisition of the data

4. Heterogeneus cortical afferents to the Locus Coruleus in the Macaca *fascicularis* monkey

The following persons collaborated in this project listed in alphabetic order.

Ubero Mar: First author. Conception. Acquisition of the data. Analysis of the data Interpretation of the results and writting the manuscript
Amaral David: Acquisition of the data
Evrard Henry: Conception. Acquisition of the data. Interpretation of the results and writting the manuscript
Hernandez Diana: Conception. Acquisition of the data.
Insausti Ricardo: Conception. Acquisition of the data. Interpretation of the results and writting the manuscript
Logothetis Nikos: Acquisition of the data

4. Results

4.1 Heterogeneus prefrontal projections to the midbrain ventral tegmental area in the macaque monkey

ABSTRACT

The orbital and medial prefrontal cortex (OMPFC) is divided on the basis of its connectivity into orbital 'viscerosensory' (OPFC) and medial 'visceromotor' (MPFC) networks. Previous reports proposed that both networks exert a strong influence onto the ventral tegmental area (VTA) activity through interposed diencephalic nuclei, and influence VTA function through sparse direct connections. Here, we analysed the density and topographical organization of the projections of the OMPFC areas projections to VTA in the macaque monkey. Injections of biotin dextran amine or fluororuby in distinct OMPFC resulted in anterogradely labelled fibres with varicosities in VTA. The density of labelled fibres varied with the location of the injection site, so that each network had areas contributing more projections than others. Overall deposits in the medial network produced more labelling than injection in the orbital network. Specifically, deposits in areas 25 and medial 9, and the intermediate agranular insula (lai) of the "medial" network produced relatively dense labelling. In contrast, injections in areas 10o, 11m and 12m produced sparse or no labelling. In the orbital network, only injections in area 13b and in the posterior median agranular insula (lapm) produced relatively dense labelling with no major difference between areas. Injections in the remainder OMPFC areas including areas 10mr, 46d and 12r produced no labelling. A comparison of the spatial distribution of the labelled fibres in VTA revealed a considerable overlap of the projections from the different areas; only a trend for more lateral and rostral distribution in medial areas relative to orbital areas was noticed. Our results suggest for the first time a complex organization of prefrontal cortex afferents to VTA. This diversity of inputs to the VTA could provide new insight in the top-down control of dopamine release, and in the study of new possible targets for the treatment of neurological disorders.

INTRODUCTION

The connections between the prefrontal cortex (PFC) and the ventral tegmental area (VTA) are critical for memory, novelty detection and reward. At the cellular level, they play a key role in behaviorally relevant burst firing of DA within VTA (Gariano et al., 1988; Murase et al., 1993). Impairment of this control has been associated to the pathophysiology of schizophrenia (Sesack et al., 2002) and drug addiction (Lodge et al., 2011; Laurelle et al., 1996). Most of the experimental studies on the cortical control of DA release have been investigated in rodents. In this species excitatory (glutamatergic) projections or inhibitory (GABAergic) intermediary synapses has been described (with the ventral pallidum, nucleus accumbens and pedunculo-pontine) into the different DA and non-DA subpopulations of the VTA (Lammel et al., 2012; Grace et al., 2007).

Still, little is known about the anatomical organization of the projections from the PFC to VTA in nonhuman primates, and in particular which PFC areas contribute most with projections to VTA, and whether these projections are topographically organized. The rodent PFC is not comparable to primates and is composed mostly by agranular cortices (Ongur et al., 2000). The rat PFC is subdivided into only a few “areas” (infralimbic, prelimbic and cingulate areas) that do not include a proper lateral prefrontal cortex and barely has an equivalent of monkey area 10 (Burgess et al., 2007). These cytoarchitectonic differences between rat and primate can account for a higher parcellation of the different PFC areas based on their different set of connections and functions found in primates (Price, 2007). This is a factor to be kept in mind when considering the density of projections, and the presence of superior cognitive processing functions in primates.

In addition, whereas some authors claim that rat PFC (prelimbic and infralimbic) projections contributes denser projections to VTA (Hurley et al., 1991 and Takagishi et al.,1991, Geiser et al.,2006) than PFC does in monkeys (Frankle et al., 2006), other authors suggest that the density of the connections is low in both species (Sesack and Pickel, 1992). Most of what is known about the organization of the PFC projections to VTA comes from the rodent literature and there is, to this date, no data suggesting that the vast expansion and diversification of the monkey PFC may be accompanied with a more complex and heterogeneous organization than in rodents. Along with the cortical expansion, subcortical nuclei and regions such as the VTA might have expanded and/or reorganized in order to relate with new areas in the cortex. So far it has been assumed that the rodent and primate VTA shares the same overall organization (Sesack and Grace, 2010). However, VTA in rats has been described as being made up to 8 small nuclei (Gasbarri et al., 1994b) while in monkeys, some authors refer only up to 2 nuclei (Mc Ritchie et al., 1998;Wilhelmus et al., 2000; Cho et al., 2010).

In the present study we examined the organization of the projections of the different areas and subareas of the PFC to VTA in macaque monkeys. We observed that only a distinct set of cortical areas contribute major projections to VTA. Particularly, the areas of the PFC that are first affected

by cocaine exposure (Beveridge et al., 2008 and Porrino et al.,2000) and present strong interconnections with the Ventral striatum involved in motivation (further information see Joel et al.,2000), send direct projections to the VTA (Ferry et al.,2000).

MATERIALS AND METHODS

The present data were obtained from 25 adult cynomolgus or rhesus macaques (*Macaca fascicularis or mulatta*, respectively; 5-10 kg) in three different laboratories (Price, Insausti, and Evrard). All cases from Price's laboratory and some cases from the Insausti's laboratory were prepared and used in the context of prior tract-tracing studies (Carmichael and Price, 1995b, a, 1996; Kondo et al., 2003; Insausti and Amaral, 2008; Saleem et al., 2008). The animals were treated according to the guidelines of the American Physiological Society, the NIH and the European Parliament and Council Directive 2010/63/EU on the protection of animals used for experimental and other scientific purposes. All animal protocols were reviewed and approved by the Animal Studies Committee of Washington University, St.-Louis, USA, and the Ethical Committee of Animal Research of the University of Castilla-La-Mancha (UCLM), Spain, or the German authorities (*Regierungspräsidium*).

Surgery and tracer injections

Anesthesia was induced by an intramuscular injection of ketamine (10mg/kg) and xylazine (0.67mg/kg) for of MRI, surgical procedures and also at the time of perfusion (see below). During surgery, the anesthesia level was maintained by intubation with isoflurane. Thereafter, the animal was placed in a Kopf stereotaxic frame for craniotomy. After surgery, a long lasting analgesic, buprenorphine (0.1mg/Kg, i.m) was given to the animal upon recovery.

Most of the PFC injections had the stereotaxic coordinates for the injection site were calculated from the MRI obtained in a Phillips Intera 1.5T (Insausti's laboratory). However, for tracer injections into deep cortical areas, a tungsten electrode was inserted along the expected track of the pipette for electrophysiological recordings of spontaneous activity which allowed to determine the vertical coordinates of the structural boundary between grey and white matter or the bottom of the brain to correct the vertical coordinates determined by the MRI.

Retrograde tracer (Fast Blue [FB; 3 %]) and anterograde tracers (biotinylated dextran amine [BDA; Molecular probes 10%]) and two bidirectional tracers (FluoroRuby [FR; Molecular Probes 5% or 10%], and Lucifer Yellow [LY; Molecular Probes 5% or 10%]) were injected. The injections were made through an air pressure system using 25 msec air pulses. The air pressure was adjusted so that very small volumes of tracer were injected in each pulse (for details, see Kondo et al., 2005). To avoid spread of the tracer into areas along the pipette track, the micropipette was left in place for 30 minutes after the injection was completed.

Perfusion and histological processing

After a survival period of two weeks, the animals were anesthetized with ketamine i.m, followed by sodium pentobarbital (25-30mg/kg i.v. or intraperitoneally). After the animals were deeply anesthetized, they were perfused transcardially with saline, followed of 4% paraformaldehyde solutions at pH 6.5 and pH 9.5 (Carmichael et Price, 1994) and 10% sucrose at pH 9.5. Then the brain was removed and placed in 30% sucrose in phosphate-buffered until it sank. Three days later, the brain was frozen in isopentane cooled with dry ice and cut into 10 collated coronal sections series of 50 µm (T.HSU et al 2007). FR and LY were processed immunohistochemically with avidin-biotin-horseradish peroxidase technique; BDA was processed with the avidin-biotin-peroxidase method (Carmichael and Price 1994).

Data analysis and presentation of illustrations

Sections were examined with light microscope. Injection sites and axonal varicosities were manually plotted by using a microscope-digitalized system (AccuStage, Shoreview, MN). For sparse labeling, each fiber was plotted as a single point. However for densely labeled areas, 4 points indicate moderately dense varicosities greater than 10 fibers / per surface unit; a rating of 6-8 points indicate strong labeling, greater than 25 fibers / per surface unit. We mapped in Sequential linear passes across the section. Midbrain boundaries were drawn onto printed plots by using camera lucida drawings on adjacent sections stained for Nissl.

We evaluated the relative strength of connections but not absolute values, as it is not possible to compare absolute values because of factors such as differences in transport levels between tracers, injection volumes and location of each injection. Midbrain areas were analyzed bilaterally. Coronal series of sections were prepared in order to visualize the distribution and density of the labeling. Because individual maps were prepared for each case, we could not compare the overlap labeling.

.

Nomenclature

The terminology used for the VTA nuclei was adapted from Paxinos and the borders of each nuclei were defined according to the morphology of the cells in the Nissl staining and the boundaries of the area along the rostro-caudal VTA level. Based on functional studies, two main cell clusters within the VTA were defined.

The most caudal and medial part was related to anticipation reward and novelty, while the rostral and medial part was exclusively modulated by novelty (Krebs *et al*., 2011) and our anatomical results and immunohistochemistry support this division (see Hernandez-Mombiela et al., in

preparation). According to our division, the VTA consists into: proper VTA, lateral VTA or PBP; ventral VTA or PN and tail of the VTA. However for consistency, we will show the labeling obtained in the entire nucleus of the VTA.

RESULTS

Injection sites in PFC

Figure 1. Illustrates a representative injection site from case M315 with an injection of BDA in the area 12o. In most cases, like in M315, the injection site was confined to the cortical grey matter and included layers III and/or V. They all had a dense central 'core' around the tip of the micropipette penetration track and a more diffuse 'halo' extending for approximately 100 to 300 µm around the core. Injection sites for BDA always appeared larger and denser than injection sites for comparable volumes of FR and LY (not shown).

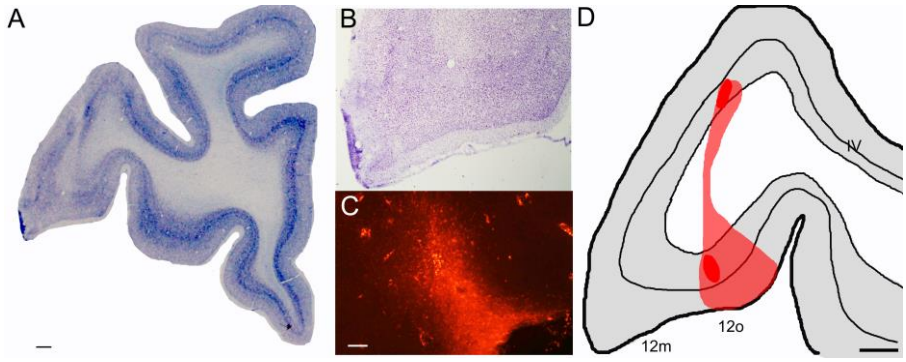

Figure 1. Representative example of an injection site (case M315). (A) Nissl-stained coronal section photomicrographa the level of the deposit (B-C) Higher magnification view of the injection site in Nissl and BDA. (D) Drawing of the maximal extent of the deposit. Scale bar 1mm

The anterograde labelling from a total of 27 anterograde tracer injections made in PFC or anterior insula was analysed in the present report. Figure 2 shows the location of each injection site in a standard map of the PFC.

Two injections were made in orbitofrontal cortex area 10o (OM38BDA and OM65FR). Three injections were made in medial prefrontal-cingulate areas 24b and 25 (cases OM34BDA, OM32FR/BDA and OM49BDA), and ten injections were made in orbital prefrontal cortex areas 11m, 11l, 12m,12r, 12, 13b, 13l (OM40BDA, OM27BDA, OM30BDA, OM29BDA, M2.15BDA, M3.15BDA, OM28BDA, OM79FR, OM65 LY, and OM42BDA). Two injections were made in anterior insula in areas Iai/Ial and Iam/Iamp (M615FR, OM68BDA). Five injections were made in lateral prefrontal cortex areas 9, 46v, 46d and multiple injection site in area 45,46v,12 (M105BDA, M305BDA, M205BDA, M405BDA and OM69LY).

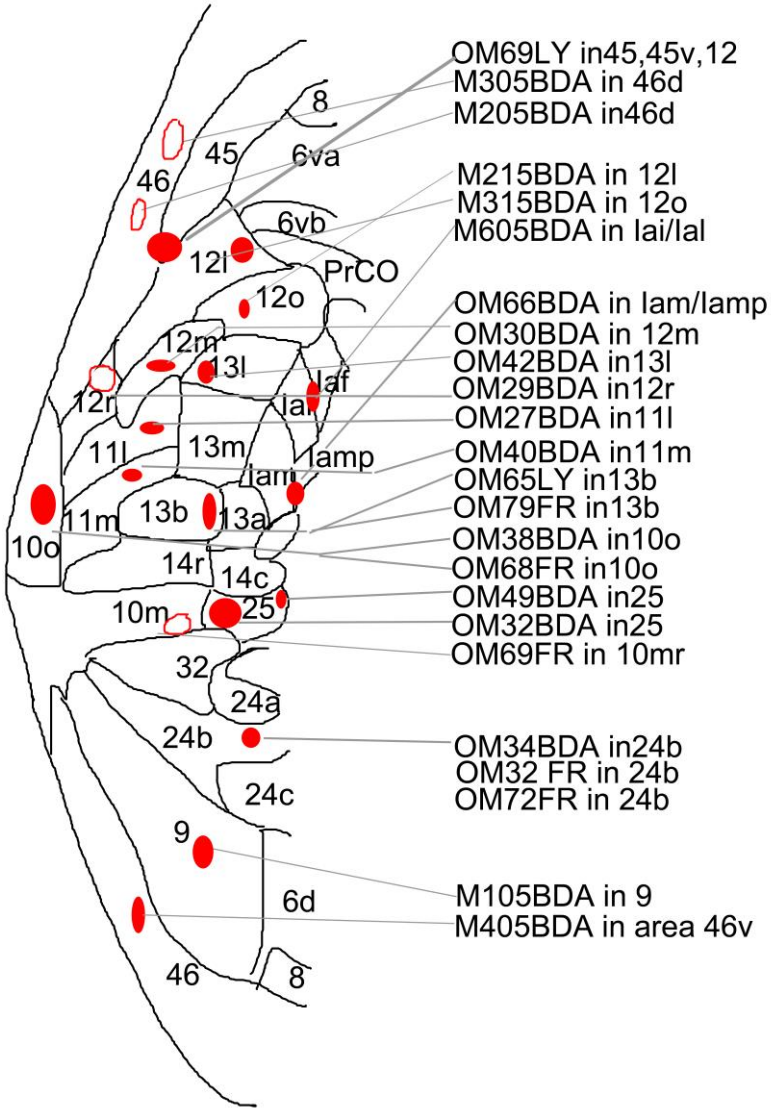

Figure 2: Topology of the injection sites in PFC using a relative collation of all injection sites onto a standard map of PFC. The ellipsoid shapes represent both the core and halo of the injection site. The ellipsoid shapes filled in red indicate the injection sites that produced anterograde labeling in VTA. The empty ellipsoid shapes indicate injection sites that did not produced labeling in VTA.

Some of the injections listed above spread to more than one architectonic area. In case OM66, the large BDA injection included both lam and lamp. In case M615, the injection included areas lai/lal. In case OM72FR, the injection spread to areas 24a' and b'. In case OM69, it included areas 45,46v and 12. Single injections of various small-middle sizes were also made in the same area; 46v (M3.05BDA and M4.05BDA) and area 13 and subareas 13b, 13l (M605BDA, OM65LY, OM42BDA, M315BDA).

As some of the tracers (FR, LY) are transported both retrogradely and anterogradely, we verified the injections by examining the location of anterogradely labelled fibres in the striatum (Haber et al., 1995) and neurons in the Amygdala (Carmichael et al .,1995).

Anterograde labelling in VTA

Architectonic organization of VTA.

A pre-requisite to the description of the distribution of anterograde labelling in VTA is a mapping of VTA to use as a reference. Figure 3 shows an architectonic map of VTA and various neighbouring nuclei or regions of the midbrain across 4 representative anteroposterior levels of the left VTA. The absence of the mammillary nuclei at the most rostral level indicated somewhat the rostral end of VTA at approximately -10.80 mm from the antero-posterior Bregma (AP) which correspond to our level 0 in Figure 3. VTA was co-existent with and ventral to the obvious red nucleus (RN and then its magnocellular part, RMC) throughout its almost entire rostro-caudal extent (level 1350 to 3150), and it was intermingled within the fibres of the third (oculomotor) nerve at the level of 2500. At its middle level, VTA was located dorsal to the interpeduncular fossa (IF), which, with the middle line nucleus, splitted VTA into two distinct sides. At more caudal levels, IF was replaced by the interpeduncular nucleus (IP) at (AP -14.40 mm; level 2500). The level where RM led to RMC also indicated the beginning of the tail of the VTA. The level of decussation (xscp) delimits the caudal level of the VTA that will continue further caudally until reaching AP 16.40mm (not shown).

General observation on the anterograde labelling.

All of the injections reported here produced anterograde labelling and in some cases retrograde labelling in VTA. Figure 4 shows examples of labelled fibres (4A) and neurons (4B) in VTA. The size of the segment of labelled fibres varied depending on the injection site; however the general overview showed short-medium fibres. Anterograde labeled fibers were counted on the contra- and ipsilateral sides. The labeling was bilateral, although the number of anterogradely labeled fibers in the ipsilateral side represented barely 5 % of the number of labeled fibers in the contralateral side; this observation is consistent with prior anterograde studies (Frankle and Haber, 2006).

The intensity of labeling varied, with most labeled fibers being moderately to intensely labeled, regardless of the tracer used, with the exception that immunohistochemically series showed greater density than the fluorescence series. The amount of labeling also varied with the size of the injection site. For example two different deposit sizes placed in area 25 (case OM32BDA and OM49BDA) showed more labeling in the larger deposit. In the following text the labeling in the OMPFC is described and analyzed arranged in networks.

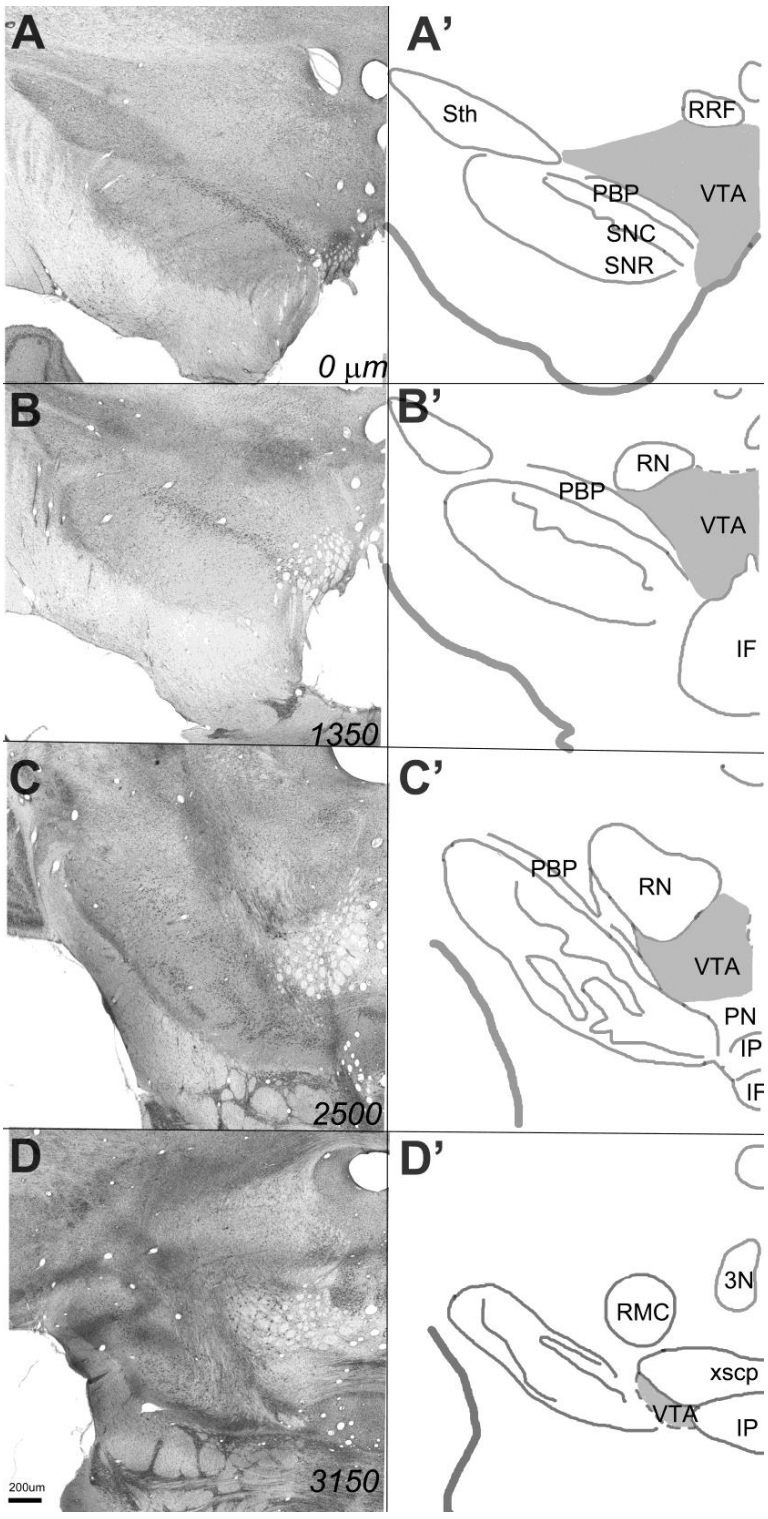

Figure 3. Architectonic mapping on a series of (A-D) coronal photography's of Nissl and the corresponding drawing (A'-D') through the rostro-caudal axis of the VTA. STh: Hypothalamic nucleus; RRF: Retrorubral Field; PBP: Parabrachial Pigmentosus nucleus; SNC: Sustancia Nigra Compacta; SNR: Sustancia Nigra Reticulata; RN: Red nucleus; IF: Interpeduncular Fossa; IP: Interpeduncular nucleus; RMC: Red magnocellular nucleus; xscp: decussation. Scale bar 200um

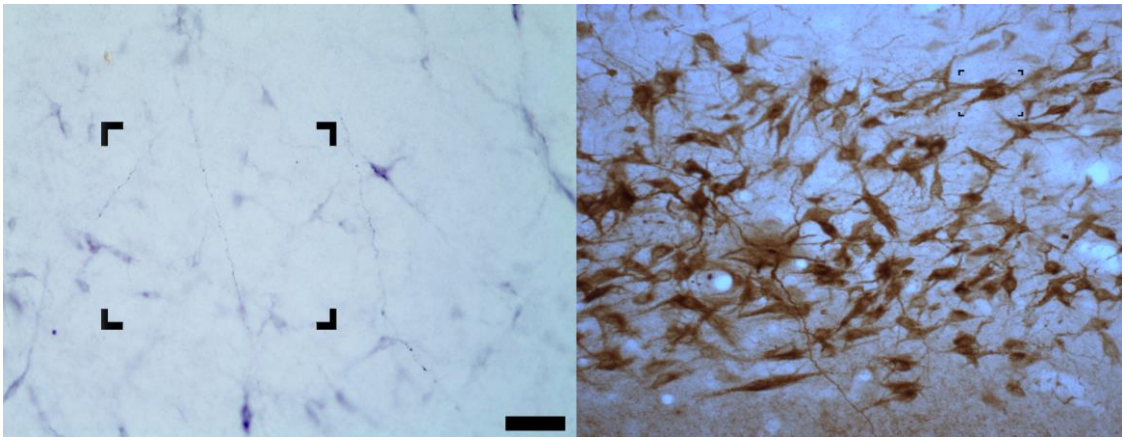

Figure 4. Photomicrographs of examples of labelled fibers bearing varicosities in VTA (A) and neurons (B) labeled with injections of FluoroRubi. Scale bar 1mm

Largely, the MPFC deposits resulted in the densest labeling of all PFC areas. The MPFC projections are representative of the labeling observed. The distribution of the projections within the VTA nuclei was characterized by broadly dispersed fibers, with clusters of denser labeling and patches of sparse labeling, generally within the anterior VTA that varied according to the PFC area explored. The property of bidirectionality in the used tracers allowed the observation of some neurons. The rostrocaudal location of the labelling was approximately similar regardless of the location of the injection site in the PFC. However the medio-lateral distribution within the different subnuclei showed a small tendency for more lateral and rostral distribution sites in MPFC relative to OPFC.

The following paragraphs describe the general density and location of the anterograde labelling in VTA. Figure 5 shows the plot of anterograde labelling in sets of coronal sections through the ventral midbrain for selected cases. The outline of the nuclei in these plots is a direct mirroring of the map shown in Figure 3. The different cases are arranged in 6 groups, from “dysgranular MPFC” to “eulaminar LPFC”.

Dysgranular MPFC.

The projections from the area 24b, case OM32 FR (Fig. 5A) and case OM32BDA (not shown) (Kondo et al., 2005) showed scarce projections into the rostral and middle levels of the VTA, mostly to the lateral VTA and to a subgroup of cells in the ventral part but not into the SN (Freedman 2000; Mar et al., 2013; Frankle et al., 2006). However, in area 25, case OM32BDA (Fig. 5B) the density of the projections was greater, despite that the pattern of distribution was similar to area 24b (Price 1998; An X et al.,1998 case 36; Frankle et al.,2006; Mar et al.,2013).

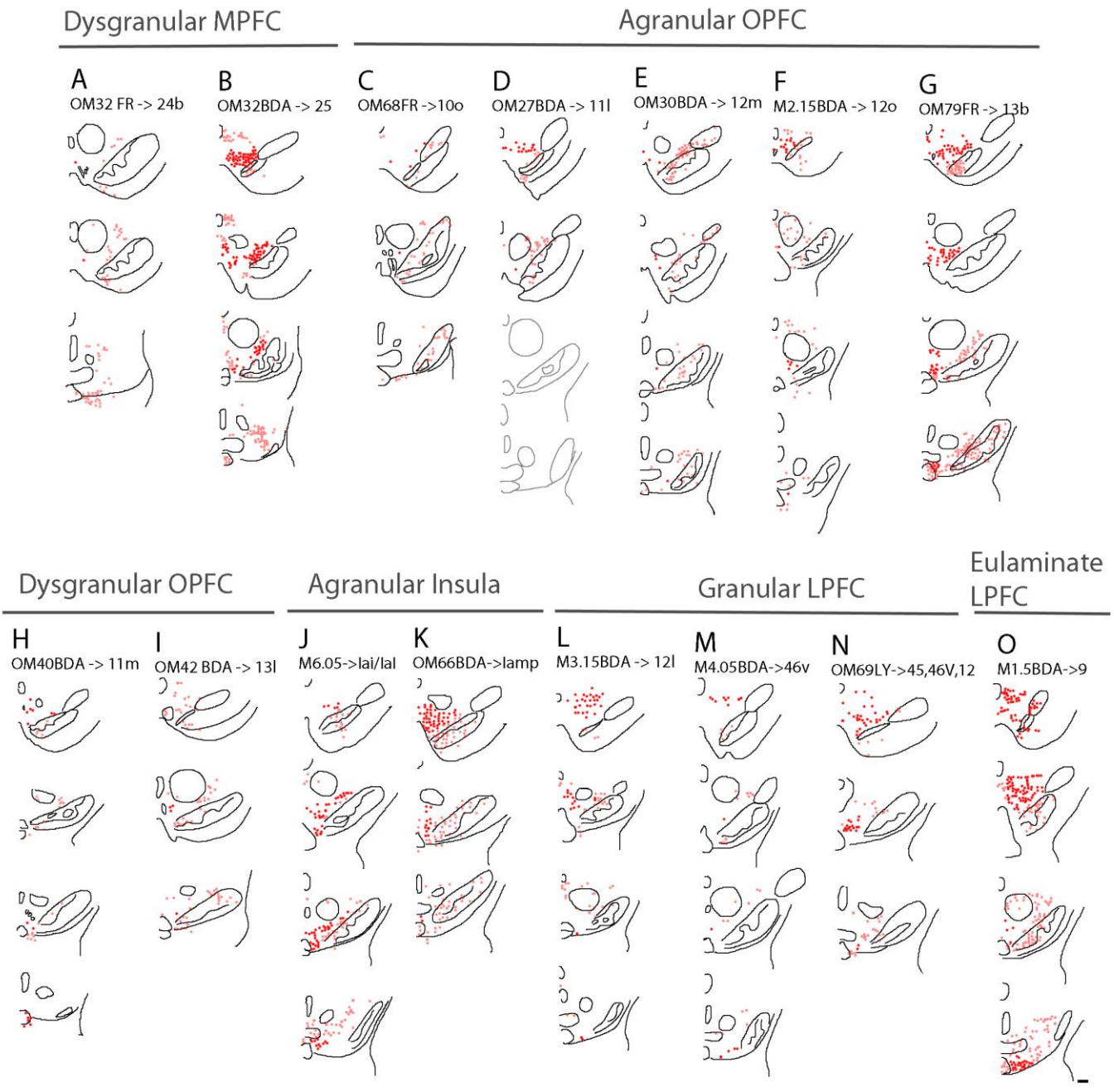

Figure 5: (A-O) Plot of anterograde labeling in the midbrain, produced with injections of tracers in the PFC. The dark red labeling corresponds to labeling in VTA. The pink labeling corresponds to labeling outside VTA. Scale bar= 1mm

Agranular OPFC

In the frontopolar cortex, two cases (Fig. 5C) OM68FR (Hsu et al., 2007) and OM38BDA (Shown in Saleem et al., 2008) received small tracer injections orbitofrontal cortex subarea 10o. No major difference in the VTA/SN projection was observed, although it was present in the hypothalamus. Labelled fibres were distributed in the rostral and middle parts of the lateral VTA and SNC (Results confirmed in AN X. et al., 1998 case OM36BDA).

Further modest projections arose from area 11l, case OM27BDA (Fig5.D) (shown in Hsu et al., 2007) with small-medium size injections of BDA resulted in a similar density and pattern distribution as the projections from the dysgranular area 11m. It contributed with some fibbers to the rostral, ipsilateral VTA, lateral (PBP), ventral (PN) and a few along SNC. Major differences were found within area 12. Four cases OM30BDA (Saleem et al., 2008) (Fig. 5E) OM29BDA (D.T. Hsu et al., 2007) (not shown), M3.15FR (Fig. 5E) and M2.15FR (Fig. 5F) of small-medium size injections placed in the caudal area 12r, rostral 12m and 12 show two distinct patterns. Area 12r yielded negative results, while areas 12 and 12m resulted in a decreasing rostro-caudal gradient projection to VTA and lateral VTA, but also from 12m to the SNC (Ongur et al., 2008). Moreover, three more cases OM79FR (Fig. 5G) OM65LY (Not shown) (Kondo et al., 2005), and OM72 (not shown) with medium size injections of FR, LY and BDA showed heavy projections from area 13b. No major differences dependent on the tracer were noticed (Frankle et al., 2006, case 133). The labelling was mostly ipsilateral and all over the VTA and SN.

Dysgranular OPFC

In the frontopolar cortex, one medium size injection OM69FR (not shown) in the 10mr produced no labelling un the VTA (Saleem et al., 2014).However, two cases, one case OM40BDA (shown in Hsu et al., 2007) (Fig. 5H) with small-medium size injections of BDA in area 11l resulted in positive fibbers projection to the rostral, ipsilateral VTA, lateral (PBP), ventral (PN) and a few along SNC. Another case OM42BDA (Fig. 5I) (Saleem et al.,2008) in area 13l resulted in la week labelling along the rostral and middle parts of the VTA but almost not in the SN.

Agranular Insula

Two cases (Fig. 5K and J) were injected in different parts of the insula, one in the agranular insula (Iam/Iamp, OM66BDA) and another case in area IaI/IaL (M6.05BDA). Projections from the Iam/Iamp showed strong projections along the VTA and SN (An et al., 1998; Price 1998; Ongür et al., 1998). Area IaI/IaL showed projections to VTA, although less dense and no labelling in the SN.

Granular LPFC

Three cases M205 and M305 (not shown) of medium size injections of BDA in area 46d gave few labelled fibres in the rostral-most part of the VTA, but not in the SN; although in case M405 (Fig. 5M) with a mid-injection size of BDA in area 46v presented scarce labelling in the VTA. One extra case with a big injection size of LY in area 45,46v and 12 (Fig. 5N) showed ipsilateral projections along the VTA particularly in the PBP nucleus and non in the SN.

Eulaminate or pseudolaminate LPFC

In the lateral prefrontal cortex, only injections in area 9 produced dense labelling. One case M105 (Fig. 5O) with a mid-size BDA deposit in area 9 showed strong ipsilateral labelling distributed all along VTA and SN.

Topographic distribution and overlap of anterograde labelling in VTA

The anterograde labelling in VTA occurred throughout the entire rostro-caudal extent of VTA, with however a preferential labelling in the rostral half, and no cases with only caudal portions of the VTA labelled. We found subtle differences in the medio-lateral distribution within the VTA region, depending on the network. For instance orbital PFC projections distributed more medial with the exception of area 11m (Fig. 5). Injections in the medial prefrontal cortex produced a similar pattern projection from the area 25 and insula that in turn are the areas that project most to VTA. Finally in the lateral PFC, despite that the projections are scarce we found that area 46 labelling distributes more along the lateral parts of the midbrain while area 9 projects strongly all along VTA. This could be due to the fact that part of area 9 belongs to the medial prefrontal network

To study the possible overlap or the spreading of the projection labeling within the VTA coming from different PFC areas, we paid attention to cases that had more than one injection in the PFC. Two cases were valid for this study. OM32 received injections of FR in area 24b and of BDA in area 25. OM72 received injections of FR in areas 24a'/24b' and LY in area 23b. OM69 received injections of FR in 10mr and LY in area 45, 46, 12 (not shown). The results from the first case (Fig 5.A-B) showed that the projections that arise in area 25 target the most medial and lateral parts of the VTA while projections from area 24b only reach a subgroup of ventral cells lying at the base of VTA. In the second case (data not shown), the injection in area 23b produced sparse labelling in the rostral midlevel of VTA and the injection in area 24a'/24b' produced no labelling. In the third case, no labelling was found from area 10mr and from the forth injection, rostro-medial levels of the VTA showed positive fibbers.All together, this simple comparative examination suggests that the PFC projections to VTA may have some subtle degree of internal topographic organization.

Injection sites in VTA

To confirm the projections inferred from the analysis of the anterograde labelling in VTA, retrograde tracers injections were made in or around VTA. Injections within VTA involved different adjacent nuclei and were placed at different rostro-caudal levels or more lateral. Out of the seven cases injected (see Methods), only three produced technically reliable retrograde labelling (M2-15FB, M3-15FB and M9-9FB). Figure 6 depicts the injections sites in the VTA drawn coronal drawings. The

injections were relative small and showed a core and a hallo of deposit. Injections within VTA involved different nuclei and were placed at different rostro-caudal levels or more lateral.

One injection of FB was made in rostral VTA (M3-15; Fig. 6D). One injection of FB was made in the lateral aspect of the middle AP extent of VTA (M2-15; Fig. 6E).

One injection of FB was made in the caudal end of VTA (M9.09 Fig. 6I). All sites were relatively small and did not extensively spread to adjacent regions.

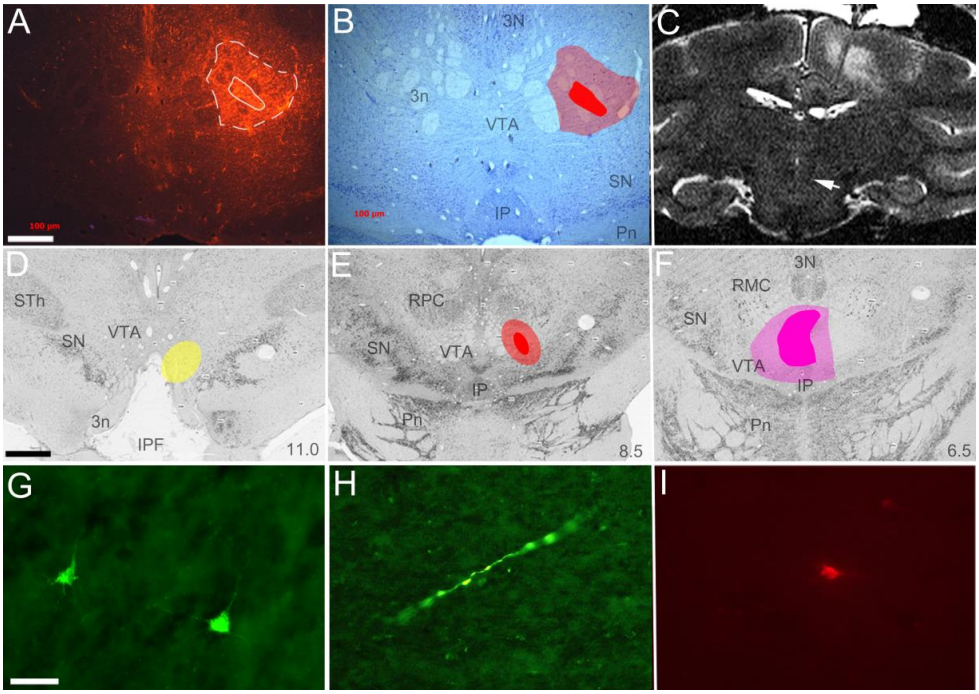

Figure 6: Photomicrographs of adjacent coronal fluorescent (A) and Nissl-stained (B) sections showing Pdex injection site in case cm28; the core and halo (circled by continuous and dashed lines, respectively) and their plots onto Nissl-stained photomicrographs of VTA, respectively. C. MRI section showing the location of the fused silica micropipette used to inject Pdex in VTA. D-F. Injection sites from cases cm018Rdex ('yellow'), cm017Rdex ('green'), cm020Rdex ('purple') and cm024Pdex ('red') depicted on a set of 3 photomicrographs through four representatives AP levels of VTA. G-I. Photomicrographs of representative retrograde (G) and anterograde (H, I) labelling produced with an injection of Rdex (G, H) or BDA (I) in VTA. Left is medial and top is dorsal. Scale bar = 150 µm (A, B), 1 mm (D-F), and 20 µm (G-I).

Retrograde labelling in PFC

Figures 7-9 show plots of the retrograde labelling into individual coronal maps of PFC and at a more posterior level passing through the ventral striatum in all three cases: M3.15 BDA (Fig. 7), M2.15 (Fig. 8), and M9.09 (Fig. 9). All three injections in VTA produced retrograde labelling in the ventral striatum and in PFC; however the density of the labelling greatly varied with the location of the injection site in VTA, in a manner that fitted the results obtained with the anterograde labelling.

Rostral VTA.

The FB injection in rostral VTA in M3.15 produced a relatively dense to moderate labelling in several distinct architectonic areas in PFC, the insula and the cingulate cortex (Fig. 7). The pattern of labelling confirmed the anterograde labelling obtained in VTA with injections in PFC. Namely, MPFC and insular areas showed in general more labelling than OPFC and LPFC areas. The labelling seemed to decrease in a top down density from the most medial to lateral areas starting from the Prefrontal Cortex. The strongest labelling was produced in area 25, the anterior insula and some subdivisions of area 13, in complete accordance with the anterograde labelling. Moderate labelling was produced in areas 24b and 9; and the lowest labelling occurred in areas 10, 11 and 46. In detail, we can see that in some areas the projections arise from a particular group of cells within that area, for example in area 9.

.

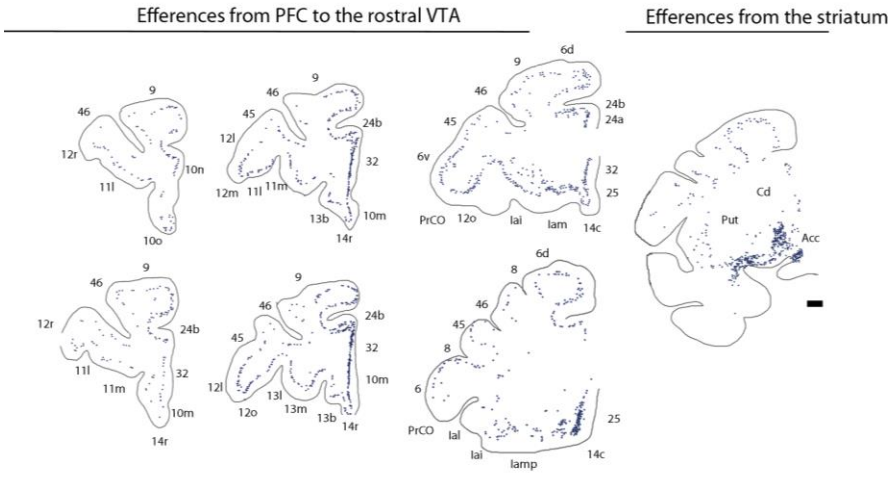

Figure 7: Plots of retrograde labelled cells in the cortex and ventral striatum from an injection placed in the rostral VTA, case M3.15FB. The labeling is represented by individual dots, and corresponds to retrograde labeling within the PFC. Scale bar = 1 mm.

These results confirm the observations found in the anterograde labelling and confirm the idea of subparcellation of the PFC in primates. For example, the dorsal and ventral parts of area 46 have clearly different patterns of labelling, from non-existing projections in the dorsal part, to some labelling in the ventral part. On the other hand, unlike the rest of the injections described below (Fig8 and Fig. 9), the rostral VTA also receive strong projections from the VS suggesting a possibly rely in this structure through the indirect pathway projection to the VTA.

Lateral VTA.

One injection placed in the most lateral part of the VTA, M2.15 of a retrograde FB in the Para-brachial Pigmentosus nucleus (pbp) and the deep mesencephalic tegmentum, showed a similar pattern of labeling as in M3.15, except the most caudal levels of area 24 and along the insula

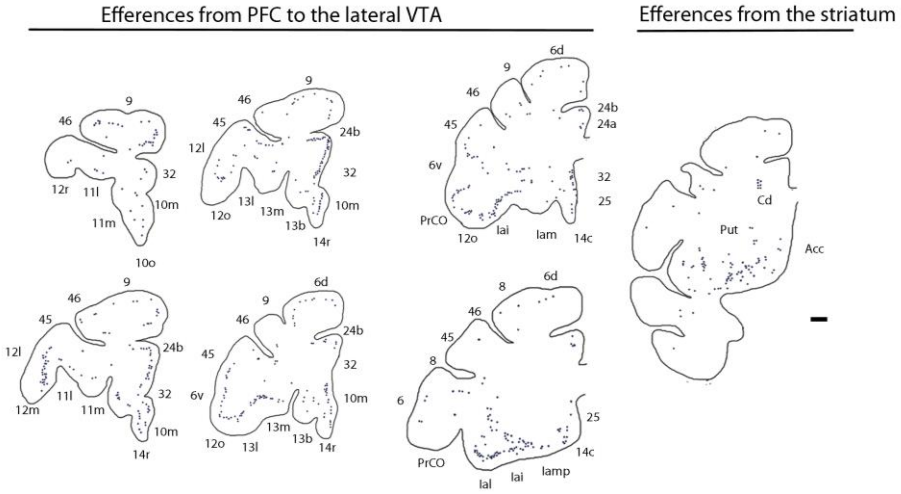

Figure 8: Plots of retrograde labelled cells in the cortex and ventral striatum from one injection placed in the lateral VTA, case M2.15FB. The labeling is represented by individual dots to represent retrograde labeling within the PFC. Scale bar = 1 mm.

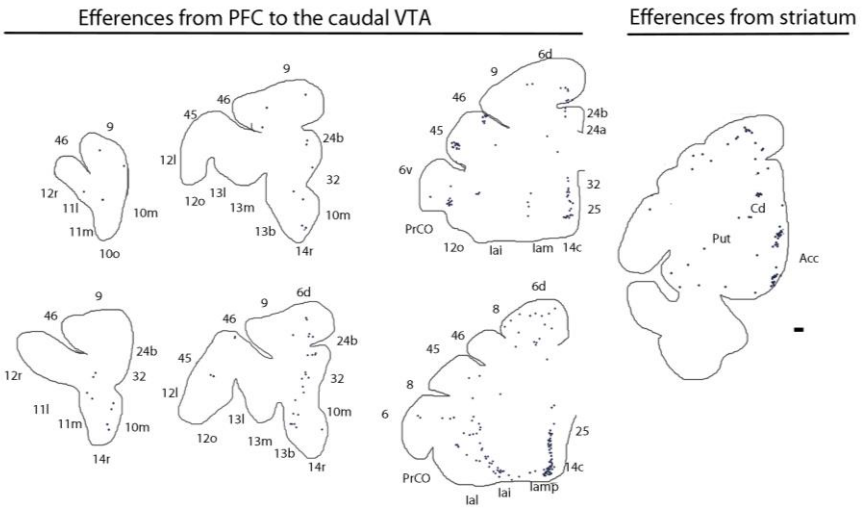

Figure 9: Plots of retrograde labelled cells in the cortex and ventral striatum from one injection placed in the caudal VTA, case M9.09FB. The labelling is represented by individual dots to represent retrograde labelling within the PFC. Scale bar = 1 mm

Caudal VTA.

The injection of FB in caudal VTA in case M2.15 produced a somewhat different density of labelling in PFC, although the overall pattern of areal labelling was similar. The results fits with the pattern projections shown from the different PFC areas along the VTA, although there were some differences. The projections to the caudal VTA, mainly arised from the MPFC and very few projections from the lateral cortex, areas 10, 11 and 46, and almost no projections from area 9.

However, this internal variability could be due to the possibility that the injection did not reach particular parts of VTA that may harbour the terminals from this area, an idea that is in conflict with the quasi-absence of topography in our anterograde labelling experiments.

DISCUSSION

The present study confirms the existence of projections from PFC to VTA in the macaque monkey. In addition to prior studies (Frankle et al., 2006), the present study reveals that not all PFC areas project to VTA and that some areas (in particular the cortical limbic areas 25, Iam/p and 13b) send relatively heavy projections to VTA, contrary to prior assumptions that PFC projections to VTA are only mild compared to the projections from the ventral striatum. The patterns of labelling in VTA suggest the existence of a subtle topography in the organization of the cortical projections to VTA. The next paragraphs will first compare our results to prior studies in primates and rodents, and then discuss the possible functional meaning of the PFC projections to VTA.

Comparison with prior tracing studies in primates and rodents

Consistent with our findings, previous studies observed that overall, the projections in primates are not strong, and it has been suggested that the projections in primates are weaker compared to rodents. (Frankle et al., 2006). In contrast, one recent study conducted in rats suggested that projections from the PFC are also weaker in rodents relative to projections from the striatum, subthalamic nuclei and dorsal raphe (Watabe et al., 2013). This discrepancy in the density of projections between both species might be because only some areas of the PFC of the rodents are compared to the whole PFC cortex in primates. Particularly they compared the infralimbic (homologous with area 25 in monkeys) and prelimbic cortex (comparable with area 32) and dorsolateral anterior cingulate cortex (homologous with area 24b) that in primates also send heavier projections compared to the rest of the prefrontal cortical areas.

Further anatomical evidence in primates has reported projections to the midbrain, although the objective of the study was different, to adjacent areas. Ongür and Price (1998) found labeling arising from area 25, 12o and Iai, but (not from area Iam and 12m) in the VTA on their study of connections

with the hypothalamus. Other studies are more specific looking for projections from areas of the PFC such as area 25 (Freedman et al., 2000) without too much detail on the projections to the VTA, showing medium density labeled fibers in the rostral VTA. Chiba et al., (2001) reported projections also from area 25, 24 and 10. Although those projections are confined, it has been postulated that they could have a profound top down effect on the regulation of the DA neuron activity. One possibility could be through the release of modulator peptides that are known to promote burst firing within VTA (Skriboll et al., 1981). Other possibility is that the increase of the neuron activity wouldn't be only synaptic (Rosseti et al.,1998), as the extracellular glutamate released could also affect the DA cells not directly target inducing burst firing (Lodge et al.,2006) and activation to silent neurons (Grace and Bunney et al.,1984b).

It should be noted also, that the projections from the PFC networks are segregated. Previous anatomical studies in rodents show different density of projections from the medial and orbital PFC to the brainstem (Sesak et al., 1989), comparable to our study in primates. Thus, despite the fact that the architectonic parcellation of the rat PFC is not as diversified and expanded as in primates (Burman et al., 2009 and Cavada et al., 2003), and despite the fact that rat PFC areas do not seem to harbor the vast functional diversity of the abundant monkey PFC areas (Price, 2007), the PFC regions that show heaviest projections to the midbrain appear to be comparably similar in rodents and primates. However, some of the monkey PFC areas are not comparable to any rat PFC areas, in particular in lateral PFC.

Those common area, named as "limbic cortex" share a cytoarchitectonic organization. They are composed by agranular and dysgranular areas that lack layer IV or have a rudimentary layer IV, that are not present in rodent PFC (Berger et al., 1991). In most cases, they occupy the 'edges' of the cortex as a ring above and below the corpus callosum (Barbas 2015). These converging observations perfectly fit with our results except for the projections from area 9. However the part from the area 9 that projects to VTA is the middle part of area 9, a part that has a pseudolaminar grade of complexity, not a canonical 6-layered isocortical organization.

Organization of the PFC projections

In the study of the organization of the PFC projections, we observed that projections from the MPFC distributed in the most dorso-lateral part of the midbrain, the VTA nucleus, than the projections arising from the OPFC, distributed more in the ventral (PN) and medial VTA, except in some cases that also distributes in the lateral (PBP). These results are supported by studies in rodents that demonstrated an inner organization of the projections within the VTA dependent on the medio-lateral axis, so that more medial cell groups innervate more medial and rostral structures while lateral cells innervate more lateral and caudal structures (Loughing and Fallon 1984).

Interestingly, one hypothetical schema shown by Williams et al., in 1998 demonstrated by rotating 45 degrees the prefrontal cortex sections that the topographical organization of the connections with the midbrain perfectly matched not only in the medio-lateral axis but in the dorsoventral axis as well.

On the other hand, functional studies proposed a feedback loop from VTA neurons to the mPFC after observing burst firing in pyramidal cells of the layer V of the mPFC induced by DA, via D2 receptors (Wang et al., 2004). In detail, only those DA cells that project back to the MPFC area innervated (Carr and Sesack, 2000a,b) but also, the GABAergic cells of the VTA that projects to the nucleus accumbens (Sesack and Carr, 2002). Those findings agreed with our observations of retrograde labeling produced after deposits of bidirectional traces such as LY and FR that showed that some of the connections are reciprocal (data not shown) (Further information see Williams et al., 1998; Saleem et al., 2014 Gaspar et al., 1992 and Porrino et al.,1982).

To explain these possible results, we looked carefully at studies of the indirect pathway projections from the PFC trought the striatum to the midbrain (Ferry et al, 2000) and we found out that the areas projecting the most to VTA are the same areas that do project the most to the ventral striatum that in turn projects the most to the VTA, through the indirect pathway (Haber et al., 2010).Those areas have in common a particular feature; they are dysgranular and are distributed all along the corpus callosum (Barbas 2015). The density of the projections shows a decreasing gradient in the midbrain, as far as the cortex is from the limbic structures. The results suggest that the limbic system is a robust system shared by rodent and primates with the only exception of the subparcellation of the PFC projections to the midbrain.

Functional interpretation

In 2012, Logde et al, demonstrated the importance of the segregated direct control of the DA from the MPFC and OPFC network. He showed that each network carries independent but complementary information that can regulated differentially the DA system (Asher A. et al, 2011).

In response to cognitive tasks, it has shown that the mPFC fires with high frequency bursts enhancing a dramatically increase of DA activity (Chagnac-Amitai et al., 1990; Chang et al., 2010). However, a single pulse of tonic activation of the mPFC can also induce inhibition in less than the half of the DA cells population (Lodge et al., 2011; Tong et al., 1998). This is because; only previously excited cells receive monosynaptic (glutamatergic) inputs from the mPFC. In contrast, the phasic activation of the OPFC regulates negatively the DA activity (Lodge in 2011) by stopping the positive feedback loop with the mPFC. Clinical studies have reported the importance of this negative control that occurs for example, during over expectation (Schoenbaum et al., 2009). During reward expectation DA activity is enhanced while the activity of the OPFC is decreased; although, the opposite happens when unexpected reward (Takahashi et al., 2009). The mechanism of this activity

has been demonstrated anatomically by Carr (2000), and it is more likely through the activation of secondary GABAergic cells from the NA or within the VTA.

However, if this would be true, we would expect projections from the OPFC only restricted to the tail of the VTA, which is the part of the nuclei that contains the most of the GABAergic cells (Bourdy et al., 2012). Our results although, do not support this idea. In fact, the projections from the OPFC are localized mostly in other nuclei than the proper VTA (PB and PN), suggesting that these nuclei might contain GABAergic cells. Taken together, it can be hypothesized that direct projections from the different subareas of the PFC might be implicated in different aspects of cognition by means of controlling VTA activity.

Technical limitations

Technical limitations such as different sizes and layers involved in the injection, the different characteristics of the tracers in terms of sensitivity and efficacy of transport may be responsible for some variability in the results. One important feature to take into account is the involvement of the deep layers of the PFC, particularly layer 5 by the injection site (Gabbot et al., 2005). Functional studies have supported this idea by showing that the layer five pyramidal cells of the cortex are responsible for the increase of VTA activity (De Felipe J. et al., 1992; Gabbot et al., 2005). In our study, most of the injections target almost all the layers, although in some cases, the spread of the tracer in the halo might not have been enough to transport the tracer effectively. This fact could, for example, explain the differences in density of the projections observed in the study. Moreover, the retrograde labeling produced by injections in the VTA, we found that in some areas of the PFC, only subgroup of cells projected downstream. For example area 9, labeled only a few cells, thus indicating that the projections depends on the size and the location of the injection. Therefore some negative cases in which we did not observe labeling could be due to size and injection site that didn’t reach that particular group of cells that project to the VTA.

BIBLIOGRAPHY

An. X, Bandler R, Ongür D, Price JL (1998). Prefrontal cortical projections to longitudinal columns in the midbrain periaqueductal gray in macaque monkeys. J Comp Neurol.Nov 30;401:455-79.

Asher A, Lodge DJ (2012). Distinct prefrontal cortical regions negatively regulate evoked activity in nucleus accumbens subregions. Int J Neuropsychopharmacol. Oct;15:1287-94.

Barbas H.(2015) General cortical and special prefrontal connections: principles from structure to function. Annu Rev Neurosci. Jul 8;38:269-89

Barbas, H. & G.R. Blatt. (1995). Topographically specific hippocampal projections target functionally distinct prefrontal areas in the rhesus monkey. Hippocampus **5:** 511–533.

Baxter MG, Murray EA (2002). The amygdala and reward. Nat Rev Neurosci. Jul;3 :563-73. Review

Berger, B., Gaspar, P., & Verney, C. (1991). Dopaminergic innervation of the cerebral cortex: unexpected differences between rodents and primates. Trends in neurosciences, 14, 21-27.

Beveridge, T. J., Gill, K. E., Hanlon, C. A., & Porrino, L. J. (2008). Parallel studies of cocaine-related neural and cognitive impairment in humans and monkeys. Philosophical Transactions of the Royal Society B: Biological Sciences, 363, 3257-3266.

Björklund A, Dunnett SB (2007). Dopamine neuron systems in the brain: an update. Trends Neurosci. 2007 May;30194-202. Epub 2007 Apr 3. Review.

Borra, E., Gerbella, M., Rozzi, S., & Luppino, G. (2013). Projections from caudal ventrolateral prefrontal areas to brainstem preoculomotor structures and to basal ganglia and cerebellar oculomotor loops in the macaque. Cerebral Cortex, bht265.

Bourdy R, Barrot M. (2012) A new control center for dopaminergic systems: pulling the VTA by the tail. Trends Neurosci. Nov; 35:681-90.

Burgess, P. W., Dumontheil, I., & Gilbert, S. J. (2007).The gateway hypothesis of rostral prefrontal cortex (area 10) function. Trends in cognitive sciences, 11, 290-298.

Burman KJ, Rosa MG (2009). Architectural subdivisions of medial and orbital frontal cortices in the marmoset monkey (Callithrix jacchus). J Comp Neurol. 2009 May 1;514:11-29.

Bush, G., Luu, P., & Posner, M. I. (2000). Cognitive and emotional influences in anterior cingulate cortex.Trends in cognitive sciences, 4, 215-222.

Carmichael ST, Price JL (1995). Limbic connections of the orbital and medial prefrontal cortex in macaque monkeys. J Comp Neurol. Dec 25;363(4):615-641.

Carmichael ST, Price JL (1995). Sensory and premotor connections of the orbital and medial prefrontal cortex of macaque monkeys. J Comp Neurol. Dec 25;363:642-664

Carmichael, S. T., Clugnet, M. C., & Price, J. L. (1994). Central olfactory connections in the macaque monkey. Journal of Comparative Neurology, 346 403-434.

Carr DB, Sesack SR (2000). GABA-containing neurons in the rat ventral tegmental area project to the prefrontal cortex. Synapse. Nov;38:114-23.

Carr DB, Sesack SR (2000). Projections from the rat prefrontal cortex to the ventral tegmental area: target specificity in the synaptic associations with mesoaccumbens and mesocortical neurons. J Neurosci. May 15;20:3864-73.

Cavada C, Compañy T, Tejedor J, Cruz-Rizzolo RJ, Reinoso-Suárez F(2000). The anatomical connections of the macaque monkey orbitofrontal cortex. A review. Cereb Cortex. 2000 Mar;10:220-42. Review

Chagnac-Amitai Y, Luhmann HJ, Prince DA (1990). Burst generating and regular spiking layer 5 pyramidal neurons of rat neocortex have different morphological features. J Comp Neurol. Jun 22; 296:598-613.

Chandler DJ, Lamperski CS, Waterhouse BD (2013). Identification and distribution of projections from monoaminergic and cholinergic nuclei to functionally differentiated subregions of prefrontal cortex. Brain Res. Jul19;1522:38-58

Chandler DJ, Waterhouse BD, Gao WJ (2014). New perspectives on catecholaminergic regulation of executive circuits: evidence for independent modulation of prefrontal functions by midbrain dopaminergic and noradrenergic neurons. Front Neural Circuits. May 21;8:53. eCollection . Review

Chang CH, Berke JD, Maren S (2010). Single-unit activity in the medial prefrontal cortex during immediate and delayed extinction of fear in rats. PLoS One. Aug 5;5:e11971.

Chiba T, Kayahara T, Nakano K, (2001). Efferent projections of infralimbic and prelimbic areas of the medial prefrontal cortex in the Japanese monkey, Macaca fuscata. Brain Res. Jan 5;888:83-101.

DeFelipe J, Fariñas I (1992). The pyramidal neuron of the cerebral cortex: morphological and chemical characteristics of the synaptic inputs. Prog Neurobiol. Dec;39:563-607. Review.

Ferry AT, Ongür D, An X, Price JL (2000). Prefrontal cortical projections to the striatum in macaque monkeys: evidence for an organization related to prefrontal networks. J Comp Neurol. Sep 25;425:447-70.

Frankle WG, Laruelle M, Haber SN (2006). Prefrontal cortical projections to the midbrain in primates: evidence for a sparse connection. Neuropsychopharmacology. Aug;31:1627-36.

Freedman LJ, Insel TR, Smith Y (2000). Subcortical projections of area 25 (subgenual cortex) of the macaque monkey. J Comp Neurol. May 29;421:172-88

Frey S, Petrides M (2000). Orbitofrontal cortex: A key prefrontal region for encoding information. Proc Natl Acad Sci U S A. Jul 18;97:8723-7.

Gabbott PL, Warner TA, Jays PR, Salway P, Busby SJ (2005). Prefrontal cortex in the rat: projections to subcortical autonomic, motor, and limbic centers. J Comp Neurol. 2005 Nov 14;492:145-77.

Gaspar, P., Stepniewska, I., & Kaas, J. H. (1992). Topography and collateralization of the dopaminergic projections to motor and lateral prefrontal cortex in owl monkeys. Journal of Comparative Neurology, 325 1-21.
Geisler S, Derst C, Veh RW, Zahm DS (2007). Glutamatergic afferents of the ventral tegmental area in the rat. J Neurosci. May 23;27:5730-43
Grace AA, Bunney BS (1984). The control of firing pattern in nigral dopamine neurons: burst firing. J Neurosci. 1984 Nov; 4: 2877-90.
Grace AA, Floresco SB, Goto Y, Lodge DJ (2007). Regulation of firing of dopaminergic neurons and control of goal-directed behaviors.Trends Neurosci. May; 30:220-7
Haber SN (2003). The primate basal ganglia: parallel and integrative networks. J Chem Neuroanat. Dec;26:317-30. Review.
Haber SN, Knutson B (2010). The reward circuit: linking primate anatomy and human imaging. Neuropsychopharmacology.Jan;35:4-26. doi: 10.1038/npp.2009.129. Epub . Review.
Haber SN, Kunishio K, Mizobuchi M, Lynd-Balta E (1995). The orbital and medial prefrontal circuit through the primate basal ganglia. J Neurosci.Jul;15:4851-67.
Hsu DT, Price JL (2007). Midline and intralaminar thalamic connections with the orbital and medial prefrontal networks in macaque monkeys. J Comp Neurol. Sep 10;504:89-111.
Hurley KM, Herbert H, Moga MM, Saper CB (1991). Efferent projections of the infralimbic cortex of the rat. J Comp Neurol. Jun 8;308:249-76.
Insausti R, Amaral DG, Cowan WM (1987). The entorhinal cortex of the monkey: III.Subcortical afferents. J Comp Neurol.Oct 15;264:396-408.
Joel, D., & Weiner, I. (2000). The connections of the dopaminergic system with the striatum in rats and primates: an analysis with respect to the functional and compartmental organization of the striatum. Neuroscience, 96, 451-474.
Jonides, J., Smith, E. E., Koeppe, R. A., Awh, E., Minoshima, S., & Mintun, M. A. (1993). Spatial working- memory in humans as revealed by PET.Letters to nature (623-625)
Kahn I, Shohamy D (2013). Intrinsic connectivity between the hippocampus, nucleus accumbens, and ventral tegmental area in humans. Hippocampus. Mar;23:187-92.
Kondo H, Saleem KS, Price JL (2005). Differential connections of the perirhinal andparahippocampal cortex with the orbital and medial prefrontal networks in macaque monkeys. J Comp Neurol. Dec 26;493:479-509
Lewis DA, Foote SL, Goldstein M, Morrison JH (1988).The dopaminergic innervation of monkey prefrontal cortex: a tyrosine hydroxylase immunohistochemical study. Brain Res. May 24;449 :225-43.
Lodge DJ (2011). The medial prefrontal and orbitofrontal cortices differentially regulate dopamine system function. Neuropsychopharmacology. May;36:1227-36.
Lodge DJ, Grace AA (2006). The laterodorsal tegmentum is essential for burst firing of ventral tegmental area dopamine neurons. Proc Natl Acad Sci U S A. Mar 28;103:5167-72.
Loughlin SE, Fallon JH (1984). Substantia nigra and ventral tegmental area projections to cortex: topography and collateralization. Neuroscience. Feb;11:425-35.
Miller, E. K., & Cohen, J. D. (2001). An integrative theory of prefrontal cortex function. Annual review of neuroscience, 24, 167-202.
Ongür D, An X, Price JL (1998). Prefrontal cortical projections to the hypothalamus in macaque monkeys. J Comp Neurol. Nov 30;401:480-505.
Ongür D, Price JL (2000). The organization of networks within the orbital and medial prefrontal cortex of rats, monkeys and humans. Cereb Cortex.Mar;10:206-19. Review.
Petrides, M., Alivisatos, B., Meyer, E., & Evans, A. C. (1993). Functional activation of the human frontal cortex during the performance of verbal working memory tasks. Proceedings of the National Academy of Sciences, 90, 878-882.
Porrino, L. J., & Goldman-Rakic, P. S. (1982). Brainstem innervation of prefrontal and anterior cingulate cortex in the rhesus monkey revealed by retrograde transport of HRP. Journal of Comparative Neurology, 205, 63-76.
Porrino, L. J., & Lyons, D. (2000). Orbital and medial prefrontal cortex and psychostimulant abuse: studies in animal models. Cerebral Cortex, 10, 326-333.
Preuss TM (1995). Do rats have prefrontal cortex? The rose-woolsey-akert program reconsidered. J Cogn Neurosci. Winter;7:1-24.
Price JL, Amaral DG (1981). An autoradiographic study of the projections of the central nucleus of the monkey amygdala. J Neurosci. Nov;1:1242-59.
Price, J. L. (1999). Prefrontal cortical networks related to visceral function and mood. Annals of the New York Academy of Sciences, 877, 383-396.
Price, J.L., F.T. Russchen & D.G. Amaral. (1987). The limbic region. II: The amygdaloid complex. *In* Handbook of Chemical Neuroanatomy, Vol. 5: Integrated Systems of the CNS, Part I. A. Bjorklund, T. Hokfelt & L.W. Swanson, Eds: 279– 388. Elsevier Science Publishers. Amsterdam.
Rolls ET (2000) The orbitofrontal cortex and reward. Cereb Cortex. Mar;10:284-94. Review.
Romanski LM (2007). Representation and integration of auditory and visual stimuli in the primate ventral lateral prefrontal cortex. Cereb Cortex. Sep;17
Rossetti ZL, Marcangione C, Wise RA (1998). Increase of extracellular glutamate and expression of Fos-like immunoreactivity in the ventral tegmental area in response to electrical stimulation of the prefrontal cortex. J Neurochem. Apr;70:1503-12.
Rudebeck PH, Buckley MJ, Walton ME, Rushworth MF(2006). A role for the macaque anterior cingulate gyrus in social valuation. Science. Sep1;313:1310-2.
Saleem KS, Kondo H, Price JL (2008). Complementary circuits connecting the orbital and medial prefrontal networks with the temporal, insular, and opercular cortex in the macaque monkey. J Comp Neurol. Feb 1;506:659-93.

Saleem KS, Miller B, Price JL, (2014). Subdivisions and connectional networks of the lateral prefrontal cortex in the macaque monkey. J Comp Neurol. May 1;522:1641-90.
Saunders R.C., D.L. Rosene & G.W. Van Hosen (1988). Comparison of the efferents of the amygdala and the hippocampal formation in the rhesus monkey: II.Reciprocal and non-reciprocal connections. J. Comp. Neurol. 271: 185–207.
Sesack SR, Carr DB (2002). Selective prefrontal cortex inputs to dopamine cells:implications for schizophrenia. Physiol Behav. Dec;77:513-7. Review
Sesack, S. R., & Pickel, V. M. (1992). Prefrontal cortical efferents in the rat synapse on unlabeled neuronal targets of catecholamine terminals in the nucleus accumbens septi and on dopamine neurons in the ventral tegmental area. Journal of Comparative Neurology, 320, 145-160.
Skirboll LR, Grace AA, Hommer DW, Rehfeld J, Goldstein M, Hökfelt T, Bunney BS (1981). Peptide-monoamine coexistence: studies of the actions of cholecystokinin-like peptide on the electrical activity of midbrain dopamine neurons. Neuroscience.;6:2111-24.
Sugihara, T., Diltz, M. D., Averbeck, B. B., & Romanski, L. M. (2006). Integration of auditory and visual communication information in the primate ventrolateral prefrontal cortex. The Journal of Neuroscience, 26, 11138-11147.
Takagishi M, Chiba T,(1991). Efferent projections of the infralimbic (area 25) region of the medial prefrontal cortex in the rat: an anterograde tracer PHA-L study.Brain Res. Dec 6;566:26-39.
Takahashi YK, Roesch MR, Stalnaker TA, Haney RZ, Calu DJ, Taylor AR, Burke KA, Schoenbaum G (2009). The orbitofrontal cortex and ventral tegmental area are necessary for learning from unexpected outcomes. Neuron. Apr 30;62:269-80.
Thiebaut de Schotten M, Dell'Acqua F, Valabregue R, Catani M(2012). Monkey to human comparative anatomy of the frontal lobe association tracts. Cortex. Jan;48:82-96
Uylings HB, Groenewegen HJ, Kolb B (2003). Do rats have a prefrontal cortex? Behav Brain Res. Nov 30;146:3-17. Review.
Wallis JD (2011). Cross-species studies of orbitofrontal cortex and value-based decision-making. Nat Neurosci. Nov 20;15:13-9. doi: 10.1038/nn.2956.Review
Williams SM, Goldman-Rakic PS (1998). Widespread origin of the primate mesofrontal dopamine system. Cereb Cortex. Jun;8:321-45.

4.2 Hippocampal formation and Amygdala projections to the ventral tegmental area in the macaque monkey

ABSTRACT

The primate limbic system is composed of mesencephalic and diencephalic structures including the ventral tegmental area (VTA), the hippocampal formation (HF) and the amygdala (Amy). Amy is composed of different nuclei including the basal (B), basal accessory (BA), lateral (L), central (CeA), peryamigdaloid (PAC), paralaminar (PL) and medial (M) nuclei. The HF it is made up of the dentate gyrus (DG), Ammon Horn's fields (CA fields), Subiculum (S), Presubiculum (PrS), Parasubiculum (Pas) and entorhinal cortex (EC). In the present study, we examined the distribution of anterograde labelling produced in VTA with injections of biotin dextran amine or phaselous vulgaris lectin in distinct architectonic regions within Amy and HF. This examination confirmed prior evidence that CeA sends strong projections to VTA but it also revealed for the first time that other Amy nuclei do indeed projects to VTA as well. The lateral of B and dorsal part of BA provided the heaviest projections, and PAC and some specific parts of PL provided moderate projections. Injections in L, the medial part of B, the ventral part of BA and other parts of PL did not produce any labelling in VTA. Injections in HF produced in general sparse or no labelling with the exception of the Subiculum. Injections in EC produced labelling in VTA only if they spread to adjacent Amy nuclei, suggesting that EC does not project to VTA. The sources of these limbic afferent to VTA were all confirmed by the examination of the distribution of perikaryal labelling produced in Amy and HF with injections of retrograde tracers in VTA. A comparison of the spatial distribution of the anterogradely-labelled fibres in VTA revealed a considerable overlap of the projections from the different regions of Amy and HF with only a subtle trend to the rostral half of VTA, or distributed throughout the entire rostrocaudal extent of VTA, suggesting a coarse internal topography within the organization of the limbic projections to the midbrain. The present study reveals the existence of new direct monosynaptic projections to the VTA that may have a crucial role in the descending limbic control of dopamine release, in addition to classically known indirect polysynaptic projections. These direct projections could play a crucial role in optimizing the descending control of dopamine release in key limbic regions involved in the emotional valuation during reward and learning processing.

INTRODUCTION

Mesencephalic nuclei such as the ventral tegmental area (VTA) exert a broad and powerful modulation of hippocampal and amygdalar functions through the release of dopamine (DA). DA regulates the hippocampal formation (HF) during reward (Marting et al., 2011) and novelty detection (Ljunberg et al., 1992), and the amygdala (Amy) during fear conditioning (Blair et al., 2001; Fudge et al., 2010) and reward memory (Murray 2007, Gaffan et al., 1993). In turn, both HF and Amy has a potent excitatory (glutamatergic) effect on VTA (Harris et al., 2004; Jin et al., 2014; Floresco et al., 2001) that, along with inhibitory projections from the ventral pallidum (VP), peduncle pontine (PPT), and lateral dorsal tegmentum (LDT) (Floresco et al., 2001), controls the tonic and phasic release of DA during enhanced motor activity, cognition, and reward (Chergui et al, 1993; Johnson et al 1992b; Floresco et al., 2003). In the pathological side of the system, the desregulation of the DA neuromodulation has been associated with various serious psychiatric disorders such as autism, attention deficit, hyperactivity epilepsies (Janak et al., 2015), anxiety (Rauch et al., 2003) and Alzheimer (Gib et al., 1989). While there is a wealth of evidence for multiple indirect polysynaptic pathways substantiating the descending control of VTA by the limbic system in both rodents and primates (see below), the existence and organization of direct monosynaptic projections from HF and Amy to VTA has not yet been completely elucidated, in particular in non-human primates for which there are to date much less tract-tracing studies than in rodents.

Prior tracing studies, mostly in rodents, emphasized that the excitatory influence of HF on the activity of the DA cells of VTA occurs through two distinct polysynaptic pathways, one arising from the ventral hippocampus via the shell of the nucleus accumbens (NA) (Floresco et al., 2001) and another one from the dorsal hippocampus via the lateral septum (LS) and/or the rostro-lateral part of the NA (Rossato et al., 2009; Luo et al., 2011). In addition to these indirect projections, a recent functional imaging study in humans suggested a direct pathway from the ventral hippocampus (S and VCA1) to VTA during emotion and reward (Khan et al., 2013). Despite the lack of anatomical evidence for direct monosynaptic projection from the HF to the midbrain, retrograde tracer studies evidence direct projections from the VTA to the DG/CA1 (Amaral et al., 1980) and EC (specifically to midportions of the EC, Insausti et al., 1987).

In the case of the Amy, excitatory influence has been suggested to occur through a direct monosynaptic projection from the central (CeA) in monkeys (Price et al., 1981; Fudge et al., 2001; Fudge et al., 2000), in rats (Pardo-Bellver et al., 2012) and in cats (Holstege et al., 1985), and through indirect polysynaptic pathways from the basolateral (BLA) and paralaminar (PL) nuclei and the intercalated cells loosely situated between the Amy nuclei (Millhouse et al., 1986) via LS, the reuniens nucleus of the medial thalamus and the Nucleus Accumbens (NA) (Price et al., 1981; Fudge et al., 2012). A recent study in rodents however indicated that most projections from CeA end in the neighboring substantia nigra with only limited direct projections to VTA (Lee et al., 2010).

Furthermore, dopamine fibers occur not only in CeA but also in the parts of the basal and basolateral nuclei (Sadikot and Parent, 1990), both of which could also potentially send direct projections to VTA.

While most knowledge on the efferent projections to VTA come from rodent work, the existence and organization of projections from HF and Amy to VTA in primates cannot be simply derived from tract-tracing studies in rodents. For example, it is often assumed that the rodent and primate VTA share the same overall organization (Sesack and Grace, 2010); however, up to 8 nuclei have been defined for the rat VTA (Gasbarri et al., 1994b) whereas only 2 nuclei are usually mentioned for the monkey VTA (Wilhelmus et al., 2000; Cho et al., 2010; Mc Ritchie et al., 1998). Similarly, while the hippocampus *per se* remains fairly similar across species, the entorhinal cortex (EC) which is a major part of HF has two general areas in rats, the lateral and the medial, although a further number of subdivisions closer to the primate EC has also been described (Insausti et al., 1998), in primates we recognized 7 different areas (Amaral and Insausti 1987; Amaral and Insausti 1990). Specific nucleus of Amy in primates are relative enlarged (Pitkänen et al., 1988; Turner et al., 1980; Andy et al., 1968; Stephan et al.,1977) and shows particular cytoarchitecture features (Chareyon et al.,2011) responsible for the different processing of the incoming information that are not necessarily present in rodents. Specifically, the basal nucleus of Amy (B) which shows strong connections with HF, the prefrontal cortex (PFC), VS and other Amy nuclei (except for the lateral nucleus; L), heavily projects, all along with L, to the central Amy nucleus (CeA) inducing the enlargement of this structure in primates. Thus, in order to better appreciate the organization of the efferent to VTA in primates, a proper examination in the laboratory species closer to humans is needed.

In order to know how the information related to one hypothetical value, evaluated by the Amy and HF, could possibly modulate the DA cells of the VTA, one major source of the DA to the cortex and striatum (Haber et al., 2003), we examine the distribution of anterograde labelling produced in VTA with injections of tracers in various parts of HF and Amy, and the distribution of retrograde labelling in HF and Amy produced with injections of tracers in VTA in macaque monkey.

MATERIALS AND METHODS

The present data were obtained from a total of 71 adult male cynomolgus or long tailed macaque monkeys (*Macaca fascicularis*) that received microinjections of anterograde tracers in the HF or amygdala; seven monkeys received microinjections of retrograde tracers in or around the VTA. The experiments (tracer injections) were conducted, chronologically, at the MIND institute of the University of California in Davis, CA, USA, at the Max Planck Institute for Biological Cybernetics in Tuebingen, Germany, and at the University of Albacete in Spain. All procedures were approved by the corresponding local authorities and followed the directives of the National Institute for Health (USA) or the European Union directives 86/609/CEE. The tracer injections at the MIND institutes

were made in the context of separate studies that have for the most part been published in prior reports (Amaral et al., 1981). The tracer injections in Spain and Germany were made mainly in the context of the present study and have not been reported elsewhere yet.

Tracer injection

The procedure of the tracer injection varied with the institution in which it was made. The anatomical guidance alternatively used basic stereotaxic, MRI guidance or a mix of both. The injections were made using Hamilton syringes or glass micropipettes, pressure injections or iontophoresis. Nevertheless, all tracers and the criteria to define the quality of an injection site were the same.

For the MRI, each monkey was placed in an MRI-compatible stereotaxic frame under anaesthesia. MRI scan images were obtained with a 1.5T Philips scanner using a coil placed over the top of the head of the animal (Spain) or with a 7T Bruker scanner using a 3-part head coil (Germany). For each individual animal, stereotaxic coordinates were calculated for every single desired injection in Amy, HF or VTA and compared with the atlas of Szabo and Cowan (1984) or of Saleem and Logothetis (2008). In some cases, additionally, electrophysiological recordings were made to refine the coordinates for deep injections (Amaral et al., 1981).

For the surgery, the animal was sedated by an intramuscular injection of ketamine (8 mg/kg) followed by sodium pentobarbital (25 mg/kg, i.v.); the anaesthesia was then induced and maintained either by intubation with isofluorane or remifentanil. The animal was placed in the Kopf stereotaxic frame. The skin was incised and the cranium trepanned above the region of interest. For most of the HF injections, the injection sites were determined using stereotaxic coordinates derived from the MRI. However, for some of the tracer injections into deep cortical areas, an insulated tungsten electrode was inserted along the expected track of the pipette for electrophysiological recordings of spontaneous activity of the structural boundaries between grey and white matter or the bottom of the brain which allowed determining the exact vertical coordinates determined firstly by the MRI. Once the target identified, retrograde tracer (Fast Blue [FB; 3 %]; Cholera Toxin B [CTb 1%]; fluorescent dextrans [FD; 10%]) or anterograde tracers (biotinylated dextran amine [BDA; Molecular probes 10%] and Phaseolus Vulgaris [PHAL; 2.5 %]) were injected in the brain. The injections were made through a micropipette using 25-msec air or hydraulic pressure pulse (BDA, FB, CTb, and FD) or using iontophoresis (PHAL) with 7 second-ON and 7 second-OFF pulses during 45 min. The air pressure was adjusted so that very small volumes of tracer were injected in each pulse (Kondo et al., 2005). To avoid spread of the tracer into areas along the pipette track, the micropipette was left in place for 15-30 minutes after the injection was finished. After surgery, the skull and skin were closed, and a long lasting analgesic and antibiotics were given to the animal after anaesthesia.

Fixation and histological processing

After a survival period of approximately two weeks, the animals were sedated with ketamine followed by sodium pentobarbital (25-30mg/kg i.v. or i.m.). Then, the animals were euthanized with a lethal dose of pentobarbital and perfused transcardially with saline, followed of 4% paraformaldehyde solutions at pH 6.5 and pH 9.5 (Pitkanen et al., 1998) and 10% sucrose at pH 9.5. Then the brain was removed and placed in 30% sucrose in phosphate-buffered saline (PBS) until it sank. Three days later, the brain was frozen with dry ice and cut into 5 to 10 collated series of 50 microns coronal sections (Cowan et al., 1972). BDA was processed histochemically with biotin-horseradish peroxidase technique, and PHAL was visualized immunohistochemically, and counterstained with Giemsa, that allowed the visualization of the diaminobenzidine reaction product. FB and FD are readily visible via epifluorescence. CTb was visualized using standard CTb immunohistochemistry (Evrard and Craig, 2008).

Data analysis and presentation of illustrations

Mounted sections were examined under bright field and epifluorescence microscope. Injection sites, anterogradely-labelled axonal varicosities (in VTA), and retrogradely-labelled perikarya (in HF and Amy) were manually plotted using a microscope-digitalized system (Minnesota Datametrics, St. Paul NM). For sparse labelling, each fibre segment was plotted as a single point. However for dense labelled areas, 4 points indicated medium dense varicosities greater than 10 fibres/ per surface unit and a rating of 6-8 points indicated strong labelling with a density range greater than 25 fibres/ per surface unit . In some cases, strong background staining had to be subtracted out. We mapped the injection sites and the labelling in successive linear traverses across the section. Finally, architectonic boundaries were drawn onto printed plots by using camera lucida with adjacent sections stained for Nissl. The labelling was analysed bilaterally. Coronal maps were prepared to visualize the distribution and the density of labelled varicosities or cell bodies. Because each map was prepared for each case, we could not directly compare the overlap of the labelling (see Results). Also, the relative strength of connections was qualitatively estimated but absolute values could not be determined. The reason why we could not compare absolute values are inherent to the tracing methods used; it was because of different factors such as differences in the efficiency of the transport between the different tracers, the variability in the volumes of the injection site and difficulty of the reproducibility of injection sites in the same location.

Nomenclature

The terminology used for VTA nuclei was adapted from Paxinos (2007) and the borders of each midbrain nucleus composing and surround VTA were defined according to the morphology of the cells in the Nissl staining along the rostro-caudal axis of VTA. A detailed description is provided in the Results section.

According to Amaral and Insausti, we considered 7 different Amy regions: the basal nucleus (B) that included a magnocellular (Bmc), intermediate (Bi) and parvicellular (Bpc) division; the basal accessory nucleus (BA) that included a magnocellular (ABmc), parvicellular (ABpc) and ventromedial (ABvm) division; the lateral nuclei (L) that contained a dorsal (Ld), dorsal intermediate (Ldi), ventral intermediate (Lvi) and ventral (Lv) division; the central nucleus (CE); the medial nucleus (M); the cortical nucleus (CO); the paralaminar nucleus (PL); the periamygdaloid cortex (PAC); and the amygdalo-hipocampal area (AHA) (Chareyron et al., 2011).

For the hippocampal formation we distinguished: the Dentate Gyrus (DG), the Ammon's fields (CA1, CA2, and CA3), the subicular complex (Subiculum, Presubiculum, Parasubiculum) and entorhinal cortex (EC). EC is the region that receives the information from the polysensory association regions of the neocortex and it is one of the major sources of HF inputs to Subiculum and the gateway of the information from the HF (Van Hoesen and Pandya 1975). EC was differentiated into seven different levels: two rostral levels (E_O and E_R), two lateral levels (E_{LR}, E_{Lc}), one intermediate (E_I) and two caudal (E_C, E_{CL}).

RESULTS

Injection sites in the HF and amygdala

A total 87 anterograde tracer injections were placed in different parts of the amygdala and HF, including 17 injections in the hippocampus and DG, 15 injections in EC (with 8 injections that included also some parts of the amygdala), and 27 injections in the amygdala. The photomicrographs and drawings in Figure 1 shows example of injection sites in HF and Amy. All injection sites consisted in a dense core surrounded by a distinct paler halo. Injection sites for BDA mostly appeared larger and denser than injection sites for comparable volumes of PHAL, which is largely due to the better control of the injections with iontophoresis (but lower tracing gain). Injection spread was generally greater in vertical penetration than medio-lateral. In most cases, the halo of the injection sites was small and confined to one architectonic region with no spread or with spread of varying size to adjacent regions, as described below. The following paragraphs describe all of the injections of anterograde tracers. Figures 2, 3 and 4 show a schematic composite collating all of representative injection site onto simplified maps of the amygdala, hippocampus, and EC, respec-

tively. The ellipsoid shapes represent both the core and halo of the injection site. The ellipsoid shapes filled in red indicate the injection sites that produced anterograde labelling in VTA. The empty ellipsoid shapes indicate injection sites that did not produced labelling in VTA. Injections were made in the left or right hemisphere but were all illustrated on the right side for consistency.

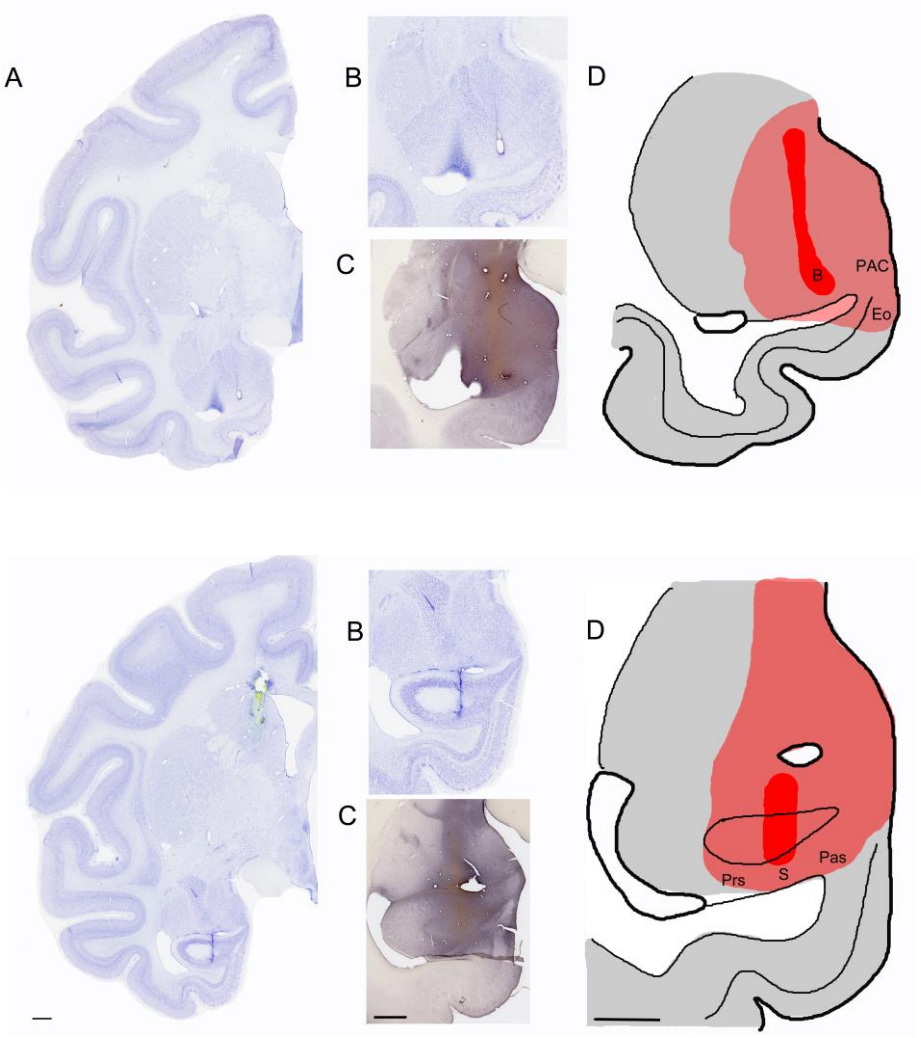

Figure 1. From the top to the bottom: examples of injections sites in Amygdala (M1-09BDA) and Hippocampal Formation (M4-08BDA). (A) Photograph of coronal section of half of the hemisphere of the monkey brain (B) Detail of the Injection site in Nissl (C) Detail of the injection site BDA (D) Drawing of the injection site in red the core and in pink the hallux. Scale bar =1mm

Amygdala.

Twenty seven injections were placed in different regions of Amy (Fig. 2). Two injections were made in PAC; one spread to AHA (M2-15BDA) and the other one to the piriform cortex (M5-05 BDA). (Both AHA and the piriform cortex were located at a level posterior to the level shown in the standard map.) Eight injections were centred in Bmc; six injections were confined within Bmc (M2L-03BDA; M1-03RBDA, M6-97BDA, M4-09BDA, M6-94PHAL; M2-03PHAL); one spread to Bi (M3-

95BDA) and another one to Bi and L (M5-97PHAL). Seven injections were centred in Bi (M1-95PHAL; M6-98BDA; M7-98BDA; M12-98PHAL; M6-94PHAL), including two that spread to Bpc (M11-98BDA, M2-98BDA). One injection was confined to Bpc (M4-97BDA). Four injections were made in PL (M12-91PHAL; M2-95LPHAL; M3-98PHAL; M3-10BDA) with a minimal spread to Bpc. Three injections were made in L, two in Lv (M11-88PHAL, M6-91PHAL) and one in Ld (M8-89PHAL). Two injections were made in ABpc (M15-98BDA; M14-97BDA).

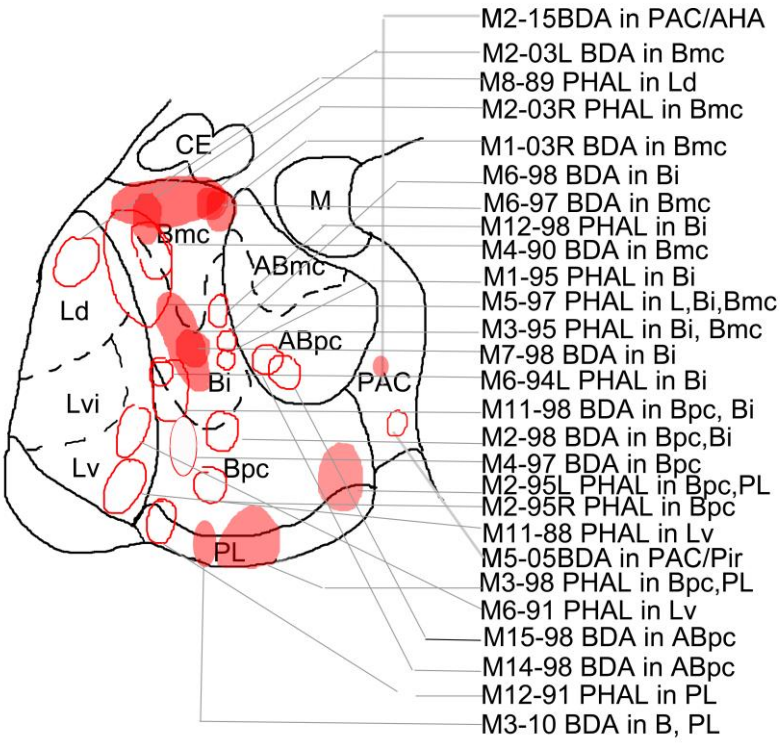

Figure 2. Topology of the injection sites in Amy using a relative collation of all injection sites onto a standard map of Amy. The ellipsoid shapes represent both the core and halo of the injection site. The ellipsoid shapes filled in red indicate the injection sites that produced anterograde labeling in VTA. The empty ellipsoid shapes indicate injection sites that did not produced labeling in VTA.

Entorhinal cortex.

Twenty three injections aimed EC (Fig. 3). Four injections were made in the rostral E_R (M06-98BDA; M12-98BDA, M3-98BDA and M10-97PHAL), one in E_C (M10-98BDA), one in E_I (M3-15BDA) and two in E_{CL} (M6-11BDA and M5-08BDA). Other injections included different parts of EC; one included E_I and E_O (M7-09BDA), one included E_I, E_C and E_{CL} (M3-98FR), three injections included E_C and E_{CL} (M2-97PHAL, M10-96PHAL and M13-98FR), one included E_{LC} and E_{CL} (M1-97PHAL), and one included E_{LC} and E_{LR} (M11-97BDA).

Eight injections centred in EC spread to some parts of Amy or HF. One injections made in E_{lr} included AB (M8-09BDA); another that included E_O and E_R also spread to AB (M1-07BDA).

Injections in E_o included also PAC and B (M1-09BDA) or PAC (M7-09BDA), and one injection that included E_O, E_R and E_{LR} also spread to Bpc (M11-09BDA). Finally, two injections included PAC, Prs and EC (M4-10BDA), or Prs and E_I (M6-09BDA).

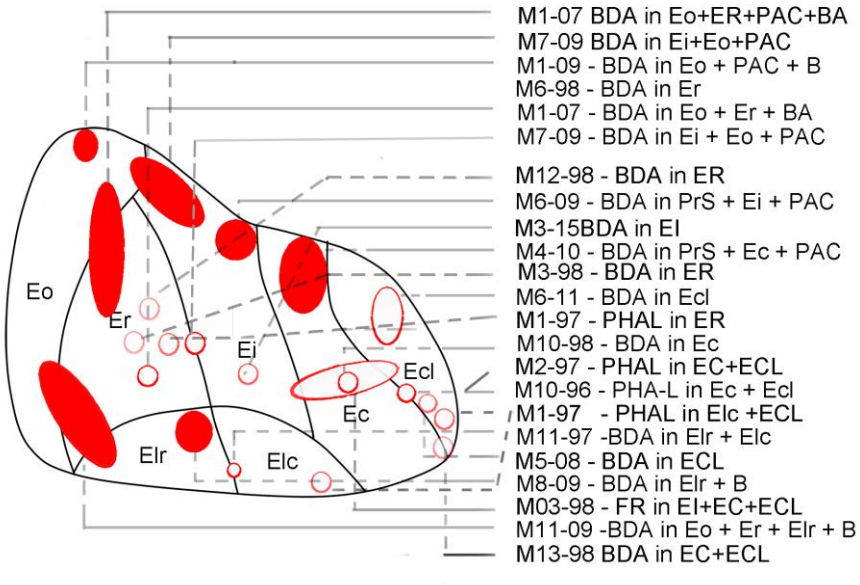

Figure 3. Topology of the injection sites in EC using a relative collation of all injection sites onto a standard map of EC. The ellipsoid shapes represent both the core and halo of the injection site. The ellipsoid shapes filled in red indicate the injection sites that produced anterograde labeling in VTA. The empty ellipsoid shapes indicate injection sites that did not produced labeling in VTA.

Hippocampus and Subiculum.

A total of 30 injections were placed in the hippocampus and Subiculum. Because most of these injections did not produce labelling in VTA (see below) and because many injections sites over-lapped, only subsets of resentative injections were mapped onto the standard composite map (Fig. 4). Seven injections were placed in DG (M2-01PHAL; M2-01BDA; M4-01PHAL; M4-01BDA; M1-02PHAL; M2-02BDA; M10-02PHAL) among which two are shown in Figure 4 (M02-02BDA; M04-01PHAL). Five injections were made in CA3 (M4-02PHAL; M3-02PHAL; M4-02BDA; M10-02BDA; M9-03BDA) among which one is represented (M10-02BDA). One injection was made in CA1 (M2-04PHAL; not shown). Fourteen injections were made in CA3 (M2-04BDA; M1-92PHAL; M5-92PHAL; M9-92LPHAL; M9-92RPHAL; M11-92PHAL; M13-92PHAL; M27-92PHAL; M10-93PHAL; M1-05BDA; M5-02PHAL; M07-02BDA and M07-03PHAL; M9-93PHAL), among which three were represented (M5-02PHAL; M2-04BDA and M7-03PHAL). Eleven injections were made in CA1 (M2-92PHAL; M10-92PHAL; M28-92PHAL; M30-92PHAL; M1-93PHAL; M2-93PHAL; M9-93BDA; M8-09PHAL; M8-03BDA; M14-03BDA and M14-03PHAL) among which two were shown (M2-92PHAL and M9-93BDA). Finally, one injection was placed in CA2 (M10-93BDA). Three large injections

included some parts of the subicular complex. One contained PreS, S, PaS and CA1 (M04-08BDA), and two others included PAC and EC (M04-10BDA) or PAC and EI (M06-09BDA). In all but a few cases, the tracer injections involved most layers of grey matter and did not extend to the white matter. Furthermore, single and larger injections included different parts of the EC.

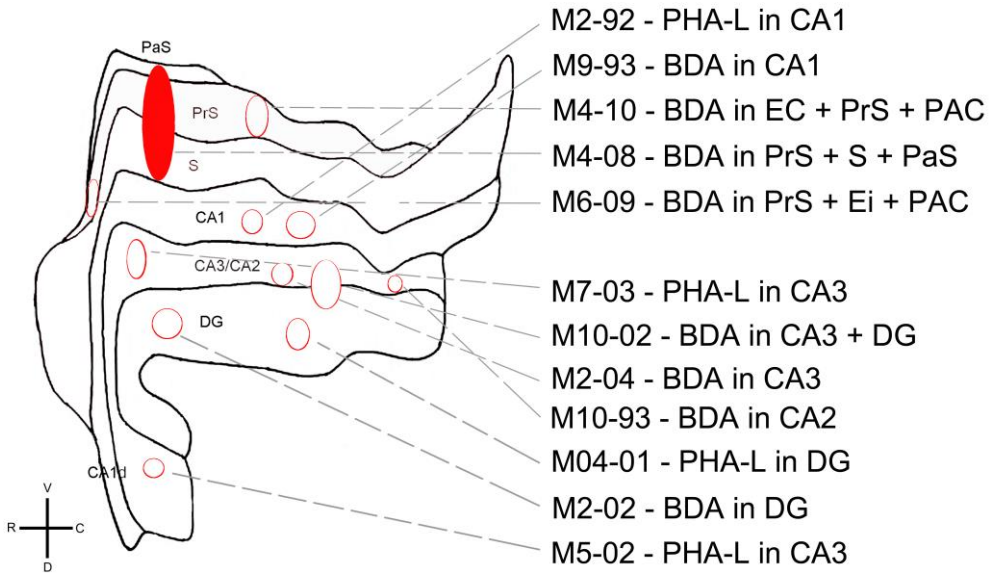

Figure 4. Topology of the injection sites in hippocampus using a relative collation of all injection sites onto a standard map of hippocampus. The ellipsoid shapes represent both the core and halo of the injection site. The ellipsoid shapes filled in red indicate the injection sites that produced anterograde labeling in VTA. The empty ellipsoid shapes indicate injection sites that did not produced labeling in VTA.

Injection sites in VTA

To confirm the projections inferred from the analysis of the anterograde labelling in VTA, retrograde tracers injections were made in or around VTA. Injections within VTA involved different adjacent nuclei and were placed at different rostro-caudal or medio-lateral levels. Out of the seven cases injected (see Methods), only three produced retrograde labelling (M2.15FB, M3.15FB and M9.9FB). Figure 5 depicts the injections sites in the VTA, as drawn coronal sections. The injections were relatively small and showed a core and a halo of deposit. Injections within VTA involved different nuclei and were placed at different rostro-caudal or medio-lateral levels.

One injection of FB was made in rostral VTA (M3.15; Fig. 5D). One injection of FB was made in the lateral aspect of the middle AP extent of VTA (M2.15; Fig. 5E). One injection of FB was made in the caudal end of VTA (M9.09 Fig. 5I). All sites were relatively small and did not spread extensively to adjacent regions.

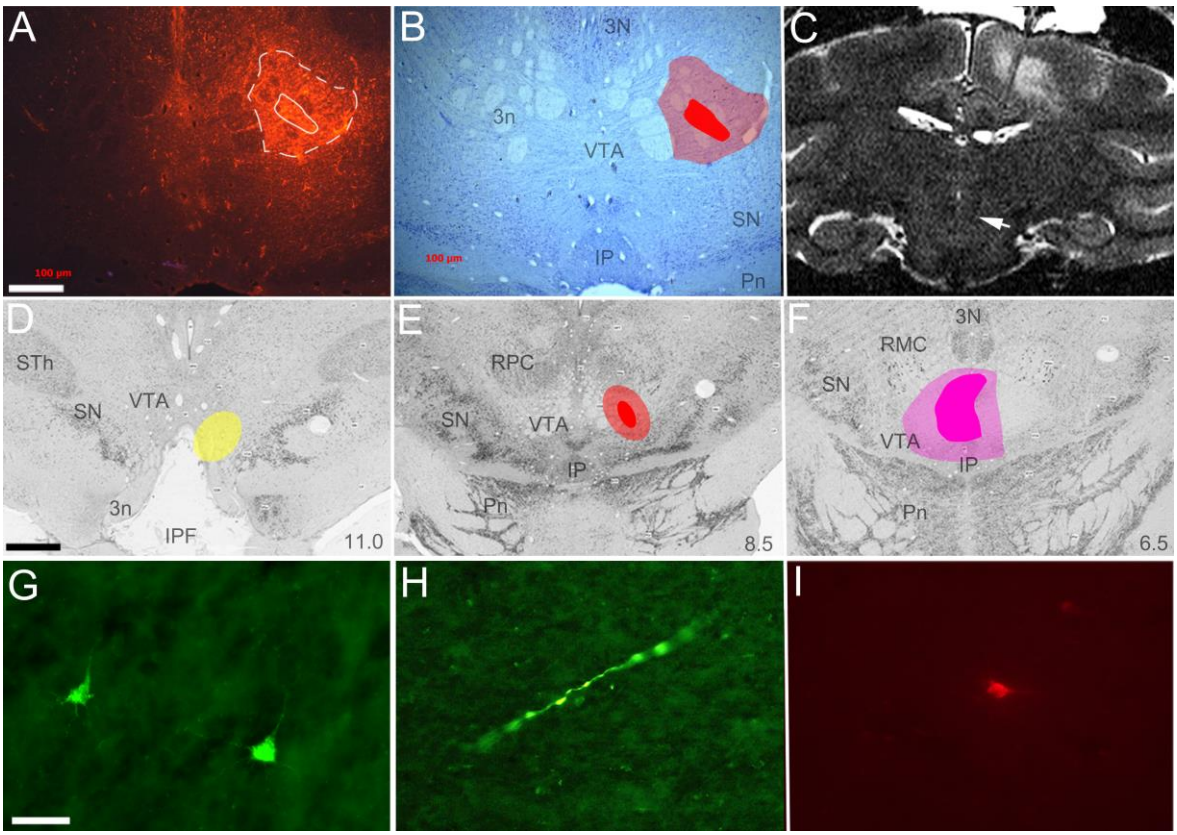

Figure 5. Photomicrographs of adjacent coronal fluorescent (A) and Nissl-stained (B) sections showing Pdex injection site in case cm28; the core and halo (circled by continuous and dashed lines, respectively) and their plots onto Nissl-stained photomicrographs of VTA, respectively. C. MRI section showing the location of the fused silica micropipette used to inject Pdex in VTA. D-F. Injection sites from cases cm018Rdex ('yellow'), cm017Rdex ('green'), cm020Rdex ('purple') and cm024Pdex ('red') depicted on a set of 3 photomicrographs through four representatives AP levels of VTA. G-I. Photomicrographs of representative retrograde (G) and anterograde (H, I) labelling produced with an injection of Rdex (G, H) or BDA (I) in VTA. Left is medial and top is dorsal. Scale bar = 150 µm (A, B), 1 mm (D-F), and 20 µm (G-I).

Anterograde labelling in VTA

Architectonic mapping of VTA.

A prerequisite to the description of the distribution of anterograde labelling in VTA is a mapping of VTA to use as a reference. Figure 6 shows an architectonic map of VTA and various neighbouring nuclei or regions of the midbrain across 4 representative anteroposterior levels of the left VTA. The absence of the mammillary nuclei at the most rostral level indicated somewhat the rostral end of VTA at approximately -10.80 mm from the antero-posterior Bregma (AP) which correspond to our level 0 in Figure 6. VTA was co-existent with and ventral to the obvious red nucleus (RN and then its

magnocellular part, RMC) throughout its almost entire rostro-caudal extent (level 1350 to 3150), and it was intermingled within the fibres of the third (oculomotor) nerve at the level of 2500. At its middle level, VTA was located dorsal to the interpeduncular fossa (IF), which, with the middle line nucleus, splitted VTA into two distinct sides. At more caudal levels, IF was replaced by the interpeduncular nucleus (IP) at (AP -14.40 mm; level 2500). The level where RM led to RMC also indicated the beginning of the tail of the VTA. The level of decussation (xscp) delimits the caudal level of the VTA that will continue further caudally until reaching AP 16.40mm (not shown).

General observation on the anterograde labelling in VTA.

All of the injections in this study produced anterograde and sometimes retrograde labelling in the VTA. Figure 7 presents examples of anterogradely labelled fibres bearing varicosities and neurons with BDA in VTA. The morphology of the labelled fibres was consistent with the presence of synaptic terminals in this region. Thicker labelled fibres of passage were found mostly around the oculomotor nucleus; that is not in VTA. Although it could be possible that some collateral of retrogradely label cells could be found, we almost did not find any retrograde labelled cells with BDA (which is sometimes both anterograde and to some extent retrograde) and found none with PHAL (almost exclusively anterograde). Moreover, labelled fibres contained varicosities and were arborized, keeping a consistent morphology of axon terminals and not collaterals (Haber et al., 2000). The size of the labelled fibres varied depending on the injection site; however the general overview showed short-medium labelled fibres segments. The number of anterogradely-labelled fibre segments in the contralateral midbrain represented barely 5 % of the number of labelled cells in the ipsilateral.

The projections within the VTA were characterized by broadly dispersed fibres mixed with clusters of denser labelling. The labelling was distributed mainly in the rostral half of the main VTA, while some labelling extended to the lateral PBP, and scarce to no labelling was seen in ventral PN or SN, with the exception of the SN pars compacta (SNc; Fig. 6) in a few cases (see below). There was no apparent medio-lateral variation in the abundance of labelling at single anteroposterior levels. There was however a dorso-ventral variation with no labelling in the ventral area confined to PN.

The abundance of labelling in VTA depended to some extent according to the exact position of the injection site within a given region. For example two injections place in BI (M7-98BDA and M1-95PHAL) produced labelling and no labelling, respectively, suggesting a complex internal topography. However, in general, the abundance of labelling mainly varied according to the localization of the injection site across the greater subdivisions HF or Amy. Most labelling in the VTA was obtained with injections made in the Basal nucleus, followed by PL, PAC and the subicular complex. There was no labelling produced with injections in Amy's L and AB, in EC proper, or in the hippocampus with the exception of the Subiculum. In the following text we will describe the labelling from injections in Amy, EC and hippocampus, successively. When one injection included different areas of HF or EC but the same part of Amy, we compared them in terms of HF and EC.

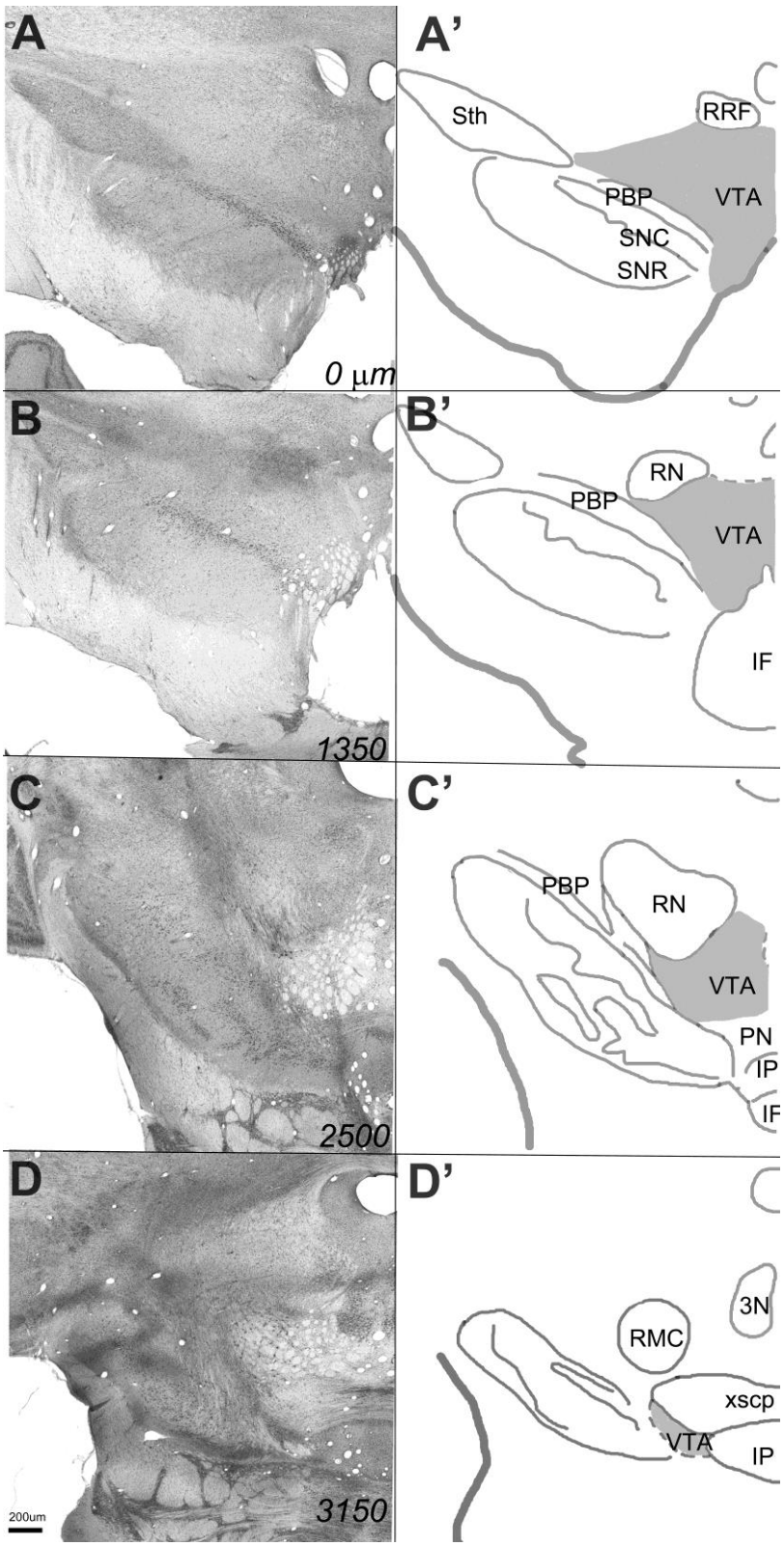

Figure 6. . Architectonic mapping on a series of (A-D) coronal photography's of Nissl and the corresponding drawing (A'-D') through the rostro-caudal axis of the VTA. STh: Hypothalamic nucleus; RRF: Retrorubral Field; PBP: Parabrachial Pigmentosus nucleus; SNC: Sustancia Nigra Compacta; SNR: Sustancia Nigra Reticulata; RN: Red nucleus; IF: Interpeduncular Fossa; IP: Interpeduncular nucleus; RMC: Red magnocellular nucleus; xscp: decussation. Scale bar 200um

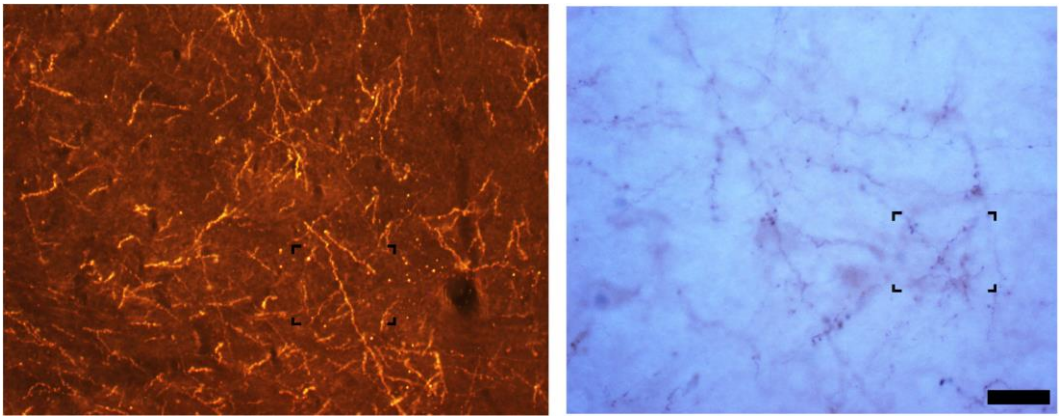

Figure 7. Photomicrographs showing examples of fibres bearing varicosities in VTA labelled with injections of BDA in the amygdala (A) and hippocampus (B). Scale bar= 1mm

Labelling from Amy injections.

Only the injections made in B and PL, and one small injection made in PAC did produce antero-grade labelling in VTA (Fig. 2; filled ellipsoids). Despite repeated injections, none of the injections made in L, AB, or yet other parts of Amy produced labelling in VTA (Fig. 2; empty ellipsoids). Figure 8A-H shows the plots of anterogradely labelled fibres with varicosities in (dark red) and around (pink) VTA on consecutive coronal sections of the ventral midbrain in 8 representative cases in which an injection of BDA of PHA-L produced labelling. While labelling was obtained in several cases with injections in B, only 5 out of 15 injections in B produced labelling (Fig. 2). The three injections made in the dorsal most portion of Bmc all produced moderate labelling in VTA and in SNc (e.g., M1.03, Fig. 8A; M2-03, Fig. 8B). The more ventral injections (M4-90 and M5-95; Fig. 2) did not label VTA. Out of the 9 injections that touched Bi, only the two injections made in the centre (including one also spreading to Bmc) produced labelling in VTA (M3-95PHAL, Fig. 8E); his labelling was however scarce and mainly distributed in the lateral parts of the VTA. Only the one multiple injection (M3-95PHAL; Fig 8E) showed labelling in the VTA itself. In all cases however, the projections to the SN were very poor. None of the injections made only in Bpc showed labelling in the midbrain (M4-97BDA, M2-95PHAL; Fig. 2) but also the injections that included both Bpc and the ventral margin of Bi did not produce labelling (M11-98BDA and M2-98BDA), suggesting all together that Bpc does not project to VTA. Three out of 4 injections including PL produced labelling in VTA (M2-95PHAL; M3-98PHAL; M3-10BDA; Fig. 2 and Fig. 8G), suggesting that at least the central and medial parts of PL projects to VTA, or that the labelling originates from a subgroup of cells called the intermediate cells and that are mainly GABAergic and dispersed in between the PL and Bpc nuclei of Amy. Finally, none of the injections centred in L showed labelling in the midbrain even the ones that also included other parts of the Amy (M5-97PHAL) (Fig. 2). Similar results were observed after single injections in ABpc (Fig. 2).

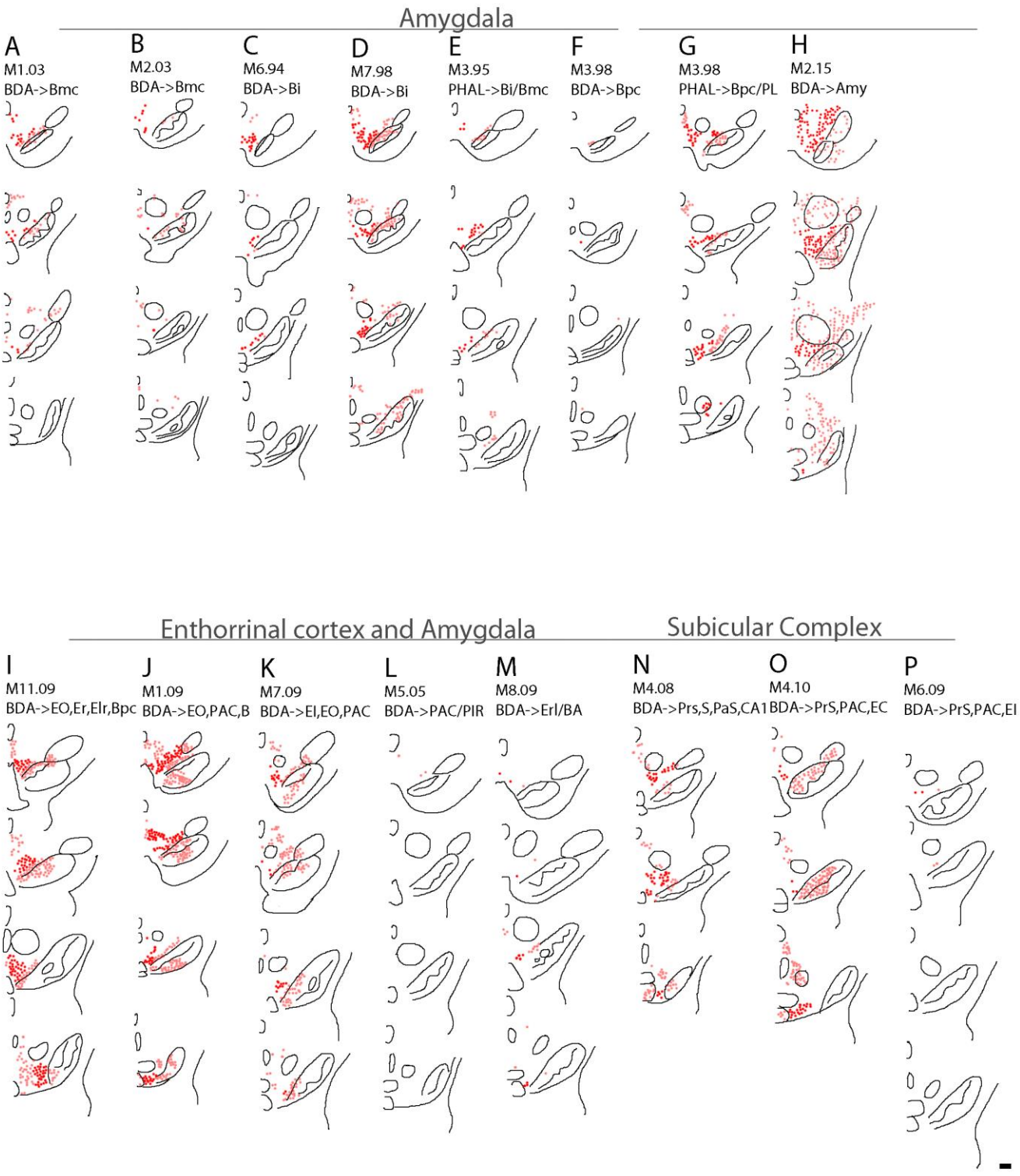

Figure 8. (A-O) Plot of anterograde labeling in the midbrain, after injections of tracers in Amy or HF. The dark red labeling corresponds to labeling in VTA. The pink labeling corresponds to labeling outside VTA. Scale bar= 1mm

Labelling from EC injections.

Among the different injections aiming EC, only the injections that spread to Amy or the Subiculum complex produced labelling in VTA (Fig. 3; Fig. 8 I-M). Injection M11-09BDA centred in E_r but spreading to other parts of the EC and Bpc produced strong labelling along the VTA that included several nucleuses (Fig. 8I). All injections made in E_o that spread to some parts of the Amy, including M1-09BDA, also produced a strong labelling in VTA and various other midbrain nuclei (Fig. 8J).

Sparse labelling was produced by an injection in E_o but with spread to PAC instead Bpc (M7-09BDA; Fig. 8K); supporting the prior observation that PAC contributes with less projections than Bpc (see above). All of the injections in E_o also spread to E_{LR} and/or E_i. However, none of the injections confined to these two EC regions produced labelling in VTA (e.g., M3-15BDA; Fig. 3). Like for E_o, only the injections in E_{RL} that spread to B (M8-09BDA) produced labelling in VTA (Fig. 8M); and one injection centred to E_l that spread to PAC and PrS also produced sparse labelling in VTA (M6-09BDA; Fig. 8P). However, none of the other injections in E_l that did not spread to Amy or HF produced labelling.

Particularly interesting is to compare the previous case mentioned before (M6-09BDA; Fig. 8P) with the case that also included PAC and PrS but E_c (M4-10BDA; Fig. 8O) that produced stronger labelling, suggesting that maybe E_c could project to VTA. However, one single injection placed in E_c that did not spread to PAC or PrS also did not produce labelling in the midbrain suggesting that the presence of fibres after larger injections in E_c were due to the PrS and/or PAC. Finally, none of the injections that included E_R, E_{Lc}or E_{CL} and that did not spread to Amy produced labelling.

Labelling from the hippocampus and Subiculum complex.

None of the injections confined to the different fields of the hippocampus proper produced labelling VTA. Only one injections that reached the Subiculum (M4-08; Fig. 4) produced moderate labelling in VTA, which is in agreement with the three cases in which labelling was produced in VTA likely because of the spread of EC-centred injections to PrS (see above and Fig. 8N-P).

Topographic distribution of the anterograde labelling

Only scant evidence or trends for a topographic were observed. For instance, in the Basal nucleus of the Amy we didn't found any topography since the density of the labelling within the Bmc changed substantially depending on the location of the injection. Moreover, one dual injection including Bmc but most of the Bi (M3-95PHAL) showed scarce labelling mainly in the lateral portions of the VTA. Injections in PL (M3-98PHAL; M2-95BDA) produced moderate labelling in comparison with the ones mentioned before; in general this labelling was situated more into the medial than lateral parts of the VTA. One injection placed in B, without specify the subnucleus, PAC and some parts of EC (M1-09 BDA) showed the strongest labelling within the VTA with medio-lateral preference and with a

presence all along VTA. However, this result is not conclusive due to the fact that we can't elucidate which area is the responsible for this projection. Three further injections that included PAC (M4-10BDA; M7-09BDA; M609BDA) showed labelling mainly in SN and some in the middle VTA, however, another injection placed in PAC (M12-91PHAL), showed no projections to the midbrain.

On the other hand, to estimate the overlap or the dispersion of the labelling produced in VTA with different Amy and HF injections; we examined dual cases, monkeys which had more than one injection with differently-coloured tracers. For example in case M2-03, injections placed in different parts of the Bmc (M2-03LBDA and M2-03RPHAL; see Fig. 2) showed that different parts of this subnuclei produced different amount of labelling (perhaps due to the different tracers) although in both cases the labelling was distributed all along the rostral and middle parts of the VTA, without apparent difference in distribution.

Retrograde labelling in HF and Amy

Figure 9-11 show plots of the retrograde labelling onto individual coronal maps of the medial temporal lobe passing through the ventral striatum in all three cases: M3-15FB (Fig. 9), M2-15FB (Fig. 10), and M9-09FB (Fig. 11). All cases showed labeling in the ventral striatum (data not shown) but only two of them showed labeling in Amy. Some isolated cells were found in the Basal, Lateral and Basal accessory nuclei cells, and a band of intercalated cells described before only from the injection placed in the rostral VTA (M3-15FB; Fig 9). Strong labelling also was found in the central, cortical and medial nuclei of the Amy from injections in the lateral VTA (M2-15FB; Fig 10). Only projections from the Subiculum and rostral entorhinal cortex showed projections, and therefore target the rostral VTA (M3-15FB; Fig 9). In contrast, caudal VTA (M9-09FB; Fig 11) showed scarce or no projections from the amygdalo-hippocampal complex, in agreement with the anterograde results observed above. However, projections from the striatum were found, but it varied greatly with the location of the injection site in VTA.

Rostral VTA.

The FB injection in rostral VTA in M3-15FB produced a relatively dense to moderate labelling in several distinct architectonic areas in the Amy. The pattern of labelling confirmed the anterograde labelling obtained in VTA with injections in the B nucleus and the Intercalated nuclei of the Amy Further projections were found arising from the Subiculum. These results confirm idea of "patchy" projections from the different subgroups of cells within the Amy.

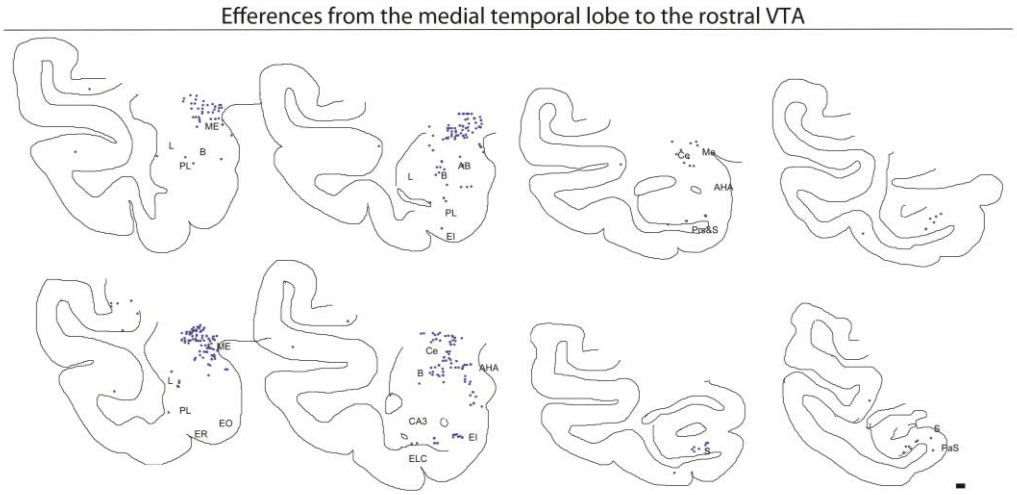

Figure 9: Plots of retrograde labeled cells in the HF and Amy from one injection placed in rostral VTA, case M3-15FB. The dots correspond to individual neurons labeled retrogradely within the medial temporal lobe. Scale bar = 1 mm

Lateral VTA.

The FB injection in lateral VTA in M2-15FB produced a relatively weak labeling in the Amy in similar architectonic areas than in case M3-15FB. The pattern of labeling confirmed the anterograde results obtained in VTA with injections in the B nucleus of the Amy. However, no projections were found from the HF suggesting that the targets to the different groups of the VTA could be topographically organized.

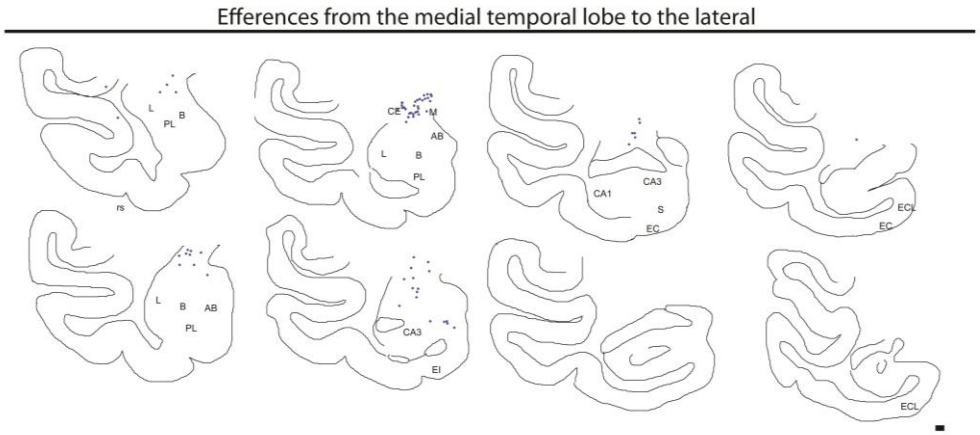

Figure 10: Plots of retrograde labelled cells in the HF and Amy from one injection placed in the lateral VTA, case M2-15FB. The dots correspond to retrograde labelling within the medial temporal lobe. Scale bar = 1 mm

Caudal VTA.

The FB injection in caudal VTA in M9-09FB produced a very scarce or no labeling in the Amy and HF, suggesting that the tail of the VTA might be modulated independently from the rostral and middle parts of the nucleus.

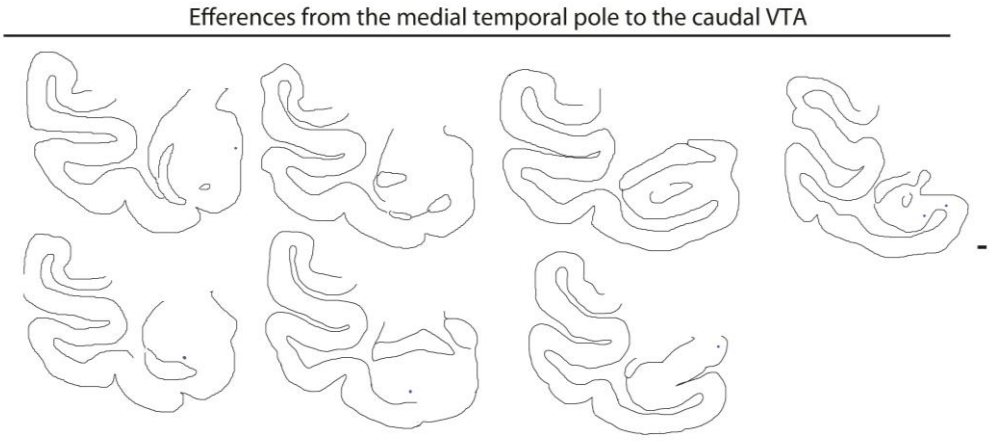

Figure 11: Plots of retrograde labelled cells in the HF and Amy from one injection placed in the caudal VTA, case M9-09FB. The dots correspond to retrograde labeling within the medial temporal lobe. Scale bar = 1 mm

DISCUSSION

Prior anatomical studies concluded that the main flow of information from Amy and HF to VTA goes through interposed nuclei (ventral pallidum, ventral striatum and medio dorsal nucleus of the thalamus) (Price et al., 2010). In the present study, we showed the existence of substantially less dense projection, than the classical mesolimbic pathway, but still very consistent direct monosynaptic projections to VTA from Amy nuclei other than CeA and from the Subiculum of the HF. In Amy, the projections generally originated from the basal nucleus with major internal variations possibly depending on the subgroup of cells implicated in the injection more than the subnuclei itself. The labelled fibres were distributed within the main VTA and in the lateral part (PBP) without any clear topography, although there was a preference for the anterior half of the VTA. In HF, the projections to rostral-middle VTA originated exclusively from the Subiculum. A careful differential analysis of the labelling produced by injections centred in other parts of HF (DG, CA1-3) and EC showed that none of these regions provides projections to the VTA Supporting this idea, studies carried out in rodents by Chandler et al., in 2014 demonstrated that the connections within the VTA are organized upon their different cell groups. Particularly, it has been found only labeled neurons in the rostral part of the VTA after placing retrograde tracers in a particular location of CA1, CA3 and DG (Swanson *et*

al., 1982), and much more restricted projections from the caudal VTA (Schwab *et al*., 1978). This kind of topography is not apparent in the studies with retrograde tracers in the nonhuman primate (Amaral and Cowan, 1980; Insausti et al., 1987). However we propose a rough topography in anterograde tracer experiments in different parts of the Amy and HF.

The next paragraphs discus the present results in light of the organization of the classical poly-synaptic pathways ending in VTA but also interconnecting the different structures considered in this study (e.g., HF with Amy); we indeed found that this prior anatomical insight and the models that they afforded provided the most powerful interpretational leverage for the present data.

Connections between HF and Amy

The interconnections between Amy and the hippocampus were shown by Amaral in 1986. AB and PAC have strong interconnection with CA1 and EC, Bpc with the DG/S and EC, Bmc only with EC, and L with PrS, PaS and EC. Years later Pitkänen et al. (2000) showed the topography of the connections between Amy and the different fields of EC. Injections made in Ld and Lv produced labelling all over EC except to E_{Lc} and E_c/E_{CL}. Particularly injections in Ld had more tendencies to project to E_O, E_R, and E_{lr} while Lv showed more projections to E_R and E_l. Moreover, only injections placed in Bi/Bpc and Bpc/PL showed labelling in the E_O, E_R and E_{Lr}. Finally, the projections from the AB only rise to the E_O and E_R levels. Our results supports this idea by showing injections in Bpc/PL also produced labelling in the midbrain along with, maybe, the rostral parts of the EC (E_r and E_{Lr}), which, as we have described above, are also strongly interconnected with Bi/Bpc and PL. If the projections from E_r and E_{Lr} were true, this would suggest a possible pathway from a well-connected set amygdalo-hippocampus “partners” to the midbrain.

HF projections to VTA

So far, there exist no prior anatomical evidences of direct efferent projections from HF to the VTA. There is however one recent functional study that suggests a direct correlation between those structures (Khan et al., 2013). Earlier retrograde tracer studies in nonhuman primates suggested the existence of interconnections from the midbrain to the HF, particularly to Ammon’s horn, DG, Subiculum and EC (mainly E_I and E_C) (Amaral *et al*., 1980; Insausti *et al*., 1987). In rodents, anterograde injections placed in VTA supported this idea by producing labelling in HF, particularly in the stratum oriens and molecular layer of the Subiculum, pyramidal and molecular layer of CA1, the stratum oriens of CA3 and DG (Gasbarri *et al*., 1994a). Going against the idea of reciprocal connection, our results indicate that only the Subiculum projects back to VTA.

It seems that the projections from HF are not homogeneous and arise with a particular inner topography. In 1998, Moser proposed a dorso-ventral organization within the HF in rodents, related

to its inner interconnections (Swanson et al., 1977). Consistent with this idea, anatomical evidences found two performant pathways from the EC, one superior and one inferior that target the dorsal and the ventral hippocampus respectively (Fanselow et al., 2010) demonstrating that the different parts of the Subiculum might have also different interconnections. The distribution of the indirect, polysynaptic projections from the dorsal and ventral HF to the midbrain shows that the ventral hippocampus (ventral Subiculum) sends projections to VTA through the Nucleus Accumbens (NA). In parallel, the dorsal hippocampus (including CA3) sends projects to VTA, but via the Lateral Septum (Luo et al., 2011). Although in these studies did not show direct connections, they suggested the existence of topography within the Subiculum. Our results demonstrate direct projections from the Subiculum, but due to the fact that the labelling analysed here was produced with rather large injections in the Subiculum we cannot confirm the idea of the topography. Future smaller injections in different parts of this structure would be necessary to prove the topography and verify the existence of parallel pathways (direct and indirect) sharing a similar pattern of topographic organization.

Amy projections to VTA

Direct projections to the VTA from CE have been previously reported in primates, and additional projections from the ME, Co and BLA nuclei were also reported in rodents (Watabe et al., in 2012; Geiser et al., 2007). Our results show that other nuclei than CE project to VTA in the monkey. These projections come essentially from Bmc and PL, the former could correspond in part the rodent's BLA. Our study also suggests that the Amy projections are not homogeneous and arise only from particular sub-populations of projecting neurons. So far, this inhomogeneous topography has been only described for the CE, ME and stria terminalis without paying any particular attention to other parts of the brain (Price et al., 1981, Fudge et al., 2000 and 2001; Pardo et al., 2012). A review of the literature addressing the topographical organization of the Amy projections revealed that most of the neurons of origin of projections within Amy are organized in patches that have never been clearly reported or described in detail by the authors of these earlier studies. Although this patchy distribution has never been described so far (only illustrated in figures in prior papers), it is reminiscent of the patchy distribution of the Amy neurons retrogradely labelled from our injections of tracers in VTA in the present study. Identifying whether these groups of cells represent a particular class of Amy projecting neurons will be critical for our elucidation of the influence of Amy of limbic processes and on VTA.

We aimed at understanding the importance of the internal organization of the projections from different parts of Amy to the midbrain. Two main types of cells have been described in Amy: the principal (pyramidal) and secondary (inhibitory). The inhibitory cells are found mainly in PAC and Bmc, but not in PL and CE. They are mainly activated by pyramidal cells within the Amy more than

from the projections from the BLA, and controlled by cortical inputs; it has been suggested that they could play a role in an inhibitory feedback loop (Smith et al., 2000). This loop is a neuronal system

for adaptation to the environment in which the individual has to learn which stimuli are associated to a reward or punishment is more relevant described as sparse encoding. For one specific task, only few neurons from the population will respond to a given stimuli inhibiting the rest of the cells population in the heterogenic functional amygdala. As an example, complementary roles have been found between the B and CE during aversive stimuli and fear conditioning eliciting downstream tonic and phasic responses respectively (Knapsa et al., 2007). Another example hypothesize that phasic changes of the CE mediate tonic behaviour such as sexual and exploratory behaviours whereas plastic changes of the BLA enable phasic responses such as surveillance. It seems therefore, that the CE could enhance a tonic modulation of the VTA either by GABAergic inputs to the DA cells or through glutamatergic inputs to the GABAergic cells of the VTA to control salient behaviours. Since CE is not activated during fear conditioning but it is the BLA, it would be really interesting to elucidate how they would regulate the behaviour dependent on the fear context.

Furthermore, despite most of the behaviours require some level of positive (reward) or negative (aversive stimuli) emotion to motivate a response, during contextual fear conditioning might also require some learning and therefore, it might be a feature in which DA midbrain neurons would sustain trough DA release the fear learning or to avoid it. Consistent with our hypothesis, in rats a disruption in the VTA and subsequently DA release has been shown to impair retrieval of previously learned fear conditioning (Nader and LeDoux, 1999, Ilango et al., 2012; Guarraci et al., 1999) highlighting the importance of direct connections within the VTA.

However, contradictory with the assumption that the DA would be released back into the Amy into CE nucleus, one of the main gateways of the Amy, studies in primates have shown that the major DA release targets are the magnocellular subdivisions of the B (Bmc) and BA (Cho et al., 2010) suggesting that the projections from the VTA to CE might be non-DA (Taylor et al., 2014). Other structures such as the M and PAC also receive projections but they are either less dense or scarce. Those observations suggest that the projections from the VTA to the Amy could be inhibitory and therefore end up the positive feedback loop of DA release into the cortex.

Along with HF, rodent BLA has been shown to play a role in the modulation of the long-term memory potentiation by emotional and motivational influence (Almaguer-Melian et al., 2003). Prior contributions proposed a polysynaptic model of projections from HF to VTA for the encoding of memory and learning (Lisman *et al*., 2005; Lisman J, 2011). This model suggests that the connectivity within the HF-VTA circuit forms a loop in which the information about objects and their spatial location converges in EC via the perirhinal and parahippocampal cortices. Most of the stored information in the HF circuit goes through the perforant pathway, which includes many interposed structures. Inputs from layer II of the EC reaches the DG, and in step-wise fashion, to CA3-CA, where the information is compared with that arriving from layer III of the EC, and send from the S to

the midbrain to enhance DA release in the VTA, and possibly memory consolidation. However, our results suggest a faster or more direct pathway from the S, presumably glutamatergic (Floresco et al., 2001; Legault et al., 2001) that receives direct inputs with novel information from the perirhinal (Kosel et al., 1983) and parahippocampal cortex (Witter et al., 2000). Another possible but not clearly supported source of projections would origin in the EC, presumably glutamatergic (Mooser et al., 2010) with spatial memory (along with the dorsal hippocampus (Tannenholz et al., 2014) (Mooser et al., 1993) that would pre-activate the VTA.

Technical limitations

The strength of the input to the VTA varied considerably across the injections from sparse to absent. Beside true anatomical variations, one of the reasons for this variation could be the viability of the PHAL injections in comparison with the BDA, and the different sizes of the injections. Another technical problem could be that some of the injections placed in EC may have not reached the deepest layers of EC, the output of the cortex and therefore from where the projections to VTA would depart (Sewards et al., 2003). Furthermore, despite our anterograde results, we observed retrograde labelled cells in the EC after placing injections within the VTA, because the FB tracer could label passing fibres, we cannot prove that those cells are projecting to the VTA. Moreover, because our study was aimed to understand subnuclei specific projections, we used small injections within the Amy, which some of them could have been too small or not reached enough principal cells to see projections in the midbrain. Despite these limitations, the high degree of reproducibility of the main data highlighted in this contribution using up to 87 injections of tracers in about 60 monkeys strongly support the viability and robustness of our finding of novel direct projections from specific parts of Amy and HF to VTA.

BIBLIOGRAPHY

Almaguer-Melian, W., Martinez-Marti, L., Frey, J. U., & Bergado, J. A. (2003). The amygdala is part of the behavioural reinforcement system modulating long-term potentiation in rat hippocampus. *Neuroscience*, *119*, 319-322.

Amaral DG, Cowan WM (1980). Subcortical afferents to the hippocampal formation in the monkey. J Comp Neurol. Feb 15;189:573-91

Andy OJ, Stephan H (1968). The septum in the human brain. J Comp Neurol. Jul;133:383-410.

Aransay A, Rodríguez-López C, García-Amado M, Clascá F, Prensa L (2015). Long-range projection neurons of the mouse ventral tegmental area: a single-cell axon tracing analysis. Front Neuroanat. May 19;9:59.

Blair HT, Schafe GE, Bauer EP, Rodrigues SM, LeDoux JE (2001) Synaptic plasticity in the lateral amygdala: A cellular hypothesis of fear conditioning. Learn Mem 8:229–242.

Brennan, P. A., & Kendrick, K. M. (2006). Mammalian social odours: attraction and individual recognition. Philosophical Transactions of the Royal Society B: Biological Sciences, 361, 2061-2078.

Canteras, N. S., Simerly, R. B., & Swanson, L. W. (1995). Organization of projections from the medial nucleus of the amygdala: a PHAL study in the rat. Journal of Comparative Neurology, 360, 213-245.

Canteras, N.S., and L.W. Swanson (1992) Projections of the ventral subiculum to the amygdala, septum, and hypothalamus: A PHA-L anterograde tract-tracing study in the rat. J. Comp. Neurol. 324: 180-194.

Chandler, D. J., Waterhouse, B. D., & Gao, W. J. (2014). New perspectives on catecholaminergic regulation of executive circuits: evidence for independent modulation of prefrontal functions by midbrain dopaminergic and noradrenergic neurons. Frontiers in neural circuits, 8.

Chareyron LJ, Banta Lavenex P, Amaral DG, Lavenex P (2011). Stereological analysis of the rat and monkey amygdala. J Comp Neurol. Nov 1;519:3218-39.

Chergui K, Charléty PJ, Akaoka H, Saunier CF, Brunet JL, Buda M, Svensson TH, Chouvet G (1993). Tonic activation of NMDA receptors causes spontaneous burst discharge of rat midbrain dopamine neurons in vivo. Eur J Neurosci. Feb 1;5:137-44.

Cho YT, Fudge JL (2010). Heterogeneous dopamine populations project to specific subregions of the primate amygdala. Neuroscience.Feb 17;165:1501-18.

Eichenbaum, H., Yonelinas, A. R., & Ranganath, C. (2007). The medial temporal lobe and recognition memory. Annual review of neuroscience, 30, 123.

Fanselow, M. S., & Dong, H. W. (2010). Are the dorsal and ventral hippocampus functionally distinct structures?. *Neuron*, *65*, 7-19.

Floresco SB, Todd CL, Grace AA (2001). Glutamatergic afferents from the hippocampus to the nucleus accumbens regulate activity of ventral tegmental area dopamine neurons. J Neurosci. Jul 1;21:4915-22

Floresco SB, West AR, Ash B, Moore H, Grace AA (2003). Afferent modulation of dopamine neuron firing differentially regulates tonic and phasic dopamine transmission. Nat Neurosci. Sep;6:968-73

Fudge JL, Haber SN (2000). The central nucleus of the amygdala projection to dopamine subpopulations in primates. Neuroscience.;97:479-94

Fudge JL, Haber SN (2001) Bed nucleus of the stria terminalis and extended amygdala inputs to dopamine

Fyhn, M., Hafting, T., Treves, A., Moser, M. B., & Moser, E. I. (2007). Hippocampal remapping and grid realignment in entorhinal cortex. *Nature*, *446*, 190-194.

Gaffan, D., Murray, E. A., & Fabre-Thorpe, M. (1993). Interaction of the amygdala with the frontal lobe in reward memory. European Journal of Neuroscience, 5, 968-975.

Gasbarri A, Packard MG, Campana E, Pacitti C (1994a). Anterograde and retrograde tracing of projections from the ventral tegmental area to the hippocampal formation in the rat. Brain Res Bull 33:445-52.

Geisler S, Derst C, Veh RW, Zahm DS (2007). Glutamatergic afferents of the ventral tegmental area in the rat. J Neurosci. 2007 May 23;27:5730-43.

Gibb, W. R., Mountjoy, C. Q., Mann, D. M., & Lees, A. J. (1989). The substantia nigra and ventral tegmental area in Alzheimer's disease and Down's syndrome. Journal of Neurology, Neurosurgery & Psychiatry, *52*, 193-200.

Guarraci, F. A., & Kapp, B. S. (1999). An electrophysiological characterization of ventral tegmental area dopaminergic neurons during differential pavlovian fear conditioning in the awake rabbit. Behavioural brain research, 99, 169-179.

Haber, S. N., Lynd, E., Klein, C., & Groenewegen, H. J. (1990). Topographic organization of the ventral striatal efferent projections in the rhesus monkey: an anterograde tracing study. *Journal of Comparative Neurology*, *293*, 282-298.

Hargreaves, E. L., Rao, G., Lee, I., & Knierim, J. J. (2005). Major dissociation between medial and lateral entorhinal input to dorsal hippocampus. *Science*, *308*(5729), 1792-1794.

Harris, G. C., Wimmer, M., Byrne, R., & Aston-Jones, G. (2004). Glutamate-associated plasticity in the ventral tegmental area is necessary for conditioning environmental stimuli with morphine. Neuroscience, 129, 841-847.

Holstege G, Meiners L, Tan K (1985). Projections of the bed nucleus of the stria terminalis to the mesencephalon, pons, and medulla oblongata in the cat. Exp Brain Res;58:379-91.

Ilango, A., Shumake, J., Wetzel, W., Scheich, H., & Ohl, F. W. (2012). The role of dopamine in the context of aversive stimuli with particular reference to acoustically signaled avoidance learning. Frontiers in neuroscience, 6.

Insausti R, Amaral DG, Cowan WM (1987). The entorhinal cortex of the monkey: III. Subcortical afferents. J Comp Neurol. 1987 Oct 15;264:396-408.

Janak, P. H., & Tye, K. M. (2015). From circuits to behaviour in the amygdala. *Nature*, *517*, 284-292.**Ji, J.,** & Maren, S. (2008). Differential roles for hippocampal areas CA1 and CA3 in the contextual encoding and retrieval of extinguished fear. Learning & Memory, 15, 244-251.

Jin, Z., Bhandage, A. K., Bazov, I., Kononenko, O., Bakalkin, G., Korpi, E. R., & Birnir, B. (2014). Expression of specific ionotropic glutamate and GABA-A receptor subunits is decreased in central amygdala of alcoholics. Frontiers in cellular neuroscience, 8.

Johnson SW, Seutin V, North RA. (1992b) Burst firing in dopamine neurons induced by N-methyl-D-aspartate: role of electrogenic sodium pump. Science. Oct 23;258:665-7
Jonas, P., & Lisman, J. (2014). Structure, function, and plasticity of hippocampal dentate gyrus microcircuits. Frontiers in neural circuits, 8, 107.
Kahn, I., & Shohamy, D**.** (2013). Intrinsic connectivity between the hippocampus, nucleus accumbens, and ventral tegmental area in humans. Hippocampus, 23, 187-192.
Kentner, A. C., Deslauriers, K., Parkinson, M., Fouriezos, G., & Bielajew, C. (2004). Interhemispheric involvement of the anterior cortical nuclei of the amygdala in rewarding brain stimulation. *Brain research*, *1003*, 138-150.
Kevetter, G. A., & Winans, S. S. (1981). Connections of the corticomedial amygdala in the golden hamster. II. Efferents of the "olfactory amygdala".
Knapska, E., Radwanska, K., Werka, T., & Kaczmarek, L. (2007). Functional internal complexity of amygdala: focus on gene activity mapping after behavioral training and drugs of abuse. Physiological reviews, 87, 1113-1173.
Kosel, K. C., Van Hoesen, G. W., & Rosene, D. L. (1983). A direct projection from the perirhinal cortex (area 35) to the subiculum in the rat. Brain Research, 269, 347-351.
Krettek, J.E., and J.L. Price (1978a) Amygdaloid projections to suhcortical structures within the basal forebrain and brainstem in the rat and cat. J.Comp. Neurol. 178:225-254.
LeDoux JE, Cicchetti P, Xagoraris A, Romanski LM (1990). The lateral amygdaloid nucleus: sensory interface of the amygdala in fear conditioning. J Neurosci. Apr;10:1062-9.
LeDoux, J. (2007). The amygdala. *Current Biology*, *17*, R868-R874.
Legault, M., & Wise, R. A. (2001). Novelty-evoked elevations of nucleus accumbens dopamine: dependence on impulse flow from the ventral subiculum and glutamatergic neurotransmission in the ventral tegmental area. European Journal of Neuroscience, 13, 819-828.
Lisman, J. E., & Grace, A. A. (2005). The hippocampal-VTA loop: controlling the entry of information into long-term memory. Neuron, 46, 703-713.
Lisman, J., Grace, A. A., & Duze, E. (2011). A neoHebbian framework for episodic memory; role of dopamine-dependent late LTP. Trends in neurosciences, 34, 536-547.
Ljungberg T, Apicella P, Schultz W (1992). Responses of monkey dopamine neurons during learning of behavioral reactions. J Neurophysiol. Jan;67:145-63.subpopulations in primates. Neuroscience. 104:807-27.
Logothetis NK, Eschenko O, Murayama Y, Augath M, Steudel T, Evrard HC, Besserve M, Oeltermann (2010) A. Hippocampal-cortical interaction during periods of subcortical silence. Nature.
Luo AH, Tahsili-Fahadan P, Wise RA, Lupica CR, Aston- Jones G.(2011) Linking context with reward: a functional circuit from hippocampal CA3 to ventral tegmental area.Science. 2011 Jul 15;333:353-7.
Majak, K., & Pitkänen, A. (2003). Projections from the periamygdaloid cortex to the amygdaloid complex, the hippocampal formation, and the parahippocampal region: A PHA-L study in the rat. *Hippocampus*, *13*, 922-942.
Martig AK, Mizumori SJ (2011). Ventral tegmental area and substantia nigra neural correlates of spatial learning. Learn Mem. Mar 29;18:260-71.
Millhouse, O. E. (1986). The intercalated cells of the amygdala. Journal of Comparative Neurology, 247, 246-271.
Moser E., Witter MP, Moser M-B (2010) Entorhinal cortex. In: Handbook of Brain Microcircuits. Shepherd GM, Grillner, S Eds. Oxford Univ Press, Oxford, UK pp175-192.
Moser, E., Moser, M. B., & Andersen, P. (1993). Spatial learning impairment parallels the magnitude of dorsal hippocampal lesions, but is hardly present following ventral lesions. The Journal of neuroscience, 13, 3916-3925.
Moser, M. B., & Moser, E. I. (1998). Functional differentiation in the hippocampus. Hippocampus, 8, 608-619.
Murray, E. A. (2007). The amygdala, reward and emotion. Trends in cognitive sciences, 11f, 489-497.
Nader, K., & LeDoux, J. (1999). Inhibition of the mesoamygdala dopaminergic pathway impairs the retrieval of conditioned fear associations. Behavioral neuroscience, 113, 891.
Pardo-Bellver C, Cádiz-Moretti B, Novejarque A, Martínez-García F, Lanuza E (2012) Differential efferent projections of the anterior, posteroventral, and posterodorsal subdivisions of the medial amygdala in mice. Front Neuroanat. Aug 21;6:33.
Pitkänen A, Kemppainen S (2002). Comparison of the distribution of calcium-binding proteins and intrinsic connectivity in the lateral nucleus of the rat, monkey,and human amygdala. Pharmacol Biochem Behav. Mar;71:369-77. Review.
Pitkänen, A., Pikkarainen, M., Nurminen, N., & Ylinen, A. (2000). Reciprocal connections between the amygdala and the hippocampal formation, perirhinal cortex, and postrhinal cortex in rat: a review. Annals of the New York Academy of Sciences, 911, 369-391.
Price JL, Russchen FT, Amaral DG. (1987). The limbic region. II. The amygdaloid complex. In: Bjorklund A, Ho¨kfelt T, Swanson LW, editors. Handbook of chemical neuroanatomy. vol.5. Integrated systems of CNS. Part I. Amsterdam: Elsevier. p 279–388.
Price, J. L., & Amaral, D. G. (1981). An autoradiographic study of the projections of the central nucleus of the monkey amygdala. The journal of Neuroscience, 1, 1242-1259.
Price, J. L., & Drevets, W. C. (2010). Neurocircuitry of mood disorders. Neuropsychopharmacology, 35(1), 192-216.
Rauch, S. L., Shin, L. M., & Wright, C. I. (2003). Neuroimaging studies of amygdala function in anxiety disorders. Annals of the New York Academy of Sciences, 985, 389-410.
Rossato, J. I., Bevilaqua, L. R., Izquierdo, I., Medina, J. H., & Cammarota, M. (2009). Dopamine controls persistence of long-term memory storage. Science, 325, 1017-1020.
Russchen FT (1982). Amygdalopetal projections in the cat. II. Subcortical afferent connections. A study with retrograde tracing techniques. J Comp Neurol. 1982 May 10;207:157-76.
Schwab, M. E., Javoy-Agid, F., & Agid, Y. (1978). Labelled wheat germ agglutinin (WGA) as a new, highly sensitive retrograde tracer in the rat brain hippocampal system. Brain research, 152, 145-150.

Sesack, S.R., A.Y. Deutch, R.H. Roth, and B.S. Bunney (1989) Topographical organization of the efferent projections of the medial prefrontal cortex in the rat: An anterograde tracct-tracing study with Phaseolus vulgaris leucoagglutinin. J. Comp. Neurol. 290:2 13-242.
Sesack, S. R., & Grace, A. A. (2010). Cortico-basal ganglia reward network: microcircuitry. Neuropsychopharmacology, 35, 27-47.
Sewards, T. V., & Sewards, M. A. (2003). Input and output stations of the entorhinal cortex: superficial vs. deep layers or lateral vs. medial divisions?. Brain Research Reviews, 42, 243-251.
Smith, Y., Paré, J. F., & Paré, D. (2000). Differential innervation of parvalbumin-immunoreactive interneurons of the basolateral amygdaloid complex by cortical and intrinsic inputs. Journal of Comparative Neurology, 416, 496-508.
Stephan H, Andy OJ (1977). Quantitative comparison of the amygdala in insectivores and primates. Acta Anat (Basel). 1977;98:130-53.
Strange, B. A., Witter, M. P., Lein, E. S., & Moser, E. I. (2014). Functional organization of the hippocampal longitudinal axis. Nature Reviews Neuroscience, 15, 655-669.
Swanson, L. W. (1982). The projections of the ventral tegmental area and adjacent regions: a combined fluorescent retrograde tracer and immunofluorescence study in the rat. Brain research bulletin, 9, 321-353.
Tannenholz, L., Jimenez, J. C., & Kheirbek, M. A. (2014). Local and regional heterogeneity underlying hippocampal modulation of cognition and mood. Frontiers in behavioral neuroscience, 8.
Turner BH, Mishkin M, Knapp M (1980). Organization of the amygdalopetal projections from modality-specific cortical association areas in the monkey. J Comp Neurol. Jun 15;191:515-43.
Van Hoesen G, Pandya DN (1975). Some connections of the entorhinal (area 28) and perirhinal (area 35) cortices of the rhesus monkey. I. Temporal lobe afferents. Brain Res. Sep 12;95:1-24.
Watabe-Uchida M, Zhu L, Ogawa SK, Vamanrao A, Uchida N (2012). Whole-brain mapping of direct inputs to midbrain dopamine neurons. Neuron. Jun 7;74:858-73.
Witter, M. P., Naber, P. A., van Haeften, T., Machielsen, W. C., Rombouts, S. A., Barkhof, F., ... & Lopes daSilva, F. H. (2000). Cortico-hippocampal communication by way of parallel parahippocampal-subicular pathways. Hippocampus, 10, 398-410.

4.3 Heterogeneous Cortical Projections to the Locus Coeruleus in the Macaque Monkey

ABSTRACT

Functional studies in rodents have demonstrated that the *Locus coeruleus* (LC) is directly activated by the prefrontal cortex; however, the anatomical related pathways are poorly understood. In this work, we examined the projections from the prefrontal cortex and anterior insular cortex to the *Locus coeruleus* (LC) in the macaque monkey. Anterograde tracers were injected in several distinct prefrontal and insular areas. All the studied areas reported labeling in LC, and the density of this labeling varied depending on the location of the injection site. Overall, injections placed in agranular or dysgranular areas produced a stronger labeling compared to those injections involving granular areas. Thereby, Injections in the agranular insular area (Iam) produced a very strong labeling in the core of LC, followed by injections placed in the medial part of the orbital prefrontal cortex (13b, 13l) and the medial prefrontal cortex (32, 24 and 25). In contrast, injections in granular areas of the orbital prefrontal cortex (11m and 11l) and the dorsolateral cortex (46d, 46v) produced sparse labeling. An exception was the granular area 9 that gave rise to a strong labeling compared to other granular areas. In most cases, the anterograde labeling occurred in the rostral part of the LC; however, injections in area 13 produced labeling throughout the rostrocaudal extent of LC. These data demonstrate a direct top-down input to LC from agranular/dysgranular limbic areas in the prefrontal and insular cortex. These connections might underlie the role that LC has in certain cognitive functions such as decision-making and memory processing.

INTRODUCTION

The noradrenergic system has an important role in brainwide neuromodulation, taking part in sleep-wake cycle, sympathetic regulation, neural plasticity and drug abuse, as well as higher cognitive processes such as decision-making and memory processing. The majority of noradrenergic neurons are concentrated in LC that provides the sole source of noradrenaline (NA) to the neocortex and hippocampus (Berridge and Waterhouse, 2003). Substantial evidence indicates that NA exerts a potent modulatory influence on prefrontal cortex (PFC) functions, such as attention, working memory and decision-making (Aston-Jones et al., 2000; Kerns et al., 2004; Milstein et al., 2007; Ramos and Arnsten, 2007) by acting on different adrenoreceptors (Lim et al., 2010). These connections are important in the evaluation of the contextual relevance and emotional valence of novel stimuli in order to promote the adaptive responses by the medial prefrontal cortex (MPFC) (Radley et al., 2008). In turn, the PFC modulates LC activity through both NMDA and non-NMDA receptors (Jodo and Aston-Jones, 1997). Functional studies in rodents demonstrate that the MPFC phasically activates LC neurons either directly or through indirect connections, and that MPFC also provides a resting tonic excitatory influence on LC activity, since the inactivation of the MPFC suppresses LC firing (Jodo et al., 1998). Thus, the activity of the PFC on the regulation of cognitive and emotional processing influences LC function. Moreover, Aston-Jones et al. (2007) showed that LC neurons responses are driven by decision processes rather than by sensory or motor activities per se, and that this decision-related activation of LC serves to facilitate behavioral responses. All these functional evidences reinforce the idea that LC is involved in the modulation of higher cognitive processes (Jodo et al., 1998; Bush et al., 2000; Radley et al., 2008).

Anatomical data support the possibility of the existence of direct, PFC projections to LC, although the vast majority of our knowledge is based on studies made in rodents. These data show that the PFC directly innervates the rostromedial dendritic peri-LC zone (Zhu and Aston-Jones, 1996; Luppi et al., 1996; Lu et al., 2012). Few studies have been undertaken in the primate claiming that only certain architectonic areas in the PFC (see discussion) project directly to the core of LC (Arnsten and Goldman-Rakic, 1984; Freedman et al., 2000; Rajkowski et al., 2000; Chiba et al., 2001; Zhu et al., 2004).

In the present work, we investigate which specific architectonic areas directly terminate on the LC and whether these projections present a particular distribution within the nucleus.

MATERIALS AND METHODS

Subjects

The present data were obtained from 20 adult cynomolgus macaques (*Macaca fascicularis,* 3-8 kg) in three different laboratories (USA, Price; Spain, Insausti, and Germany, Evrard). All monkeys from the Price's lab and some monkeys from the Insausti's lab were prepared and used in the context of prior tract-tracing studies (Carmichael and Price, 1995b, a, 1996; Kondo et al., 2003; Insausti and Amaral, 2008; Saleem et al., 2008; Mohedano-Moriano et al., 2015). The cases were examined and analyzed in relation to the connections with the LC.

The animals were treated according to the guidelines of the American Physiological Society, the NIH and the European Parliament and Council Directive 2010/63/EU on the protection of animals used for experimental and other scientific purposes. All animal protocols were reviewed and approved by the Animal Studies Committee of Washington University, St.-Louis, USA, the Ethical Committee of Animal Research of the University of Castilla-La-Mancha (UCLM), Spain, or the German authorities (*Regierungspräsidium*).

Tracer injection

All tracer injections were made during aseptic surgery under general anesthesia. Prior to surgery, each monkey was anesthetized (see below) and placed in an MRI-compatible stereotaxic frame. An MRI scan (T1 MPRAGE 3D image, with 0.8 or 1.0 mm isometric voxels) was then obtained by using a 1.5 T scanner, using a receive-only or volume coil placed over the top of the head of the animal. Stereotaxic coordinates for each desired injection site in the PFC that was specific for each individual animal were derived from the MR images. These individual-specific coordinates were compared with coordinates from the atlas of Szabo and Cowan (1984). Electrophysiological recording was used to further refine the coordinates for deep injections (see below). For the surgery (also for MRI), anesthesia was induced by intramuscular injection of ketamine (10 mg/kg) and xylazine (0.67 mg/kg). The animals were then intubated, and surgical anesthesia was initiated with a gaseous mixture of oxygen, nitrous oxide, and halothane or isofluorane. Once anesthesia was established, the animals were placed in a stereotaxic apparatus, and the scalp was incised. Craniotomies were made in the skull at the sites indicated by the stereotaxic coordinates. In certain cases were the injection site was located in deep cortical layers of OMPFC, a tungsten electrode was used in order to determinate the depth of the base of the brain (Saleem et al., 2008). After surgery, a long-lasting analgesic, buprenorphine (0.1 mg/kg, i.m.), was given as the animal was brought out of anesthesia.

Aqueous solutions of the anterograde tracer biotinylated dextran amine [BDA; Molecular Probes, Eugene, OR; 10%]), and two bidirectional tracers (Fluoro Ruby [FR; Molecular Probes, 5% or 10%], and Lucifer Yellow [LY; Molecular Probes, 5% or 10%]) were injected in different portions of the PFC. The injections were made through micropipettes where the tracer was delivered with an air pressure system (Saleem et al., 2008). The volume of tracers injected varied between 0.1 to 1.2 µl, depending on the sensitivity of tracers. To avoid spread of tracer into areas along the pipette track, the micropipette was left in place for 30 minutes after the injection was finished. With this procedure, there was little spread of tracer into the overlying cortex or white matter.

Perfusion and histological processing

After a survival period of 2 weeks, the animals were anesthetized with ketamine (10 mg/kg, i.m.), followed by sodium pentobarbital (25–30 mg/kg, i.v.), and perfused with a pH shift fixation method as described by Carmichael and Price (1994), with slight modifications (Saleem et al., 2008). In this method, the animals were first perfused transcardially with warm heparinized saline, followed by a sequence of cold 4% paraformaldehyde in 0.1M sodium acetate buffer (pH 6.5), then 4% paraform-aldehyde in 0.1M borate buffer (pH 9.5), and finally 4% paraformaldehyde and 10% sucrose in borate buffer. The brain was blocked sterotaxically, removed, photographed, and then placed in 20% and than transferred to 30% sucrose in 0.1 M phosphate buffer (pH 7.2–7.4) at 4ºC. After 3-4 days, the brain blocks were frozen in dry ice and isopentane, and cut coronally at 50µm thickness on a sliding microtome. An alternating series of sections was processed for each tracer, usually one section out of 10 in each series, with 500µm intervals between adjacent sections. BDA was processed directly with the avidin-biotin-peroxidase method. The other tracers FR, and LY, were processed immunohistochemically with an avidin-biotin-horseradish peroxidase method (Carmichael et al., 1994). For these tracers, the sections were first processed to block the biotin from the injected BDA (Avidin-Biotin Blocking Kit; Vector, Burlingame Burlingame, CA) and then incubated for 3–3.5 days in the primary antibody (anti-tetramethylrhodamine [for FR] and anti-LY: Molecular Probes; Nos. A-6397 and A-5750; 1:1,000). The sections were then processed with the appropriate biotinylated secondary antibody and avidin-biotin staining kit (Vector) with diaminobenzidene as the chromogen (for other details see Saleem et al., 2008). The immunostaining was enhanced with a silver/gold intensification method, which made the labeled axons and cells visible with dark field illumination (Carmichael and Price, 1994). Additional series of adjacent sections were processed with Nissl staining for cytoarchitectonic study.

Data analysis and illustrations

The spatial distribution of labeled terminals was analyzed with an epifluorescence microscope coupled to a computerized charting system (MD-Plot, Datametrics, Minnesota, USA), and each labeled fiber was plotted as a single point. Subcortical boundaries and other landmarks were added to these plots by camera lucida drawings of adjacent Nissl-stained sections. The relative strength or densities of connections was evaluated; however, the absolute values were not determined due to factors such as differences between tracers in transport efficacy, injection volumes and location of each injection. LC labeling was analyzed bilaterally, and maps were prepared to visualize the distribution and density of the terminal fields.

Nomenclature

Subdivisions of the PFC were determined according to prior architectonic and tract-tracing studies that subdivided the entire PFC into 23 architectonic areas, and the anterior insula into 7 architectonic areas (Carmichael and Price, 1994; Evrard et al., 2014). The core of LC was subdivided into a central region of high cellular density and a region with sparser cellular density, as described in *Chapter 1* (Figure 1).

RESULTS

Injection sites in the prefrontal cortex

In most cases the injection site was confined to the cortical grey matter and included layers III and/or V. They all had a dense central ‘core’ around the tip of the micropipette penetration track and a more diffuse ‘halo’ extending for approximately 100 to 300 µm around the core. Figure 1 shows an example of injection site from case M02-15 with an injection of FR in area 12.

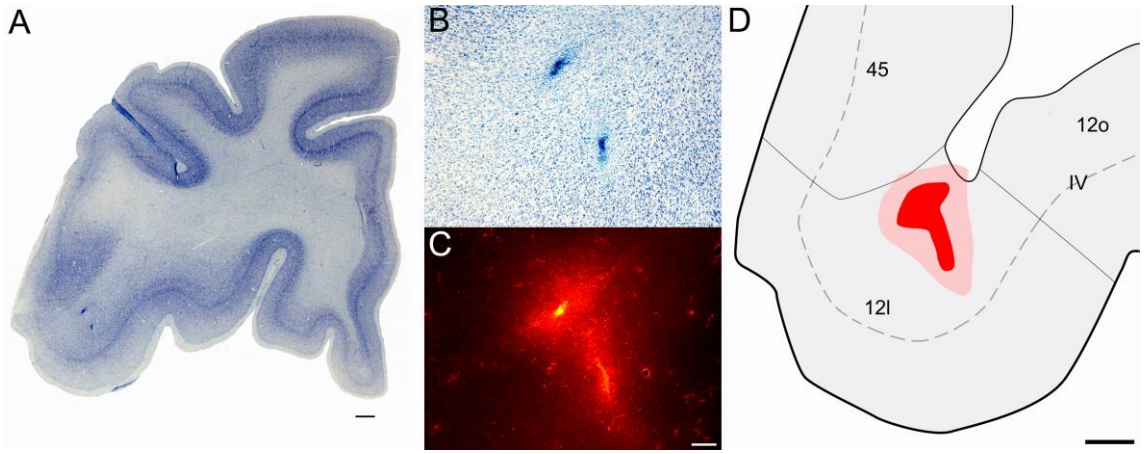

Figure 1. Location of the injection site in Case M02-15. A, Low-magnification photomicrograph of a Nissl-stained coronal section of the prefrontal cortex (*Macaca fascicularis*); B and C, Higher-magnification photomicrograph of contiguous sections mounted for nissl and fluorescence respectively. D, Representation of the injection site over the corresponding cytoarchitectonic areas.

A total of 28 injections of anterograde or bidirectional tracers were made in several distinct architectonic areas in the agranular insula anterior to the limen, and in the orbital, medial and lateral PFC. In light of the finding reported here (see below), the cases are ordered throughout the text according to the degree of granularity of the injected areas: agranular insula areas (Iam, Iamp, Iai, Ial), dysgranular cingulate areas (24, 25 and 32), dysgranular orbital and medial PFC areas (13b, 13l, 12r), granular orbital and medial PFC areas (12m, 12o, 11m, 11l, 10m, 10o), and granular lateral PFC areas (12l, 46 and 9).

Figure 2 depicts the injection sites collated all together in a standard unfolded map of PFC. The round and ellipsoidal shapes represent both the ‘core’ and ‘halo’ of each injection site. Injections were made in the left or the right side of PFC in different cases, but in Figure 2 all are illustrated in left PFC for consistency.

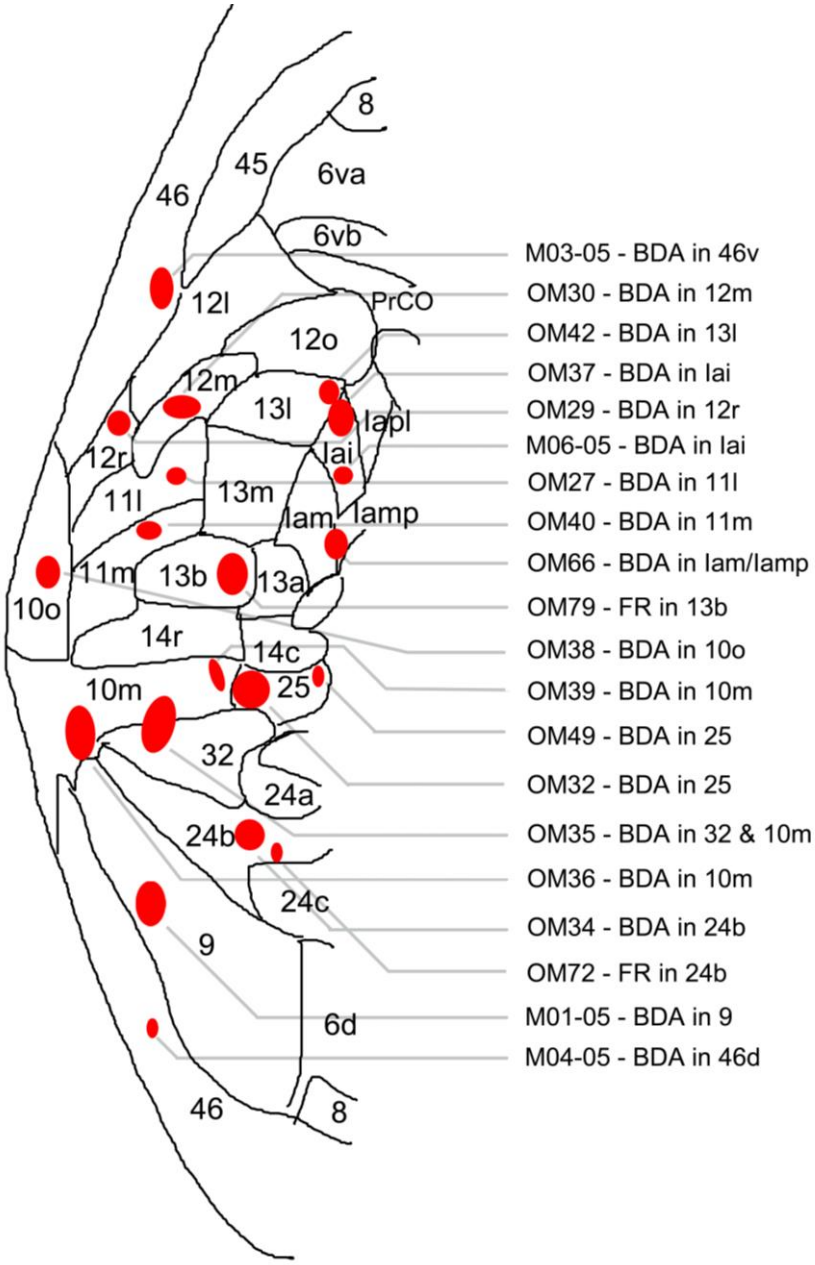

Figure 2. Unfolded map showing the location of the injection sites in the prefrontal cortex and anterior insular cortex

Three injections were made in the anterior insula. One large injection of BDA filled all the layers of Iam and Iamp (OM66). Two smaller injections of BDA were confined to the deep layers of Iai (OM37) or Ial (M06-05), respectively.

Six injections were made in dysgranular MPFC areas. Most injections were confined to one area including two injections in area 24b (OM32-FR and OM34) and two injections in area 25 (OM32-BDA, and OM49-BDA). Among the injections in area 25, in case OM32, the injection had a medium size and involved all the layers, whereas in case OM49 the injection was small and limited to deep layers (IV-VI). One injection in area 32 spread to area 10m (OM35) but a differential analysis of anterograde labeling in LC indicates that most, if not all the labeling from that injection

arose from area 32. Five injections were made in the rostral pole of PFC, in distinct subdivisions of area 10 with two injections in area 10mr (OM69 and OM36), one injection in area 10m (OM39) and one injection in area 10o (OM38).

Six injections were made in the orbital PFC. These injections included one injection in area 13b (OM79), two injections in area 13l (OM28 and OM42), one injection in area 11m (OM40) and one in area 11l (OM27), one injection in area 12r (OM29), one in area 12m (OM30), and one in area 12l (M02-15).

Finally, four injections were made in the lateral PFC with one injection in area 9 (M01-05), 2 injections in area 46v (M03-05) and one injection in area 46d (M04-05).

Anterograde labeling in *Locus coeruleus*

Most of the injections reported here produced anterograde labeling in LC. Figure 3A and B show photomicrographs of representative anterograde labeling in LC. The labeled fibers were sinuous, and displayed varicosities. The majority of the terminal fields reached the sparse periphery of the core of LC, although in some cases (see below) the labeled fibers were present also in the dense core. The labeling was distributed mainly in the ipsilateral LC with only about 5% of labeling present in contralateral LC. The highest density of labeling was located mainly in the rostral levels of LC, although in some cases the labeling was also distributed throughout the entire rostro-caudal extension of the nucleus (e.g., OM79, see below).

Figure 4A and B show how individual fiber segments were plotted and counted. The density of labeled fibers varied greatly according to the location of the injection site. The histogram in Figure 3C illustrate this variation using, for each area injected, an average of the ratio of the number of fiber segments labeled from one specific area relative to the total number of fibers labeled in the case with most labeling (OM66).

Overall, injections placed in agranular or dysgranular areas produced a stronger labeling compared to those injections involving granular areas. Thereby, Injections in the agranular insular area (Iam) produced a very strong labeling in the core of LC, followed by injections placed in the medial part of the orbital prefrontal cortex (13b, 13l) and the medial prefrontal cortex (32, 24 and 25). In contrast, injections in granular areas of the orbital prefrontal cortex (11m and 11l) and the dorsolateral cortex (46d, 46v) produced sparse labeling. An exception was the granular area 9 that gave rise to a strong labeling compared to other granular areas. The next paragraphs describe the distribution and density of labeling in LC for all relevant cases illustrated in Figures 5 and 6.

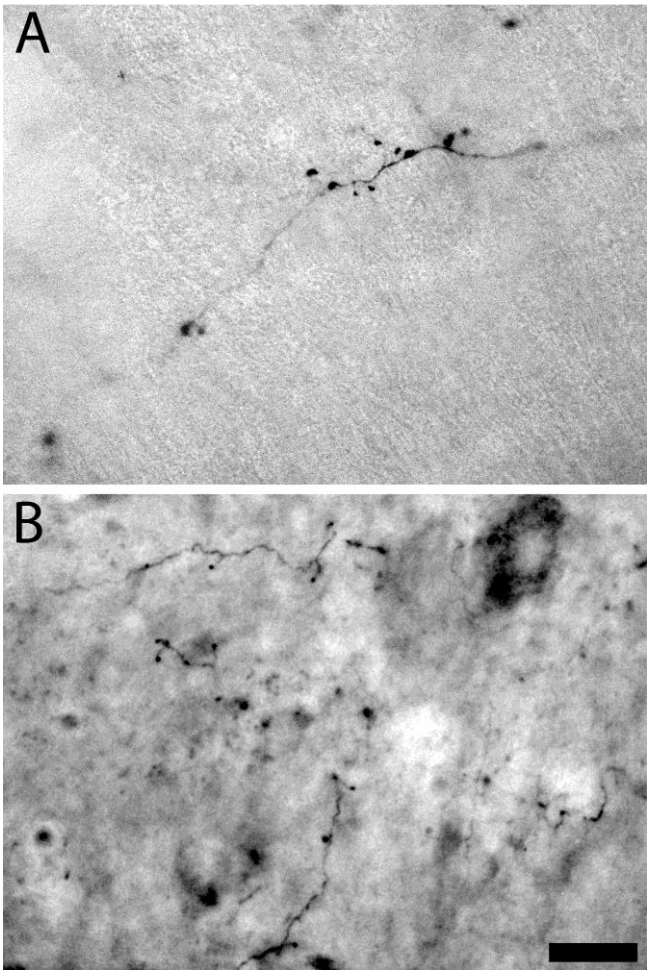

Figure 3. Photomicrographs of BDA-positive labeled fibers in the *Locus coeruleus*. Scale bar: 20 μm.

Orbital prefrontal cortex and anterior insula.

Injections in the OPFC showed an overall rostro-caudal gradient in the density of the fibers sent to LC. Areas located rostral and medial in the OPFC (10o, 11m, 11l) projected very lightly compared to areas located more caudal and lateral (13b, 13l, Iam/Iamp).

Out of all of the areas examined here, the tracer injection located in Iamp/Iamp (case OM66) showed the highest density of anterograde labeling in LC (Fig. 5A). The labeled fibers distributed along the whole extension of the nucleus in both the core and the periphery. Injections in areas Iai and Ial that surround Iam and Iamp produced much less labeling. Notably, two small injections of BDA in cases OM28 and OM37 were placed in the rostral and caudal portions of Iai respectively, and the labeling obtained varied in density and distribution (Fig. 5B and C). The injection in the rostral part of Iai showed scarce labeling in the dorsal portion of the nucleus, whereas the caudal Iai showed a higher number of labeled fibers, but the distribution was located in the rostro-medial portion of LC.

High density of fibers was found after the injection of FR in area 13b (case OM79; Fig. 5D). The resulting labeling distributed all over the extension of LC in both the dense and sparse parts of the

core, but it was more abundant in the rostral portion. Similar density of labeling was obtained after a small BDA injection into area 13l, although the spatial distribution of the labeling was slightly different showing preference for the lateral location within LC (Fig. 5E).

Finally, two BDA injections in area 11, one placed in 11m (case OM40; Fig. 6E) and the other in 11l (case OM27; Fig. 6F) showed few labeled fibers along the rostro-medial extension of the nucleus, specifically localized in the sparse part of the core. A small BDA injection in area 12m (OM30; Fig. 6G) produced sparse labeled fibers in the rostral LC.

Medial prefrontal cortex.

Although all the injections produced a moderate to dense labeling, the distribution of fibers and boutons varied substantially across the different cases of these series.

The densest labeling resulted from deposits in area 32. One BDA injection involving area 10mc and area 32 (case OM35; Fig. 5F) resulted in moderate to dense labeling. The labeled terminals likely arose in area 32 since area 10mc projection is very light; therefore the bulk of the labeling in this case may originate substantially in area 32.

Injections in area 24b (cases OM34 and OM72; Fig. 5G and H) showed moderate density of labeling throughout the rostro-caudal extension of LC, and some fibers reached the dense part even though most of the fibers were distributed in the sparse part of the core.

Two injections in area 25 produced an anterograde labeling of moderate density and a similar spatial distribution of the fibers along the rostral to medial extension of the sparse portion of the core (Fig. 5I and J), mainly localized in the medial part close to the forth ventricle. Like in the previous cases, the caudal pole presented very few (1-2) labeled fibers while the bulk of the labeling was preferentially located in the rostromedial part of LC.

Finally, injections in different rostro-caudal portions within area 10m produced different labeling density. The BDA injection in the rostral part of 10m in case OM35 (Fig. 6D) produced a denser labeling, compared to the caudal part of 10m (case OM39; Fig. 6C), although the caudal deposit was smaller. The sparse labeled fibers obtained with the injection in 10mc were localized in the rostral periphery of the core of LC without entering the most compact part of the core. In contrast, the labeled fibers arising in 10mr were distributed throughout both the compact and the sparse portions, and covered all the extent of the LC, even though the caudal labeling was sparser than in rostral LC. The BDA deposit in area 10o (OM38) did not show any anterograde labeling in LC (Fig. 6A).

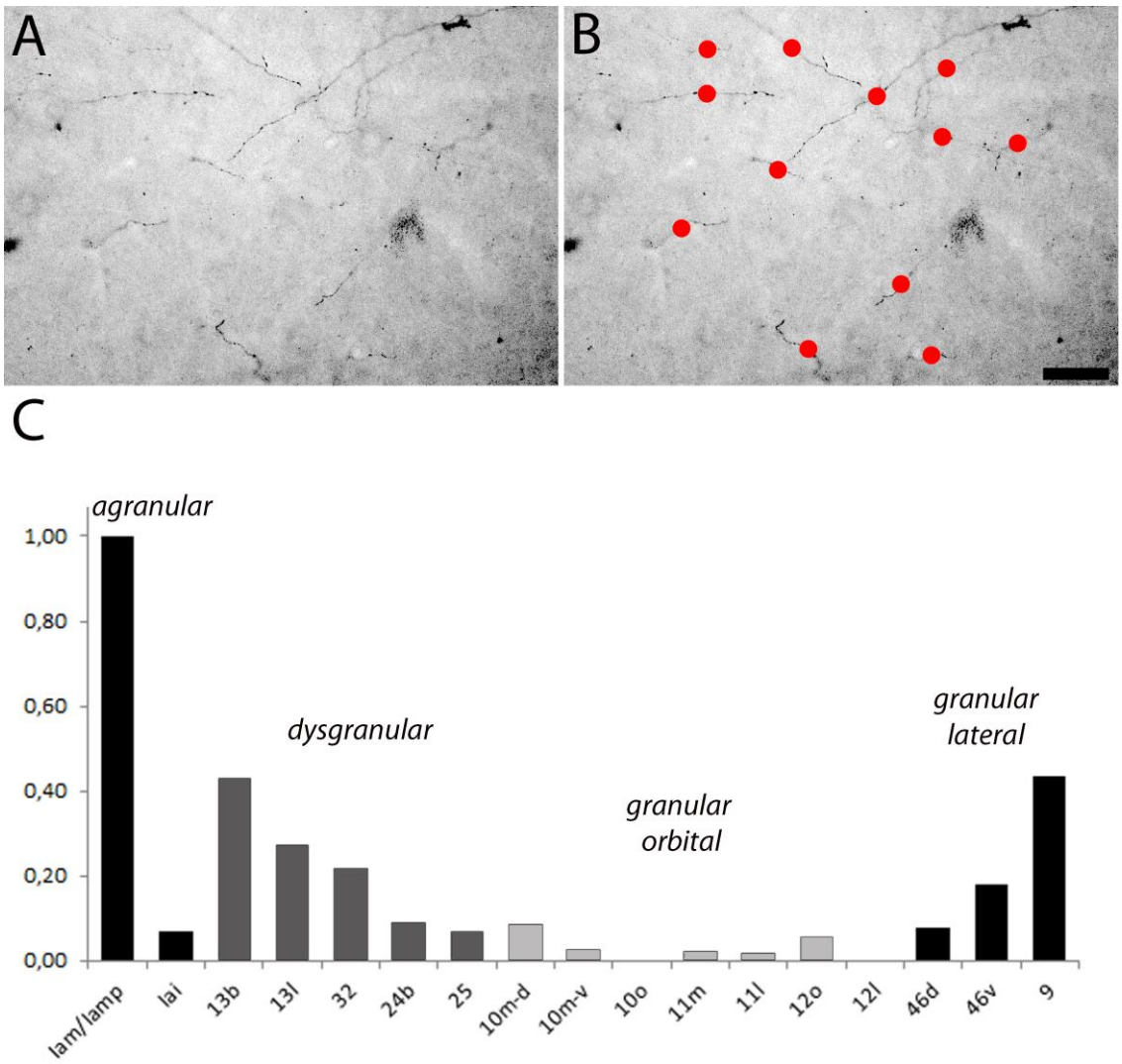

Figure 4. A and B, photomicrographs of the labeled axons in the *Locus coeruleus*. Each red dot represents one fiber. C, graph representation of the relative number of labeled fibers in LC after injections in different architectonic areas within the prefrontal cortex and anterior insular cortex. Scale bar: 20 μm.

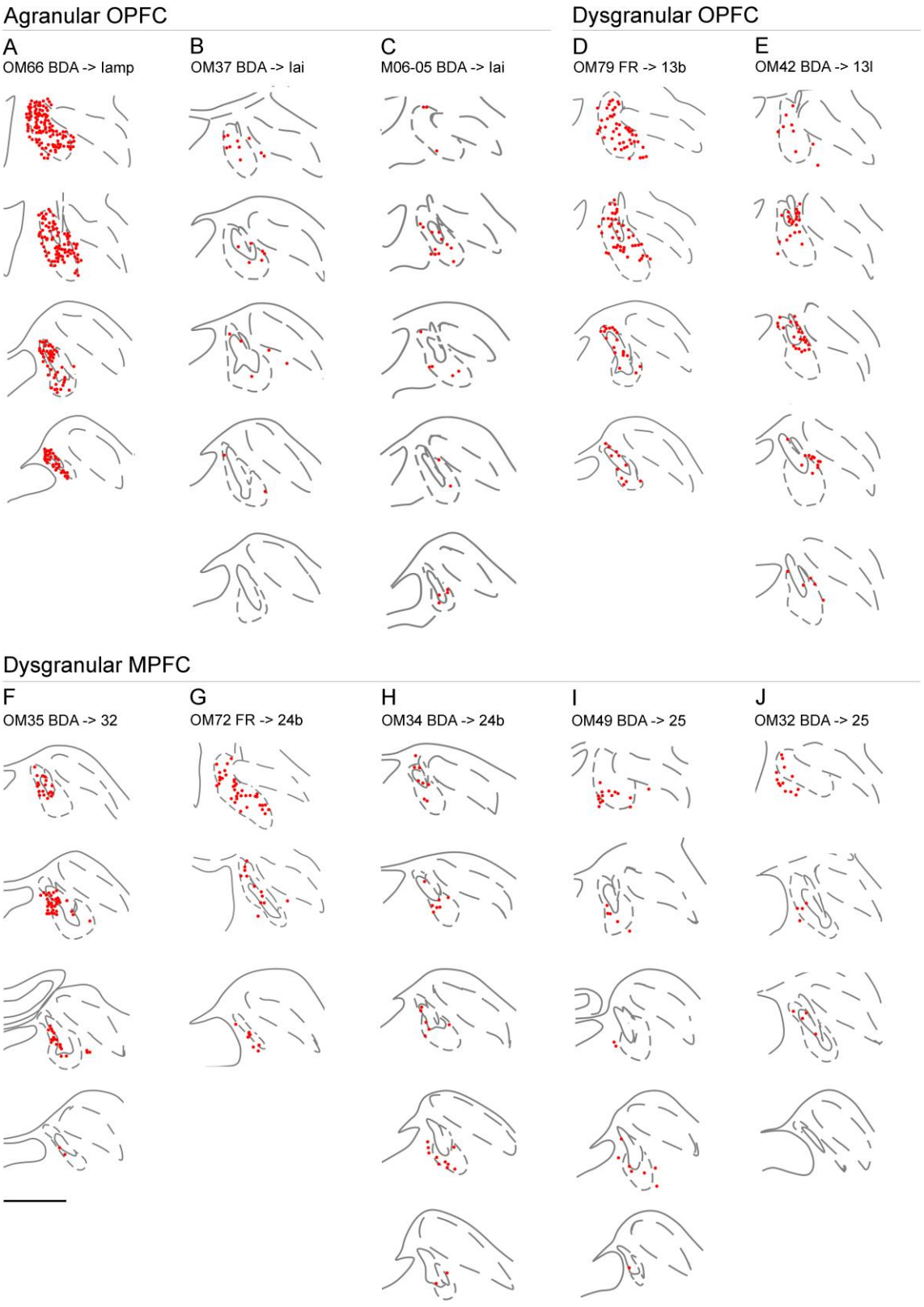
Agranular OPFC
Dysgranular OPFC
A
OM66 BDA -> lamp
B
OM37 BDA -> lai
C
M06-05 BDA -> lai
D
OM79 FR -> 13b
E
OM42 BDA -> 13l
Dysgranular MPFC
F
OM35 BDA -> 32
G
OM72 FR -> 24b
H
OM34 BDA -> 24b
I
OM49 BDA -> 25
J
OM32 BDA -> 25

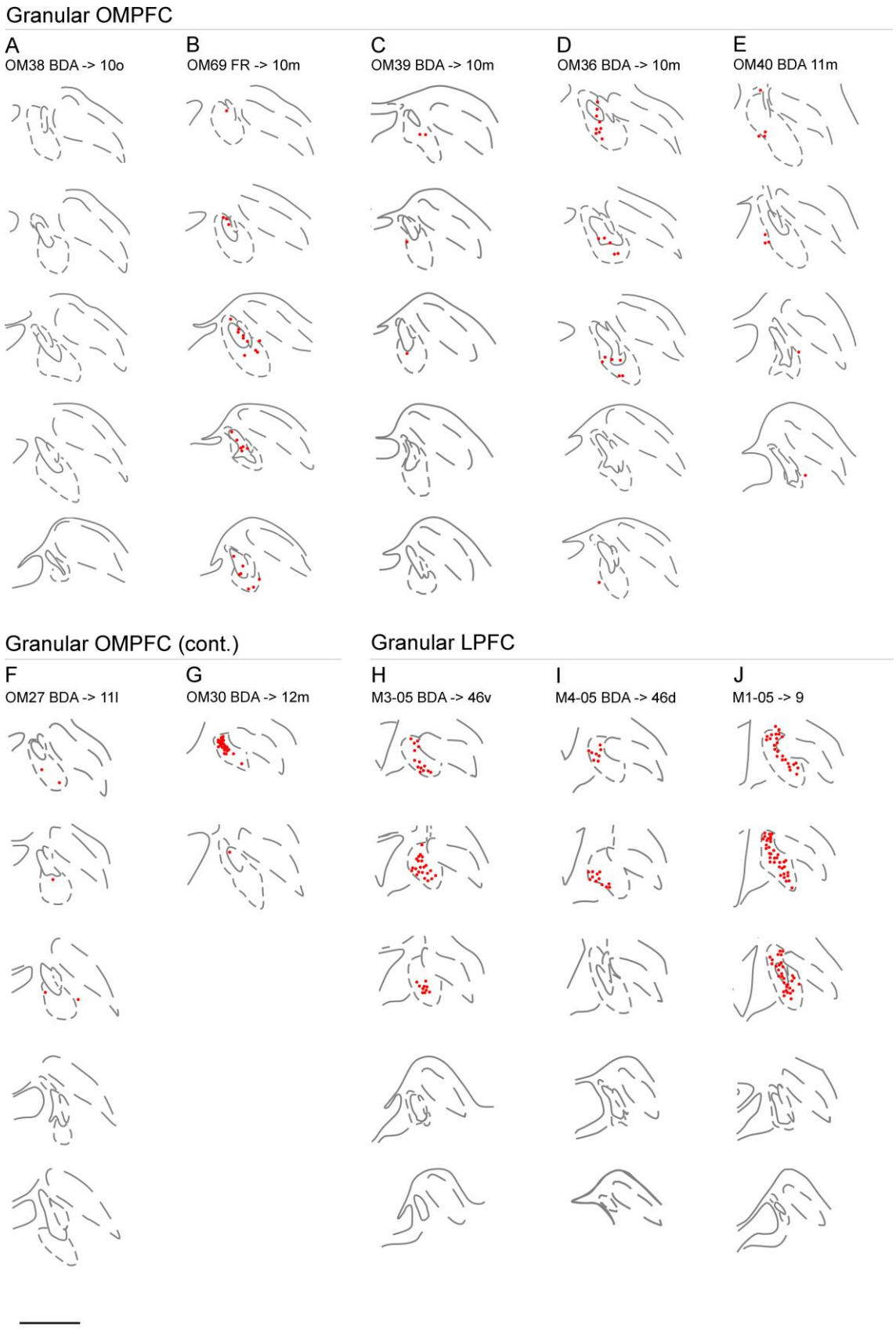

Figure 5-6. Drawings depicting the labeling obtained in the *Locus coeruleus* after injections of anterograde tracers in the prefrontal cortex and anterior insula. Each red dot represents 1 labeled fiber. Scale bar:2mm

Lateral prefrontal cortex.

Only area 9 deposits (case M01-05; Fig. 6J) produced a relatively high number of labeled fibers in the LC. These labeling was mainly distributed in the rostral LC, and some fibers entered the core in the most anterior portion of the nucleus. Two medium-size BDA injections in both 46d and 46v showed labeling in the most anterior rostral part of LC that is the rostral pole, and the density of which were higher in 46v compared to 46d (Fig. 6H and I, respectively).

DISCUSSION

The results in the present study show the existence of direct cortical projections from the insula, MPFC, OPFC and LPFC to LC. These projections are heterogeneous and show a crude topographical distribution in their terminal fields within LC. Interestingly, most of the studied areas innervate the core of LC, and most of them project directly to the densest part of the nucleus suggesting a modulatory influence of LC activity.

Methodological considerations

The BDA as anterograde tracer specifically labels axons and terminal arborizations that often show varicosities in the projected areas. We were able to detect and chart the projection at higher magnification despite that they were often scarce, very thin, and difficult to identify. Dark-field illumination also helped with the observation of these thin fibers.

In all tract-tracing experiment, the size of the injection site can markedly influence the density of the anterograde labeling. Yet, in the present study, large injections followed by sparse labeling were as large as injections where deposits resulted in much more dense labeling. This indicates that although injection size was an important factor in the density of cortical projections to LC, it did not confound the difference between dense projecting areas (agranular/dysgranular cortices) and those that did not. Retrograde labeling with injections of tracer in LC in our laboratory (unpublished results) and in prior studies (Aston-Jones et al., 2007) largely supports this heterogeneity.

The morphology of the LC and adjacent structures (represented in figures 6 and 7) varied slightly from animal to animal depending on the size of the animal and the angle of section, but this did not modify the overall results.

Comparison with prior studies in primates and rodents

Little is known about the cortical inputs in the primate LC. There are only few studies on the cortical afferents to LC in the monkey. Arnsten and Golman-Rakic (1984) showed the existence of direct cortical projections to LC in the nonhuman primate, although they suggested that the only cortical input to LC arises in the dorsomedial and dorsolateral PFC (areas 10 and 9), and they target the rostromedial part. Posterior studies suggested that only area 25 in the MPFC send moderate to scattered projections to the LC in the monkey (Freedman et al., 2000; Chiba et al., 2001). Aston-Jones and colleagues reported that OPFC and ACC also contribute to innervate LC (SfN 2000, 2002, 2004; Aston-Jones et al., 2007), and this clearly supports our data. Also, consistent with the present study, all these prior works showed that only about 5% of the total projections were contralateral.

A few previous anatomical studies in rodents described the existence of connections between the cerebral cortex and the LC, with a weak projection arising in the medial prefrontal, infralimbic and insular cortices, without reference to any specific topography (Cedarbaum and Aghajanian, 1978; Sesack et al., 1989; Luppi et al., 1995). A more recent tract-tracing study suggests that MPFC afferent terminals specifically innervate the rostromedial peripheral LC region in the rat (Lu et al., 2012). This rostral distribution of the terminals is consistent with our results in the nonhuman primate. Our experimental data show that most of the PFC areas target preferentially the rostral-to-medial part of the nucleus. The caudal pole is usually devoid of afferents, although some areas such as Iamp, and 13 send projection homogeneously throughout the whole extension of LC. A major difference between rodents and our results in the nonhuman primate is that all the PFC areas (except 10o) directly target the core of LC, while in rodents the terminal fields are localized in the peripheral-LC, where the dendritic processes lie. Another important difference is that the monkey PFC sends overall qualitatively denser inputs to LC compared to the intensity of the projection described for rodents.

Functional interpretations

There is a wealth of functional evidence that indicates that PFC regulates the LC in the rodent. Jodo et al. (1997, 1998) suggested that the PFC has a potent excitatory influence on LC activity. Single pulse electrical stimulation (1 mA, 0.3-0.5 ms) of both the dorsomedial PFC and prelimbic cortex activate the 81% and 16% of the LC neurons respectively, and train stimulation (20 Hz for 0.5 s) activated a larger percentage of LC neurons (92% and 82%); however, electrical stimulation of the LPFC had no effect on LC activity (Jodo et al., 1998). Our anatomical results are in agreement with these data since the injections placed in rostrolateral PFC barely produced labeling in LC. Moreover, chemical inactivation of the MPFC suppressed LC firing. This indicates that MPFC also provides a

resting tonic excitatory influence on LC activity (Jodo et al., 1998).

The cortical limbic system occupies the edges of the cortex as a ring above the corpus callosum and the base of the brain, where all cortical sensory, high-order association and motor systems abut (Barbas 2015). Our data show that the limbic prefrontal cortex (agranular and dysgranular areas) has a major input on LC compared to granular areas. The possibility arises that there might be a correlation between the laminar pattern existent across the different PFC areas and the intensity of the projections to LC. Overall, the agranular areas (Iam/Iamp) send the strongest input to LC, followed by the dysgranular areas in the MPFC and OPFC. The LPFC showed scarce labeling with the exception of DMPFC (area 9). This might be due to the fact that the injection site was precisely located in the most rostral portion of the dorsomedial area 9, which is very close and related to the dysgranular limbic cortex. Besides area 9, the areas 11, 12, 14 and 10 (granular) among others, produced scarce labeling in LC.

According to a recent structural model, feedforward connections project to less granular areas, and feedback projections originate from less granular areas (Barbas, 2015). Our data indicate that less granular areas do project to the LC at the same time that they present feedback projections to other cortical areas.

Despite its broad projection to the entire neuraxis, the LC is not homogeneous since there exists an inner specific organization of its cells with respect to the functions of its efferent targets (Chandler et al., 2013). Combining anatomical, molecular and electrophysiological methods, it was shown that different populations of cells in LC in the rat project specifically to different discrete prefrontal and primary motor cortex areas, with minimal overlapping and that LC cells innervating specific subregions of PFC are distinct from those terminating in M1 both in neurochemical content and electrophysiogically (Chandler et al., 2014).

In turn, LC receives direct inputs from numerous brain structures, with substantial degree of topography, based on the rat model (Luppi et al., 1995; Valentino et al., 1996; Van Bockstaele et al., 1999, 2001). The central nucleus of the amygdala and the bed nucleus of the stria terminalis send afferent fibers mainly to the rostrolateral peripheral-LC (Ennis et al., 1991), the ventrolateral part of the periaqueductal grey area sends afferent fibers mainly to the rostromedial peripheral-LC (Ennis et al., 1991), the ventral tegmental area targets the rostral pole (Deutch et al., 1986), and the dorsal raphe nucleus to the caudal part of the peripheral-LC region (Lu et al., 2012), suggesting selective afferent patterns.

The present study demonstrates a direct top-down input to LC from agranular/dysgranular limbic areas in the prefrontal cortex and the anterior insula. These connections might underlie the areal-specific role of high cognitive, motivational and emotional processes in the control of LC activity and NA release in the brain.

BIBLIOGRAPHY

Arnsten AF, Goldman-Rakic PS (1984). Selective prefrontal cortical projections to the region of the locus coeruleus and raphe nuclei in the rhesus monkey. Brain Res 306(1-2):9-18.

Aston-Jones G, Iba M, Clayton E, Rajkowski J, Cohen J (2007). The locus coeruleus and regulation of behavioral flexibility and attention: clinical implications. In Brain Norepinephrine: Neurobiology and Therapeutics, ed. Ordway GA, Schwartz MA and Frazer A. Cambridge University Press. Pp 136-235.

Aston-Jones G, Rajkowski J, Cohen J (2000). Locus coeruleus and regulation of behavioral flexibility and attention. Prog Brain Res 126: 165–182.

Barbas H (2015). General cortical and special prefrontal connections: principles from structure to function. Annu Rev Neurosci 38: 269-289.

Berridge CW, Waterhouse BD (2003). The locus coeruleus-noradrenergic system: modulation of behavioral state and state-dependent cognitive processes. Brain Res Rev 42: 33-84.

Bush G, Luu P, Posner MI (2000). Cognitive and emotional influences in anterior cingulate cortex. Trends Cogn Sci 4:215-222.

Carmichael ST, Price JL (1994). Architectonic subdivision of the orbital and medial prefrontal cortex in the macaque monkey. J Comp Neurol 346(3):366-402.

Carmichael ST, Price JL (1995a). Limbic connections of the orbital and medial prefrontal cortex in macaque monkeys. J J Comp Neurol 363(4):615-641.

Carmichael ST, Price JL (1995b). Sensory and premotor connections of the orbital and medial prefrontal cortex of macaque monkeys. J Comp Neurol 363(4):642-664.

Carmichael ST, Price JL (1996). Connectional networks within the orbital and medial prefrontal cortex of macaque monkeys. J Comp Neurol 371(2):179-207.

Cedarbaum JM, Aghajanian GK (1978). Afferent projections to the rat locus coeruleus as determined by a retrograde tracing technique. J Comp Neur 178: 1-16.

Chandler DJ, Gao WJ, Waterhouse BD (2014). Heterogeneous organization of the locus coeruleus projections to prefrontal and motor cortices. PNAS 111: 6817-6821.

Chandler DJ, Lamperski CS, Waterhouse BD (2013). Identification of projections from monoaminergic and cholinergic nuclei to functionally differentiated subregions of prefrontal cortex. Brain Res 1522: 38-58.

Chiba T, Kayahara T, Nakano K (2001). Efferent projections of infralimbic and prelimbic areas of the medial prefrontal cortex in the Japanese monkey, *Macaca fuscata*. Brain Res 888: 83–101.

Deutch AY, Goldstein M, and Roth RH. (1986). Activation of the locus coeruleus induced by selective stimulation of the ventral tegmental area. Brain Res 363: 307-314.

Ennis M, Behbehani M, Shipley MT, Van Bockstaele EJ, Aston-Jones G (1991). Projections from the periaqueductal grey to the rostromedial pericoerulear region and nucleus locus coeruleus: new evidence of anatomical and physiological specifity. Physiol Rev 63: 844-914.

Evrard HC, Logothetis NK, Craig AD (2014). Modular architectonic organization of the insula in the macaque monkey. J Comp Neurol 522:64-97.

Freedman LJ, Insel TR, Smith Y (2000). Subcortical projections of area 25 (subgenual cortex) pf the macaque monkey. J Comp Neurol 421: 172-188.

Insausti R, Amaral DG (2008). Entorhinal cortex of the monkey: IV. Topographical and laminar organization of cortical afferents. J Comp Neurol 509(6):608-641.

Jodo E, Aston-Jones G (1997). Activation of locus coeruleus by prefrontal cortex is mediated by excitatory amino acid inputs. Brain Res 768(1-2): 327-32.

Jodo E, Chiang C, Aston-Jones G (1998). Potent excitatory influence of prefrontal cortex activity on noradrenergic locus coeruleus neurons. Neurosci 83(1): 63-79.

Kerns JG, Cohen JD, MacDonald III AW, Cho RY, Stenger VA, Carter CS (2004). Anterior cingulate conflict monitoring and adjustments in control. Science 303: 1023-1026.

Kondo H, Saleem KS, Price JL (2003). Differential connections of the temporal pole with the orbital and medial prefrontal networks in macaque monkeys. J Comp Neurol 465(4):499-523.

Lu Y, Simpson KL, Weaver KJ, Lin RCS (2012). Differential distribution patterns from medial prefrontal cortex and dorsal raphe to the locus coeruleus in rats. Anat Rec 295: 1192-1201.

Luppi PH, Aston-Jones G, Akaoka H, Chouvets G, Jouvet M (1995). Afferent projections to the rat locus coeruleus demonstrated by retrograde and anterograde tracing with cholera-toxin b subunit and *Phaseolus vulgaris leucoagglutinin*. Neurosci 65(1): 119-160.

Milstein JA, Lehmann O, Theobald DE, Dalley JW, Robbins TW (2007). Selective depletion of cortical noradrenaline by anti-dopamine beta- hydroxylase-saporin impairs attentional function and enhances the effects of guanfacine in the rat. Psychopharmacol (Berl) 190: 51-63.

Mohedano-Moriano A, Muñoz-López M, Sanz-Arigita E, Pró-Sistiaga P, Martínez-Marcos A, Legidos-Garcia ME, Insausti AM, Cebada-Sánchez S, Arroyo-Jiménez MM, Marcos P, Artacho-Pérula E, Insausti R (2015). Prefrontal cortex afferents to the anterior temporal lobe in the Macaca fascicularis monkey. J Comp Neurol 523: 2570–2598.

Radley J, Williams B, Sawchenko PE (2008). Noradrenergic innervation of the dorsal medial prefrontal cortex modulates hypothalamo-pituitary-adrenal responses to acute emotional stress. J Neurosci 28(22): 5806-5816.

Rajkowski J, Lu W, Zhu Y, Cohen J, Aston-Jones G (2000). Prominent projections from the anterior cingulate cortex to the locus coeruleus in the Rhesus monkey. Soc Neurosci Abstr 26: 838.15.

Ramos BP, Arnsten AF (2007). Adrenergic pharmacology and cognition: focus on the prefrontal cortex. Pharmacol Ther 113: 523–536.

Saleem KS, Kondo H, Price JL. (2008). Complementary circuits connecting the orbital and medial prefrontal networks with

the temporal, insular, and opercular cortex in the macaque monkey. Journal of Comparative Neurology 506(4):659-693.
Sesack SR, Deutch AY, Roth RH, Bunney BS (1989). Topographical organization of the efferent projections of the medial prefrontal cortex in the rat: an anterograde tract-tracing study with Phaseolus vulgaris leucoagglutinin. J Comp Neurol 290(2):213-42.
Szabo J, Cowan WM (1984). A stereotaxic atlas of the brain of the cynomolgus monkey (*Macaca fascicularis*). J Comp Neurol 222: 265-300.
Valentino RJ, Chen S, Zhu Y, Aston-Jones G (1996). Evidence for divergent projections to the brain noradrenergic system and the spinal parasympathietic system from Barrington's nucleus. Brain Res 732: 1-15.
Van Bockstaele EJ, Bajic D, Proudfit H, Valentino RJ (2001). Topographic architecture ofstress-related pathways targeting the noradrenergic locus coeruleus. Physiol Behav 73: 273-283.
Van Bockstaele, E. J., Peoples, J., & Telegan, P. (1999). Efferent projections of the nucleus of the solitary tract to peri-locus coeruleus dendrites in rat brain: Evidence for a monosynaptic pathway. *Journal of Comparative Neurology*,*412*(3), 410-428.
Zhu, Y., & Aston-Jones, G. (1996). The medial prefrontal cortex prominently innervates a peri-locus coeruleus dendritic zone in rat. In *Soc Neurosci Abstr* (Vol. 22, p. 601).athway. J Comp Neurol 412(3):410-28.
Zhu, Y., Iba, M., Rajkowski, J., & Aston-Jones, G. (2004). Projection from the orbitofrontal cortex to the locus coeruleus in monkeys revealed by anterograde tracing. In *Society for Neuroscience Abstracts* (Vol. 30, pp. 211-213).

4.4. Hippocampal Formation And Amygdaloid Projections To The Locus Coeruleus In The Nonhuman Primate

ABSTRACT

The Locus coeruleus (LC) modulates the limbic system through direct projections to the hippocampal formation (HF) and amygdala (Amy) that in turn, regulate noradrenergic activity necessary for memory processing. Whether this regulation courses through direct projections or through indirect connections is unknown. Only the central nucleus of the amygdala has been reported to target directly and regulate the activity of LC. Here, we examine whether such modulation of the HF and Amy could be relayed by direct afferents to LC. Deposits of biotin-dextran amine, Phaseolus vulgaris leucoagglutinin or tritiated aminoacids in the dentate gyrus, hippocampus (CA1-3), entorhinal cortex, and subiculum, as well as in different deep nuclei of the amygdaloid complex, resulted in anterograde labeling that was analyzed. Overall, deposits in the subiculum resulted in the highest number of labeled fibers and presumably synaptic terminals in LC, particularly localized throughout the entire rostrocaudal extent of the lateral portion of the nucleus. Injections placed in the entorhinal cortex produced labeling, but the deposit spread into the amygdala and a differential analysis suggests that the labeling produced with injections centered in EC actually likely originate in the Amy. Injections in CA1-3 or dentate gyrus did not produce any labeling. Within the amygdala, only the injections made in the basal and the paralaminar nuclei produced labeling in the lateral portion of LC, similar to the labeling produced after deposits into the subiculum. Prior studies showed that both subiculum and the basal nucleus of the amygdala receive projections from LC. The present study shows that these projections are bidirectional in primates and that the spatial distribution of both subiculum and amygdala overlaps within the lateral portion of locus coeruleus, suggesting a role for LC in memory processing under emotional context.

INTRODUCTION

The noradrenergic (NA) system has been shown to be involved in memory processing (Roullet and Sara 1998; Tronel et al., 2004; McGaugh and Roozendaal, 2008), as well as synaptic plasticity in the hippocampus and amygdala (Tully and Bolshakov, 2010). The majority of the NA neurons are allocated in the brainstem, the most important of which is the *Locus coeruleus* (LC), which fires at critical periods during learning, off-line memory consolidation and retrieval (Sara, 2009).

LC phasically responds to novel salient stimuli arising from ascending sensory afferents (Aston-Jones and Bloom, 1981) and modulates the limbic system, and in particular the to the hippocampal formation (HF) and amygdala (Amy) through direct projections (Jones and Moore, 1977; Bowden et al., 1978; Fallon et al., 1978; Amaral and Cowan, 1980; Loughlin et al., 1986; Insausti et al., 1987; Wilcox and Unnerstall, 1990). Those, in turn might regulate the noradrenergic activity necessary for memory processing. Whether this regulation courses through direct or through interposed (indirect) connections is largely unknown.

There is no anatomical data demonstrating the existence of direct inputs from the HF to LC. In fact, there are studies in both rodents and primates indicating that the only cortical region showing direct projections to the LC is the prefrontal cortex (PFC, Cedarbaum and Aghajanian, 1978; Arnsten and Golman-Rakic, 1984; Luppi et al., 1995; Freedman et al., 2000; Chiba et al., 2001; Aston-Jones and Cohen, 2005; Lu et al., 2012). Regarding the amygdaloid complex, only the central nucleus of the amygdala (CeA) has been shown to send a rather strong projection to LC in both rodents and monkeys (Price and Amaral, 1981; Ennis et al., 1991; Luppi et al., 1995). No evidence for other amygdala nuclei projections to the LC exists, to the best of our knowledge.

However, functional studies indicate that HF and Amy might project to the LC and, therefore, regulate the activity of NA-LC under certain conditions. Pharmacological studies in rodents revealed that, after a learning experience, there is a time window during which the NA system is activated to reinforce long-term memory processing (Sara et al., 1999; Tronel et al., 2004). On the other hand, the Amy might also improve the retrieval of emotional memories by modulating central arousal by the LC (Davis and Whalen, 2001). Furthermore, functional MRI demonstrated that both Amy and LC are functionally connected during the successful retrieval of memories that were encoded in an emotional context (Sterpenich et al., 2006).

In this study, we used anterograde tract-tracing in the macaque monkey to test whether HF and Amy project directly to LC, and to examine the topographical organization of these projections.

MATERIALS AND METHODS

Subjects

The present data were obtained from 55 young adult *Macaca fascicularis* monkeys (mean weight 3.3 kg, range 2.5–4.5 kg), which had been prepared and used in previous studies (Pitkänen and Amaral, 1998; Bonda, 2000; Pitkänen et al., 2002; Freese and Amaral, 2005; Mohedano-Moriano et al., 2015). The cases were reexamined and the connections with LC analyzed. In addition, anterograde tracers were injected into different subfields of the EC in 3 more monkeys.

All procedures were carried out under an approved University of California-Davis Institutional Animal Care and Use Protocol, and strictly adhered to National Institutes of Health policies on primate animal subjects. Likewise, experiments were conducted according to the guideline of the European Community on welfare of research animals (directive 86/609/EEC) and the supervision and approval of the Ethical Committee of Animal Research of the University of Castilla-La Mancha (UCLM), Spain.

Surgery and tracer injection

Animals were tranquilized with an initial intramuscular dose of ketamine HCl (8 mg/Kg), fitted with a tracheal cannula, and brought to a surgical level of anesthesia with isoflurane. All surgeries were performed under sterile conditions, and the animal's heart rate, respiration, temperature, and blood oxygenation were monitored throughout the procedure. The animal was placed in a Kopf stereotaxic apparatus; a midline incision was made, and a small burr hole was drilled in the skull at a position appropriate for the injection of tracer. The coordinates were based on the atlas of Szabo and Cowan (1984). The dorsoventral coordinate for the injection was determined by recording extracellular unit activity along the injection trajectory, as described previously (Amaral and Price, 1984). Postoperatively, the monkeys received analgesics as needed and prophylactic doses of antibiotics.

Different anterograde tracers were injected in the hippocampal formation and the deep amygdala nuclei. The tracer *Phaseolus vulgaris* leucoagglutin (PHA-L) was iontophoretically injected as a 2.5% solution of in 0.1 M sodium phosphate buffer, pH 7.4 (5-µA pulsed DC current, 7 seconds on and 7 seconds off, for 40–45 minutes). The ^{3}H-aminoacid injections contained an equal amount of ^{3}H-leucine and ^{3}H-proline (L-[4-5-3H] leucine; L-[2, 3-3H] proline, respectively, New England Nuclear, Dupont, DE, USA), vacuum evaporated and reconstituted to a final concentration of 100 µC/µl (see Insausti and Amaral, 2008 for details). Injections of biotin dextran amine (BDA, 10.000 MW, lysine fixable, 10%, Molecular Probes, Eugen, OR, USA) were injected either by iontophoresis (Freese and Amaral, 2005) or by pressure (Muñoz and Insausti 2005; Mohedano-Moriano et al., 2008).

To avoid spread of tracer along the pipette track, the micropipette was left in place for 30 minutes after the injection was finished

Perfusion and histological processing

After a 2-week survival period, the animals were the animals were anesthetized with ketamine (10 mg/kg, i.m.), followed by sodium pentobarbital (25–30 mg/kg, i.v.), and transcardially perfused with 0.5 L of cold 1% paraformaldehyde in 0.1 M phosphate buffer followed by 7.0 L of cold 4% paraformaldehyde in 0.1 M phosphate buffer. The brain was blocked stereotaxically, postfixed for 6 hours in 4% paraformaldehyde, and then cryoprotected in 10% glycerol and 2% dimethyl sulfoxide (DMSO) in 0.1 M phosphate buffer (pH 7.4) for 24 hours, then 20% glycerol, 2% DMSO in 0.1 M phosphate buffer for 72 hours. Blocks were subsequently sectioned or stored at –80ºC until they were sectioned into either 30 or 50 μm sections in the coronal plane on a microtome where the stage was frozen with dry ice. After rinses in phosphate buffer, the sections were mounted onto acid cleaned, gelatin-coated slides and stained by the Nissl method with 0.25% thionin. BDA and PHA-L was processed directly with the avidin-biotin-peroxidase method (ABC Elite Kit, Vector, Burlingame, CA).

Data analysis and illustrations

The spatial distribution of labeled terminals was analyzed with an epifluorescence microscope coupled to a computerized charting system (MD-Plot, Datametrics, Minnesota, USA), and each labeled fiber was plotted as a single dot. Subcortical boundaries and other landmarks were added to these plots by camera lucida drawings of adjacent Nissl-stained sections.

The relative strength or densities of connections was evaluated, although factors such as differences between tracers in transport levels, injection volumes and location of each injection precluded the estimation of absolute values. LC labeling was analyzed bilaterally in coronal sections, and maps were prepared to visualize the spatial distribution and density of the terminal fields across the rostrocaudal extension of the nucleus. Only those fibers contained presumed synaptic buttons or varicosities were represented in the maps.

Nomenclature

Hippocampal formation.

The hippocampal formation includes the, dentate gyrus, hippocampus, subiculum, presubiculum, parasubiculum and entorhinal cortex (Insausti and amaral, 2012). The entorhinal cortex was divided into seven subfields according to the nomenclature of Amaral et al. (1987): olfactory entorhinal subfield (Eo), rostral entorhinal subfield (Er), intermediate entorhinal subfield (Ei), lateral rostral entorhinal subfield (Elr), lateral caudal entorhinal subfield (Elc), caudalentorhinal subfield (Ec) and caudal limiting entorhinal subfield (Ecl).

Amygdaloid complex.

In this study, we used the nomenclature of Price et al. (1987); Amaral et al. (1992) and Pitkänen & Amaral (1998) for the monkey amygdaloid complex with slight modifications. The deep nuclei of the amygdala consist of the lateral nucleus (dorsal, dorsal intermediate, ventral intermediate, and ventral divisions), the basal nucleus (magnocellular, intermediate, and parvicellular divisions), the accessory basal nucleus (magnocellular, parvicellular and ventromedial divisions) and the par-alaminar nucleus.

Locus coeruleus.

Anatomically, the LC is composed of a densely packed group of neurons (nuclear core) and a surrounding peripheral zone with more loosely packed neurons (figure 1), which is asymmetrically distributed and contains mostly dendrites. The core of LC is divided into dorsal and ventral parts cytoarchitectonically distinct, since the cells in the dorsal division are more densely packed and a majority of these cells in the dorsal division are aligned obliquely in a dorsolateral to ventromedial orientation when viewed in the coronal plane of the brain (obliquely in the brainstem, and thence in the LC. The less dense part of LC core starts in the rostral pole of LC, and extends caudally, mainly ventral to the more densely packed part; at midlevel of the rostrocaudal extent, the less dense part spreads both medially, where some sparse medium-size cells are interspersed into the laterodorsal tegmentum, and laterally beyond the mesencephalic tract of the fifth cranial nerve.

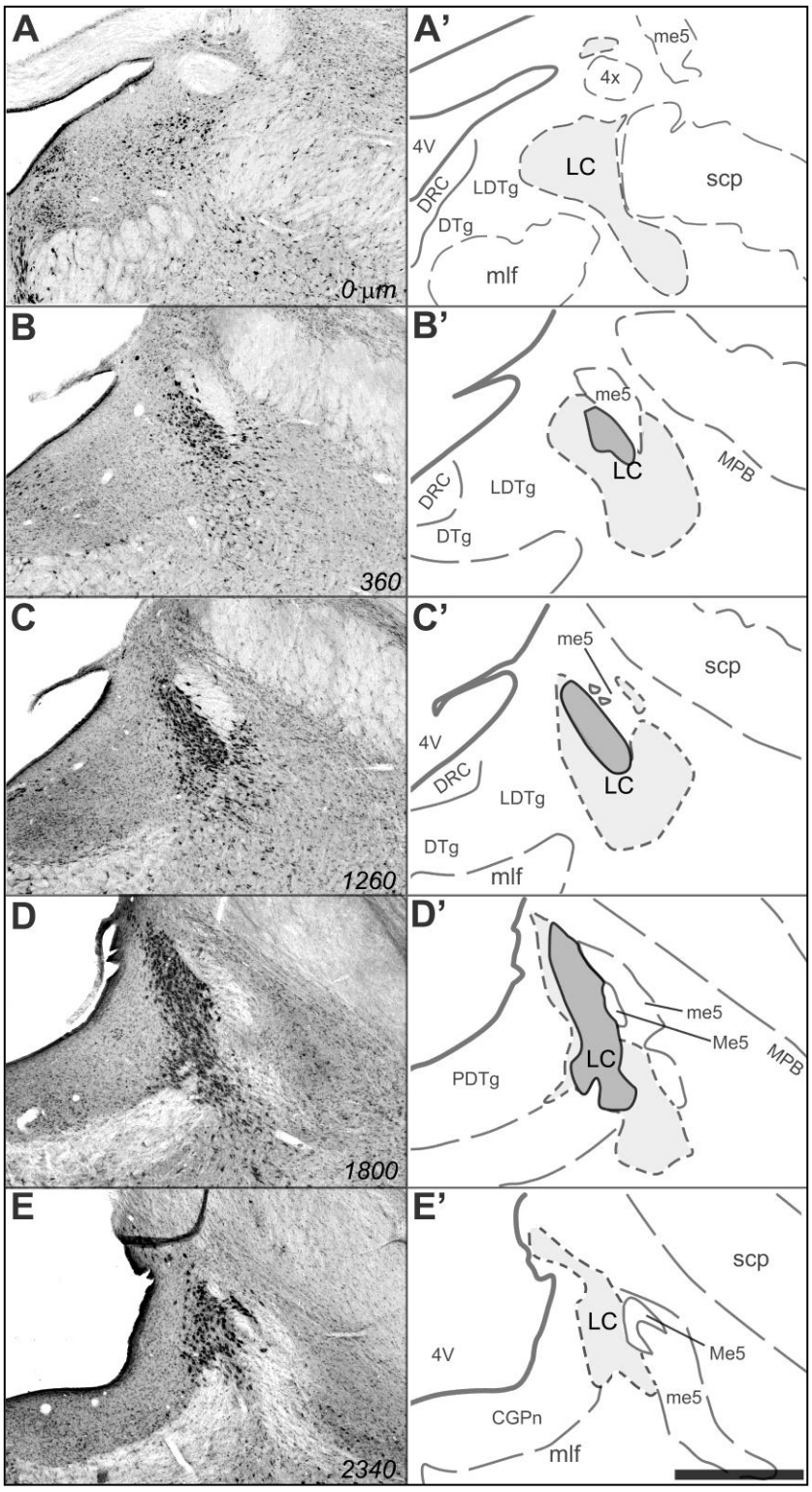

Figure 1. Cytoarchitecture. Coronal sections of LC in the monkey from rostral (A) to caudal (E), and the corresponding drawing (A'-E'). Abbreviations: 4V, fourth ventricle; 4x, trochlear decussation; CGPn, cg pons; DRC, dorsal raphe caudal; DTg, dorsal tegmentum; LDTg, laterodorsal tegmentum; LC, locus coueruleus; me5, mesencephalic tract 5; Me5, mesencephalic nucleus 5; mlf, medial longitudinal fascicle; MPB, medial parabrachial nucleus; scp, superior cerebelar peduncle. Scale bar: 1mm

RESULTS

Injection sites

Table 1 presents the list of cases, the tracer injected in each case and the location of the injection site. We analyzed the labeling obtained from 71 injections (Table 1) that included DG (n=13), CA1 (n=5), CA2 (n=2), CA3 (n=7), Subiculum/Presubiculum (n=4), EC (n=17) and Amygdala (n=35). Figures 2, 3 and 4 show the collation of all these injections sites onto standard maps of the hippocampus, entorhinal cortex, and amygdaloid complex, respectively.

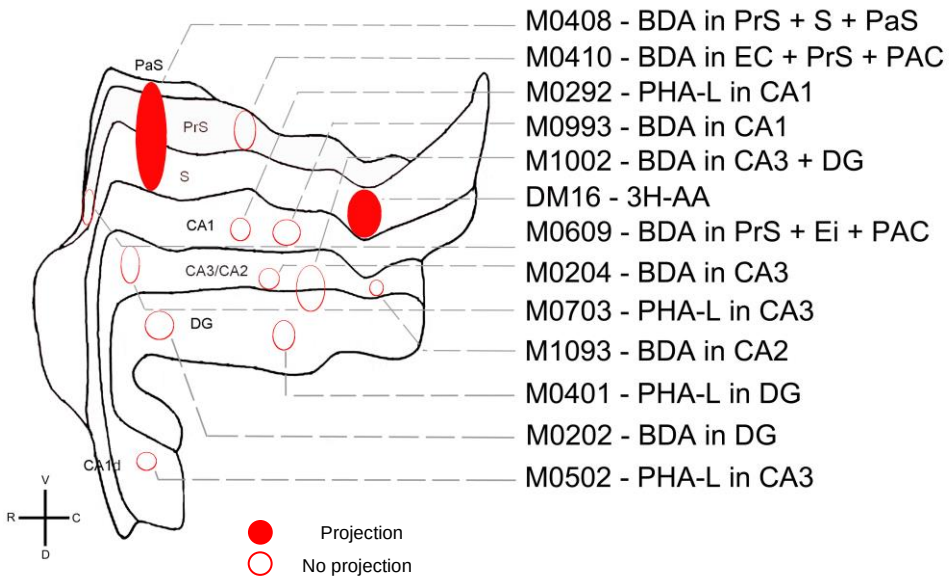

Figure 2. Flat map of the hippocampus, subiculum, presubiculum and parasubiculum.The circles represent the injection sites. Filled circle: project; empty circle: do not project.

Figures 5A-B and 6A-B show examples of injection sites in subiculum and amygdala, respectively. PHA-L and BDA injection sites were identified under both dark and bright field (Fig. 5 and 6) illumination; ^{3}H-aminoacid injection site was identified under dark field illumination (not illustrated). Due to differences in the amount of the tracer injected and variations in tracer uptake, the injection sites varied in shape and size. The injections of BDA injected by pressure were usually bigger than those injected iontophoretically, where the injections were well restricted to a small region.

The BDA injected by pressure in the EC involved layers I-VI. The tracer did not extend to the white matter in any of the cases, but in some of them the Amy was involved along the tract (See Table 1). The pressure injections of BDA in the Amy were also bigger and the diffusion area usually spread to contiguous nuclei within the Amy. Finally, the iontophoretic injections of BDA and PHA-L in the HF or Amy involved just a small group of cells in a restricted portion, and the layers involved in the EC varied among the different cases.

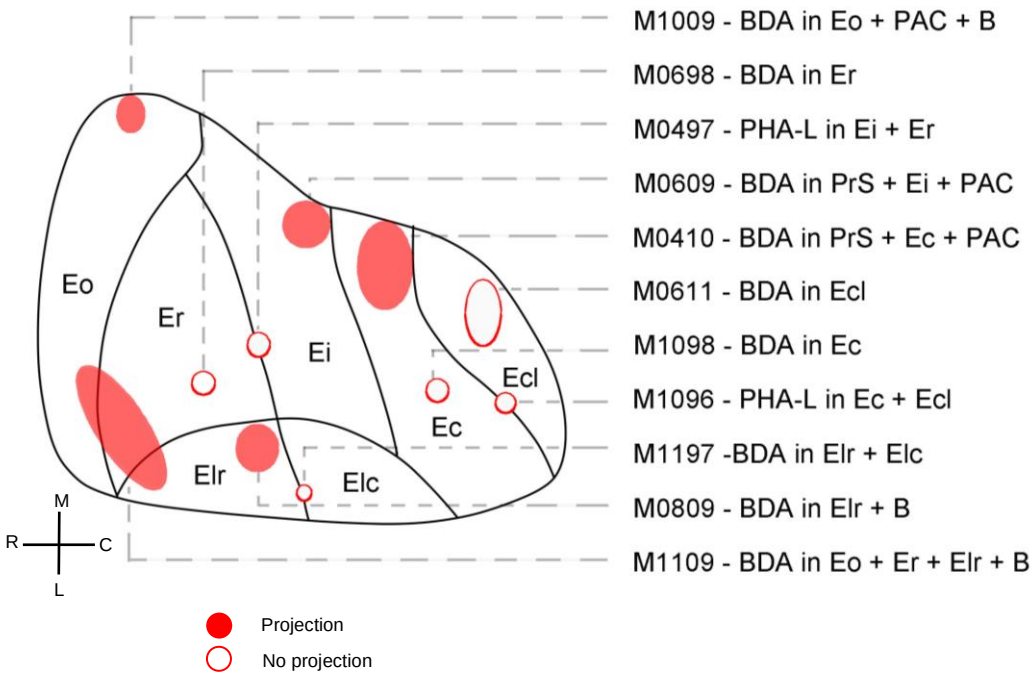

Figure 3. Unfolded map of the entorhinal cortex. The circles represent the injection sites.

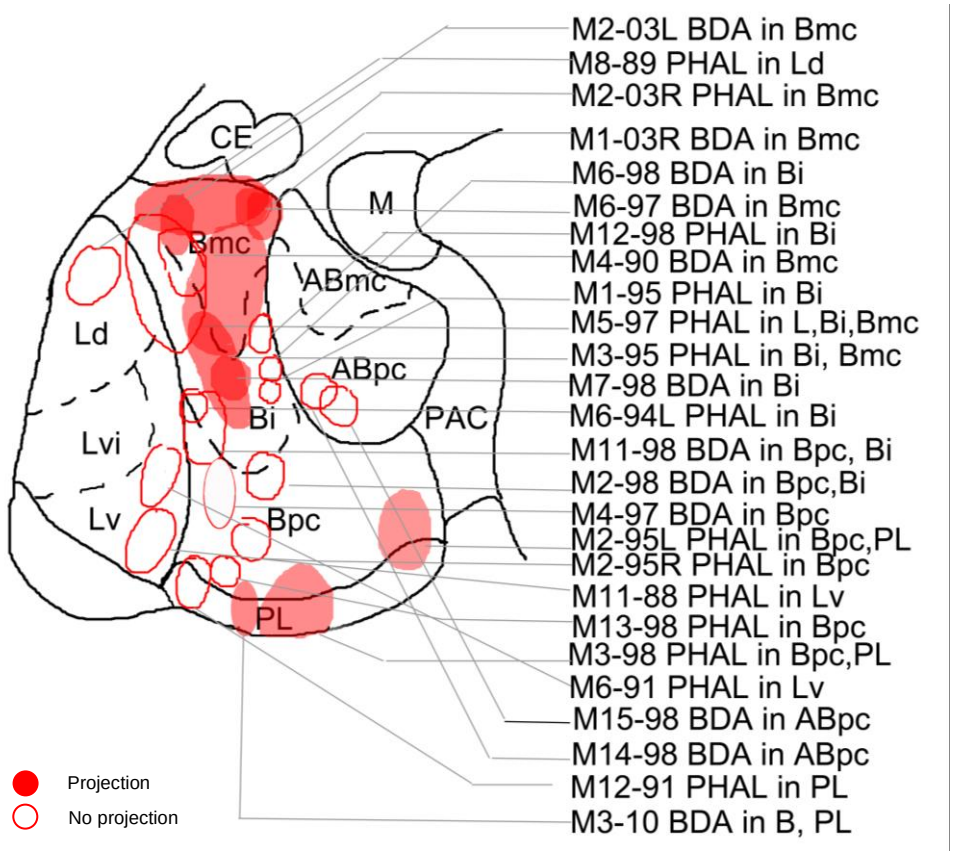

Figure 4. Bidimensional map representing the location of the injection sites in the amygdaloid complex. The circles represent the injection sites.

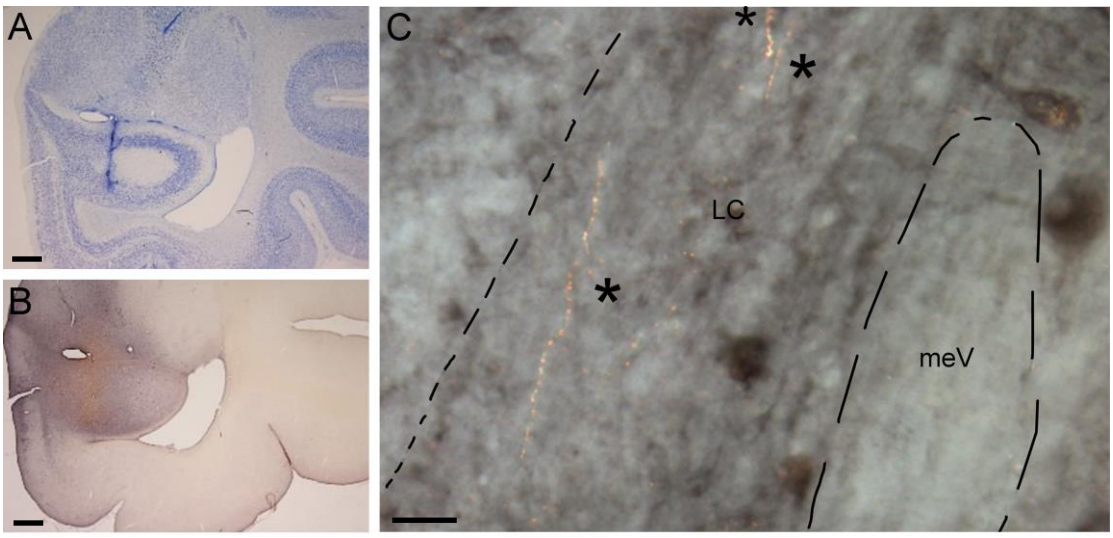

Figure 5. Photomicrographs of coronal section of the injection site in subiculum (M04-08). A. Nissl. B, BDA. C, Darkfield photomicrograph of anterograde labeling in LC. Asterisks indicate labeled fiber. Scale bar: 100μm (A and B), 20μm (C). For abbreviations see legend of figure 1.

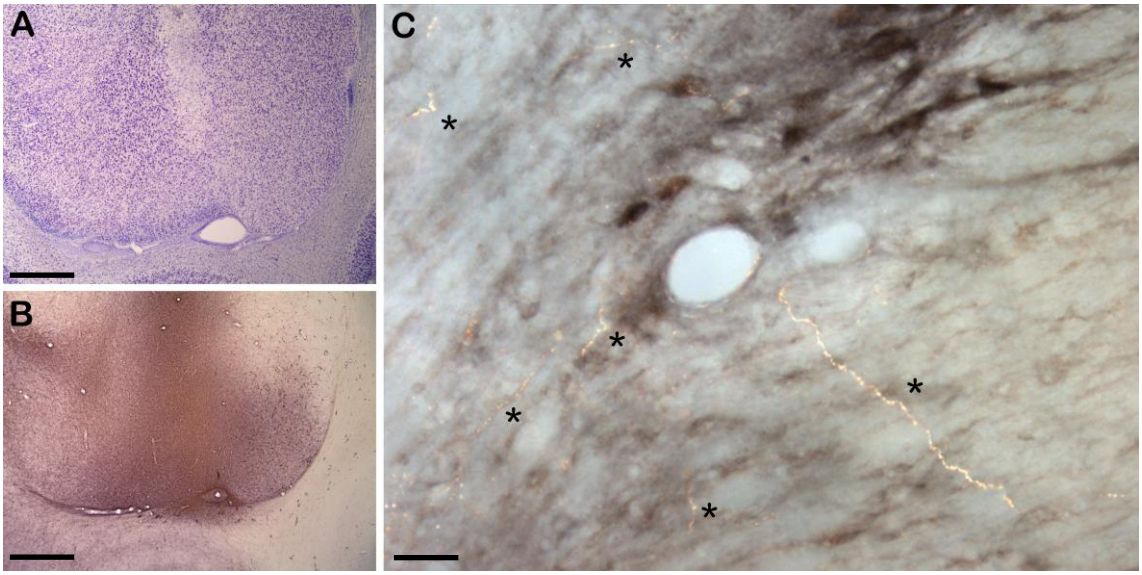

Figure 6. Photomicrographs of coronal section of the injection site in the basal nucleus of the amygdala (M03-10). A. Nissl. B, BDA. C, Darkfield photomicrograph of anterograde labeling in LC. Asterisks indicate labeled fiber. For bbreviations see legend of figure 1. Scale bar: 100μm (A and B), 20μm (C).

			INJECTION SITE																							
			HIPPOCAMPAL FORMATION													AMYGDALA										
				Hippocampus			Subicular Complex			Entorhinal Cortex						Lateral			Basal			Accesory Basal	Paralaminar			
	CASE	TRACER	DG	CA1	CA2	CA3	Sub	PrS	PaS	Eo	Er	Ei	Elr	Elc	Ec	Ecl	Ld	Lvi	Lv	Bmc	Bi	Bpc	ABpc	PL	PAC	AHA	Labeling
1	M01-02	PHA-L																									-
2	M02-02	PHA-L																									-
3	M02-02	BDA																									-
4	M03-02	PHA-L																									-
5	M04-01	BDA																									-
6	M04-01	PHA-L																									-
7	M04-02	PHA-L																									-
8	M04-02	BDA																									-
9	M10-02	PHA-L																									-
10	M11-92	PHA-L																									-
11	M02-04	PHA-L																									-
12	M09-03	BDA																									-
13	M10-02	BDA																									-
14	M02-92	PHA-L																									-
15	M09-93	BDA																									-
16	M14-03	BDA																									-
17	M28-92	PHA-L																									-
18	M10-93	BDA																									-
19	M07-03	BDA																									-
20	M9-92	PHA-L																									-
21	M05-02	PHA-L																									-
22	M07-03	PHA-L																									-
23	M02-04	BDA																									-
24	DM16	3H-AA																									+
25	M04-08	BDA																									+
26	M06-09	BDA																									-
27	M04-10	BDA																									+
28	M12-98	BDA																									-
29	M3-98	BDA																									-
30	M12-97	PHA-L																									-
31	M02-97	PHA-L																									-
32	M11-97	BDA																									-
33	M10-87	3H-AA																									+
34	M10-96	PHA-L																									-
35	M10-98	BDA																									-
36	M06-11	BDA																									-
37	M04-97	PHA-L																									-
38	M06-98	BDA																									-
39	M10-09	BDA																									+
40	M08-09	BDA																									+
41	M03-10	BDA																									+
42	M11-09	BDA																									+
43	M4-90	BDA																									-
44	M8-89	PHA-L																									-
45	M11-88	PHA-L																									-
46	M6-91	PHA-L																									-
47	M12-91	PHA-L																									-
48	M1-95	PHA-L																									-
49	M2-95L	PHA-L																									+
50	M2-95R	PHA-L																									+
51	M3-95	PHA-L																									+
52	M4-97	BDA																									-
53	M5-97	PHA-L																									-
54	M6-97	BDA																									+
55	M6-94L	PHA-L																									-
56	M3-98	PHA-L																									+
57	M2-98	BDA																									-
58	M6-98	BDA																									-
59	M11-98	BDA																									-
60	M7-98	BDA																									+
61	M13-98	PHA-L																									-
62	M14-98	BDA																									-
63	M15-98	BDA																									-
64	M12-98	PHA-L																									+
65	M1-03R	BDA																									+
66	M1-03L	PHA-L																									+
67	M2-03R	PHA-L																									+
68	M2-03L	BDA																									+
69	M14-97	BDA																									-
70	M6-98	PHA-L																									+
71	M12-98	PHA-L																									+

TABLE 1. Anterograde tracer injections in the hippocampal formation[1] and the amygdala[1]. + Symbol refers to the presence of labeled fibers (> 1), - symbol refers to the absence of labeling (<1).

The anterogradely labeled fibers had a sinuous shape with a high number of varicosities (figures 5C, and 6C), mainly distributed in the ipsilateral hemisphere; however there was scarce labeling also into the contralateral hemisphere that did not represent more than the 5% of the total labeled fibers.

Figures 8 and 9 show the plots of anterograde labeling in sets of coronal sections through LC. Overall, the subiculum and the basal magnocellular nucleus of the amygdala deposits resulted in the heaviest labeling in the core of LC. The majority of the terminal fields were located in the sparse part of the core, although in some cases (e.g. M02-03R, M02-03L, M04-08, M08-09, M03-10) the labeled fibers were present also in the densest part of nucleus. Overall, the most of the labeling was located in the rostrolateral portion of LC, although in some cases a sparse labeling was observed in the medial portion of the LC at caudal levels of the nucleus. Moreover, not all the injections produced labeling in LC

Hippocampal Formation

The subiculum was the region of all the HF that projected most heavily to the LC. Injections in DG and hippocampal fields (CA3, CA2 and CA1) did not produce any labeling; the deposits in EC labeled axons in LC, although in some cases some nuclei of the Amy were involved, and the resulting labeling in LC could have been also originated in the diffusion zone of the deposit.

Subiculum

The data obtained from the analysis of two injections in Sub (figure 2), one with BDA (M04-08; figure 8G) and one with 3H-AA (DM16; not shown but see Table 1), revealed a strong input to LC. The injection of 3H-AA, showed a moderate concentration of silver-aggregates in the lateral part of the ipsilateral nucleus. The BDA injection also showed that the terminal fields in LC were distributed ipsilaterally, and adopted the form of long fibers running longitudinally to the coronal plane and mainly localized within the lateral portion of the core of LC, close to the mesencephalic tract of the fifth cranial nerve. Even though there were fibers throughout the whole rostrocaudal extension of the nucleus, most of them were innervating the rostral levels.

Three injections included the PrS (cases M04-08, M06-09, and M04-10; see figure 2). The case M06-09 had an injection of BDA that involved the PrS, Ei and PAC and no labeled axons were found in the LC (Fig. 8D). Therefore, it seems that the PrS does not project directly to LC. In the case M04-10, the BDA injection targeted PrS, EC and AHA and produced moderate to sparse labeling within the ipsilateral core of LC (Fig. 8F).

However, some axons also reached the core of the contralateral LC. Since neither PrS nor EC (see below) seemed to send projections, it is likely that the labeling seen in LC could arise in AHA. The case M04-08 has been described above (Fig. 8G).

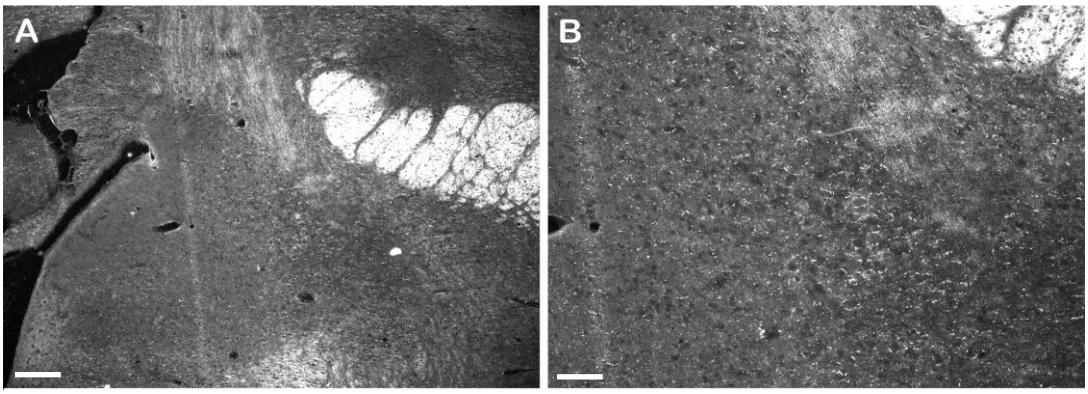

Figure 7. Darkfield photomicrographs of a coronal section showing 3H-AA labeling in the lateral part of the *Locus coeruleus* (case DM16). Scale bar: 100μm (A), 20μm (B)

Dentate Gyrus and Hippocampus

The thirteen injections at different levels of the DG were very small, and involved only a limited number of cells in the most of the cases (not shown in Figs. 7 and 8; but see Table 1). Since no labeled fibers were found in the LC, neither in the periphery nor in the core, there was strong indication that they did not project to LC. Likewise, CA fields, CA3, CA2 and CA1 did not send projections to the LC, since none of the fourteen injections of either BDA or PHA-L made iontophoretically in CA3, CA2 and CA1 fields showed labeling (see Table 1).

Entorhinal Cortex

A total of sixteen injections in different subfields of the entorhinal cortex were analyzed (see Table 1). Eleven out of sixteen injections were located in a specific subfield of the EC without involvement of other brain structures. The result of these deposits of anterograde tracer either in Eo, Er, Ei, Ec or Ecl was negative as no labeled axons were found (Table 1). However, the injection of 3H-AA in Elr (case M1087) showed moderate to light density of silver deposit in the rostroventral part of the LC (Table 1). Furthermore, five more BDA injections in EC were analyzed. In these cases, either the deposit or the periphery of the injection site spread to neighboring amygdalar nuclei, and thereby it is likely the labeling obtained arised in the Amy rather than in EC (see below).

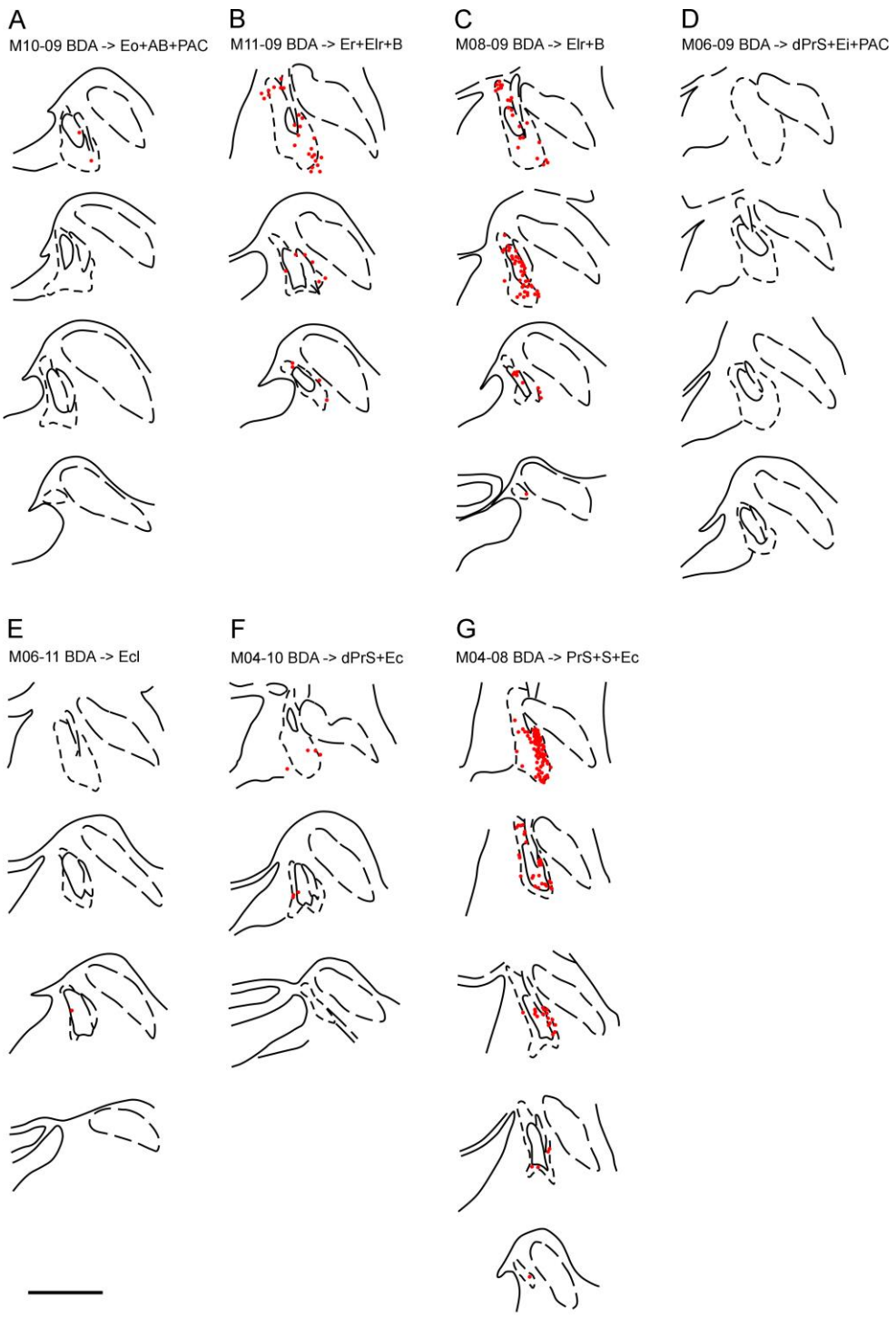
A
M10-09 BDA -> Eo+AB+PAC
B
M11-09 BDA -> Er+Elr+B
C
M08-09 BDA -> Elr+B
D
M06-09 BDA -> dPrS+Ei+PAC
E
M06-11 BDA -> Ecl
F
M04-10 BDA -> dPrS+Ec
G
M04-08 BDA -> PrS+S+Ec

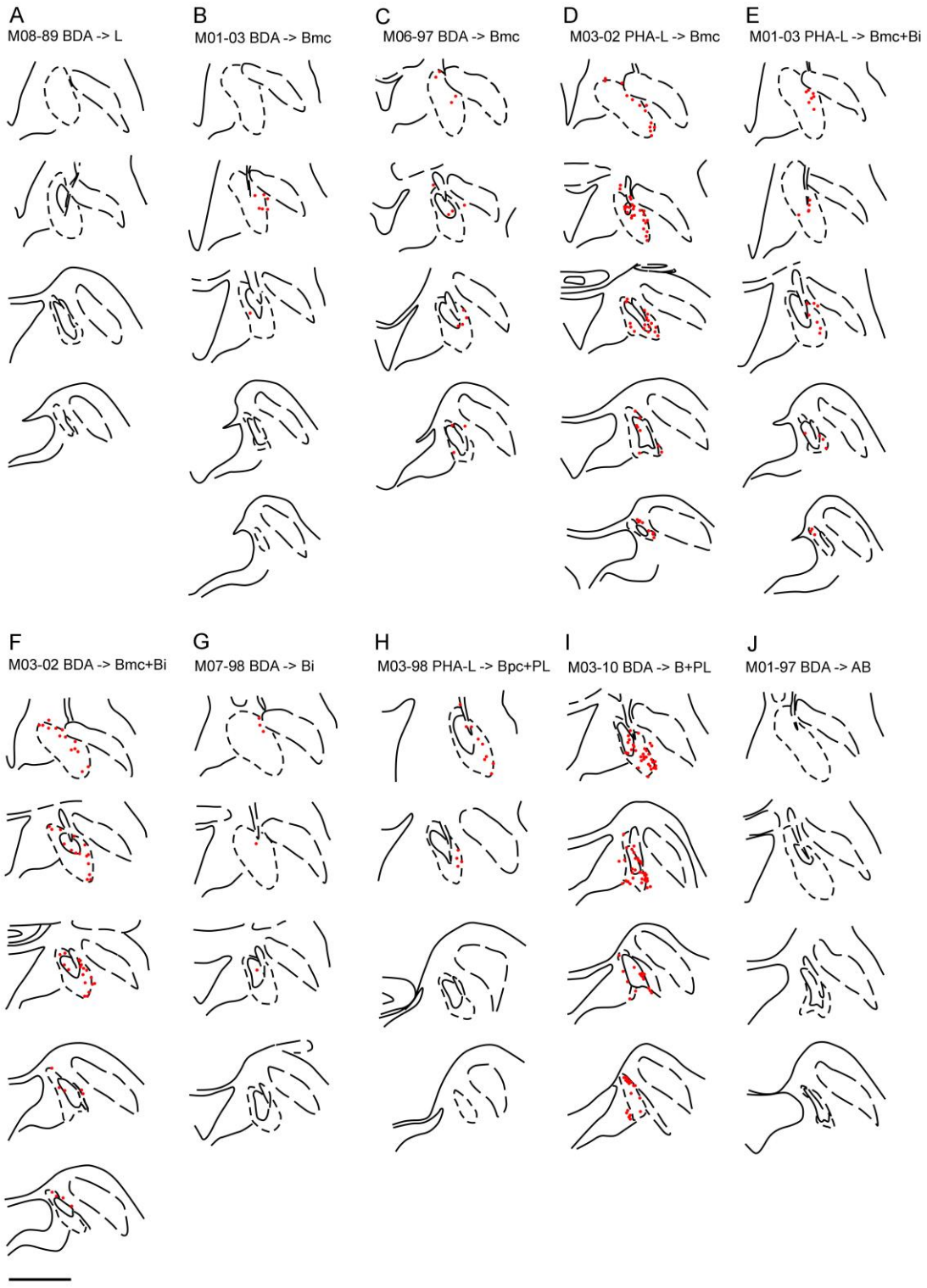

Figure 8-9. Drawings depicting the labeling obtained in the *Locus coeruleus* after injections of anterograde tracers in the hippocampal formation and the amygdala. Each red dot represents 1 labeled fiber. Scale bar: 2mm

Amygdaloid Complex

The data obtained from the analysis of 35 injections in different deep amygdaloid nuclei as well as PAC and AHA, showed that there is a complex organization of subpopulations of cells projecting to the LC. Injections in the same nucleus but involving different divisions often resulted in opposite results. For example, in both cases M6-97 (BDA; Fig. 9C) and M4-90 (BDA; not shown but see Table 1) the injection was located in Bmc; however only the first one showed labeling in LC. Therefore, it seemed that the projections of the Amy to LC could be originated in a subset of neurons.

Overall, the basal nucleus of the amygdala sends the densest inputs to LC, followed by the PL. Only some small regions in the Bi and Bpc send projections to LC. In contrast, injections in the lateral nucleus or the PAC did not show any labeling within LC.

The basal magnocellular and the paralaminar nuclei send their projections manly to the lateral part of the ipsilateral LC, and the density of fibers decreases from rostral to caudal levels of LC.

Lateral Nucleus

Four cases with injections of PHA-L in different divisions of the lateral nucleus (Ld, Lvi and Lv) did not reveal any labeled fiber, neither in the core of LC nor the periphery (M8-89, M11-88, M6-91, and M5-97. See Table 1). Therefore, it is likely that the lateral nucleus of the amygdala does not project to LC.

Basal Nucleus

In the present results, the major output from the amygdala to LC arises in the Bmc, although certain injections in Bi or Bpc also produced some labeling. These nuclei project preferentially to the rostrolateral portion of the core, but some scattered fibers are also present at caudal levels.

Within the Bmc, almost all of the deposits projected to the core of LC (e.g. M01-03, M06-97, M03-02, Fig. 9D; See figures 9B, 9C and 9D respectively). There is only one injection that did not produced labeling (M4-90. See Table 1), and was located close to Ld and Bi. On the contrary, only two injections in Bi out of 8 produced labeling in LC, and one of them also involved the Bmc (see M7-98 and M3-95 in Table 1).

Paralaminar Nucleus

The PL nucleus was included in the injection site of six experiments. In five cases, the injection site included also the basal nucleus, mainly the Bpv and the ventral part of Bi (see Table 1). The analysis of these five cases showed labeling in the core of LC, with the fibers distributing along the entire longitudinal extension of the nucleus, the majority of them in the core. However, the density of these projections in LC decreased from rostral to caudal, so that the caudal pole contained a scarce amount of fibers. The labeling was stronger in the cases where the injection was bigger, such as M08-09 (Fig. 8C) and M03-10 (Fig. 9I). Only one case (M12-91; not shown, see Table 1) out of the six did not show any labeling in LC. In this case, the injection size was small and localized very close to the lateral nucleus of the amygdala.

Accessory Basal Nucleus

Four cases with injections of BDA in the AB were analyzed. In three of them, the injections were small and strictly restricted to the ABpc (cases M14-97, M14-98, M15-98; see Table 1). No labeled axons were found neither in the core nor the periphery of LC. In one case (M10-09; Fig. 8A), the injection involved ABmc, ABpc, Bpc, PAC and Eo, and resulted in scarce labeling in the rostral part of the core. It is likely that this light labeling arose in Bpc.

DISCUSSION

The present study shows the existence of a direct input from the subiculum to the locus coeruleus. In addition, the present results demonstrate that, beyond the central nucleus, the Amy targets the LC directly through the basal and the paralaminar nuclei. It seems that these projections originate in specific groups of cells with an irregular distribution. Moreover, all the projecting cell groups innervate the core of LC, while some of them project directly to the densest part of the nucleus, what is suggestive of a direct and a presumably powerful modulatory influence on LC activity. Interestingly, the spatial distribution of the labeled fibers in LC is very similar for both the Sub and Amy, since the labeling was preferentially distributed along the lateral portion of the nucleus, mostly at rostral levels.

Methodological considerations

The BDA as anterograde tracer specifically labeled axons and terminal arborizations with varicosities. Although many of the subsequent fibers were very thin and difficult to identify, they could be observed at higher magnification even if they were scattered. Dark-field illumination also helped with the observation of these thin fibers. The size of the injection site could also be a limiting factor concerning the quantitative analysis. For example, most of the PHA-L injections in the EC were very small and confined to a reduced group of cells, while some BDA injections were considerably bigger and extended to adjacent regions.

The anatomical shape of the LC and adjacent structures represented in the drawings varied from animal to animal, depending on the size of the animal and angulation of the plane of section of the brain. However, neither the variation in shape across animals nor the variation in the plane of section altered the finding.

Hippocampal formation input to the *Locus coeruleus*

Although there are no previous anatomical reports on the existence of direct projection from the HF to LC, the present study shows that the subiculum targets directly the core of the nucleus and that

these afferents are specifically distributed throughout the rostrolateral part of LC. The entorhinal cortex might also contribute with a small input, although more experiments would be needed to demonstrate it

Despite the lack of the anatomical evidence in the literature regarding these projections, there are functional studies suggesting that the HF might influence LC activity under certain conditions. The neurons in LC are responsive to salient stimuli of various modalities (Aston-Jones et al., 1986, 1994) and this selective responsiveness of LC neurons to cognitively important stimuli points to a functional link between higher brain areas and the LC (Gibbs et al., 2010). The activation of LC leads to the release of NA in terminal fields, as well as in the somato-dendritic area of LC neurons (Singewald et al., 1994; Singewald and Philippu, 1998; Gulyas et al., 2010) and influence the functional state of LC cells to subsequent stimuli (Bouret and Sara, 2005). NA release in the LC modulates memory formation and consolidation (Gibbs et al., 2010).

Furthermore, it has been demonstrated that both N-methyl-D-aspartate (NMDA) and a-amino-3-hydroxy-5- methyl-4-isoxazolepropionic acid (AMPA) of glutamatergic receptors are present in LC, and that LC neurons are phasically activated by glutamatergic input (Jodo and Aston-Jones, 1997; Jodo et al., 1998), what is followed by the release of noradrenaline (NA) onto its targets.

The subiculum represents the principal outflow of the HF (Swanson et al., 1978) and provides massive, topographically organized innervation to limbic cortices, nucleus accumbens, lateral septum, bed nucleus of the stria terminalis, preoptic area, hypothalamus, central gray region and medulla (Canteras and Swanson, 1992; Köhler, 1990), although projections to LC have not been described. The subiculum efferent terminals are glutamatergic (Blaha et al., 1997; Floresco et al, 2001; Lisman and Grace, 2005), and therefore it is likely that the subicular input to LC described in this work may activate the nucleus.

Amygdala input to the *Locus coeruleus*

The retrograde tracer horseradish peroxidase (HRP) was initially used to demonstrate brain regions that project to LC in the rodent (Cedarbaum and Aghajanian, 1978; Clavier, 1979; Aston-Jones et al., 1986; Luppi et al., 1995). These early studies suggested that only the CeA innervates LC. Anterograde tract-tracing studies corroborated the results obtained with the retrograde tracers. Aston-Jones et al (1986) injected WGA-HRP into the CeA of the rodent and found labeled axon processes into the dorsolateral peri-LC area but not within the nuclear boundaries. This might be a major difference between rodents and primates, since our results show that the amygdala innervates the core of the LC, mainly in its rostrolateral extension.

Previous studies in monkeys (Price and Amaral, 1981) demonstrated that the Amygdala targets the core of LC and this is in accordance with our data. They described moderate labeling mainly located in the ventral portion of the nucleus arising specifically in the CeA. Our results show

variations in the distribution of the labeled axons depending on the location of the injection site; however, the overall labeling was concentrated in the lateral part of the nucleus, mainly at rostral levels. It might be possible that the CeA sends projections to the ventral part of LC while the basal nucleus of the amygdala specifically projects to the lateral portion.

In addition, our data demonstrate that the CeA is not the only amygdaloid nucleus projecting to LC, as labeled fibers were obtained after injections in Bmc, and certain portions of the PL and Bpc. This work shows that the projection system of the amygdala is quite complex, and that might exist subsets of cells specialized in their outputs, since injections located close to each other within the same nucleus reported totally different results (See Fig. 4, 8 and 9).

On the other hand, The PAC seems not to send inputs to LC, since a big injection of BDA (M06-09; Fig. 8D) that involved PAC, Ei and PrS did not produce any labeling in neither the core nor the periphery of LC. One more case was analyzed (M10-09; Fig. 8A), where the injection involved the Bpc and scattered fibers were found in one slice in the rostral LC. It is likely that this scarce labeling originated in the Bpc rather than the PAC.

Only one experiment involved AHA as injection site (M04-10; Fig. 8F). This injection also extended to the PrS and Ec. Several cases mentioned earlier with deposits in the on PrS and Ec, clearly showed that these structures do not contribute to the labeling obtained in LC; therefore it is likely that the labeling found in this case may arise in AHA. The density is moderate to light and the labeled axons are scattered distributed along the core of LC, with no specific topographic organization. More injections would be needed in order to establish the contribution that AHA might have in the input to LC.

Functional interpretation

Notably, whereas prior rodent studies proposed that basolateral amygdala regulates LC indirectly through CeA (Bouret et al., 2003), the present tracing data indicates that the primate Bmc can directly regulate LC. Although it is unclear whether the converging hippocampo- and amygdalo-coerulean projections identified here are functionally related. Prior evidence from nonhuman and human studies suggests that both could have a role in memory processing (Sara, 2010). Novelty detection is accompanied by increased hippocampal noradrenergic activity, driven by enhanced firing of LC (Sara et al. 1994; Kitchigina et al. 1997). This activation of LC activity under novelty conditions might be mediated by the direct input that Sub sends to the core of the nucleus. In turn LC might provide the saliency signal required to promote hippocampal encoding of relevant novel information through changes in synaptic strength (Lemon et al., 2009). Accordingly, the direct projections from the basal nucleus of the amygdala to LC could contribute in restoring central arousal states that promote emotional memory consolidation (Sterpenich et al. 2006).

BIBLIOGRAPHY

Amaral DG, Cowan WM (1980). Subcortical afferents to the hippocampal formation in the monkey. J Comp Neurol 189: 573-91.

Amaral DG, Price JL (1984). Amygdalo-cortical projections in the monkey (*Macaca fascicularis*). J Comp Neurol 230(4): 465-96.

Amaral DG, Price JL, Pitkänen A, Carmichael ST (1992). Anatomical organization of the primate amygdaloid complex. In: Aggleton J, editor. The amygdala: neurobiological aspects of emotion, memory, and mental dysfunction. New York: Wiley-Liss Publishers. pp. 1-66.

Arnsten AF, Goldman-Rakic PS (1984). Selective prefrontal cortical projections to the region of the locus coeruleus and raphe nuclei in the rhesus monkey. Brain Res 306(1-2):9-18.

Aston-Jones G, Bloom FE (1981). Norepinephrine-containing locus coeruleus neurons in behaving rats exhibit pronounced responses to non-noxious environmental stimuli. J Neurosci 1(8):887-900.

Aston-Jones G, Ennis M, Pieribone VA, Nickell WT, Shipley MT (1986). The brain nucleus locus coeruleus: restricted afferent control of a broad efferent network. Sci 234: 734-737.

Aston-Jones G, Rajkowski J, Kubiak P, Alexinsky T (1994). Locus coeruleus neurons in monkey are selectively activated by attended cues in a vigilance task. J Neurosci 14(7):4467-4480.

Blaha CD, Yang CR, Floresco SB, Barr AM, Phillips AG (1997). Stimulation of the ventral subiculum of the hippocampus evokes glutamate receptor-mediated changes in dopamine efflux in the rat nucleus accumbens.

Bonda E (2000). Organization of connections of the basal and accessory basal nuclei in the monkey amygdala. Eur J Neurosci 12: 1971-1992.

Bouret S, Duvel A, Onat S, Sara SJ (2003). Phasic activation of locus coeruleus by the central nucleus of the amygdala. J Neurosci 23(8): 3491-3497.

Bouret S, Sara SJ (2005). Network reset: a simplified overarching theory of locus coeruleus noradrenaline function. Trends Neurosci 28: 574-582.

Bowden DM, Graman DC, Poynter WD (1978). An autoradiographic, semistereotaxic mapping of major projections from locus coeruleus and adjacent nuclei in *Macaca mulatta.* Brain Res 145: 257-276.

Canteras NS, Swanson LW (1992). Projections of the ventral subiculum to the amygdala, septum, and hypothalamus: a PHAL anterograde tract-tracing study in the rat. J Comp Neurol 324: 180-194.

Cedarbaum JM, Aghajanian GK (1978). Afferent projections to the rat locus coeruleus as determined by a retrograde tracing technique. J Comp Neur 178: 1-16.

Chiba T, Kayahara T, Nakano K (2001). Efferent projections of infralimbic and prelimbic areas of the medial prefrontal cortex in the Japanese monkey, *Macaca fuscata*. Brain Res 888: 83–101.

Clavier RM (1979). Afferent projections to the self-stimulation regions of the dorsal pons, including the locus coeruleus, in the rat as demonstrated by the horseradish peroxidase technique. Brain Res Bull 4: 497-504.

Davis M, Whalen PJ (2001). The amygdala: vigilace and emotion. Mol Psychiatry 6: 13-34.

Ennis M, Behbehani M, Shipley MT, Van Bockstaele EJ, Aston-Jones G (1991). Projections from the periaqueductal grey to the rostromedial pericoerulear region and nucleus locus coeruleus: new evidence of anatomical and physiological specifity. Physiol Rev 63: 844-914.

Fallon JH, Koziel DA, Moore RY (1978). Catecholamine innervation of the basal forebrain. II. Amygdalasuprahinal cortex and entorhinal cortex. J Comp Neurol 180: 509-532.

Floresco SB, Todd CL, Grace AA (2001). Glutamatergic afferents from the hippocampus to the nucleus accumbens regulate activity of ventral tegmental area dopamine neurons. J Neurosci 21(13): 4915-4922.

Freedman LJ, Insel TR, Smith Y (2000). Subcortical projections of area 25 (subgenual cortex) pf the macaque monkey. J Comp Neurol 421: 172-188.

Freese JL, Amaral DG (2005). The organization of projections from the amygdala to visual cortical areas TE and V1 in the Macaque monkey. J Comp Neurol 486: 295-317.

Gibbs ME, Hutchinson DS, Summers RJ (2010). Noradrenaline release in the locus coeruleus modulates memory formation and consolidation; roles for α- and β-adrenergic receptors. Neurosci 170: 1209-1222.

Gulyas B, Brockschnieder D, Nag S, Pavlova E, Kasa P, Beliczai Z, et al (2010). The norepinephrine transporter (NET) radioligand (S,S)- [18F]FMeNER-D2 shows significant decreases in NET density in the human brain in Alzheimer's disease: a post-mortem autoradio- graphic study. Neurochem Int 56: 789-798.

Insausti R, Amaral DG (2008). Entorhinal cortex of the monkey: IV. Topographical and laminar organization of cortical afferents. J Comp Neurol 509(6):608-641.

Insausti R, Amaral DG (2012). Hippocampal formation. In Mai JK, Paxinos G (Eds.), Atlas of the Human Brain (Third Edition), Elsevier Academic Press, London (2012), pp. 896–942.

Insausti R, Amaral DG, Cowan WM (1987). The entorhinal cortex of the monkey: III. Subcortical afferents. J Comp Neurol 264: 396-408.

Jodo E, Aston-Jones G (1997). Activation of locus coeruleus by prefrontal cortex is mediated by excitatory amino acid inputs. Brain Res 768(1-2): 327-32.

Jodo E, Chiang C, Aston-Jones G (1998). Potent excitatory influence of prefrontal cortex activity on noradrenergic locus coeruleus neurons. Neurosci 83(1): 63-79.

Jones BE, Moore RY (1977). Ascending projections of the locus coeruleus in the rat. II Autoradiographic study. Brain Res 127: 25-53.

Kitchigina V, Vankov A, Harley C, Sara SJ (1997). Novelty-elicited, noradrenaline-dependent enhancement of excitability in the dentate gyrus. Eur J Neurosci 9: 41-47.

Köhler C (1990). Subicular projections to the hypothalamus and brainstem: some novel aspects revealed in the rat by the anterograde *Phaseolus vulgaris* leukoagglutinin (PHA-L) tracing method. Prog Brain Res 83: 59-69

Lemon N, Aydin-Abidin S, Funke K, Manahan-Vaughan D (2009). Locus coeruleus activation facilitates memory encoding and induces hippocampal LTD that depends on ß-adrenergic receptor activation. Cerebral Cortex 19: 2827-2837.
Lisman JE, Grace AA (2005). The Hippocampal-VTA Loop: Controlling the Entry of Information into Long-Term Memory. Neuron 46(5): 703-713.
Loughlin SE, Foote SL, Bloom FE (1986). efferent projections of nucleus locus coeruleus: topographic organization of cells of origin demonstrated by three-dimensional reconstruction. Neurosci 18(2): 291-306.
Lu Y, Simpson KL, Weaver KJ, Lin RCS (2012). Differential distribution patterns from medial prefrontal cortex and dorsal raphe to the locus coeruleus in rats. Anat Rec 295: 1192-1201.
Luppi PH, Aston-Jones G, Akaoka H, Chouvets G, Jouvet M (1995). Afferent projections to the rat locus coeruleus demonstrated by retrograde and anterograde tracing with cholera-toxin b subunit and *Phaseolus vulgaris leucoagglutinin*. Neurosci 65(1): 119-160.
McGaugh JL, Roozendaal B (2008). Drug enhancement of memory consolidation: historical perspective and neurobiological implications. Psychopharmacol 202: 3-14.
Mohedano-Moriano A, Martinez-Marcos A, Pro-Sistiaga P, Blaizot X, Arroyo-Jimenez MM, Marcos P, Artacho-Pérula E, Insausti R (2008). Convergence of unimodal and polymodal sensory input to the entorhinal cortex in the *fascicularis* monkey. Neurosci 151: 255-71.
Mohedano-Moriano A, Muñoz-López M, Sanz-Arigita E, Pró-Sistiaga P, Martínez-Marcos A, Legidos-Garcia ME, Insausti AM, Cebada-Sánchez S, Arroyo-Jiménez MM, Marcos P, Artacho-Pérula E, Insausti R (2015). Prefrontal cortex afferents to the anterior temporal lobe in the Macaca fascicularis monkey. J Comp Neurol 523: 2570–2598.
Muñoz M, Insausti R (2005). Cortical efferents of the entorhinal cortex and the adjacent parahippocampal region in the monkey (Macaca fascicularis). Eur J Neurosci 22: 1368-88.
Pitkänen A, Amaral DG (1998). Organization of the intrinsic connections of the monkey amygdaloid complex: projections originating in the lateral nucleus. J Comp Neurol 398: 431-458.
Pitkänen A, Kelly JL, Amaral DG (2002). Projections From the Lateral, Basal, and Accessory Basal Nuclei of the Amygdala to the Entorhinal Cortex in the Macaque Monkey. Hippocampus 12: 186-205.
Price JL, Amaral DG (1981). An autoradiographic study of the projections of the central nucleus of the monkey amygdala. J Neurosci 1(11): 1242-1259.
Price JL, Russchen FT, Amaral DG (1987). The limbic region. II: the amygdaloid complex. In Bjorklund A, Hokfelt T, **Swanson LW** (eds), Handbook of Chemical Neuroanatomy, Vol. 5, Integrated Systems of the CNS, Part I. Elsevier Science, Amsterdam. pp. 279-388.
Roullet P, Sara SJ (1998). Consolidation of memory after its reactivation: involvement of β-noradrenergic receptors in the late phase. Neural Plast 6: 63-68.
Sara S.J, Roullet P, Przybyslawski J (1999). Consolidation of memory for odor-reward association: β-adrenergic receptor involvement in the late phase. Learn Mem 6: 88-96.
Sara SJ (2009). The locus coeruleus and noradrenergic modulation of cognition. Nat Rev Neurosci 10(3): 211-23.
Sara SJ, Vankov A, Herve A (1994). Locus coeruleus-evoked responses in behaving rats: a clue to the role of noradrenaline in memory. Brain Res Bull 35: 457-465.
Singewald N, Philippu A (1998). Release of neurotransmitters in the locus coeruleus. Prog Neurobiol 56: 237-267.
Singewald N, Schneider C, Pfitscher A, Philippu A (1994). In vivo release of catecholamines in the locus coeruleus. Naunyn Schmiedebergs Arch Pharmacol 350: 339-345.
Sterpenich V, D'Argembeau A, Desseilles M, Balteau E, Albouy G, Vandewalle G, Degueldre C, Luxen A, Collette F, Maquet P (2006). The locus coeruleus is involved in the successful retrieval of emotional memories in humans. J Neurosci 26: 7416:7423.
Swanson LW, Wyss JM, Cowan WM (1978). An autoradiographic study of the organization of intrahippocampal association pathways in the rat. J Comp Neurol 181: 681-715.
Szabo J, Cowan WM (1984). A stereotaxic atlas of the brain of the cynomolgus monkey (*Macaca fascicularis*). J Comp Neurol 222: 265-300.
Tronel S, Feenstra MG, Sara SJ (2004). Noradrenergic action in prefrontal cortex in the late stage of memory consolidation. Learn Mem 11: 453-458.
Tully K, Bolshakov VY (2010). Emotional enhancement of memory: how norepinephrine enables synaptic plasticity. Mol Brain 3(15): 1-9.
Wilcox BJ, Unnerstall JR (1990). Identification of a subpopulation of neuropeptide Y-containing locus coeruleus neurons that project to the entorhinal cortex. Synapse 6: 284-291.

5. Discussion and Conclusion

The present thesis illustrates how much anatomical details can tell us about the principles of brain organization and suggest new testable hypotheses, in this case for the organization and function of the descending control of the brain's midbrain monoaminergic systems. The present thesis revealed that the organization of the projections to VTA and LC are much more complex than originally thought, - and more complex and rich in primates than in rodents -, but also that they are organized according to a very consistent plan made of numerous parallel circuits linking related regions in a coherent circuit. Our results unravel parts of the complex anatomical topography substantiating the monosynaptic descending cortico-limbic conections in control of the main sources of DA and NE in the nonhuman primate brain. The Ventral Tegmental Area (VTA) and Locus Coeruleus (LC) are strongly interconnected (Beckstead et al., 1979; Swanson et al., 1998; Watabe -Uchida et al., 2004; Gesiler et al., 2008) and share overall numerous sources of afferent inputs. While the same prefrontal, insular, hippocampal and amygdaloid regions project directly and indirectly to VTA and LC, the relays or intermediate regions they use in their indirect projections are not always the same. In fact, only VTA has been found to receive indirect projections via the ventral striatum (VS). Although numerous other experiments would be necessary to test the following suggestions, this anatomical distinction suggests that even though the same cortical and limbic regions project to LC and VTA, the control that they exert also through indirect projections could produce very different effects on VTA and LC separately, and this differential control could provide the basis for a divergent influence of VTA over LC, and vice versa. Notably, this reciprocal influence could be supported by parallel projections or analogous to inner topographies with the rostro-caudal and medio-lateral axes of projection topographies of VTA and LC. In particular, the main findings of this thesis are:

1. Consistent with rodents, the PFC, particularly from mPFC (area 24, 13, 25) directly project to the VTA and LC in the non-human primate.
2. Different density of projections from the subareas of the PFC reaches both VTA and LC.
3. Cortical projections are distributed topographically along the medio-lateral axis in the VTA.
4. Some of the connections between the PFC and VTA or LC are reciprocal, highlighting the parallel role of DA and NE in neuromodulating the Cortex
5. Novel direct projections to VTA (and LC) from other Amy nuclei than Ce (i.e., B, PL and PAC) that were never described before in primates. Other areas such as the L and AB showed so far no projections.
6. Distinct density of projections depending on the subnucleus of the Basal amygdala: Bmc/Bpc particularly projects to the VTA and LC.
7. The projections from the different subnuclei of the B (Bmc, Bi, and Bpc) to the deep brain structures depend on the particular clusters of cells within each subnucleus.
8. Only projections from the S of the HF has been observed to VTA and LC
9. EC does not seemto send direct projections to VTA and LC.

5. Discusión y Conclusion

La presente tesis ilustra cuanto los detalles anatómicos pueden decirnos acerca de los principios de la organización del cerebro y sugerirnos nuevas hipótesis comprobables, en este caso para la organización y funcionamiento del control descendente de los sistemas monoaminérgicos cerebrales del cerebro medio. La presente tesis reveló que la organización de las proyecciones a VTA y LC son mucho más complejas de lo que se pensaba originalmente, - y siendo más compleja y vasta en primates que en roedores -, pero también que se organizan de acuerdo con un plan muy consistente formado por muchos circuitos paralelos que se unen y relacionan regiones en un circuito coherente. Nuestros resultados develan partes de la compleja topografía anatómica que demuestran las conexiones descendentes monosináptica en el control córtico-límbico de las principales fuentes de DA y NE en el cerebro de los primates no humanos. El área ventral tegmental (VTA) y el Locus Coeruleus (LC) están fuertemente interconectados (Beckstead et al, 1979; Swanson et al., 1998; Watabe -Uchida et al., 2004; Geisler et al., 2008) y comparten globalmente numerosas fuentes de aferencias. Mientras que las mismas regiones prefrontales, insulares, hipocampales y amígdalinas proyectan directa e indirectamente a VTA y LC, los retransmisores o regiones intermedias que utilizan en sus proyecciones indirectas no siempre son los mismos. De hecho, sólo en la VTA se ha encontrado que recibe proyecciones indirectas a través del estriado ventral (VS). Aunque muchos otros experimentos serían necesarios para poner a prueba las siguientes sugerencias, esta distinción anatómica sugiere que a pesar de que las mismas regiones corticales y límbicas proyectan a LC y VTA, el control que ejercen también en las proyecciones indirectas podría producir efectos muy diferentes sobre VTA y LC de forma separada, este control diferencial podría servir de base para una influencia divergente de la VTA sobre LC, y viceversa. Cabe destacar que esta influencia recíproca podría ser apoyada por proyecciones paralelas o análogas de la topografía intena con los ejes rostro-caudal y medio-lateral de las proyecciones topograficas de VTA y LC. En particular las principales conclusiones de la tesis son:

1. *En consistencia con lo observado en roedores, el PFC, en particular el córtex prefrontal medial (área de 24,13, 25) proyecta directamente a la VTA y LC en el primate no humano.*
2. *Se han observado diferentes densidades de proyecciones desde las subáreas del PFC que alcanzan tanto VTA como LC.*
3. *Proyecciones corticales se distribuyen topográficamente lo largo del eje medio-lateral en el VTA.*
4. *Algunas de las conexiones entre el PFC y VTA o LC son recíprocas, destacando el papel neuromodulador de la DA y NE en el Córtex.*
5. *Proyecciones directas a la VTA (y LC) desde otros núcleos de la Amy aparte de Ce (es decir, B, PL y PAC) que nunca fueron descritos anteriormente en primates. Otras áreas, como la L y AB no mostraron hasta ahora proyecciones.*
6. *Distintas densidades de proyecciones dependientes del subnúcleo de la amígdala: En particular, Bmc/Bpc proyectos a la VTA y LC.*

7. *Las proyecciones de los diferentes subnúcleos del B (Bmc, Bi, Bpc) a las estructuras del tronco del encéfalo dependen de los grupos particulares de células dentro de cada subnúcleo.*
8. *Solamente se han observado proyecciones desde S de la FH a la VTA y LC.*
9. *Sin embargo, no se han observado proyecciones dese la CE a la VTA y LC.*

1. Diskussion und Schlussfolgerung

Diese Arbeit veranschaulicht in welchem Ausmaß anatomische Details etwas über die Organisationsprinzipien des Gehirns aussagen können, welche uns wiederum zu neuen prüfbaren Hypothesen führen (in diesem Fall für die Organisation und Funktionsweise der efferenten Kontrolle der monoaminergen Systeme des Mittelhirns).Zudem offenbart diese Arbeit, dass die Organisation der Projektionen zum VTA und LC weitaus komplexer sind als ursprünglich angenommen (noch komplexer und komplizierter in Primaten als bei Nagern). Weiterhin zeigt die Arbeit, dass die Organisation der Projektionen einem sehr konsequenten Plan folgt, welcher aus zahlreichen parallelen Kreisläufen besteht, die verwandte Gebiete zu einem kohärenten Kreislauf verbinden.

Unsere Ergebnisse entwirren Teile der komplexen anatomischen Topographie und bestätigen eine efferente Kontrolle monosynaptischer, kortikal-limbischer Verbindungen, unter welcher die Hauptquellen des DA und NE im Gehirn nicht-menschlicher Primaten stehen.VTA und LC sind fest miteinander verschaltet (Beckstead et al., 1979; Swanson et al., 1998; Watabe -Uchida et al., 2004; Gesiler et al., 2008) und teilen sich allgemein zahlreiche Quellen für afferente Eingänge. Während immer gleiche präfrontale, insuläre, hippocampale und amygdaloide Regionen sowohl direkt als auch indirekt in den VTA und LC projizieren, sind die nachgeschalteten, sogennante Zwischenregionen, die bei indirekten Projektionen verwendet werden, nicht immer gleich. Tatsächlich hat man herausgefunden, dass lediglich der VTA eine indirekte Projektion über das VS erhält. Obwohl zahlreiche weitere Experimente nötig wären um die folgenden Behauptungen zu untersuchen, deuten die anatomischen Unterscheidungen darauf hin, dass obwohl die gleichen kortikalen und limbischen Regionen in den LC und den VTA projizieren, die Kontrolle die sie über indirekte Projektionen haben, sehr unterschiedliche und separate Effekte auf den VTA und LC haben können. Diese unterschiedliche Kontrolle könnte eine Grundlage für einen divergenten Einfluss des VTAs auf den LC und umgekehrt bieten.Dieser reziproke Einfluss könnte insbesondere durch die parallelen Projektionen oder, analog zur inneren Topographie, durch die rostro-kaudalen und medio-lateralen Achsen der Projektionstopographien des VTA und LC unterstützt werden.Die Hauptergebnisse dieser Arbeit sind:

1. der präfrontale Kortex, insbesondere der mediale präfrontale Kortex (Region 24, 13, 25), projizieren direkt zum VTA und LC in nicht-menschlichen Primaten.

2. unterschiedliche Projektionsdichten aus den Subarealen des präfrontalen Kortex erreichen sowohl VTA als auch LC.

3. kortikale Projektionen sind topographisch betrachtet entlang der medio-lateralen Achse im VTA verteilt.

4. Manche Verbindungen zwischen PFC und VTA oder LC sind reziprok, wodurch die parallele Rolle der DA und NE bei der Neuromodulation des Kortex hervorgehoben wird.

5. Entdeckung neuer direkter Projektionen zum VTA (und LC) von anderen Amy Nuclei als Ce (i.e. B, PL, und PAC) die niemals zuvor in Primaten beschrieben wurden. Andere Bereiche wie die L und AB weisen bisher keine Projektionen auf.

6. Unterschiedliche Dichten der Projektionen (abhängig vom Subnukleus der basalen Amygdala: Bmc/Bpc projizieren ausschließlich zum VTA und LC)

7. Projektionen aus den unterschiedlichen Subnuclei des B (Bmc, Bi und Bpc) zu den tiefen Hirnstrukturen sind abhängig von bestimmten Zellverbänden innerhalb jedes Subnucleus.

8. Es wurden lediglich Projektionen vom S des HF zum VTA und LC beobachtet.

9. EC weist keine direkten Projektionen zum VTA und LC auf.